JAERI-Conf
96-005

PROCEEDINGS OF THE THIRD SPECIALISTS' MEETING ON NUCLEAR DATA FOR FUSION REACTORS

NOVEMBER 29~30, 1995, TOKAI, JAPAN

March 1996

(Eds.) Keiichi SHIBATA and Yukio OYAMA

日本原子力研究所
Japan Atomic Energy Research Institute

本レポートは，日本原子力研究所が不定期に公刊している研究報告書です。
入手の問合わせは，日本原子力研究所技術情報部情報資料課（〒319-11 茨城県那珂郡東海村）あて，お申し越しください。なお，このほかに財団法人原子力弘済会資料センター（〒319-11 茨城県那珂郡東海村日本原子力研究所内）で複写による実費頒布をおこなっております。

This report is issued irregularly.
Inquiries about availability of the reports should be addressed to Information Division, Department of Technical Information, Japan Atomic Energy Research Institute, Tokai-mura, Naka-gun, Ibaraki-ken 319-11, Japan.

編集兼発行　日本原子力研究所
印　　刷　㈱原子力資料サービス

JAERI－Conf 96－005

Proceedings of the Third Specialists' Meeting on Nuclear Data for Fusion Reactors

November 29～30, 1995, Tokai, Japan

(Eds.) Keiichi SHIBATA and Yukio OYAMA

Japanese Nuclear Data Committee
and
Japanese Research Committee on Reactor Physics
Tokai Research Establishment
Japan Atomic Energy Research Institute
Tokai-mura, Naka-gun, Ibaraki-ken

(Received January 31, 1996)

The Third Specialists' Meeting on Nuclear Data for Fusion Reactors was held at Tokai Research Establishment, Japan Atomic Energy Research Institute on the 29th and 30th of November 1995. This meeting was jointly organized by Japanese Nuclear Data Committee and by Japanese Research Committee on Reactor Physics. Forty specialists participated in the meeting, and made discussion on current status of evaluated data contained in JENDL-3.2, JENDL Fusion File and FENDL-1. Data accuracy was examined from the analyses of benchmark experiments. Finally, recommendation was given for FENDL-2, which is developed at IAEA.

Keywords: Proceedings, Nuclear Data, Fusion Reactor, Evaluation, Benchmark Test, JENDL, FENDL

JAERI－Conf 96－005

第３回核融合炉核データ専門家会議報文集

1995年11月29～30日，東海村

日本原子力研究所東海研究所
シグマ研究委員会・炉物理研究委員会
（編）柴田　恵一・大山　幸夫

（1996年１月31日受理）

第３回核融合炉核データ専門会議が1995年11月29日，30日に日本原子力研究所東海研究所で開催された。この会議は，原研シグマ研究委員会及び炉物理研究委員会の共催で行われた。会議には40名の専門家が出席し，JENDL-3.2，JENDL Fusion File及びFENDL-1の評価済みデータの現状について議論が行われた。データ精度の検証はベンマーク実験の解析により行われた。最後に，IAEAで現在作成中のFENDL-2に対するJENDLデータの推薦順位が決定された。

東海研究所：〒319－11　茨城県那珂郡東海村白方白根２－４

Organizing Committee

Yukio OYAMA (Chairman)	Japan Atomic Energy Research Institute
Satoshi CHIBA	Japan Atomic Energy Research Institute
Keiichi SHIBATA	Japan Atomic Energy Research Institute
Fujio MAEKAWA	Japan Atomic Energy Research Institute
Takamasa MORI	Japan Atomic Energy Research Institute
Koichi MAKI	Hitachi, Ltd.
Naoki YAMANO	Sumitomo Atomic Energy Industries, Ltd.

幹事

大山　幸夫　（幹事長）	日本原子力研究所
千葉　敏	日本原子力研究所
柴田　恵一	日本原子力研究所
前川　藤夫	日本原子力研究所
森　貴正	日本原子力研究所
真木　紘一	日立製作所
山野　直樹	住友原子力工業

Contents

目　　次

Preface

Research of "Fusion Neutronics" includes broad areas such as reactor design, nuclear data evaluation, cross section measurement, integral experiment, transport calculation and nuclear data processing code developments and so on. However, because this includes really many research areas, there may exist difficulty on communication among scientists in different area. Designers of fusion reactors requires design tools as nuclear data and calculation codes, nuclear data evaluator provides basic cross section data, and the other researchers works to interface between them and to establish the quality of the data and codes. These efforts are needed to closely contact each other, therefore an opportunity to meet together and to discuss among the different areas are desired.

The Third Specialists' Meeting on Nuclear Data for Fusion Reactor was held on November 29-30, 1995 at Tokai Research Establishment in Japan Atomic Energy Research Institute. This meeting aims at discussing the problems relevant to fusion reactors among evaluators of nuclear data, designers of fusion reactors and experimentalists of fusion neutronics. The meeting has been held every five years since 1985. The first meeting was held at the time of starting fusion neutronics just after completion of new intense neutron source facilities, i.e., FNS/JAERI and OKTAVIAN/Osaka University. The second meeting was at the period during JAERI/USDOE collaboration at FNS and at the time when double differential cross section measurements had been extensively performed by both groups of the Osaka University and the Tohoku University. At the same time, JENDL-3(3.1) had been completed by Japanese Nuclear Data Committee considering fusion reactor application as well as fission reactor. In this meeting, the followings problems were pointed out for further efforts.

1) Improvement of secondary gamma-ray data,
2) Necessity of Fusion File with ENDF-6 format,
3) Necessity of processing code for ENDF-6 format data,
4) Necessity of cross section sensitivity analysis,

and 5) High energy neutron data.

After the second meeting, some new integral experiments were performed at FNS, and new experimental data for nuclear heating was obtained by the direct measurement method. As for fusion reactor development, new experimental works for the ITER/EDA started especially shielding problems. Under IAEA, an international standard nuclear data file, FENDL-1 was selected and an international effort of a integral test for it also was initiated. In 1995, JENDL-3.2 and JENDL-Fusion File were completed and also tested by Japanese integral experiments. Some of problems listed in the above have been solved in the mean time. Hence the present meeting has been desired for reviewing these many activities and it has become a good chance in coincidence with international activities.

The meeting consists of seven sessions:1)Reviewing fusion reactor design and development, 2)Nuclear data evaluation and code development, 3)Integral data testing, 4)Engineering applicability, 5)Activation data, 6)PKA and KERMA data and 7)Summary and comments. The present meeting could be held by cooperation and assistance of many peoples. So I would like to thank all participants who gave lectures and comments, and also appreciate the member of the secretariat.

Yukio OYAMA

1. Fusion Reactor Design

1.1 Review of Nuclear Design in International Thermonuclear Experimental Reactor (ITER)

Koichi Maki, Satoshi Satoh*, Kei-ichiro Shibata, Yasushi Seki*
Hitachi Research Laboratory, Hitachi Ltd.
7-1-1 Omika-cho, Hitachi-shi, Ibatraki-ken 319-12
* Japan Atomic Energy Research Institute
Naka-machi, Naka-gun, Ibaraki-ken 311-01

Abstract

Main thema in nuclear design of deuterium-tritium fusion reactors are radiation shielding design, blanket nuclear design, induced radioactivity evaluation and radiation damage evaluation. In the present paper, typical designs and evaluated examples concerning these thema are reviewed on the basis of Engineering Design Activity (EDA) and Conceptual Design Activity (CDA) in International Thermonuclear Experimental Reactor (ITER).

1. Introduction

Principal design subjects in nuclear design for DT tokamak fusion reactors are radiation shielding design (below to write down as only shielding design), blanket nuclear design, induced radioactivity evaluation and radiation damage evaluation. In the present paper, these subjects are explained concerning mainly International Thermonuclear Experimental Reactor (ITER)[1] Engineering Design Activity (EDA) and partially ITER Conceptual design Activity (CDA)[2]. At first, outline of the ITER-EDA is illustrated in Chapter 2, and then shielding design is especially represented in detail in Chapter 3. The next, nuclear design of breeding blanket is described in Chapter 4, and successively induced radioactivity and radiation damage evaluations are explained in Chapter 5 and 6, respectively.

2. Outline of ITER

The ITER-EDA has been being promoted since July in 1992 according to the schedule as Fig.1 The ITER-EDA final design report will be published and finished at the

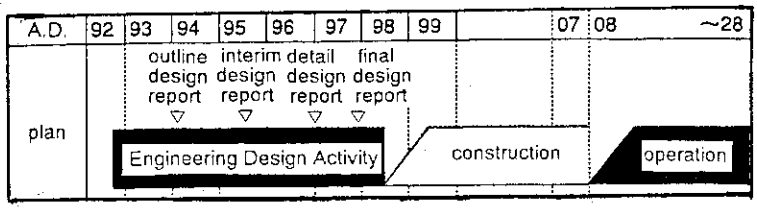

Fig.1 ITER developing schedule

Table 1. Principal design parameters of ITER[1]

Plasma major radius	8.1 m	Fusion power	1500 MW
Plasma minor radius	2.8 m	Average neutron first wall loading	1 MW/m^2
Plasma current	21 MA	Average neutron first wall fluence	
Toroidal field on axis	5.7 T	basic phase	0.3 MWa/m^2
Plasma burn time	1000 sec	extended phase	1 MWa/m^2

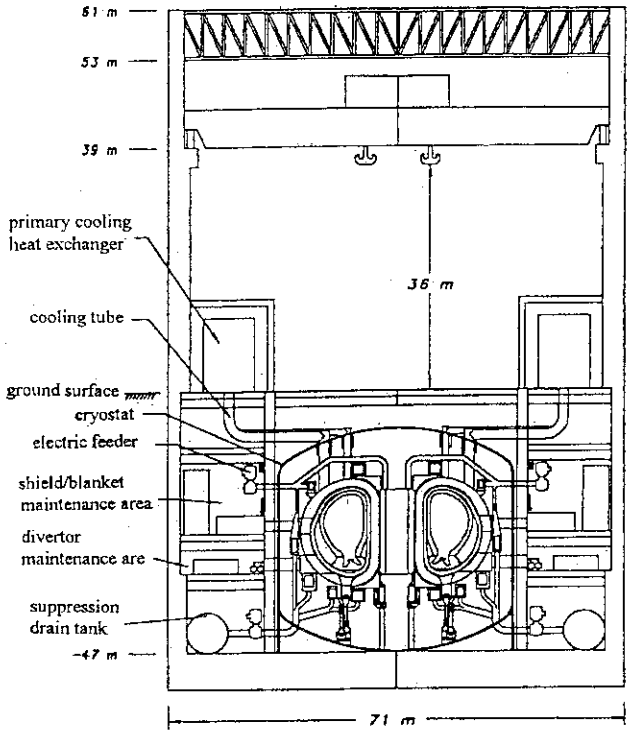

Fig.2 Elevation of tokamak building

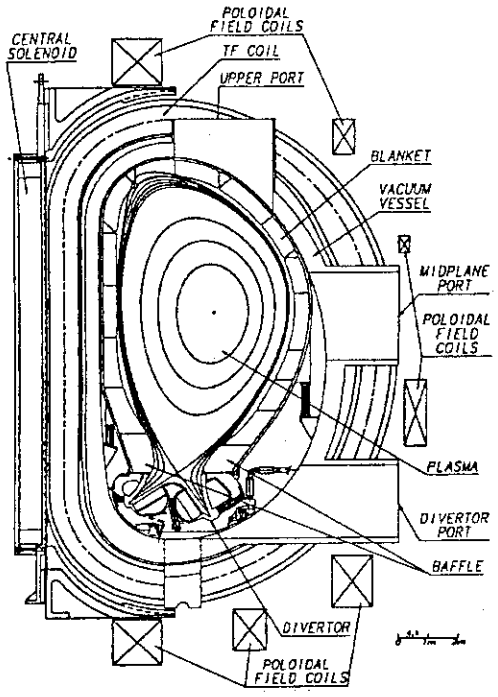

Fig.3 Poloidal cross section of ITER

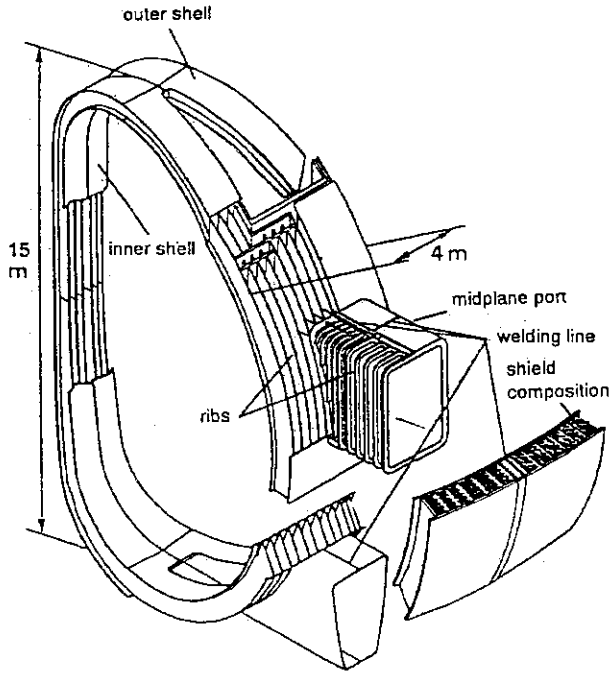

Fig.4 Vacuum vessel sector

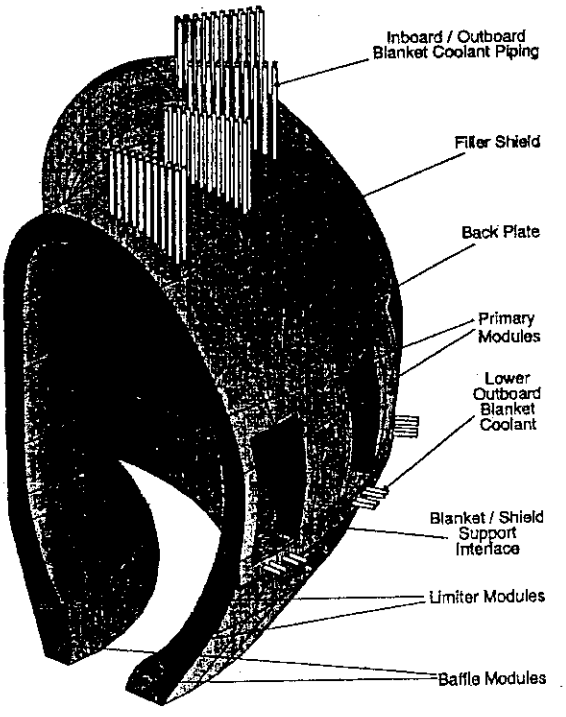

Fig.5 Shield / Blanket configuration

middle of 1998. After that, the ITER may be progressed into the construction phase.

The ITER building and the facility configuration are illustrated in Fig.2. The reactor is surrounded by the cryostat constructed with thickness of 2cm double stainless steel (SS) walls and further enclosed by approximately 1m thick biological shield mainly consisting of concrete. The poloidal cross section of ITER is shown as Fig.3. The principal design parameters are listed in Table 1. The vacuum vessel is constructed by inner and outer shells with ribs in order to enhance stiffness as shown in Fig.4. Stainless steel plates are inserted in vacuum vessel together with water in order to increase shielding ability. The shield blanket is enclosed by the vacuum vessel. The inboard shield blanket sector is divided into two rows in the toroidal direction and every row consists of seven modules in the poloidal direction, and the outboard shield blanket is divide into three rows in the toroidal direction and every row consists of eight modules in the poloidal direction as illustrated in Fig.5. The lowest modules in inboard and outboard are called baffles, which receive high heat flux of 5MW/m^2. Two modules above the baffle in the outboard are limiter modules which are touched by plasma during plasma formation period. The shield blanket modules consist of approximately 80%SS and 20%water.

3. Shielding design

At first subjects in shielding design are explained as shown in Fig.6. Shielding design is divided into two categories due to shielding objects. One is biological shielding and the other is shielding for facility itself. The former is the same as fission reactors, accelerators and radioisotope facilities. Subjects in the former are to decrease in worker's and public exposures. While the latter is important subject in fusion reactors since superconductive magnets (SCM) should be protected against radiation. That is, the subject is to decrease in nuclear heating rate and radiation damage in winding pack in superconductive magnets. Further subjects are to decrease in radiation damage, that is dpa in structural materials and functional materials, and in helium and proton production rate at rewelding positions in structural materials, and to reduce radiation damage for equipments inside and outside the reactor core.

3.1 Shielding for facility itself

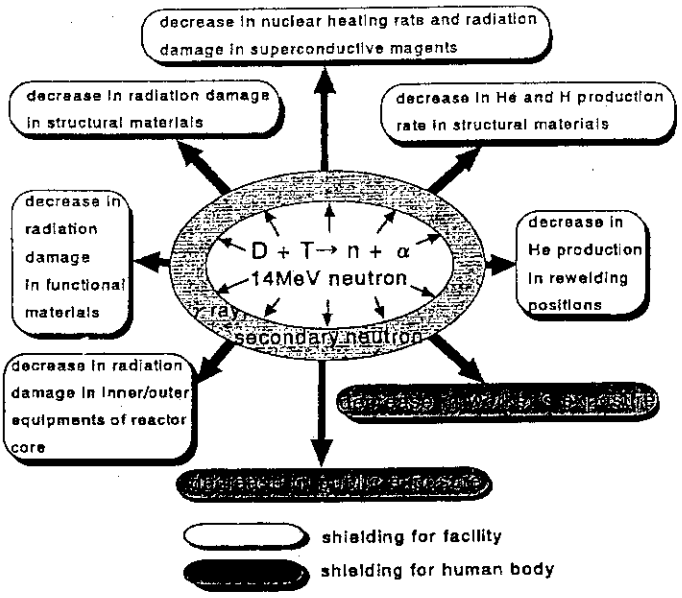

Fig.6 Subjects in shielding design for tokamak fusion reactors

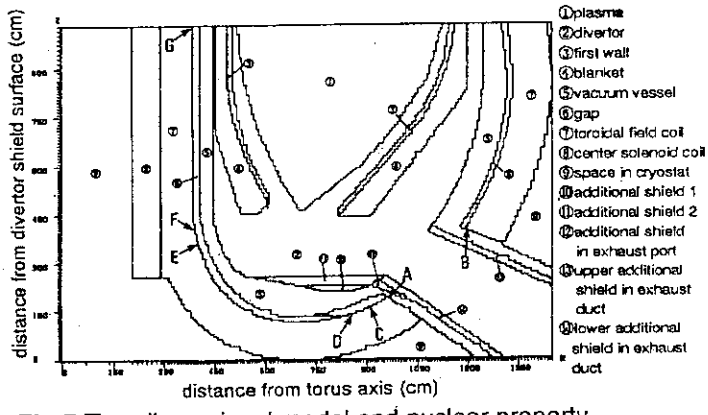

Fig.7 Two dimensional model and nuclear property evaluation positions for toroidal field coils of A, B, C, D, E, F and G.

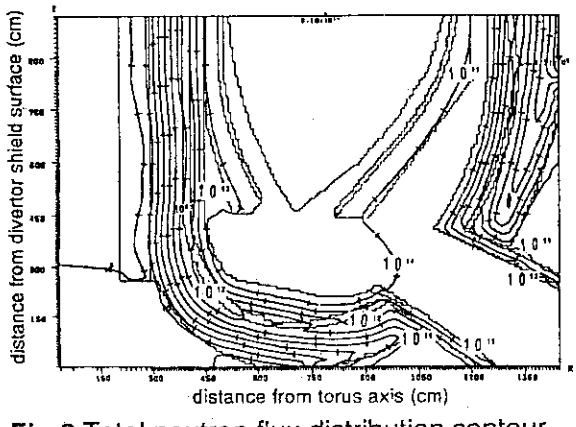

Fig.8 Total neutron flux distribution contour in lower half reactor of ITER.

The positions of insufficient shielding thickness concerning shield blanket and vacuum vessel were surveyed from the view point of protecting SCM against radiation by two dimensional transport calculation for ITER during operation with DOT3.5[3] code, group constant set FUSION40[4] and two dimensional model as Fig.7. Calculated total neutron flux distribution is presented as Fig.8. Nuclear properties in SCM

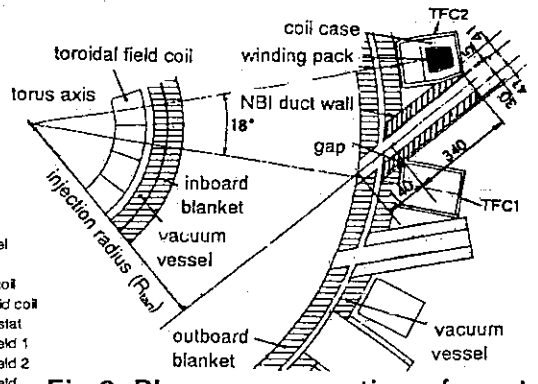

Fig.9 Plane cross section of reactor core and NBI duct in ITER (in cm).

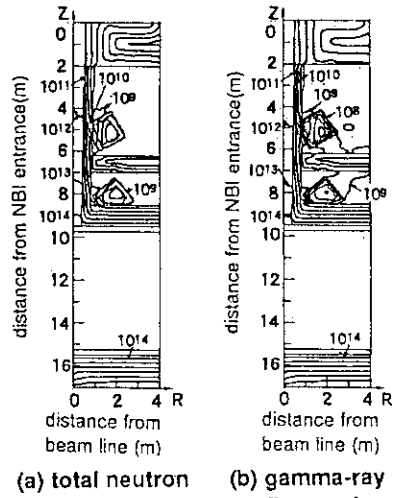

(a) total neutron flux contour (n/cm²s)

(b) gamma-ray flux contour (γ/cm²s)

Fig.10 Neutron and gamma-ray flux distributions around the NBI duct in ITER.

at the positions from A to G are illustrated in Table 2.

Table 2 Nuclear properties at positions from A to G in SCM and required additional thicknesses for shields near these positions under the condition of the first wall neutron loading of 1MW/m^2 and the first wall neutron fluence of 3MWa/m^2.

evaluated position / nuclear property (thickness)	design limit	A (30cm)	B (30cm)	C (35cm)	D (40cm)	E (50cm)	F (50cm)	G (100cm)*
nuclear heating rate mW/cm^3	1	73	10	90	42	35	22	10
insulator dose MGy	50	330	55	770	300	250	130	75
copper dpa 10^{-3}dpa	0.5	9.6	1.3	34	10	7.5	3.5	2.4
fast neutron fluence (E_n>0.1MeV) 10^{19}n/cm^2	1	2.8	0.33	5.8	2.1	1.6	0.79	0.47
required additional thickness cm	---	20	20	35	30	25	20	15

*This thickness includes 50cm liquid lithium blanket which has only half shielding efficiency of that in 80%SS+20% water shield.

Nuclear properties in superconductive toroidal field coils around the neutral beam injector (NBI) duct were evaluated. The duct and the coil configurations are shown in Fig.9. The model, and calculated neutron and gamma-ray fluxes are presented in Fig.10. The duct and the coils are modeled by two dimensional RZ model, where Z axis corresponds to duct center line. The coil of TFC2 in Fig.9 is set at the upper coil among two coils in Fig.10. Pseudo shield is inserted between the two coils in order to avoid effect of leakage neutron by gap streaming between the coil of TFC1 and the duct on nuclear properties in the coil of TFC2. Evaluated nuclear properties in TFC1 and TFC2 are listed in Table 3. According to the results, nuclear properties in TFC1 and TFC2 satisfy the design limits.

Table 3 Nuclear properties in toroidal field coils of TFC1 and TFC2 near the neutral beam injection duct for the first wall neutron loading of 1MW/m^2 and the first wall neutron fluence of 3MWa/m^2.

	design limit	TFC1	TFC2
nuclear heating rate mW/cm^3	1	0.033	0.052
insulator dose MGy	50	1.0	1.5
Copper dpa 10^{-3}dpa	0.5	0.1	0.15
fast neutron fluence (E_n>0.1MeV) 10^{19}n/cm^2	1	0.019	0.028

3.2 Biological shielding

Dose rates in reactor room and environment around the reactor building during

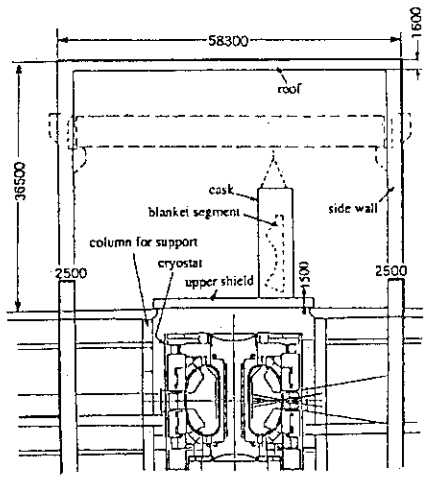

Fig.11 Cross section of reactor room and one segment that was hung in the room by a crane (measurements are in millimetres).

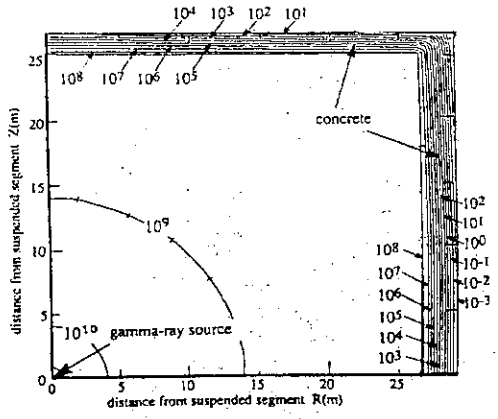

Fig.12 Gamma-ray dose-rate distribution (in microsieverts per hour) in the reactor room with one segment hanging from the ceiling (gamma-ray source intensity is 6.44 × 10^{17} γ/s for the first-wall neutron fluence of 3 MW·yr/m^2).

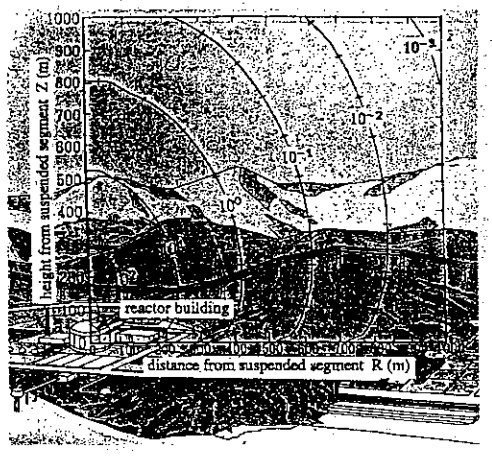

Fig.13 Skyshine gamma-ray dose rate distribution in the environment around the reactor building with one segment hung in the room from the ceiling one day after shut down (unit in μSv/y) [gamma-ray source intensity is 6.44 × 10^{17} γ/s for the first wall neutron fluence of 3MWa/m^2] [21].

hanging one activated segment from the ceiling were estimated after 3MWa/m^2 neutron fluence operation. The hanging configuration is illustrated as shown in Fig.11. According the dose rate in the room presented in Fig.12[5,6], lowest dose rate is 10^8μSv/h beside the room wall and dose rate near the module is larger than 10^{10}μSv/h. This dose rate is exchanged into absorbing dose rate to be approximately 10^4 Gy/h, which means to become ordinary semi conductor equipments damaged and loses their functions several hours or so. Skyshine

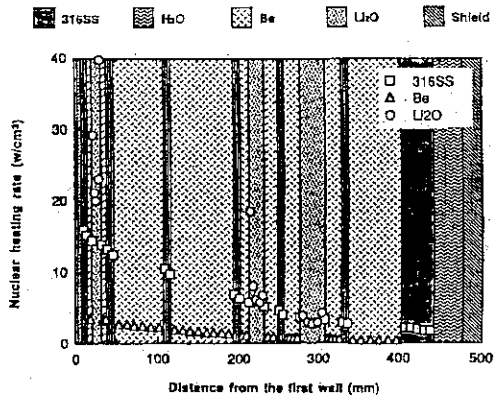

Fig.14 Nuclear heating rate distribution in the ITER ceramic breeder multi-layered pebble bed blanket for the neutron first wall loading of 1MW/m^2 by a one-dimensional cylinder model for this blanket with ANISN code.

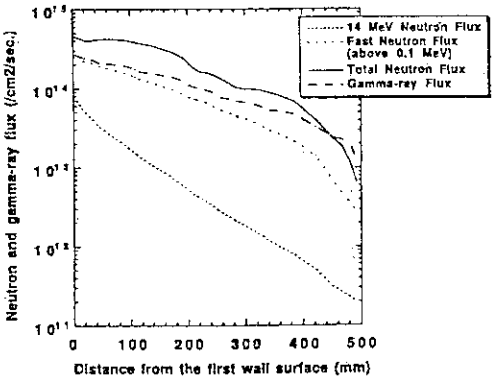

Fig.15 Neutron and gamma-ray flux distributions in the ITER ceramic breeder multi-layered pebble bed blanket for the neutron first wall loading of 1MW/m^2.

gamma-ray dose rate distribution in the environment around the reactor building under the same conditions is illustrated in Fig.13[5,6]. Considering public exposure design limit of 10μSv/y and design safety factor as 10, site boundary can be selected as the radius 400m from the reactor center.

4. Blanket nuclear design

A blanket is one of the components surrounding the plasma and has following three important roles in D-T fusion reactors:

1) to produce tritium, which is one of the fuels in DT fusion and does not exist naturally.

2) to recover thermal energy transformed into, partially through gamma-ray, from kinetic energy of neutrons.

3) to shield radiation for protection fusion reactor components such as SCM and human body against radiation exposure.

A ceramic breeder multi-layered pebble bed blanket is put as a candidate of the ITER driver blankets. Temperature of cooling water is restrained lower than 100℃ since this blanket has no object to generate electric output. The blanket has three Li_2O breeder zones, nine Be neutron multiplier zones and five cooling panels. The ceramic Li_2O and metal Be are used in the shape such as 1mm diameter pebbles. Total thickness of the blanket is 50cm and the first wall thickness 1.5cm including 0.5cm thick cooling channel. Nuclear heating rate distributions are calculated with ANISN[7] code, group constant set FUSION40[4] and one dimensional model made by material number densities averaged in each zone as shown in Fig.14[6]. Neutron and gamma-ray fluxes in the blanket are expressed as Fig.15[6]. Contribution of each breeder zone to tritium breeding ratio is summarized in Table 4. Total breeding ratio can be obtained 1.137, which is called local TBR. Net TBR is reduced since there are positions or zones where blankets cannot be equipped with, that is called blanket coverage. In fact the net TBR in ITER is approximately 0.8 because the coverage is obtained only 0.7.

Table 4 Tritium breeding ratio in every zone of the ceramic breeder blanket

	1st zone	2nd zone	3rd zone	total
$^6Li(n,\alpha)T$	0.574	0.345	0.200	1.119
$^7Li(n,n'\alpha)T$	0.011	0.003	0.004	0.018
total	0.585	0.348	0.204	1.137

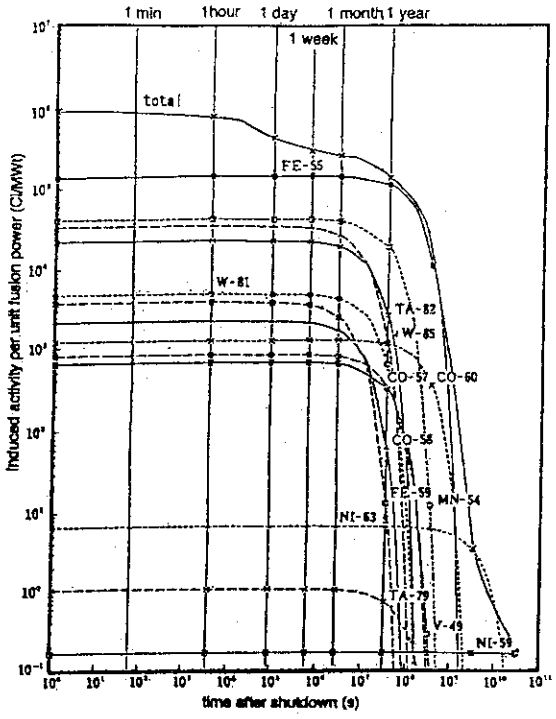

Fig.16 Time evolutions in induced activities of nuclides per unit fusion power after one year continuous operation in the steady state tokamak power reactor SSTR [24].

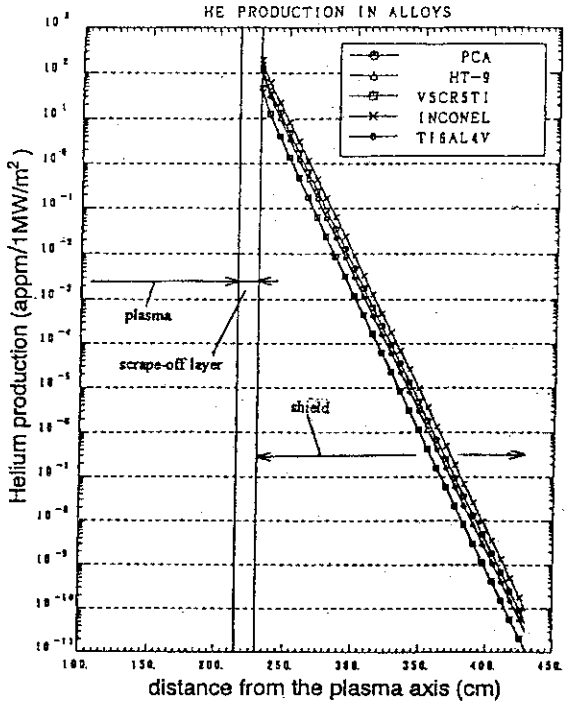

Fig.18 Helium production rates in alloys of the steel rich (80% steel and 20% water) composition versus the distance from the plasma axis [13].

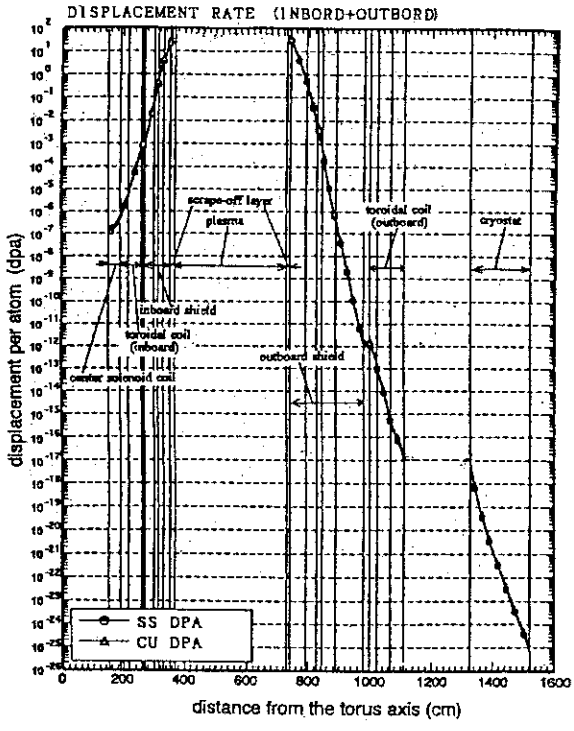

Fig.17 Displacement per atom distributions in stainless steel and copper after 3MWa/m² operation on the mid-plane of the ITER-CDA by a one dimensional model.

5. Induced activity evaluation

In fusion reactor materials constructing reactor are activated by 14MeV neutrons produced in DT fusion reaction. In activation process unstable nuclides are produced by neutron reaction with materials. The unstable nuclides decay, and release β-rays and γ-rays together with decay heat. Induced activity causes following problems in fusion reactors,

1) High dose rate by induced activity not only makes workers to be impossible to approach the machine and to maintain it directly but also shortens life time of remote maintenance machine by gamma-ray radiation damage.

2) Activated components become finally radiation waste.

3) Movable activated materials enhance risk potential for environment.

4) Decay heat by activity causes component temperature to raise in the case of loss of cooling ability or stopping cooling system.

Therefore, evaluation of induced activity is one of the most important subjects in fusion reactors. Induced activity is estimated for ferritic steel of F82H applied in SSTR (Steady State Tokamak Reactor)[8] design under the condition of neutron fluence of 4MWa/m^2 as shown in Fig.16. From this result we can understand induced activity overall the reactor 10^6Ci per fusion power 1MW.

6. Radiation damage evaluation

Items to be evaluated as radiation damage are displacement per atom (dpa), helium and proton production rates, and transmutation of nuclides. Former two items having larger effect items of them on the material properties are reviewed in this chapter.

The distributions of dpa values in stainless steel and copper are presented in Fig.17, which was obtained by calculation for ITER-CDA[2] with ANISN code under the condition of 3MWa/m^2 neutron fluence. In nuclear response function calculation stainless steel and copper are assumed to exist all regions in the ITER core. In fact stainless steel exists in all regions except cryostat, while copper exists only in SCM. From Fig.17 dpa in SS and copper for the first wall neutron fluence 3MWa/m^2 can be seen 30dpa, that is approximately 10dpa per 1MWa/m^2.

Helium production rate distribution after 1MWa/m^2 first wall neutron fluence operation is illustrated as Fig.18[9]. This was calculated by one dimensional cylinder model with ANISN code. Helium production in stainless steel can be obtained approximately 130appm for the first wall neutron fluence of 1MWa/m^2.

7. Summary

Radiation shielding design, blanket nuclear design, induced radioactivity evaluation and radiation damage evaluation are reviewed as main thema in nuclear design of ITER-EDA and -CDA.

Principal subjects in shielding design are illustrated and explained. In shielding design for facility itself, positions of shield thickness defect are cleared. In biological shielding, dose rates in reactor room and environment are estimated. In blanket nuclear design, nuclear

heating rate distribution and tritium breeding ratio are evaluated. Induced activity, and dpa and helium production rate in radiation damage are predicted for ITER. We emphasize that nuclear design is important and indispensable to fusion reactor design.

Acknowledgments

These works were performed as parts of the design study supported by Naka Fusion Research Establishment at the Japan Atomic Energy Research Institute (JAERI). The authors wish to thank Dr. S. Matsuda, department leader of the ITER Development Laboratory, and Dr. H. Takatsu of Reactor Core Engineering Laboratory in JAERI. And they also wish to thank Dr. K. Hayashi of Hitachi Engineering Corp. Ltd., for his valuable advice and comments, and K.Yamada of Business Automation Company for his supporting calculations.

References

1) ITER Technical Advisory Committee, "Executive Summary Project Management Plan for International Thermonuclear Experimental Reactor," The 4th Meeting of the Technical Advisory Committee, Garching Joint Work Site, (Nov. 1994).

2) K. Tomabechi *et al.*, ITER Documentation Series No.10, IAEA, International Atomic Energy Agency (1991).

3) W. A. Rhoades and F. R. Mynatt, "The DOT-III Two Dimensional Discrete Ordinates Transport Code," ORNL-TN-4280, Oak Ridge National Laboratory (1973).

4) K. Maki, *et al.*, Nuclear Group Constant Set FUSION-J3 for Fusion Reactor Nuclear Calculation Based on JENDL-3, JAERI-M 91-072, Japan Atomic Energy Research Institute (1991).

5) K. Maki, *et al.*, Fusion Technology **27**, 176 (1995).

6) K.Maki, *et al.*, Nuclear Design for Fusion Reactors, Journal of Plasma and Fusion Research, **71**, 987(1995).

7) W. W. Engle, "A User's Manual for ANISN, A One Dimensional Discrete Ordinate Transport Code with Anisotropic Scattering," K1693, Union Carbide Corporation, Computing Technology Center (1967).

8) Fusion Reactor System Laboratory, JAERI-M 91-081, Japan Atomic Energy Research Institute (1991).

9) S. Mori *et al.*, JAERI-M93-175, Japan Atomic Energy Research Institute, (1993).

1.2 Topics of ITER Nuclear Design

Satoshi Sato, Hideyuki Takatsu, Toshihiko Sasaki*, Toshihisa Utsumi*
Japan Atomic Energy Research Institute,
Naka-machi, Naka-gun, Ibaraki-ken 311-01
*Information Technologies Japan Inc.
Mito Tokyoseimei-kan, 3-10-17, Jonan, Mito-shi, Ibaraki-ken 310

The shielding analyses of the inboard blanket, the vacuum vessel and the toroidal field coil in ITER were conducted by Monte Carlo and 2- dimensional discrete SN methods taking the radiation streaming through the gap between the adjacent blanket modules into account, and their nuclear responses were evaluated[1]. The nuclear responses of the toroidal field coil could fully satisfy the shielding design targets. On the other hand, the helium production rates at the back of the inboard blanket were about 2 - 3 times higher than the shielding design target at the end of the operation.

1. Introduction

Blanket for International Thermonuclear Experimental Reactor (ITER) is composed of a number of shielding modules from the assembly and maintenance point of view, and there are 20 mm wide gaps between the adjacent shielding modules[2]. A bird's-eye view of the blanket configuration is shown in Fig. 1. Shielding modules are welded to the back plates to form a rigid axisymmetric structure through two connection "legs" located at the back of the module. Branch coolant pipes are also connected to the common manifolds as shown in Fig. 2. The legs and the branch pipes will be cut and rewelded in case of replacement of shielding modules with breeding modules, and damaged modules with new ones, if necessary. To evaluate the effect of radiation streaming through the gaps between adjacent shielding modules on nuclear responses of the blanket, the vacuum vessel and the toroidal field coil (TFC), shielding analyses were conducted by 2-dimensional discrete SN method. In addition, to evaluate the uncertainty due to the ray-effect in the streaming analysis by discrete SN method. Monte-Carlo analyses were also conducted.

As wide gaps are desirable from remote maintenance point of view, shielding analyses for the 20 - 100 mm wide gaps were conducted. Then the gap width which could satisfy the shielding design targets was evaluated.

2. Nuclear Responses at the Blanket and the Vacuum Vessel

Radiation transport analyses were conducted for the inboard blanket using Monte Carlo code MCNP4.2[3]. The continuous energy cross section library FSXLIB-J3[4] based on JENDL-3.1[5] was used for the transport calculation, and the constant KERMA library[6], the DPA library[7] and the helium production cross section library[8] based on JENDL-3.1 were used as the nuclear response functions.

The analysis model is shown in Fig. 3. The shielding modules were divided into the 32 mm thick first wall region and the 301.5 mm thick homogenized shielding region composed of 60.4 % SS and 39.6 % H_2O. The first wall region was divided into 5 mm thick Be armor, 5 mm thick Cu heat sink and 22 mm thick homogenized coolant region composed of 25.7 % Cu, 53.8 % SS and 18.9 % H_2O. The coolant manifold region was also homogenized, and it was composed of 15 % SS, 61.4 % H_2O and 23.6 % void. The connection legs and the back plate were composed of 100 % SS. Gaps between shielding modules and between the connection legs are 20 mm and 115.2 mm, respectively. The SS regions were incorporated behind the plasma and also behind the back plate to take the effect of the back scattering of neutron and gamma-ray into account.

For neutron wall loading of 1 MW/m^2 and neutron fluence of 3 MWa/m^2, helium production rates in SS were evaluated at the locations D1 - D5 shown in Fig. 3 using the point detector. The locations D1, D2, D3, D4 and D5 mean the gap outlet, the leg root adjacent to the gap, the back of the shield module, i. e. the bulk region, which corresponds to the root of the branch pipe, the front surface of the back plate seeing the plasma through the gap, and the vacuum vessel surface behind the gap, respectively. The helium production rate at the location D1 was evaluated by multiplying the neutron flux at the gap outlet and the helium production cross section library of SS.

In case of the 20 mm wide gap, nuclear responses are summarized in Table. 1. The helium production rates at the front surface of the back plate, D4, and the vacuum vessel, D5, are 7.9 and 2.1 appm, respectively. They are 7.9 and 2.1 times higher than the shielding design target for rewelding, i.e. 1 appm, respectively.

The helium production rates at the leg, D2, the branch pipe, D3, and the gap outlet, D1, are 2.8, 2.3 and 12.3 appm, respectively. The helium production rate at the leg root is about 1.2 times higher than that at the branch pipe root. In other words, the gap streaming effect on the increase of the helium production rate at the leg root is 20 %.

To obtain the contour of the helium production rate, radiation transport analyses were also conducted with the inboard blanket, the vacuum vessel and the TFC using 2-dimensional discrete SN code DOT3.5[9]. The energy group cross section library FUSION-40[10] based on JENDL-3.1 was used for the transport calculation. From results obtained by DOT3.5, it was found that the thickness of the shielding module required to be increased by about 50 mm in order to satisfy the shielding design target at the branch pipe.

3. Nuclear Responses at the Toroidal Field Coil

The nuclear responses at the TFC were evaluated using both Monte-Carlo and 2-dimensional discrete SN analyses. The flow chart of the evaluation procedure is shown in Fig. 4.

Relationship between the gap width and the ratio of the nuclear responses at the TFC behind the gap to the shielding design targets is shown in Fig. 5. Safety factor of 3 for each responses is taken into account here. The TFC radiation limits of nuclear heating rate in winding pack, dose to electrical insulator, fast neutron fluence and displacement damage in copper stabilizer are 5 mW/cm^3, 5 x 10^9 rad, 1 x 10^{19} n/cm^2 and 6 x 10^{-3} dpa, respectively[11]. The nuclear responses at the TFC would satisfy the shielding design targets up to the gap width of 50 mm as shown in Fig. 5.

4. Conclusion

The nuclear responses of the shielding blanket, the vacuum vessel and the TFC in ITER were evaluated taking the radiation streaming through the gap between the adjacent blanket modules into account. Through this study, the following results were obtained.

(1) The peak helium production rates at the front surface of the back plate and the vacuum vessel behind the gap are 7.9 and 2.1 times higher than the shielding design target for neutron fluence of 3 MWa/m^2.

(2) The effect of radiation streaming through the gap is to increase the helium production rate at the leg by 20 %. However, the helium production rates at the leg and the branch pipe of the blanket module are 2 - 3 times higher than the shielding design target. To satisfy the shielding design target at the branch pipes, the thickness of the shielding module needs to be increased by about 50 mm.

(3) The nuclear responses at the TFC fully satisfy the shielding design targets for the gap width of 20 mm. The gap width could be increased by up to 50 mm from the view point of TFC protection.

Acknowledgment

The authors would like to express their sincere appreciation to Drs. S. Shimamoto, S. Matsuda, M. Ohta and M. Seki for their continuous guidance and encouragement. They also would like to acknowledge all the members who supported this work.

References

1) Sato, S. et al., : To appear in 12th Topical Meeting on the Technology of Fusion Energy., 1996, Reno, USA
2) Sato, S. et al., : JAERI-Tech 95-019, (1995).
3) Briesmeister J. F., Ed., : LA-12625-M, (1993).
4) Kosako, K., Oyama, Y., Maekawa H. : JAERI-M 91-187, (1991) [in Japanese].
5) Shibata, K. et al., : JAERI-1319, (1990).
6) Maki, K. et al., : JAERI-M 91-073, (1991) [in Japanese].
7) Maki, K., Sato, S. et al., : to be published as JAERI-Data, (1996).
8) Mori, S. et al., : JAERI-M 93-175, (1993).
9) Rhoades, W. A., Mynett, F. R., : ORNL-TM-4280, (1973).
10) Maki, K. et al., : JAERI-M 91-072, (1991) [in Japanese].
11) Smith, D. et al., : "ITER BLANKET, SHIELD AND MATERIAL DATA BASE", IAEA, Vienna, 1991

Table. 1 Nuclear responces at the inboard shielding blanket and the vacuum vessel in case of the 20 mm wide gap (Neutron wall loading : 1 MW/m^2, Neutron fluence : 3 MWa/m^2)

	D1	D2	D3	D4	D5
14MeV neutron flux (/cm^2/sec.)	1.9 x 10^{12}	2.7 x 10^{11}	2.1 x 10^{11}	1.2 x 10^{12}	2.5 x 10^{11}
Total neutron flux (/cm^2/sec.)	1.8 x 10^{13}	1.1 x 10^{13}	1.9 x 10^{12}	1.5 x 10^{13}	6.9 x 10^{12}
Gamma-ray flux (/cm^2/sec.)	2.1 x 10^{13}	1.5 x 10^{13}	1.2 x 10^{13}	1.5 x 10^{13}	
Neutron heating rate (mW/cm^3)	0.080			0.054	0.015
Gamma-ray heating rate (mW/cm^3)	1.18			1.2	
Helium Production Rate (appm)	12.3	2.8	2.3	7.9	2.1

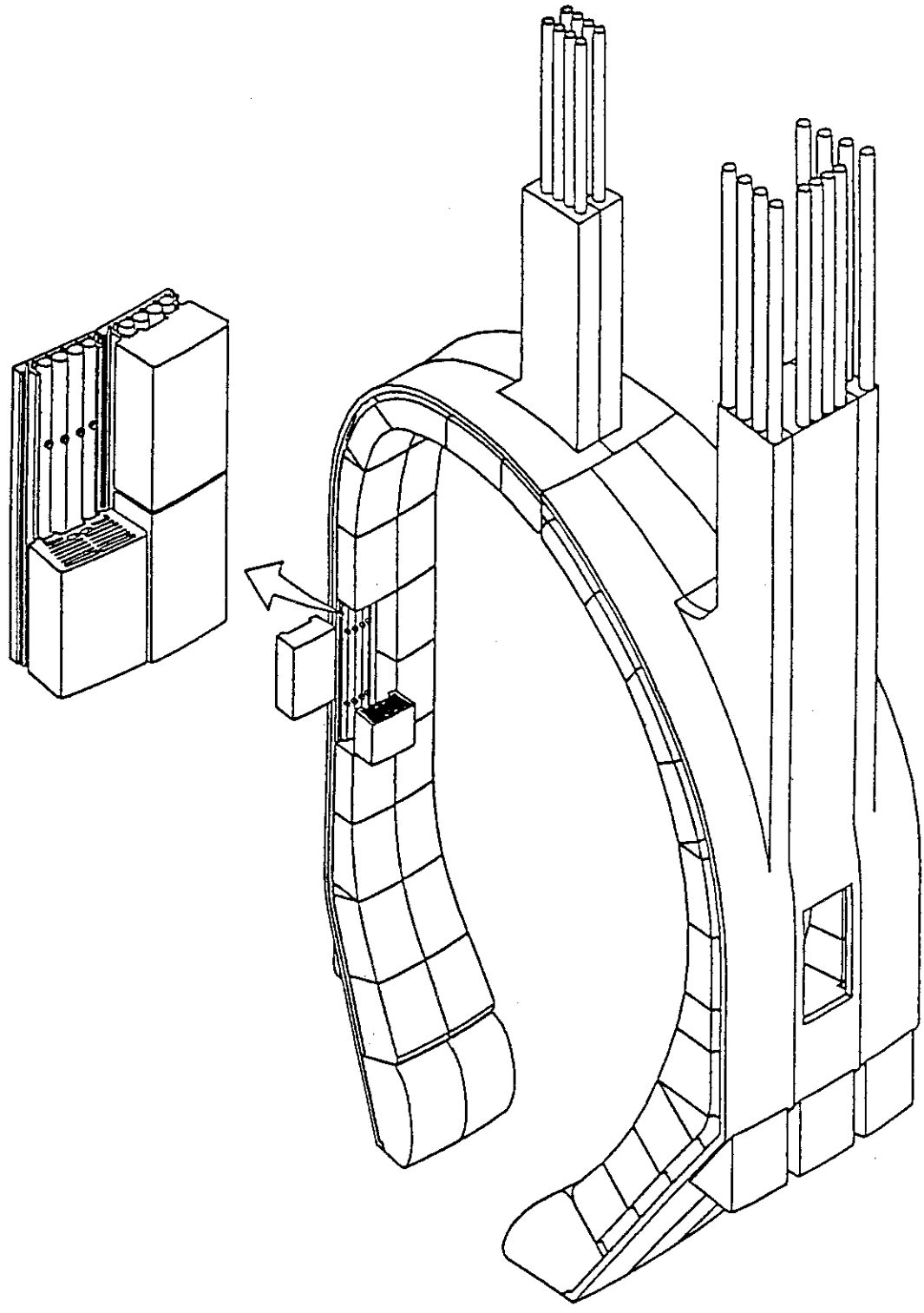

Fig. 1 A bird's - eye view of the blanket configuration

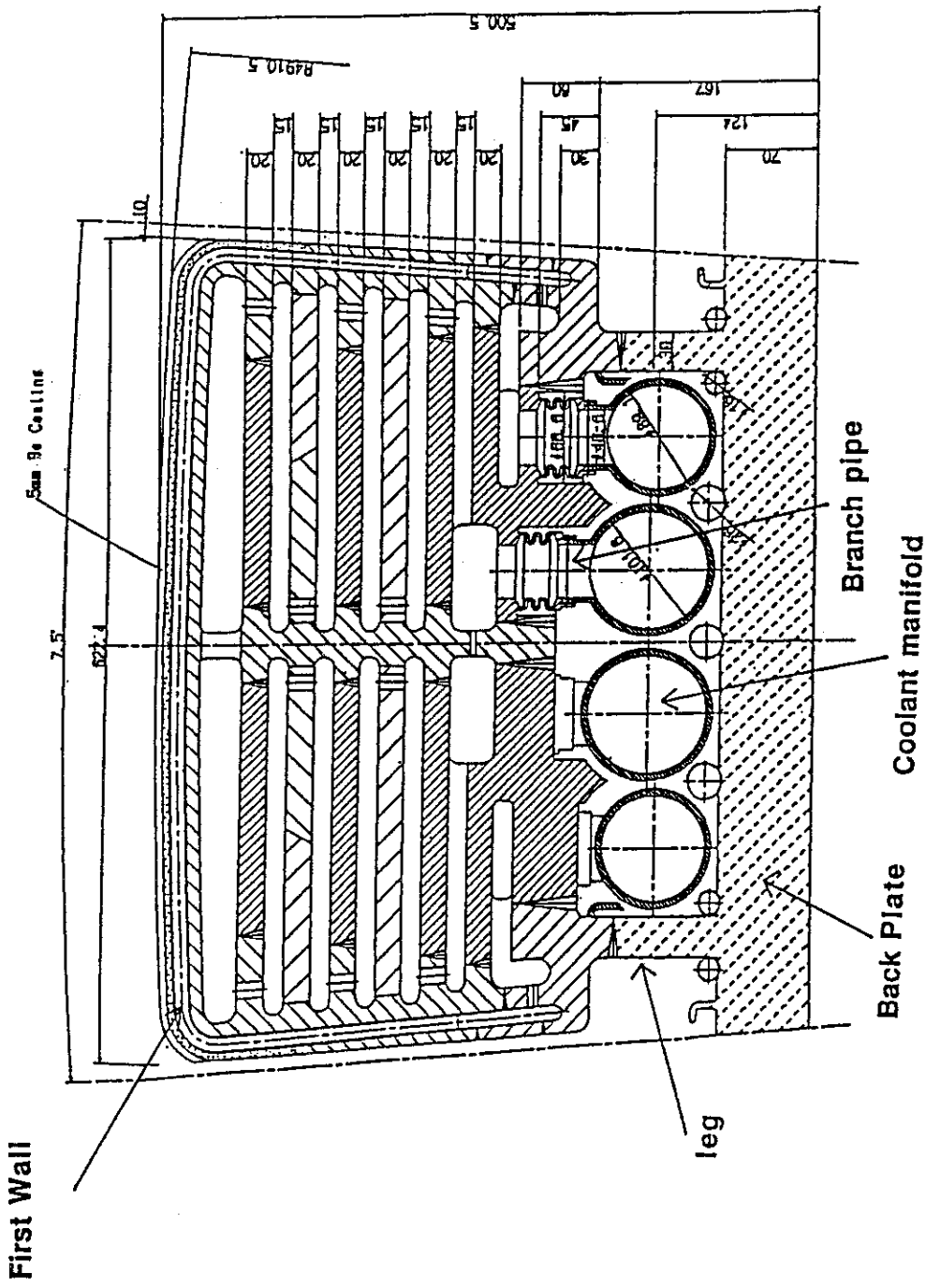

Fig. 2 A cross-sectional view of the blanket module

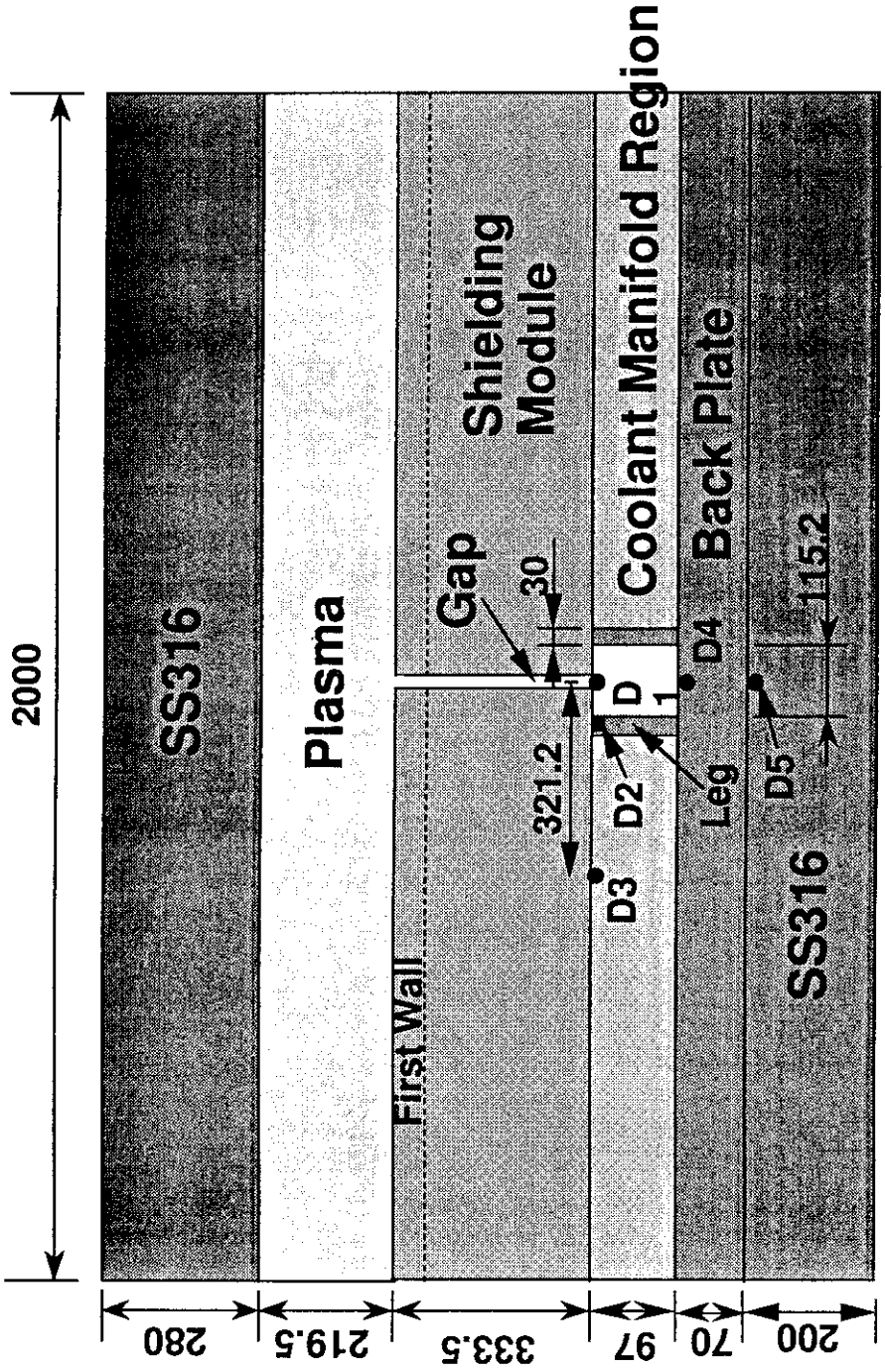

Fig. 3 Analysis model for MCNP (unit : mm)

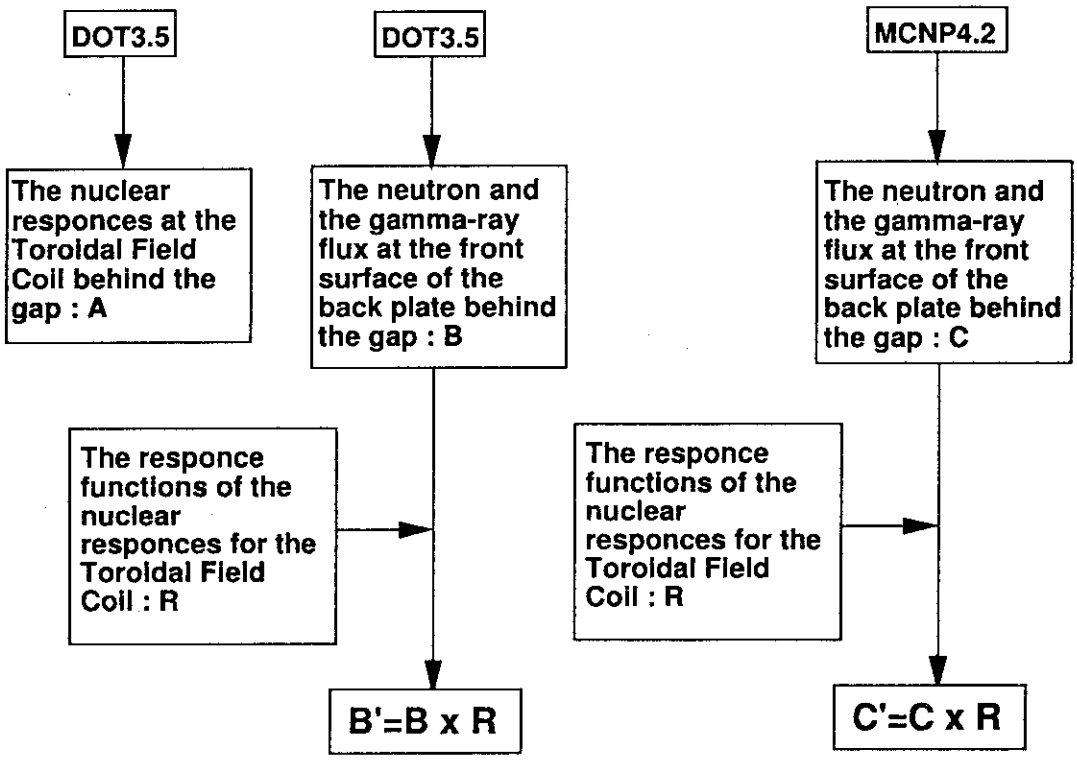

Fig. 4 The flow chart of the evaluation procedure of nuclear responces at the Toroidal Field Coil behind the gap

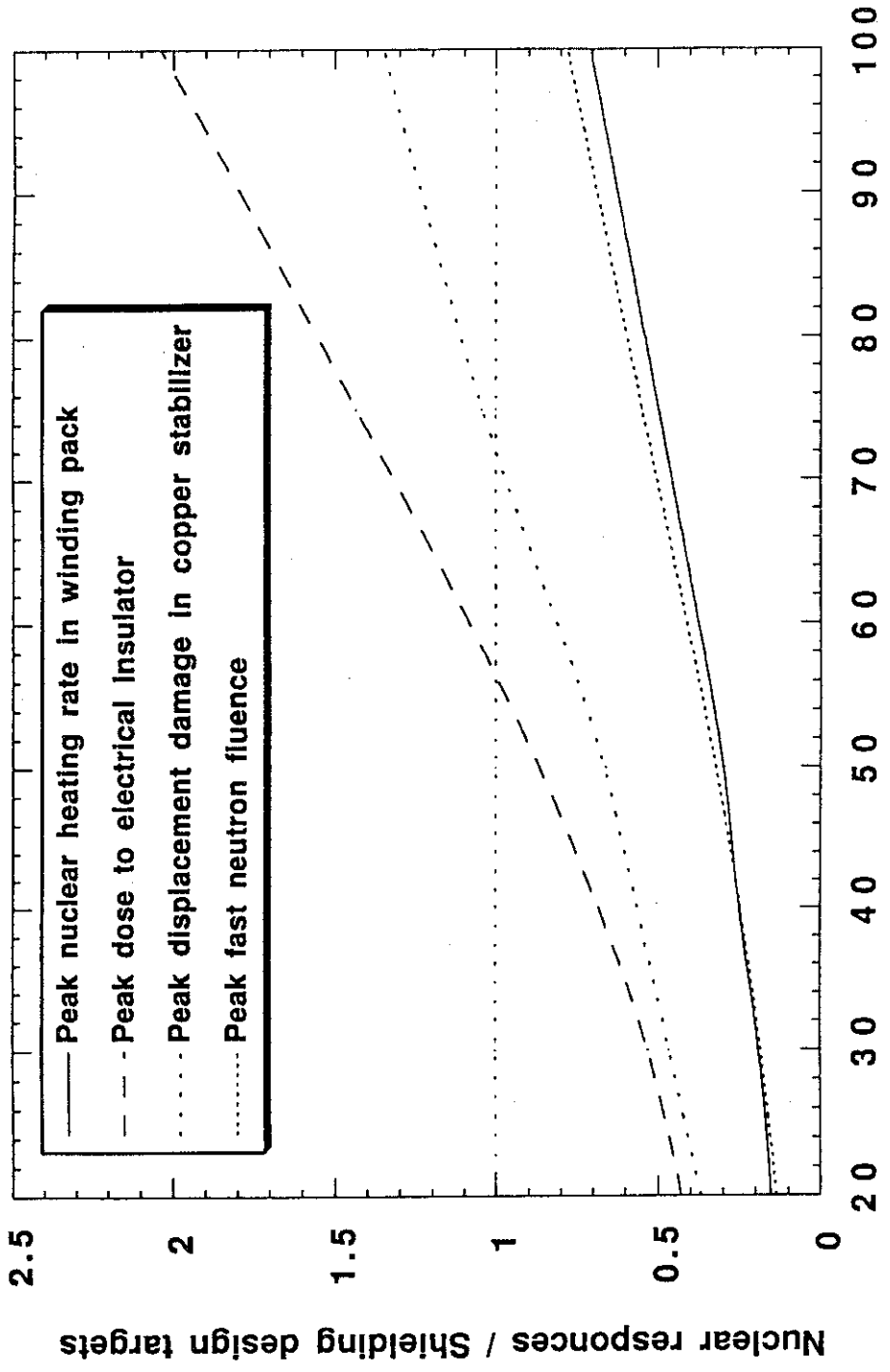

Fig. 5 Relationship between the gap width and the ratio of the nuclear responces at the Toroidal Field Coil to the shielding design targets

1.3 Status of ITER/EDA R&D Neutronics Task

Yujiro Ikeda

Department of Reactor Engineering,
Japan Atomic Energy Research Institute
Tokai-mura, Ibaraki-ken 319-11 Japan

Various R&D efforts are under way aiming at a development of the International Thermonuclear Experimental Reactor (ITER). As the D-T neutron relevant issue was recognized to be one of critical and urgent item for ITER design, four international parties have been devoted to carrying out related experiments. The status of R&D tasks for the neutronics relevant issues under the ITER/EDA framework is given in this report with emphasis of the Japanese contribution.

1. Introduction

The International Thermonuclear Experimental Reactor (ITER) development has been in the engineering design activity (EDA) phase since 1993 after the termination of the Conceptual Design Activity (CDA) Phase.The purpose of EDA is to establish and provide the reactor engineering design base of ITER which demonstrates D-T plasma burning operations with the ignition condition for 1,000 sec, providing all technical information needed for Demonstration Reactor and further. In order to support the ITER design, various critical technological R&Ds are needed to develop an adequate data base. As the ITER is the based on the D-T burning operation, we have to encounter serious problems created by D-T neutron interactions with the materials and structural elements of reactor. To assure the credible soundness of reactor itself, the neutronics are one of most crucial issues for the design, in terms of shielding for the superconducting magnet, nuclear heat deposition in the plasma facing components, induced radioactivity and dose rate after shutdown, decay heat generation and so on. In the breeding blanket design, tritium production rate should be well predicted. All issues are so critical for demonstrating the fusion reactor attractiveness. Even for ITER as the experimental reactor, the neutronics should be the mainline for establishing the safety operation scenario.

In viewing the importance of neutronics, we have proposed the R&D tasks to be undertaken in ITER/EDA. This report gives the present status and the future plan of the neutronics R&D Tasks which we have committed and to be committed, respectively.

2. Status of R&D Tasks and credits

The most critical neutronic problem for the ITER design is the radiation shielding against the nuclear heating in the superconducting magnet (SCM). First of all, a study for adequate design of experimental configuration was needed before starting the shielding experiments. In the urgent Task assignment procedure in 1993, we proposed to execute a survey calculation for optimize the experimental assembly for shield blanket test. In the mean time, a task for development and demonstration of a technique fir nuclear heating measurement with a microcalorimeter was also proposed and assigned with ITER credit in the ITER/EDA R&D urgent Task of 1993. The preparation of the experimental assembly was in parallel carried out considering its long leading time required. Assuming the Task agreements, a series of experiments was initiated for validation of shield blanket nuclear calculation.

In 1994, still the ITER/EDA was at the start of all design and R&D Tasks. In that time, four potential participants from four parties proposed a joint neutronics task and it was approved as T-16 with credit of 400 IUA (1 IUA/1k US$ in 1989) for each party. The committing organizations were Japan (JAERI/FNS), EU (ENEA-Frascati, FZK and TUD), US (UCLA) and RF (Kurchatov Institute of Atomic Energy). In 1995 and 1996, a task of T-218 was also jointly proposed by the four parties and agreed to be undertaken. The task sharing and assigned credit is shown in **Table 1.3.1**. As the recognition of the largest contribution among the parties, JAERI/FNS was assigned as the this particular Task coordinator. In this particular Task, three research items were identified to be covered; (1) inboard bulk shield by EU and RF, (2) outboard shield with penetrations by JA an US and (3) induced radioactivity/nuclear heating measurements by JA and US.

3. Previous Task Coordination and Products

In this section, the Japanese contributions under the EDA R&D Task are outlined.

3.1 Bulk Shielding Experiment and Analysis

Before starting the experiment, pre-analysis of the experimental assembly for the shield blanket was conducted in order to optimize the size taking account of the primary condition for ITER shield designs) As a result, a baseline assembly configuration was determined to be a cylindrical shape of SS-316 with and without water, dimensions of which were 1.2 m in diam. and 1 m thickness. It was also found that the a SS-316 coverage for the D-T neutron source was effective to simulate the D-T neutron environment with slow neutron components along with 14 MeV primary neutrons.

After construction the experimental assembly, extensive integral experiments were carried out with emphasis of the data acquisition in the deep location of the shield. The measurements dealt with neutron and gamma-ray spectrum fluxes, gamma-ray heating rates, spectral indices with foil activation and fission reaction rates.[2,3] Experimental analyses were performed with comprehensive nuclear data libraries, e.g., JENDL-3.2, FENDL-1.[4,5] The results of the analyses were effectively incorporated in the validation the data base, which provide substantial feedback to the shield blanket design in terms of the uncertainty range, design margin and safety factors to be considered.

3.2 Nuclear Heating Experiment

A technical development of the direct nuclear heating measurement was approved to be done under the urgent R&D Task in '93. However, due to the machine time difficulty, the Task was combined into the Task T-16 in '94. Since the fundamental technological development of heat deposition with a microcalorimeter was already completed in the last JAERI-USDOE collaboration on fusion neutronics,[6,7] the major effort was placed on the increase the detection sensitivity and extension of neutron field in a SS-316 assembly driven by 14 MeV neutrons. The tested materials were SS-316 as the reference, Be, Cu, W, Zr and Graphite (C).

The data of temperature rise measured with a calorimetric method were interpreted to the heating rate in the materials, and compared with the calculations using JENDL-3.2 base KERMA factor and FENDL-1 KERMA. As a results of this particular Task, it was demonstrated that the calorimetric technique was unique and essential for the experimental validation of the nuclear hearing relevant data base. The Task report was accepted by ITER/JCT and detailed description is to be given in the separate paper of this meeting.

3.3 Induced Radioactivity Experiment

As the extended series of the induced radioactivity experiments underway in the FNS, a

radioactivity production characteristics under pulsed mode operations was also investigated under T-16 in '94. The objective of this Task was to characterize the radioactivity production under a pulsed irradiation condition comparing to a continuous mode as a function of the pulse duty factor, pulse length and decay half-life of the radionuclides. Setting the generalized pulse length of 3 min. and changing duty factors, several radioactivity production rates were measured in both pulsed and continuous mode. The ratio of each measured production with different half-lives was agreed with calculations based on the general algorithm. The results demonstrated the validity of the algorithm and suggested a possibility for significant reduction of radioactivity under some pulsed mode operation in comparison with those after continuous operation.

4. Current and Future R&D Tasks

The Task T-218 was assigned to be done jointly by four parties, the sharing of which is shown in Table 1. The first item to commit is the outboard with penetration (streaming experiments). We are expected to provide experimental data for the effects of gap neutron streaming corresponding to a concern from the shield blanket design, i.e., a 20 mm gap between two blanket module possibly increases neutron flux at the location of back plate. It is assumed the He production rate is critical for the re-welding process from the material damage consideration. Thus, it is highly requested to validate the design calculation adequacy by experiments. In correspondence with this requirement, we have designed an experimental assembly for the streaming. In **Fig. 1.3.1**, the drawing of the assembly is shown. The assembly has been recently constructed and fixed in the wall structure between the first and the second target room at FNS. The first experiment is scheduled in December 1995. A bulk shielding experiment with simulation of superconducting magnet was also assigned to be done in T-218 by JAERI. The experiments has been completed in 1995 and the experimental analysis is in progress.

Induced radioactivity and nuclear heating experiments are also included in T-218 Task as the item 3 to be conducted jointly with US. The nuclear heating measurements for materials of Cu, Be, W, C, Cr and SS-316 in a Cu assembly was carried out in November 1995. Unfortunately, US could not contribute to the experiment due to sudden and sever budget cut of fusion program of U.S. The data are in process and the experimental analysis will be completed by the end of March 1996. The next experiments with a graphite assembly is schedule to be conducted with US participants in 1996.

Induced radioactivity experiments were simultaneously conducted with use of the neutron fields in the Cu assembly used for the nuclear heating experiment. A number of materials were irradiated in two position with different neutron spectra. The measurements of radioactivity production are in progress to cover characteristics at longer cooling times.

As the new R&D Task in '96 and '97, we proposed to a Task on Decay heat experiments. The proposed Task was in process for the Task Agreements with strong support of ITER-JCT. The Task area is the safety and environment because the data validation is directly related to the issue of cooling scenario for decay heat after reactor shutdown. Some part of experimental preparation has been in progress assuming the Task Agreement to be completed soon.

5. Summary

The ITER/EDA has in progress and the intermediate design report was accepted by ITER

council. From now on, all efforts are to be placed on the final detailed design of ITER. There are, however, a lot of R&D work needed to arrive at the credible design. In particular, neutronics related issues are of critical for the data quality assurance which is the fundamental data base for the safety and environment assessment. Unfortunately, the funding to maintain all R&D issue is limited in the ITER/EDA framework. Also, it appeared that US commitment becomes weak due to the budget cut of US DOE. Russian contribution is still uncertain as a concern. All endeavors, however, should be forced on the development of Fusion Energy . ITER program will have a turning point at the site determination in two years. After ITER site is determined, hopefully to Japan, we will have a new phase of our research activity. As mentioned, more serious commitment should be requested to neutronics society.

Assuming the D-T burning plasma machine is the nuclear machine, neutronics relevant issues are of the first priority. In order to complement the ITER/EDA, more basic approach should be continued. An international collaboration program under IEA framework has been conducted with emphasis of long term researches. The IEA deals with neutronics integral experiments on advance breeder materials, general code and data base validation, radioactivity characterization for low activation materials, and a technical development of experimental measurements required in the test program of ITER and demo reactor.

References

1) C. Konno, et al., "Pre-Analyses of SS316 and SS316/Water Bulk Shielding Experiments", JAERI-Tech 94-019 , Oct. 1994.
2) C. Konno, et al., "Bulk Shielding Experiment on Large SS-316 Assemblies Bombarded by D-T Neutrons: Vol. 1 : Experiment", JAERI-Research 94-043 Dec. 1994.
3) C. Konno, et al,. "Bulk Shielding Experiment on A Large SS316/Water Assembly Bombarded by D-T Neutrons: Volume I: Experiment" JAERI-Research 95-017 Mar. 1995.
4) F. Maekawa, et al.,"Bulk Shielding Experiment on Large SS-316 Assemblies Bombarded by D-T Neutrons: Volume II: Analysis", JAERI-Research 94-044 Dec. 1994.
5) F. Maekawa, et al.,"Bulk Shielding Experiment on A Large SS316/Water Assembly Bombarded by D-T Neutrons:Volume II: Analysis", JAERI-Research 94-018 Mar. 1995.
6) Y. Ikeda, et al., "Direct Nuclear Heating Measurements and Analyses for Structural Materials Induced by Deuterium-Tritium Neutrons," Fusion Technol. Vol. 28, [1] (1995) 156.
7) A. Kumar, et al., "Direct Nuclear Heating Measurements and Analyses for Plasma-Facing Materials," ibid., (1995) 173.
8) Y. Ikeda, et al., "Measurements and Analyses of Decay Radioactivity Induced in Simulated Deuterium-Tritium Neutron Environments for Fusion Reactor Structural Materials," ibid., (1995) 74.
9) A. Kumar, et al., "Decay Radioactivity Induced Plasma-Facing Materials by Deuterium-Tritium Neutrons," ibid., (1995) 99.

Table 1.3.1 T-218 Task Sharing and Assigned Credits

Task	Sub-Task A Inboard Blanket-Shield No Penetrations		Sub-Task B Outboard Blanket-Shield With Penetrations		Sub-Task C Measurement Technique Development[a]	
Facility	FNG		FNS		FNS	
Task Sharing	EU/RF		JA/US		US/JA	
Resources (IUA)	EU	RF	JA	US	JA	US
1994	600	400	400[b]	400[c]	200	----
1995	400	200	400	200	100	25
1996	400	200	400	200	100	25

a. For nuclear heating and radioactivity measurements.
b. Part of the credits for 1994 covered Sub-Tasks B and C.
c. Credits for 1994 covered Sub-Tasks B and C.

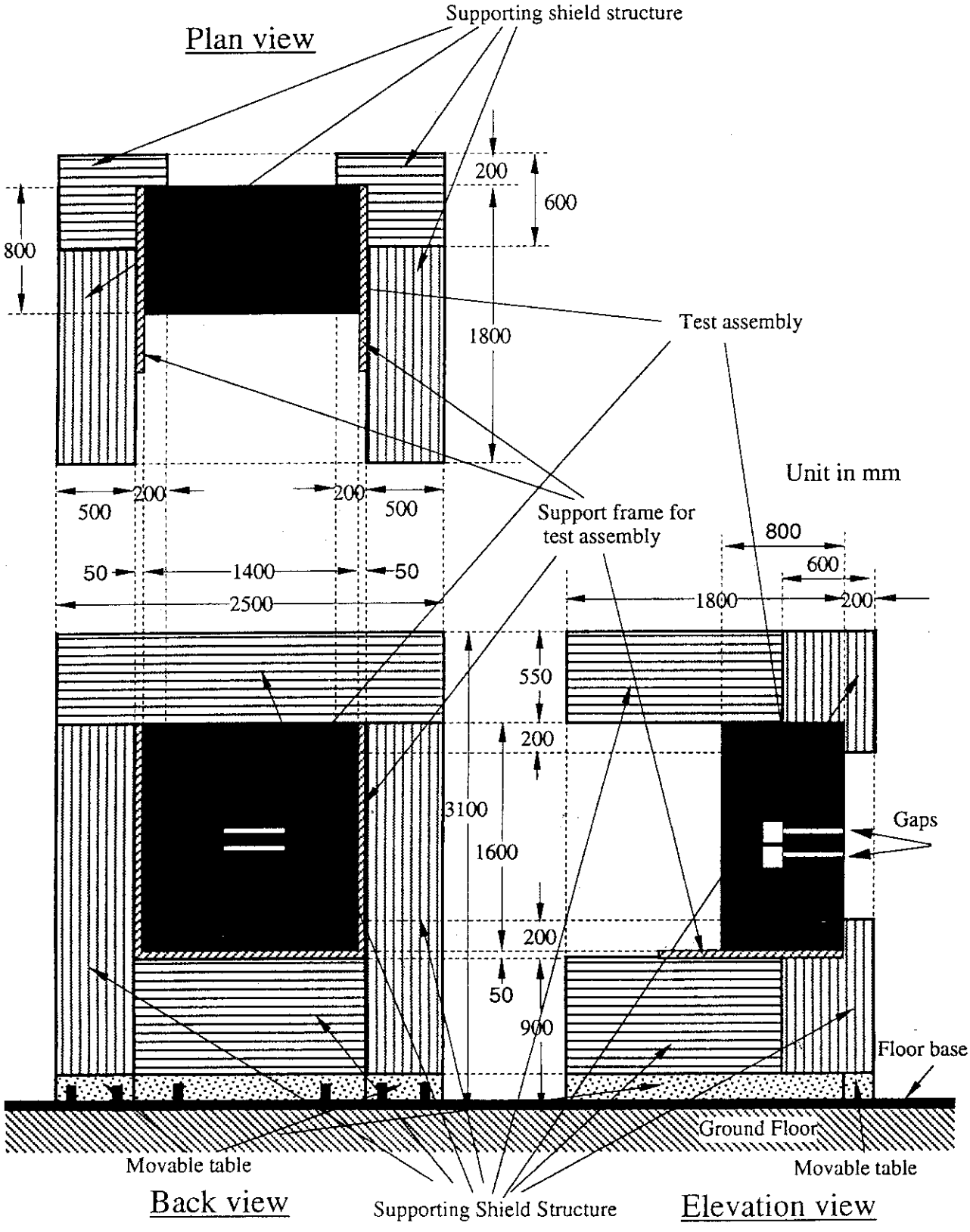

Fig. 1.3.1 Drawing of the streaming experimetal Assembly

1.4 Review of Fusion DEMO Reactor Study

Yasushi Seki
Fusion Reactor System Laboratory
Japan Atomic Energy Research Institute
Naka-machi, Naka-gun, Ibaraki-ken, Japan 311-01

Fusion DEMO Reactor is defined and the Steady State Tokamak Reactor (SSTR) concept is introduced as a typical example of a DEMO reactor. Recent DEMO reactor studies in Japan and abroad are introduced. The DREAM Reactor concept is introduced as an ultimate target of fusion research.

1. Introduction

In this paper a fusion DEMO reactor is defined as the fusion power reactor to be built after a fusion experimental reactor such the ITER (International Thermonuclear Fusion Experimental Reactor) which is jointly designed by European Union, Japan, Russian Federation and the United States. An experimental reactor is to demonstrate sustained fusion burning and to demonstrate fusion nuclear technology. DEMO means demonstration of electric power generation by thermonuclear fusion reaction. The expected time schedule for the construction of DEMO fusion reactors in the four parties fall between 2020 and 2040. The assumed plasma physics and technology should therefore be consistent with the expected time frame.

2. The Steady State Tokamak Reactor (SSTR)

The Steady State Tokamak Reactor (SSTR) concept[1] shown in Fig. 1, was proposed in 1990 as a realistic fusion power reactor to be built in the near future. The concept of SSTR was based on a small extension of the present day physics and technologies. The major feature of SSTR was the maximum utilization of a bootstrap current (which was discovered in large tokamak devices such as JET and JT-60) in order to reduce the power required for the steady state operation. The bootstrap current was assumed to contribute 75% of the required tokamak plasma current. This requirement lead to the choice of a moderate plasma current (12 MA), and high βp (2.0) for the device, which were achieved by selecting high aspect ratio (A=4) and high toroidal magnetic field (16.5 T). A negative-ion-based neutral beam injection system was used both for heating and central plasma current drive. Notable engineering features of SSTR were: the use of a uniform double walled vacuum vessel which also serves as radiation shield and significant reduction of the electromagnetic force with the use of functionally gradient material. It should be noted that reduced activation ferritic steel was selected as

the structural material available about 30 years later. The primary coolant was assumed to be pressurized water used in similar condition as the pressurized light water reactor (PWR). It was shown that a tokamak machine comparable to ITER in size can become a power reactor capable of generating about 1 GW of electricity with a plant efficiency of ~30%. Main parameters of SSTR are shown in Table 1.

Table 1 Main parameters of SSTR

Plasma major radius	Rp	7.0	m	Average temperature	<T>	17	keV
Plasma minor radius	ap	1.75	m	Average density	<n>	1.4×10^{20}	m^{-3}
Aspect ratio	A	4		Energy confinement time	τ_E	1.4	sec
Plasma current	Ip	12	MA	H-factor for Goldston scaling	H_G	1.8	
Bootstrap current	I_{BT}	9	MA	H-factor for S-O scaling	H_{S-O}	1.6	
Beam driven current	I_{BD}	3	MA	Deuterium beam energy	Eb	2	MeV
Plasma elongation	κ	1.8		NBI current drive power	P_{CD}	60	MW
Magnetic field on axis	Bt	9	T	Fusion power	Pf	3000	MW
Maximum field on coil	Bmax	16.5	T	Net electric power	Pnet	1080	MW
Plasma volume	Vp	760	m^3	Q-value	Q	50	
Beta poloidal	βp	2.0		Max. neutron wall load	Pnmax	5	MW/m^2
Beta toroidal	βt	2.5	%	Tritium breeding ratio	TBR	1.2	
Troyon coefficient	g	3.3		Divertor	Single null		

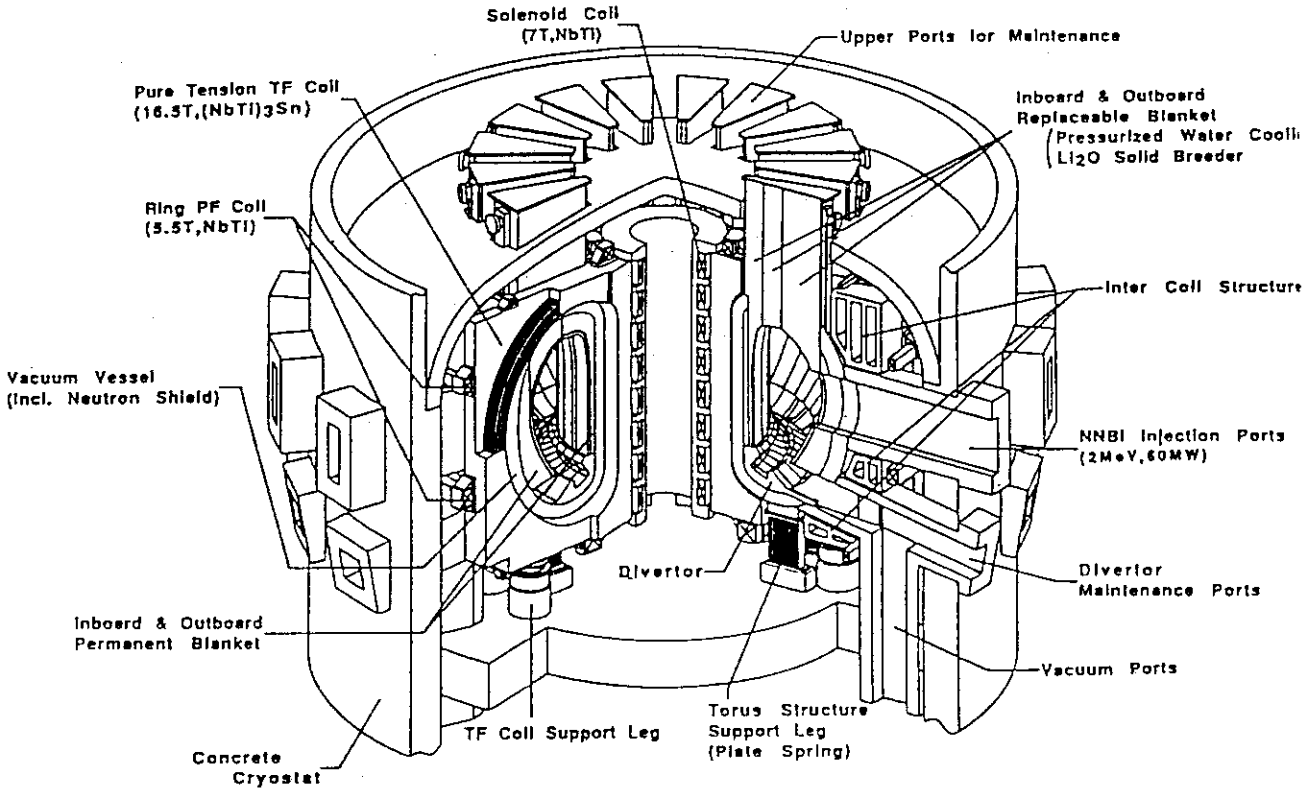

Fig.1 Overview of the Steady State Tokamak Reactor (SSTR)

3. Recent DEMO Reactor Studies

Recently, the FFHR (Force-Free Helical Reactor)[2] concept and IDLT (Inductively-operated Day Long Tokamak)[3] concept has been proposed in Japan. Both of the studies aim at realistic concepts assuming construction in the DEMO time frame.

The FFHR has a set of three helical coils arranged in force free configuration to reduce the magnetic force on helical coils. This allows to simplify the coil supporting structure and to use high magnetic field instead of relying on high plasma beta to achieve high fusion power. For the blanket, reduced activation ferritic steel is used as the structural material and molten salt FLIBE is used as the coolant.

In the IDLT studies, it is stated that tokamak DEMO reactors can be realized even with pulsed operation mode if the pulse length can be made sufficiently long to several hours. It is also stated that austenitic stainless steel could be used in low power density DEMO.

In abroad, STARLITE program[4] is on going in the US to define a DEMO reactor based on the idealistic fusion power reactor concepts such as ARIES[5]. In STARLITE program, the coolant/structural material combination selected is helium gas/reduced activation ferritic steel and liquid lithium/vanadium alloy. Recently, the Safety and Environmental Assessment of Fusion Power (SEAFP)[6] program has been completed in EU which showed the environmental and safety attractiveness of fusion reactor. The coolant/structural material combinations chosen in this study are water/reduced activation ferritic steel and helium gas/vanadium alloy.

The materials used in the DEMO reactor studies home and abroad are summarized in Table 2.

Table 2 Materials used in DEMO fusion reactor studies

Function	Material
Plasma facing surface	Beryllium, Copper, Molybdenum, Tungsten, TiC
Structural materials	Austenitic steel, Ferritic steel, Martensitic steel, Vanadium alloy
Coolant	Water, Liquid lithium, Molten salt (FLIBE), Helium gas
Tritium Breeder	Lithium oxide, Liquid lithium, Molten salt (FLIBE), Lithium Lead
Neutron Multiplier	Beryllium

4. Idealistic fusion reactor, DREAM

As seen in the previous section, the structural material for DEMO reactors are restricted to metallic alloy. Very low activation materials such as ceramic composite materials are thought not to be available in the 50 years from now time frame for DEMO. From reactor system design point of view, I believe the ideal coolant/material combination in terms of environmental safety is helium gas/SiC/SiC composite material. An idealistic reactor concept called DREAM[7] (DRasticlly EAasy Maintenance Reactor) which is shown in Fig. 2, using this material combination is being studied in JAERI. With the use of high temperature helium gas, high thermal efficiency is possible. DREAM reactor also realizes high plant availability by simplified blanket replacement scheme. Major development needs for SiC/SiC composite material such as high thermal conductivity, good irradiation resistance, non-permeability of hydrogen, have been identified and the R&D program[8] to overcome the deficiencies of the material is being coordinated.

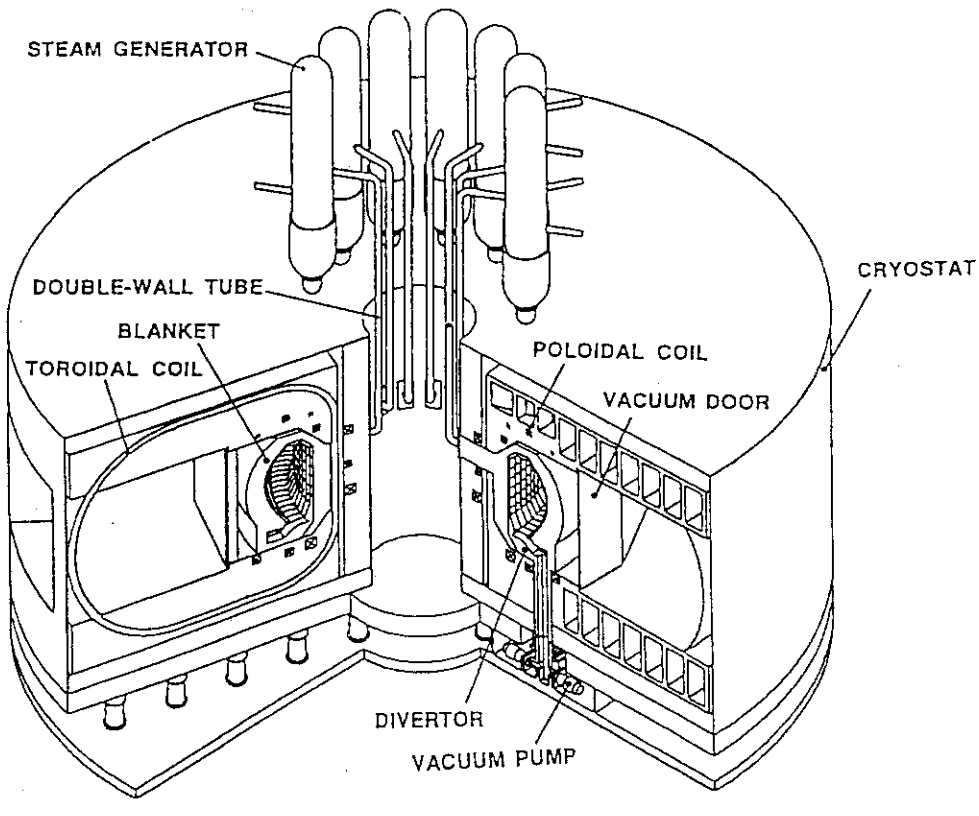

Fig.2 The DREAM (DRastically EAsy Maintenance) Reactor Concept

References

(1)Fusion Reactor System Laboratory: Concept Study of the Steady State Tokamak Reactor (SSTR), JAERI-M 91-081 (1991)

(2)SAGARA, A., MOTOJIMA, K., WATANABE, K. et al.: Fusion Engineering and Design 29 (1995) 51-56

(3)INOUE, N., OGAWA, Y., YAMAMOTO, T. et al.:14th IAEA Conf. on Plasma Physics and Controlled Nuclear Fusion, Wurzburg, IAEA-CN-56/G-1-4(1992)

(4)The ARIES Team: Starlite and ARIES Papers Presented at the 16th Symposium on Fusion Engineering (SOFE-16) UCSD-ENG-006 (1995)

(5)CONN, R. W., NAJMABADI, F. and the ARIES Team.:ARIES-I, A Steady-State, First-Stability Tokamak Reactor with Enhanced Safety and Environmental Features:Proc. 13th IAEA Conf. on Plasma Physics and Controlled Nuclear Fusion, Wurzburg, IAEA-CN-53/H-1-4 (1990) 659

(6)RAEDER, J., COOK, I., MORGENSTERN, F.H. et al.:Safety and Environmental Assessment of Fusion Power (SEAFP), EURFUBRU XII-217/95 (1995)

(7)NISHIO, S., MURAKAMI, Y., ADACHI, J. et al.: A Concept of Drastically Easy Maintenance (DREAM) Tokamak Reactor", Proc. IAEA-TCM WS on Fusion Reactor Design and Technology, Fusion Eng. Design 25 (1994) 289-298

(8)KOHYAMA, A. Edited: Proceedings of the Twelfth Fusion Reactor Materials Forum held at The Univ. of Tokyo, April 21, 1995

2. Nuclear Data Evaluation and Library

2.1 Evaluation of Light-Nuclei and Gamma-Ray Production Data

Keiichi SHIBATA
Nuclear Data Center
Japan Atomic Energy Research Institute
Tokai-mura, Naka-gun, Ibaraki-ken 319-11

Light-nuclei data contained in JENDL-3.2 and JENDL Fusion File are reviewed with emphasis on fusion applications. Comparisons are made between evaluated and measured double differential cross sections. Also presented are gamma-ray production cross sections and spectra for light and medium-heavy nuclei. The evaluation method of gamma-ray production data is described.

1. Introduction

The second revision of JENDL-3 (referred to as JENDL-3.2)[1] was made available in June 1994. In the light mass region up to A=20, the library contained 14 nuclei, i.e., ^{1,2}H, ^{3,4}He, ^{6,7}Li, ^{9}Be, ^{10,11}B, ^{12}C, ^{14,15}N, ^{16}O and ^{19}F. JENDL-3.2 adopted the conventional MF4-5 representation for double differential cross sections (DDXs) which are important in fusion neutronics calculations. On the other hand, a preliminary version of JENDL Fusion File[2] (abbreviated as JENDL-FF, hereafter) was created in order to improve the quality of DDX data by using the MF6 representation, although it contained only 7 nuclei (^{6,7}Li, ^{9}Be, ^{12}C, ^{14}N, ^{16}O, ^{19}F) in the light mass region, as of December 1995. Among the nuclei, the data of ^{6,7}Li, ^{14}N and ^{16}O were taken from JENDL-3.2 without any changes.

Concerning gamma-ray production, JENDL-3.2 contained evaluated gamma-ray production cross sections and spectra for 66 nuclei, while the gamma-ray data in JENDL-FF were taken from JENDL-3.2 except for elemental iron and nickel.

This paper reviews the evaluation method of light-nuclei and gamma-ray production data together with evaluated results.

2. Light-Nuclei Data

2.1 Cross Sections

In the light mass region, data evaluation is mainly based on available experimental data, since the applicability of nuclear models to light nuclei is uncertain. Thus, selection of experimental data is important in the course of evaluation. Figure 1 shows the ^{7}Li(n,n't)^{4}He reaction cross section[3], which is important in tritium breeding in fusion blankets. The latest evaluations JENDL-3.2 and ENDF/B-VI are based on the measurements published in 1980's, and are lower than the old ENDF/B-IV data, i.e., 20% at 10 MeV and 10% at 14 MeV. Decrease in the cross section gave an impact to the

design of fusion blankets.

R-matrix analyses are powerful in the evaluation of the following quantities: total cross sections of ^{3,4}H, ^{6}Li, ^{9}Be, ^{10,11}B, ^{12}C and ^{16}O, (n,p) cross section of ^{3}He, (n,t) cross section of ^{6}Li and (n,α) cross section of ^{10}B. The (n,t) reaction cross section[4] of ^{6}Li is shown in Fig. 2. In this case, the evaluated curve below 2 MeV was obtained from R-matrix calculations, which reproduced a resonance peak around 250 keV. Above 2 MeV, the evaluation is based on available experimental data.

Inelastic scattering and charged-particle emission cross sections of ^{9}Be, ^{10,11}B, ^{12}C, ^{14,15}N, ^{16}O and ^{19}F were calculated with nuclear models. It is difficult to predict absolute cross sections with model calculations in this mass region, but the shape of calculated excitation functions is generally reasonable. Absolute values were obtained by normalizing a calculated cross section to a measured one at a certain energy point.

2.2 Particle Emission Spectra

In the ENDF-6 format, the MF6 representation is available to describe DDX directly. So far, as for light nuclei, we have used the pseudo level representation using MF4-5. In this representation, pseudo levels were generated so as to reproduce measured DDX data. In JENDL-3.2, the DDX data of ^{6,7}Li, ^{12}C, ^{10}B and ^{14}N were evaluated with this method. In general, particle spectra from three-body reaction such as ^{6}Li(n,nd)^{4}He and ^{7}Li(n,nt)^{4}He are assumed[3] to have a shape of the three-body phase-space distribution. Figures 3 and 4 show neutron DDXs from ^{6}Li and ^{12}C, respectively.

As for ^{9}Be, the use of pseudo levels were not allowed within the framework of the ENDF format since a large part of neutron spectra comes from the (n,2n) reaction but levels with a neutron multiplicity of two do not conform to the format. Therefore, this case has been dealt with in JENDL-FF using MF6. Neutron and charged-particle spectra emitted from the n-^{9}Be reaction were calculated with a Monte Carlo code SCINFUL/DDX[5] incorporating two- and three-body reaction kinematics. In the (n,2n) reaction, the following 4 processes were considered in the calculation:

$$
\begin{aligned}
n + {}^{9}Be \rightarrow\ & ①\quad n + {}^{9}Be^{*} \\
& \qquad {}^{9}Be^{*} \rightarrow\ n + {}^{8}Be \\
& \qquad\quad {}^{8}Be \rightarrow\ 2\alpha \\
& \qquad {}^{9}Be^{*} \rightarrow\ \alpha + {}^{5}He \\
& \qquad\quad {}^{5}He \rightarrow\ n + \alpha \\
& ②\quad \alpha + {}^{6}He^{*} \\
& \qquad {}^{6}He^{*} \rightarrow\ 2n + \alpha \\
& ③\quad {}^{5}He + {}^{5}He \\
& \qquad {}^{5}He \rightarrow\ n + \alpha \\
& ④\quad 2n + {}^{8}Be \\
& \qquad {}^{8}Be \rightarrow\ 2\alpha.
\end{aligned}
$$

The calculated neutron DDXs reproduced measured spectra at 14 MeV, as seen in Fig. 5. Similar calculations of ^{6,7}Li are in progress for JENDL PKA/KERMA File.

3. Gamma-ray Production Data

3.1 Light Nuclei

For very light nuclei up to carbon, neutron capture reactions play a significant role in gamma-ray production, together with inelastic scattering to several discrete levels. In the low energy region, the capture cross section is assumed to have a dependence of $(E_n)^{-1/2}$, where E_n stands for an incident energy. On the other hand, the inverse reaction is used to evaluate the higher energy part of capture cross section if the measurements on (γ,n) reactions are available.

The capture cross sections of ^{3}He are shown in Fig. 6, where the JENDL-3.2 data are compared with those of ENDF/B-VI and with experimental data. In this case, experimental data are available in a wide energy range, and the evaluated data were obtained as follows:

$$\sigma_{n,\gamma}(E_n) = \frac{8.59\times10^{-6}}{\sqrt{E_n}} + 6.37\times10^{-8}\sqrt{E_n}\,e^{-5.11\times10^{-4}\sqrt{E_n}}$$

,where $\sigma_{n,\gamma}$ and E_n are given in units of barn and eV, respectively. In the above equation, the second term indicates p-wave capture. It should be noted that the ENDF/B-VI data assume a straight line in the entire energy region. P-wave capture is also important in the evaluation of capture cross sections of ^{16}O. It is found from Fig. 7 that the recent measurements[6] indicate a dependence of $(E_n)^{1/2}$ above several tens of keV, while the old data point is placed on the $(E_n)^{-1/2}$ line. In the energy region above 1 MeV, the JENDL-3.2 data were obtained by using the measured ^{17}O(γ,n_0) cross sections.

3.2 Structural Materials

3.2.1 Statistical-model calculations

The evaluated gamma-ray production data of structural materials were obtained from statistical-model calculations using computer codes CASTHY[7], GNASH[8] and TNG[9]. The composite formula of Gilbert and Cameron[10] was used to represent level density. The profile function of giant dipole resonance is of the Brink-Axel[11] type, i.e., a Lorentzian shape.

In the previous version JENDL-3.1, the calculated thermal spectra were replaced with measured data after a benchmark test[12] had been done, since it was too difficult for the calculations to reproduce the measurements well. As a result of this replacement, total energy was not necessarily conserved at thermal energy. In the present JENDL-3.2, this drawback was removed by taking account of experimentally determined branching ratios for primary transitions in the calculation of capture gamma-ray spectra. Evaluated

thermal spectra from natural nickel are shown in Fig. 8, where the JENDL-3.1 data are based on the experimental data[13] measured at ORNL. It should be noted that the JENDL-3.2 data are almost consistent with those of JENDL-3.1 in this case.

3.2.2 Evaluated cross sections and spectra

Evaluated gamma-ray spectra from natural Cr, Cu and ^{93}Nb at 8 MeV are shown in Figs. 9-11, together with measurements.

Total gamma-ray production cross sections of Cr and Fe are compared with experimental data in Figs. 12 and 13. In these figures, the experimental data were obtained by multiplying the spectral measurements by 4π, while the evaluated data were corrected for experimental cut-off energy of gamma-rays. As for chromium, all evaluated data are smaller than the measurements. On the other hand, the iron data of JENDL-3.2 are considerably larger than those of the other two libraries, although the measured data are consistent with JENDL-3.2. As a matter of fact, the iron and nickel data of JENDL-3.2 were obtained by renormalizing statistical-model calculations to measurements. According to a result of benchmark tests[14], however, gamma-ray heating in iron was overestimated by the JENDL-3.2 data. Therefore, we decided to adopt original model calculations of iron in JENDL-FF without renormalization. As seen in Fig. 13, the iron data in JENDL-FF are almost consistent with those in ENDF/B-VI and JEF-2.2. With the same reason, the total gamma-ray production cross section of nickel in JENDL-FF were reduced as compared with that in JENDL-3.2.

4. Concluding Remarks

Light-nuclei and gamma-ray production data in JENDL-3.2 and JENDL-FF were reviewed with a focus on fusion applications. Selection of experimental data is important in evaluation of light nuclei since it is difficult to predict cross sections using the nuclear models applying to medium-heavy mass nuclei. DDXs from light nuclei were well reproduced by evaluated data with pseudo levels. As for ^{9}Be in JENDL-FF, neutron and α-particle DDXs were calculated by taking account of 2- and 3-body reaction kinematics, and the calculations were found to reproduce measurements.

Concerning gamma-ray production, inclusion of p-wave capture is important for several light nuclei. In the medium-heavy mass region, gamma-ray production cross sections and spectra were mainly obtained from statistical-model calculations. Following the result of the benchmark test, total gamma-ray production cross sections of iron and of nickel were reduced in JENDL-FF as compared with those in JENDL-3.2.

References

1) Nakagawa T. et al.: J. Nucl. Sci. Technol., **32**, 1259 (1995).
2) Chiba S.: Private communication (1995).
3) Chiba S. and Shibata K.: "Revision and Status of the Neutron Nuclear Data of ^{6}Li and

^{7}Li", JAERI-M 88-164 (1988).
4) Shibata K.: "Evaluation of Neutron Nuclear Data of ^{6}Li for JENDL-3", JAERI-M 84-198 (1984).
5) Koyama Y.: Master thesis in Kyushu University (1993).
6) Igashira M., Kitazawa H. and Takaura K.: Nucl. Phys., **A536**, 285 (1992).
7) Igarasi S. and Fukahori T.: "Program CASTHY -Statistical Model Calculation for Neutron Cross Sections and Gamma Ray Spectrum", JAERI 1321 (1991).
8) Young P.G. and Arthur E.D.: "GNASH: A Preequilibrium, Statistical Nuclear-Model Code for Calculation of Cross Sections and Emission Spectra", LA-6947 (1977).
9) Fu C.Y.: "A Consistent Nuclear Model for Compound and Precompound Reactions with Conservation of Angular Momentum", ORNL/TM-7042 (1980).
10) Gilbert A. and Cameron A.G.W.: Can. J. Phys., **43**, 1446 (1965).
11) Axel P.: Phys. Rev., **126**, 671 (1962).
12) Cai Shao-hui, Hasegawa A., Nakagawa T. and Kikuchi Y.: J. Nucl. Sci. Technol., **27**, 844 (1990).
13) Maerker R.E.: ORNL/TM-5203 (1976).
15) Maekawa F. and Oyama Y.: Proc. 1st Research Coordination Meeting on Measurement, Calculation and Evaluation of Photon Production Data, Bologna 1994, INDC(NDS)-334, p. 139 (1995).

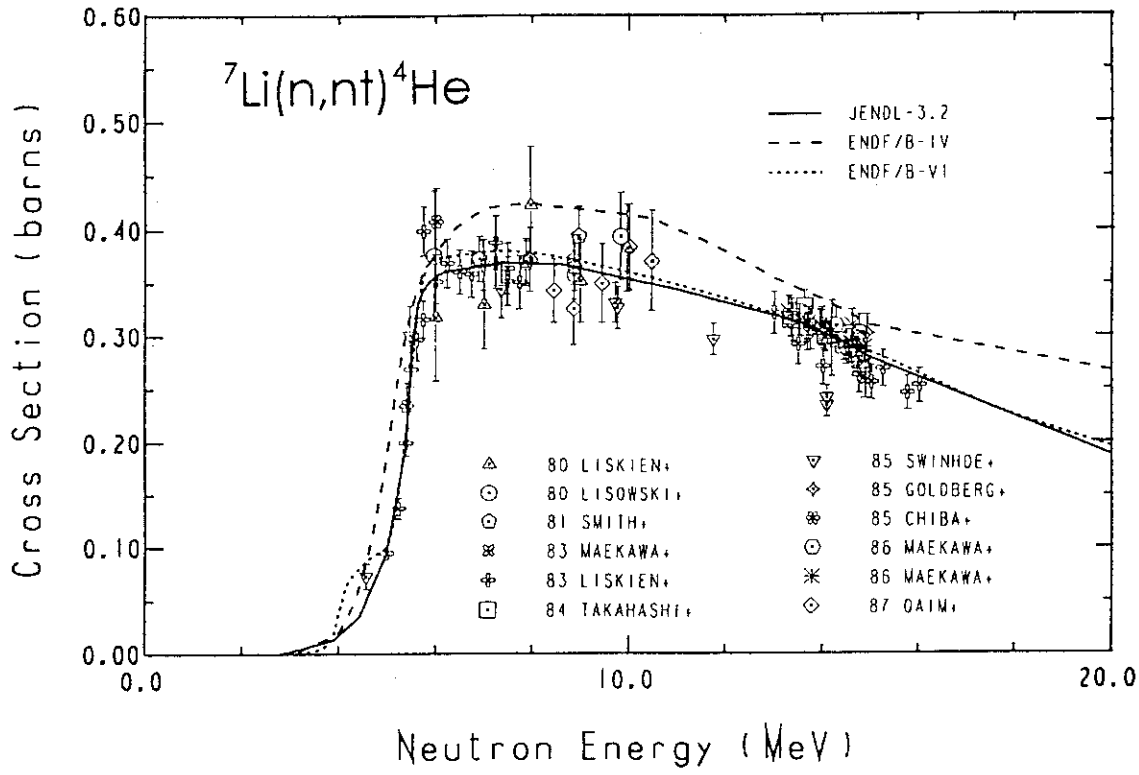

Fig. 1 ^{7}Li(n,nt)^{4}He reaction cross section.

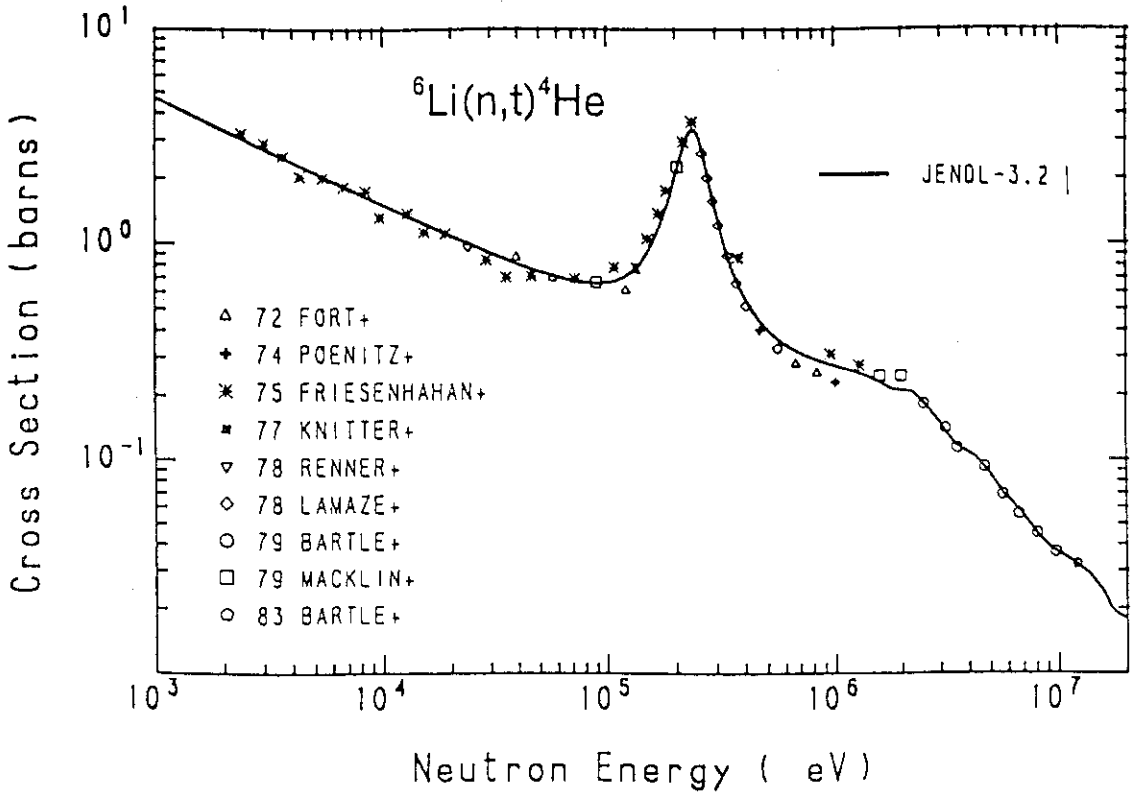

Fig. 2 ^{6}Li(n,t)^{4}He reaction cross section.

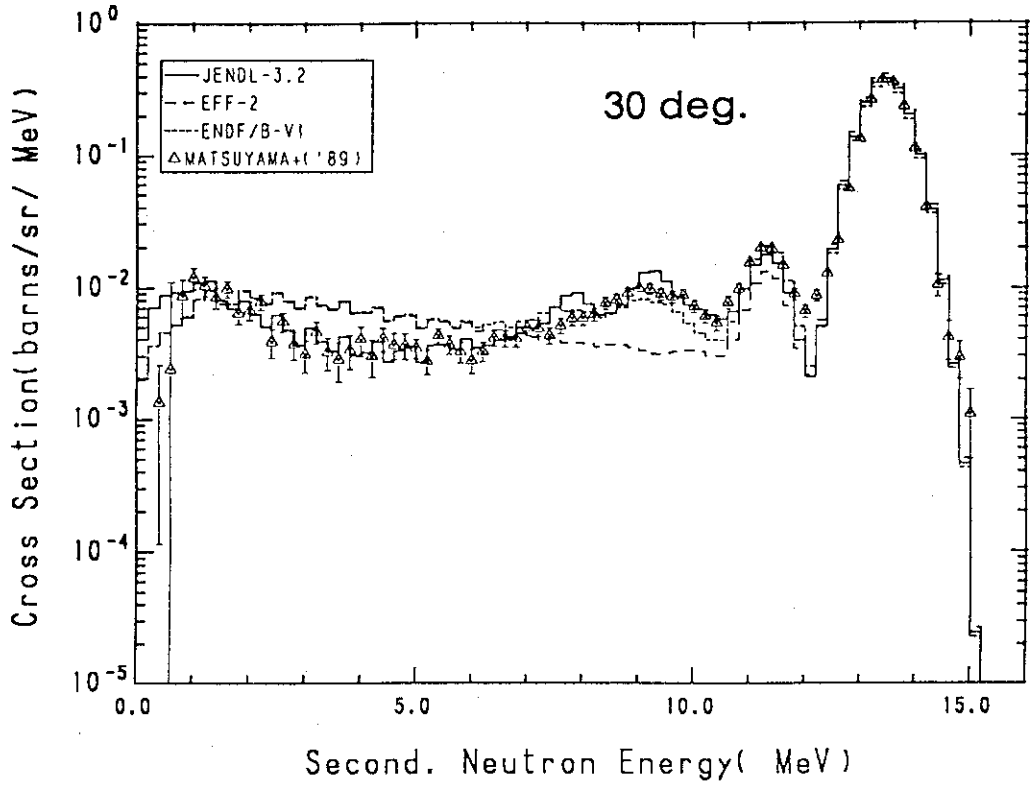

Fig. 3 DDX of ^{6}Li at 14 MeV.

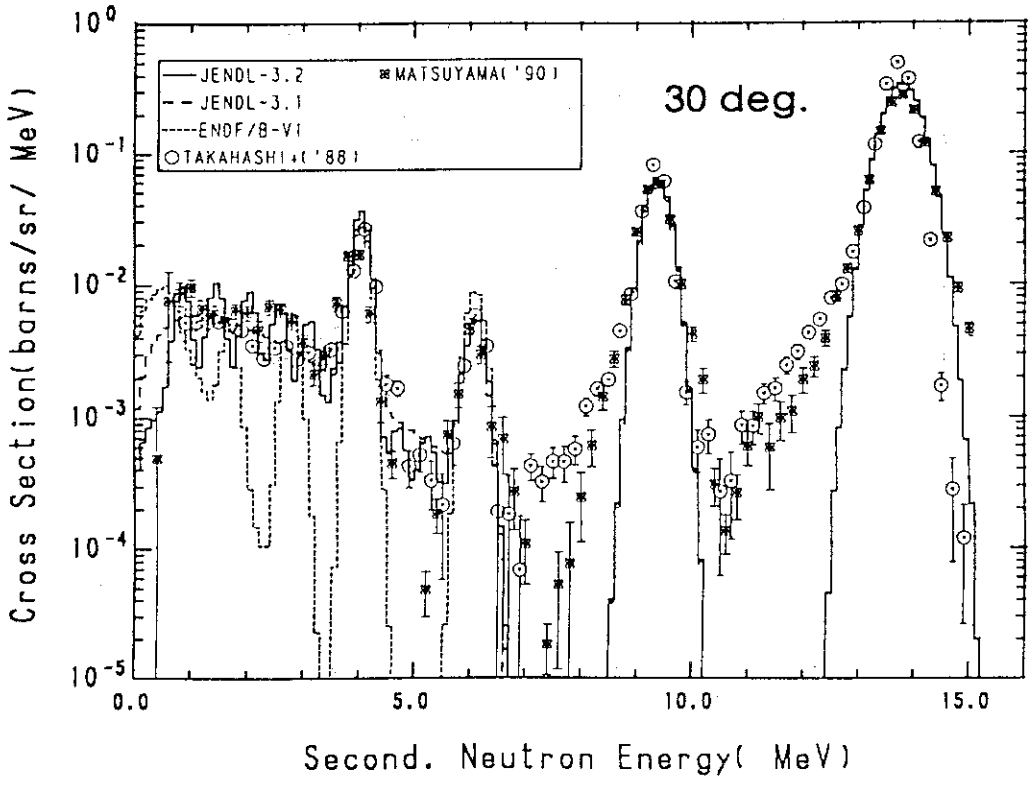

Fig. 4 DDX of ^{12}C at 14 MeV.

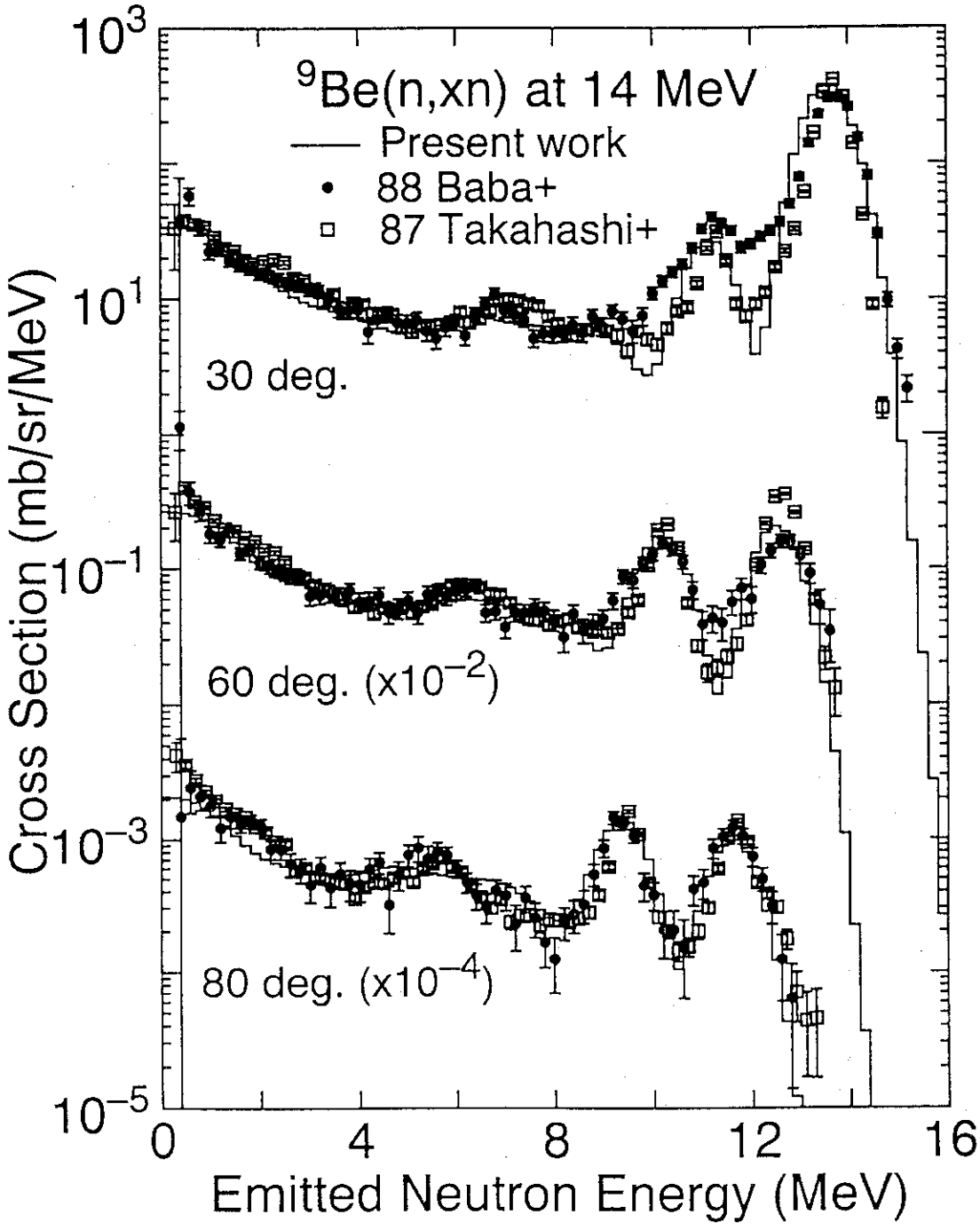

Fig. 5 DDX of ^{9}Be at 14 MeV.

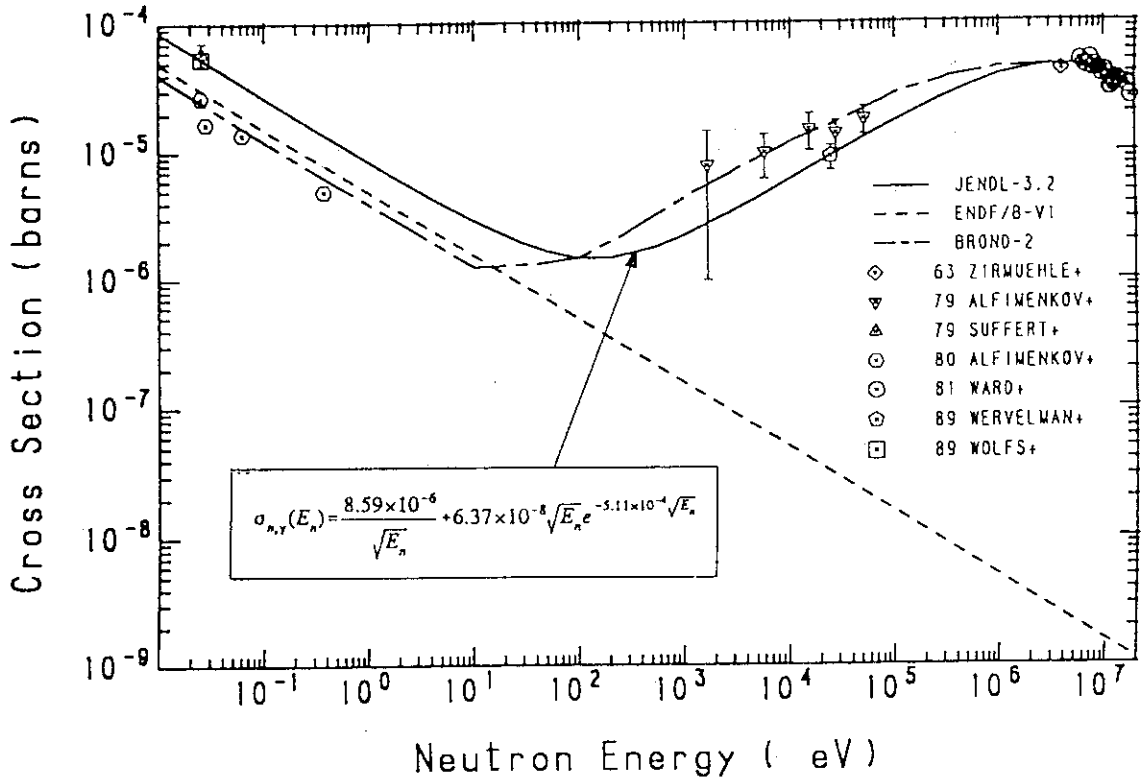

Fig. 6 $^{3}He(n,\gamma)$ reaction cross section.

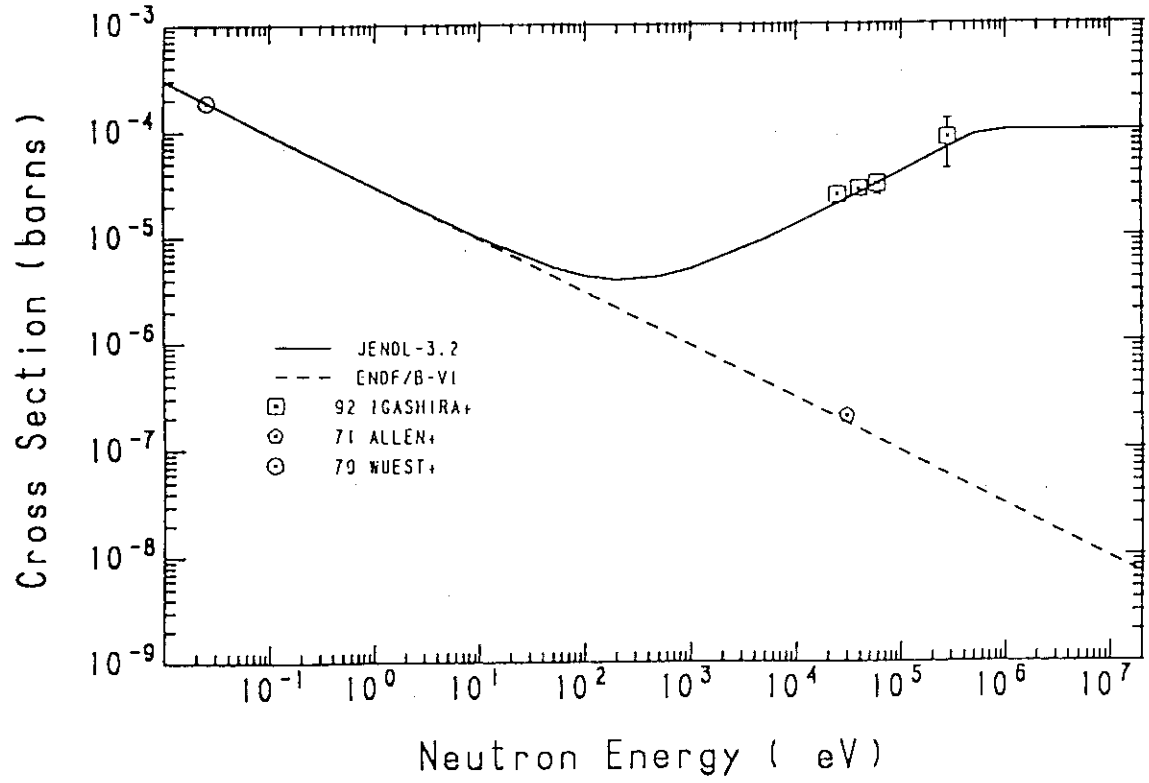

Fig. 7 $^{16}O(n,\gamma)$ reaction cross section.

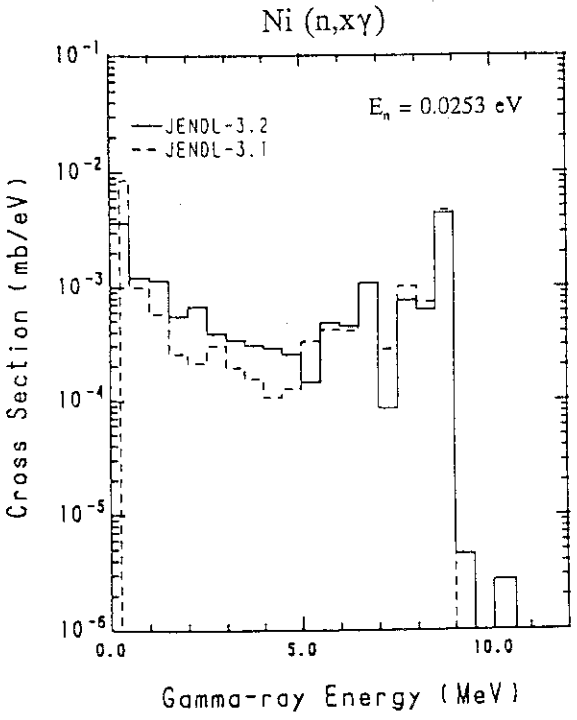

Fig. 8 Ni(n,xγ) spectra at 0.0253 eV.

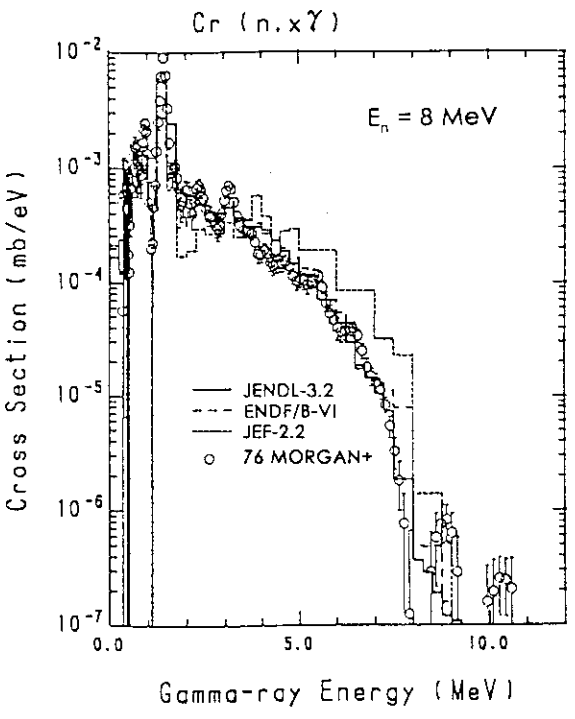

Fig. 9 Cr(n,xγ) spectra at 8 MeV.

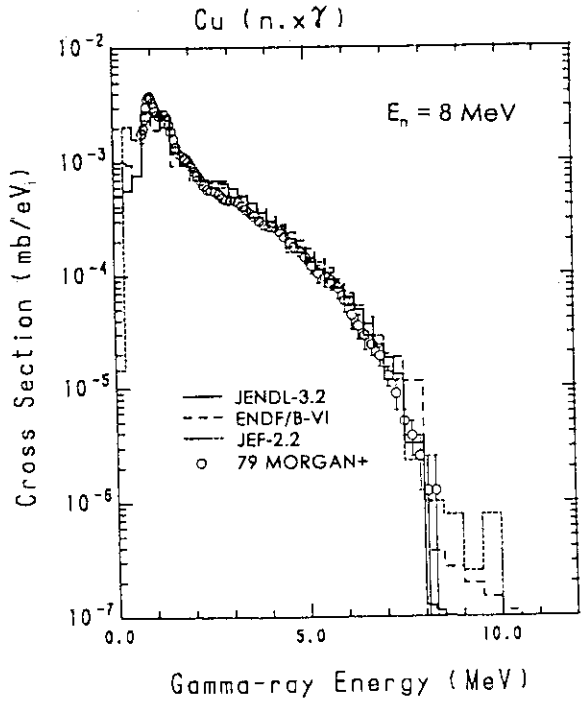

Fig. 10 Cu(n,xγ) spectra at 8 MeV.

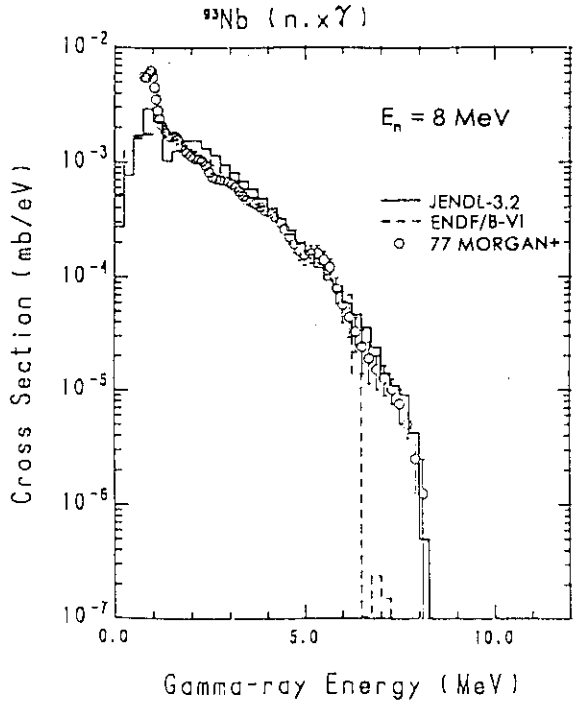

Fig. 11 ^{93}Nb(n,xγ) spectra at 8 MeV.

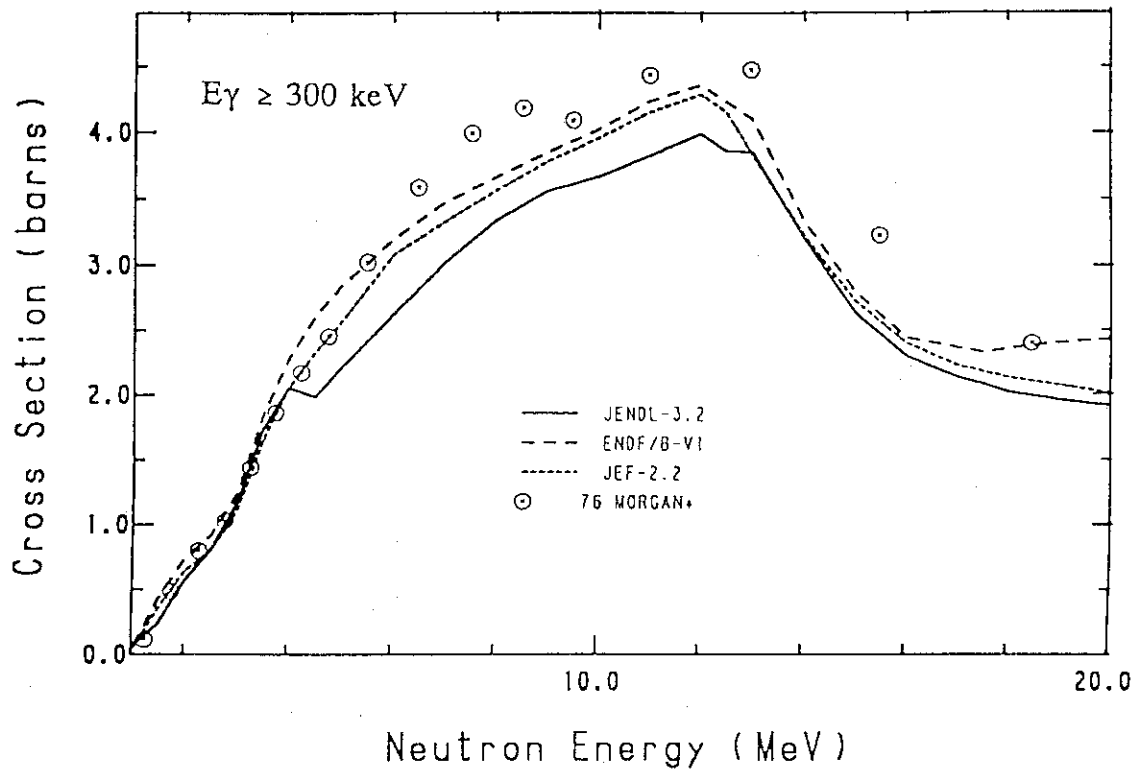

Fig. 12 Total gamma-ray production cross section of Cr.

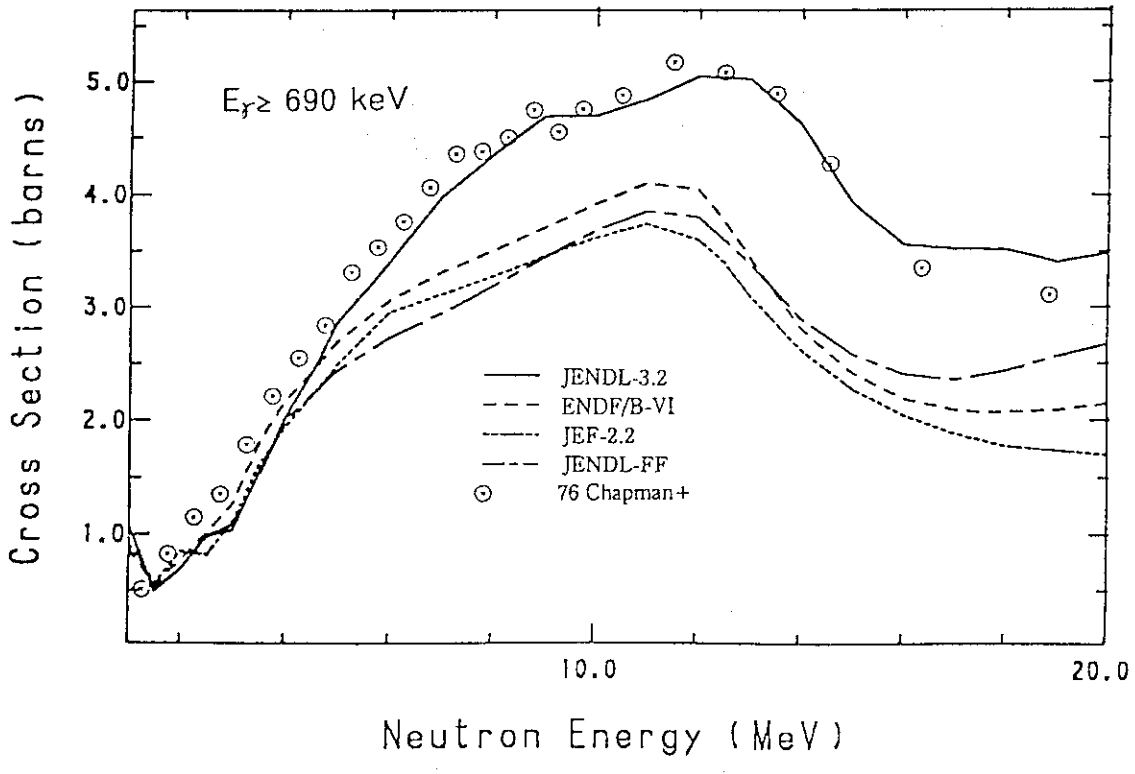

Fig. 13 Total gamma-ray production cross section of Fe.

2. 2 Evaluation of the Double-Differential Cross Sections of Medium-Heavy Nuclei for JENDL Fusion File

Satoshi Chiba, Tokio Fukahori, Baosheng Yu* and Kazuaki Kosako**

Japan Atomic Energy Research Institute
Tokai-mura, Naka-gun, Ibaraki-ken 319-11, Japan

* China Institute of Atomic Energy
Beijing, People's Republic of China

** Sumitomo Atomic Industries
Kaji-cho, Chiyoda-ku, Tokyo 101, Japan

Abstract

The status and evaluation method of the double-differential cross sections of the medium-heavy nuclei for JENDL Fusion File are presented. The data in JENDL Fusion File were compiled in ENDF-6 format with an MF=6 option to store the DDX data.

1. Introduction

The energy-angle double differential cross section (DDX) data play an important role in estimating the main characteristics of neutron fields in fission and fusion reactor applications. The neutrons produced from a fission or fusion reaction lose their energy by interacting with surrounding nuclei, inducing damage to structural materials, nuclear transmutation, radio-activities, gamma-ray heating, neutron multiplication, tritium production, etc. These processes occur at different rates depending on the energy of the incident neutrons. On the other hand, the DDX contains information on the dynamics of n + target system, which is also essential in understanding the properties of nuclear reaction mechanisms. Therefore, detailed knowledge on DDX is very important for the application and basic sciences.

In the first revision of JENDL-3[1] (JENDL-3.1), the DDXs are not given explicitly; they must be constructed as a product of cross section, angular distribution and energy distribution given independently in MF=3, 4 and 5, respectively. This representation, however, cannot reproduce the energy-angle correlation clearly observed in the incident neutron energy region above around 10 MeV where the contribution of the pre-equilibrium process is significant[2]. The data given in JENDL-3.1 were therefore found to be inadequate from both the microscopic and macroscopic points of view[3,4,5]. Furthermore, it was also pointed out that the DDXs of secondary charged

particles, not contained in JENDL-3.1, are also necessary, because these data are essential in material damage studies as basic data in calculating Primary Knock-on Atom (PKA) spectra and Kinetic Energy Release in Materials (KERMA)[6]. In such a situation, it was decided by the JENDL compilation group to prepare a special purpose file, JENDL Fusion File, to improve the accuracy of the DDX of secondary neutrons as well as those of charged particles. From discussions with users in fusion neutronics and PKA/KERMA applications, and considering future data needs, it was decided to include the following elements and their isotopes in JENDL Fusion File: ^{19}F, ^{27}Al, ^{0,28,29,30}Si, ^{0,40,42,43,44,46}Ca, ^{0,46,47,48,49,50}Ti, ^{51}V, ^{0,50,52,53,54}Cr, ^{55}Mn, ^{0,54,56,57,58}Fe, ^{59}Co, ^{0,58,60,61,62,64}Ni, ^{0,63,65}Cu, ^{75}As, ^{0,90,91,92,94,96}Zr, ^{93}Nb, ^{0,92,94,95,96,97,98,100}Mo, ^{116,117,118,119,120,122,124}Sn, ^{0,121,123}Sb, ^{0,180,182,183,184,186}W, ^{0,204,206,207,208}Pb and ^{209}Bi, where the mass number 0 indicates a natutal element. The evaluation was based on the systematics proposed by several authors, keeping various quantities given in JENDL-3.1 as much as possible. Re-evaluation of the neutron DDXs for light nuclei, ^{6,7}Li, ^{9}Be, ^{12}C, ^{14}N and ^{16}O, also started slightly later as a part of the JENDL Fusion File project. In this paper, the status and evalution methods of JENDL Fusion File for the medium-heavy elements are explained

2. General Outline of the Method of DDX evaluation

In the present work, DDXs were calculated based on systematics. As described in Ref. 9, the systematics derived by Kumabe et al.[10] was mainly used for the neutron DDX, while that of Kalbach[11] was adopted for the secondary charged particles. Various quantities required in these kinds of systematics were calculated by SINCROS-II code system[12]. DDXs measured by two Japanese groups[13-22] were taken into consideration in determining the theoretical model parameters.

In order to store the DDX data of secondary charged particles, the ENDF-6 format[23] was adopted in compiling JENDL Fusion File. The DDXs of secondary charged particles are given in a composite form (MT=203～207), not as reaction-wise spectra.

Systematics of the DDX was first proposed by Kalbach and Man[24], and other formulae were proposed later by Kumabe et al.[10] and Kalbach[11]. These formulae decompose the DDX in the following form;

$$\frac{d^2\sigma}{d\epsilon \cdot d\Omega} = \frac{d\sigma}{d\epsilon}\cdot\left[(1-f_{MSD})\cdot P(\epsilon,\Omega)_{MSC} + f_{MSD}\cdot P(\epsilon,\Omega)_{MSD}\right] \quad (1)$$

where

$$f_{MSD} \equiv \frac{d\sigma_{MSD}}{d\epsilon}\Big/\left(\frac{d\sigma_{MSD}}{d\epsilon}+\frac{d\sigma_{MSC}}{d\epsilon}\right) \equiv \frac{d\sigma_{MSD}}{d\epsilon}\Big/\frac{d\sigma}{d\epsilon} \quad (2)$$

denotes the fraction of multi-step direct cross section in the energy differential cross section (EDX), dσ/dε. The quantities $P(\epsilon,\Omega)_{MSC}$ and $P(\epsilon,\Omega)_{MSD}$ designate the angular distributions of particles emitted from the multi-step compound (MSC) and multi-step direct (MSD) processes, respectively. The various kinds of systematics give certain rules to calculate the quantities $P(\epsilon,\Omega)_{MSC}$ and $P(\epsilon,\Omega)_{MSD}$ on the assumption that they do not depend on the incident particle energy. Therefore, the EDX and f_{MSD} are the quantities which have to be known in applying the systematics.

The SINCROS-II code system consists of three main programs, EGNASH2, DWUCKY and

CASTHY2Y (see **Fig. 1**). Many evaluations for JENDL-3.1 have been carried out by using these programs, and therefore the present evaluation is a natural extension of JENDL-3.1. Another merit of using this code system is an ability to control sophisticated aspects of the multi-step statistical model calculation with a simple input by 1) building in such model parameters as optical model potential (OMP) and level density parameters (LDP) as defaults, 2) storing the discrete level structures retrieved from Evaluated Nuclear Data Structure File (ENSDF)[25] and atomic masses in databases, 3) interconnecting the databases and outputs from various programs, and 4) preparing a rich set of processing programs to convert the outputs to the ENDF format.

A schematic diagram of the method of evaluation and compilation of JENDL Fusion File is shown in **Fig. 1**. The SINCROS-II code system was used to calculate the partial reaction cross sections, particle spectra (EDXs) and the fraction of the multi-step direct reactions (f_{MSD}). The modified Walter-Guss OMP was used for neutron, and Perey and Walter-Guss combined OMP for proton as described in Ref. 12. For other particles, default OMPs (Lohr-Haeberli[26] for deuteron, Becchetti-Greenlees[27] for triton and ^{3}He, and Lemos modified by Arthur and Young[28] for α-particle) were used. The level density parameters were taken mostly from the table of Gilbert-Cameron[29] or Yamamuro[12]. However, LDP had to be adjusted to reproduce the energy spectra at low secondary neutron energy in some cases. The F2 parameter of EGNASH2 code, the Kalbach's constant divided by 100, was adjusted to reproduce the observed EDX at 14 MeV, and at 18 MeV if the experimental data are available. The parameter adjustment is designated in the middle left part of **Fig. 1** as a loop consisting of SINCROS-II, output file 15 from EGNASH2, KMDDX[30] and SPLINT89[31].

After fixing the model parameters, the DDXs were calculated and saved in the ENDF-6 format by F15TOB program[32], using the EDXs of neutrons taken from JENDL-3.1 and f_{MSD} calculated by EGNASH2. Various kinds of systematics[9] were built in F15TOB program, but Kumabe's was adopted for neutron, while Kalbach's was employed for charged particle channels mostly. When Kumabe's systematics was adopted, the DDX was expressed in a Legendre expansion form. On the contrary, when the Kalbach's systematics was used, the DDX was given compactly as a combination of (ϵ,dσ/dϵ,f_{MSD}), since an option of this systematics is available in the ENDF-6 format. The quantity f_{MSD} depends on incident neutron energy, outgoing particle energy and outgoing particle species, but was assumed to be independent of reaction channels in the present evaluation. The evaluated results of DDXs were then compared with the experimental data through PLDDX[33] and SPLINT89 codes. The evluation procedure was repeated by replacing a part of the JENDL-3.1 data with the SINCROS-II calculation by CRECTJ5[34] program until an acceptable agreement was reached between evaluated and measured data. Finally, format and physical consistency of the results were checked by ENDF utility programs[35]. DDXs of natural elements were constructed from those of isotopes. Instead of averaging the DDX of isotopes directly, the DDXs of natural elements were calculated by averaging the EDX and f_{MSD} of corresponding isotopes according to the natural abundances of them.

As described earlier, the Kumabe's systematics was used in calculating neutron DDX because this systematics can reproduce the observed data in the angular range from 30 to 150 deg., being better than the Kalbach-Man's and Kalbach's systematics[9]. However, it was found that this systematics sometimes overestimates the cross section in the very forward angles (less than 30 deg.). Therefore, a new formula was sought, by changing the A_L parameter to A_L = 0.0561 +

0.0377·L(L+1), instead of Eq. (5a) of Ref. 10. The new formula gives slightly smaller cross section in the forward and bigger values at backward angles. This change led to a better agreement with the experimental data. On the contrary, cross sections calculated by the Kumabe's oritinal formula were almost consistent with those calculated by the new one in the angular region between 40 and 150 deg. The new formula was adopted case-by-case.

3. Results of DDX Evaluation and Discussion

3.1. DDXs for neutron emission

In this sub-section, the presently evaluated neutron DDX data are compared with the experimental data and ENDF/B-VI[38] for selected elemens. In the subsequent figures, the data have been multiplied by the amount denoted in the parentheses after the angle.

^{27}Al : DDX of ^{27}Al at 14.1 MeV is given in **Fig.2.** The pseudo-level representation is adopted in ENDF/B-VI, which is a concise way to take account of the energy-angle correlation. The DDX reproduced from ENDF/B-VI can therefore reproduce the overall trend of DDX of ^{27}Al. However, the data stored in ENDF/B-VI overestimates the DDX at backward angles in the energy from 5 to 8 MeV, showing a possibility that the angular distribution of the pseudo-level is too weak. The present evaluation can reproduce the DDX of this nucleus satisfactorily.

Si : DDX of Si at 14.1 MeV is given in **Fig. 3.** The two experimental data sets show a slight disagreement at the forward angle. The data given in ENDF/B-VI seem to overestimate the data from middle to backward angles at 0 to 5 MeV region. At the forward angle, the present evaluation gives almost the same DDX as those in ENDF/B-VI, and they are in good agreement with the data reported by Baba et al. At middle to backward angles, the present evaluation gives a good agreement with the data of Takahashi et al.

^{51}V : DDXs of ^{51}V are shown in **Fig. 4.** The present evaluation gives a good overall agreement with the measured data. The data reproduced from ENDF/B-VI give too small cross sections at forward angles.

Zr : DDXs of Zr at 14.1 and 18.0 MeV are shown in **Figs. 5 and 6.** The DDXs calculated from ENDF/B-VI have a strong enhancement at low energy region. At 10 MeV region of the 14-MeV data, on the contrary, they tend to be lower than the measured cross section. The same trend is also observed at 18.0 MeV. The present evaluation can reproduce the data well.

3.2. Comparison with the (n,charged-particle) data

It is one of the main subjects of the present work to give good data on the DDX of secondary charged particles. In **Fig. 7**, energy spectra of proton, deuteron and α-particle emitted from interaction of 14-MeV neutrons with ^{93}Nb are shown. Although these quantities were not taken into consideration when various parameters in SINCROS-II calculation were adjusted, this figure may show the typical level of the spectra of secondary charged particles stored in JENDL Fusion File.

4. Concluding Remarks

The double differential cross sections of secondary neutrons and charged particles have been evaluated for medium-heavy nuclein using systematics supplemented by multistep statistical model calculations and were compiled as JENDL Fusion File. The main effort was placed to take account of the energy-angle correlation in the secondary neutron and charged particle spectra. The results were compiled in the ENDF-6 format. The presently evaluated results are in good accord with the measured cross sections on the whole.

Acknowledgements

The authors would like to thank Dr. N. Yamamuro of Data Engineering Corp. for his help in using SINCROS-II code system. They are also indebted to Drs. A. Takahashi of Osaka university and M. Baba of Tohoku university for their courtesy in providing the measured DDX data in a timely manner.

References

1) K. Shibata, T. Nakagawa, T. Asami, T. Fukahori, T. Narita, S. Chiba, M. Mizumoto, A. Hasegawa, Y. Kikuchi, Y. Nakajima and S. Igarasi : "Japanese Evaluated Nuclear Data Library, Version-3, -JENDL-3 -", JAERI 1319 (1990).
2) e.g., E. Gadioli and P.E. Hodgeson : "Pre-Equilibrium Nuclear Reactions", Clarendon Press, Oxford (1992).
3) Y. Nakajima and M. Maekawa (Ed.) : Proceedings of the Specialist's Meeting on Nuclear Data for Fusion Reactors, JAERI-M 91-062 (1991).
4) T. Fukahori, S. Chiba and T. Asami, JAERI-M 92-053 (1992).
5) T. Fukahori and S. Chiba, "Intercomparison of Evaluated Double-Differential Cross-Sections and Evaluation Method for JENDL Fusion File", Proc. Int. Conf. on Nuclear Data Evaluation Methodology, BNL, 12-16 Oct (1992), p.46 (1993), World Scientific.
6) M. Kawai, T. Fukahori and S. Chiba : "STATUS OF JENDL KERMA/PKA FILE", JAERI-M 92-027, p.28 (1992).
7) H. Kashimoto, Y. Koyama, H. Shinohara, Y. Watanabe and S. Chiba, "Study of the ^{12}C Breakup Process and Carbon Kerma Factor", JAERI-M 93-046, p.287 (1993).
8) T. Nakagawa, K. Shibata, S. Chiba, T. Fukahori, Y. Nakajima, Y. Kikuchi, T. Kawano, Y. Kanda, T. Ohsawa, H. Matsunobu, M. Kawai, A. Zukeran, T. Watanabe, S. Igarasi, K. Kosako and T. Asami, Jour. Nucl. Sci. Technol. 32, 1259(1995).
9) B. Yu, S. Chiba and T. Fukahori, J. Nucl. Sci. Technol. 29, 677(1992).
10) I. Kumabe, Y. Watanabe, Y. Nohtomi and M. Hamada : Nucl. Sci. Eng. 104, 280 (1990).
11) C. Kalbach : Phys. Rev. C37, 2350 (1988).
12) N. Yamamuro : "A NUCLEAR CROSS SECTION CALCULATION SYSTEM WITH SIMPLIFIED INPUT-FORMAT, VERSION-II (SINCROS-II)", JAERI-M 90-006 (1990).
13) A. Takahashi, JAERI-M 86-029, p.99(1986).
14) A. Takahashi, E. Ichimura, H. Sugimoto and T. Kato, JAERI-M 86-080, p.393(1986).

15) A. Takahashi, E. Ichimura, Y. Sasaki and H. Sugimoto, OKTAVIAN Report A-87-03 (1987).
16) A. Takahashi, J. Yamamoto, K. Ohshima, M. Fukazawa, Y. Yanagi, M. Ueda, J. Miyaguchi, S. Kohno, K. Yugami, H. Nonaka, E. Ichimura, H. Sugimoto and K. Sumita, OKTAVIAN Report A-87-01(1987).
17) A. Takahashi, M. Gotoh, Y. Sasaki and H. Sugimoto, OKTAVIAN Report A-92-01 (1992).
18) A. Takahashi, private communication.
19) M. Baba, M. Ono, N. Yabuta, T. Kikuchi and N. Hirakawa, Proc. of Int. Conf. on Nucl. Data for Basic and Applied Sciences, Santa Fe, N.M., U.S.A., May 13-17, p.223 (1985), Gordon and Breach.
20) M. Baba, M. Ishikawa, N. Yabuta, T. Kikuchi, H. Wakabayashi and N. Hirakawa, Proc. of Int. Conf. on Nucl. Data for Science and Technology, Mito, May 30-Jun 3, p.291(1988), Saikon Publishing.
21) M. Baba, S. Matsuyama, T. Itoh, T. Ohkubo and N. Hirakawa, J. Nucl. Sci. Technol., 31, 757 (1994).
22) M. Baba, private communication.
23) P.F. Rose and C.L. Dunford (ed.), "ENDF-102, DATA FORMATS AND PROCEDURES FOR THE EVALUATED NUCLEAR DATA FILE, ENDF-6", BNL-NCS 44945 (1991).
24) C. Kalbach and F.M. Mann : Phys. Rev. C23, 112 (1981).
25) "Evaluated Nuclear Structure Data File", maintained by BNL/NNDC.
26) J.M. Lohr and W. Haeberli, Nucl. Phys. A232, 381 (1974).
27) F.D. Becchetti, Jr. and G.W. Greenlees, "Polarizatin Phenomena in Nuclear Reactions", The University of Wisconsin Press, p.682 (1971).
28) E.D. Arthur and P.G. Young, "Evaluated Neutron-Induced Cross Sections for ^{54,56}Fe to 40 MeV", LA-8626-MS (1980).
29) A. Gilbert and A.G.W. Cameron : Canad. Jour. Phys. 43, 1446 (1965).
30) B. Yu and S. Chiba : "KMDDX", unpublished.
31) T. Nakagawa : "SPINPUT", JAERI-M 9499 (in Japanese) (1981); T. Narita, T. Nakagawa, Y. Kanemori and H. Yamakoshi : "SPLINT, A Computer Code for Superimposed Plotting of the Experimental and the Evaluated Data", JAERI-M 5769 (1974).
32) S. Chiba, program "F15TOB", unpublished.
33) B. Yu and S. Chiba : "PLDDX", unpublished.
34) T. Nakagawa : "CRECTJ5", to be published.
35) C.L. Dunford : "Release of ENDF Utility Codes, Version 6.6", unpublished memorandum, BNL/NNDC, June 13, 1990.
36) NNDC/BNL, "ENDF/B-VI".

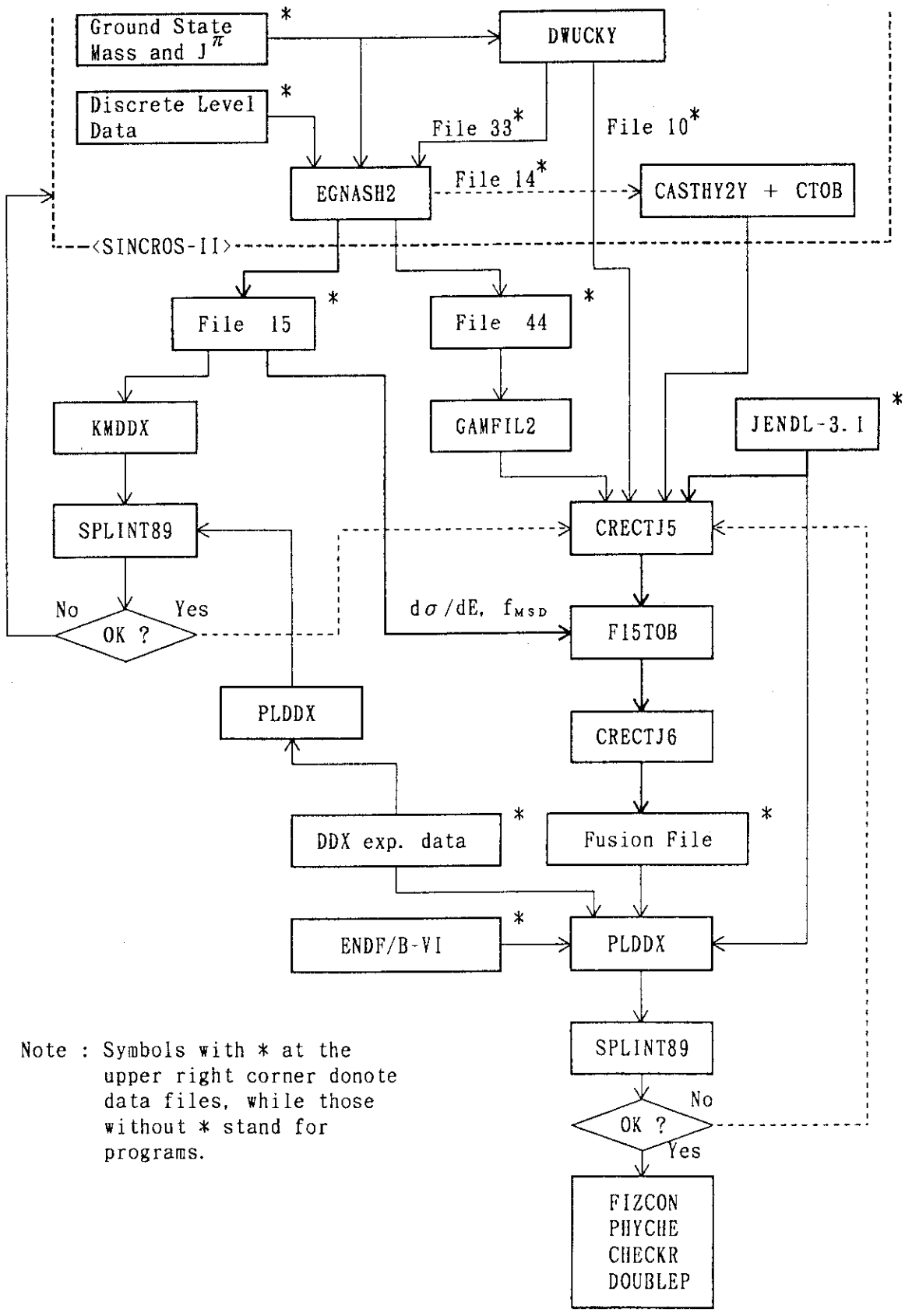

Fig. 1 Schematic flow of evaluation and compilation of JENDL Fusion File

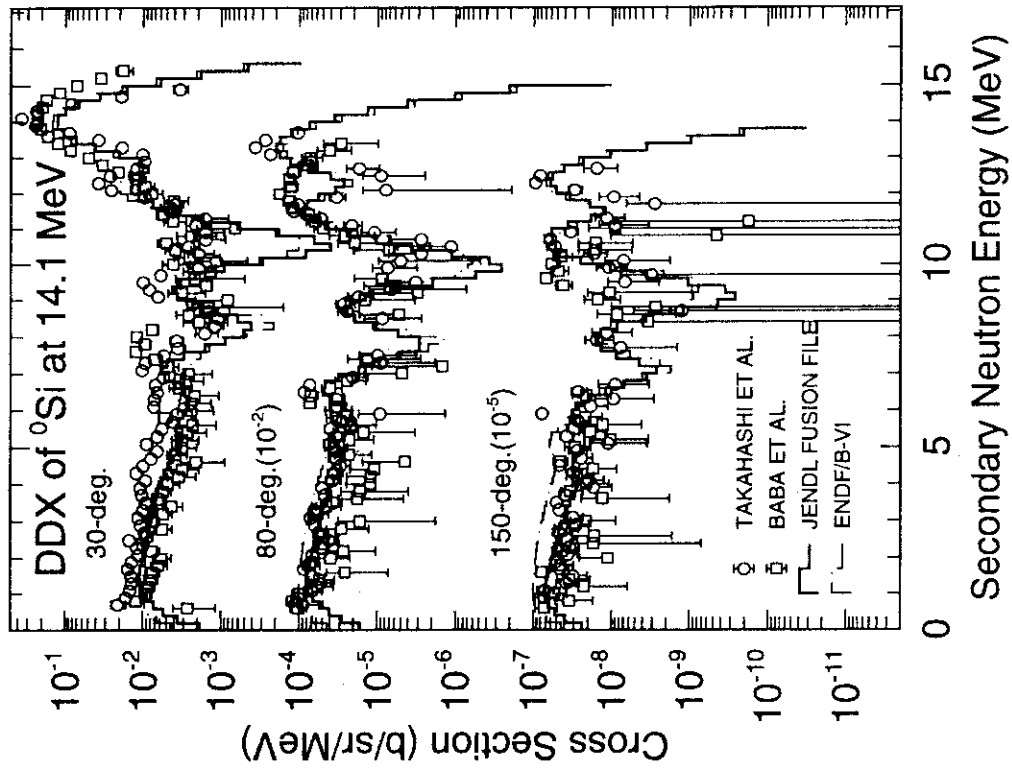

Fig. 3 DDX of ^{0}Si(n,xn) at 14.1 MeV

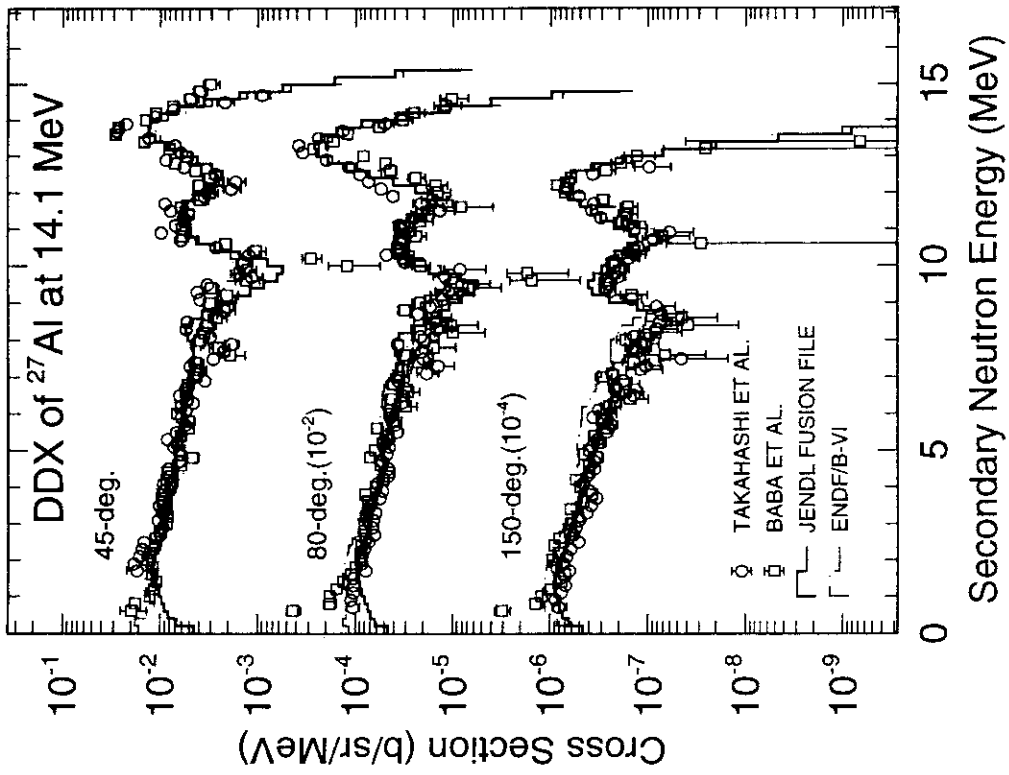

Fig. 2 DDX of ^{27}Al(n,xn) at 14.1 MeV

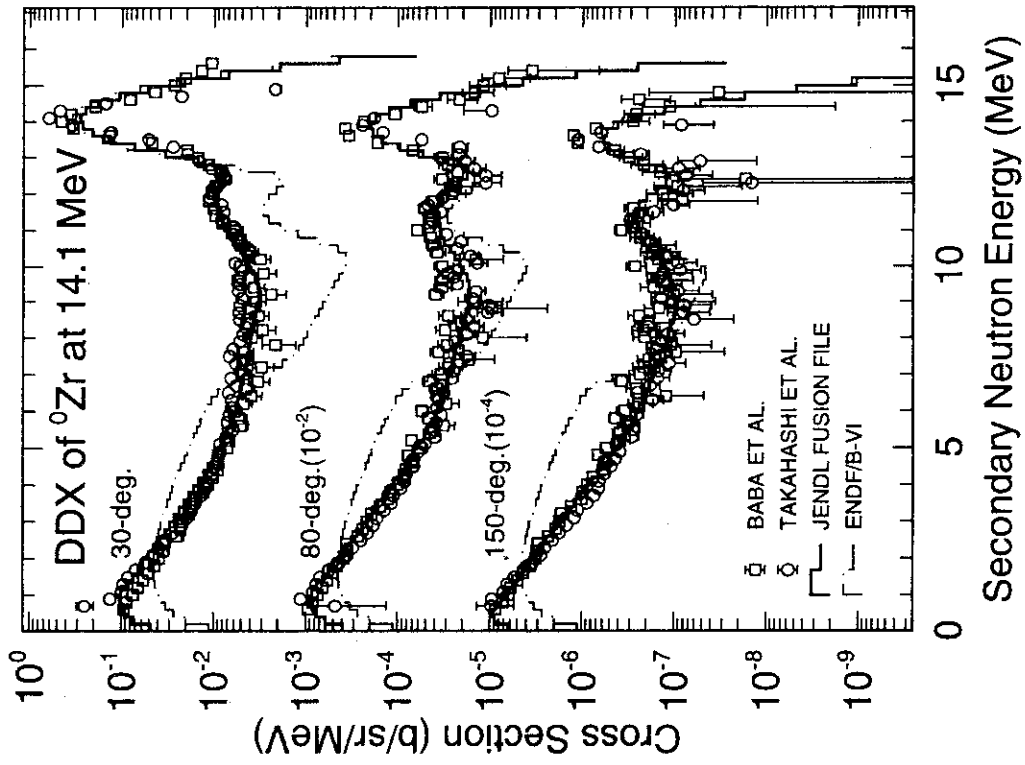

Fig. 5 DDX of ^{0}Zr(n,xn) at 14.1 MeV

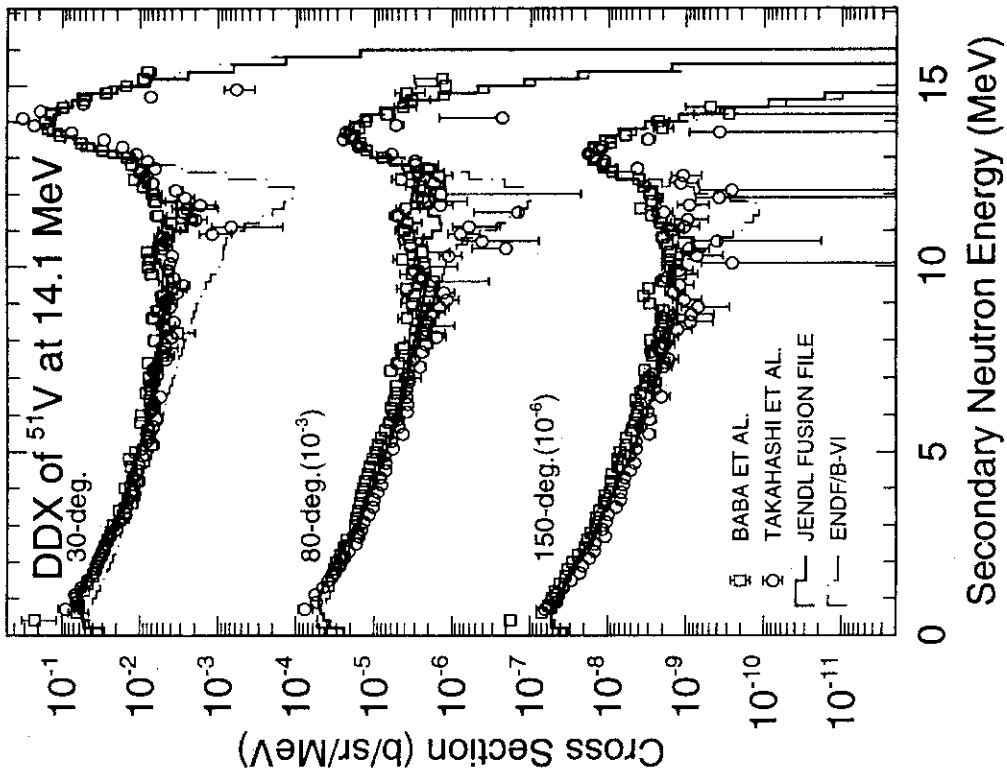

Fig. 4 DDX of ^{51}V(n,xn) at 14.1 MeV

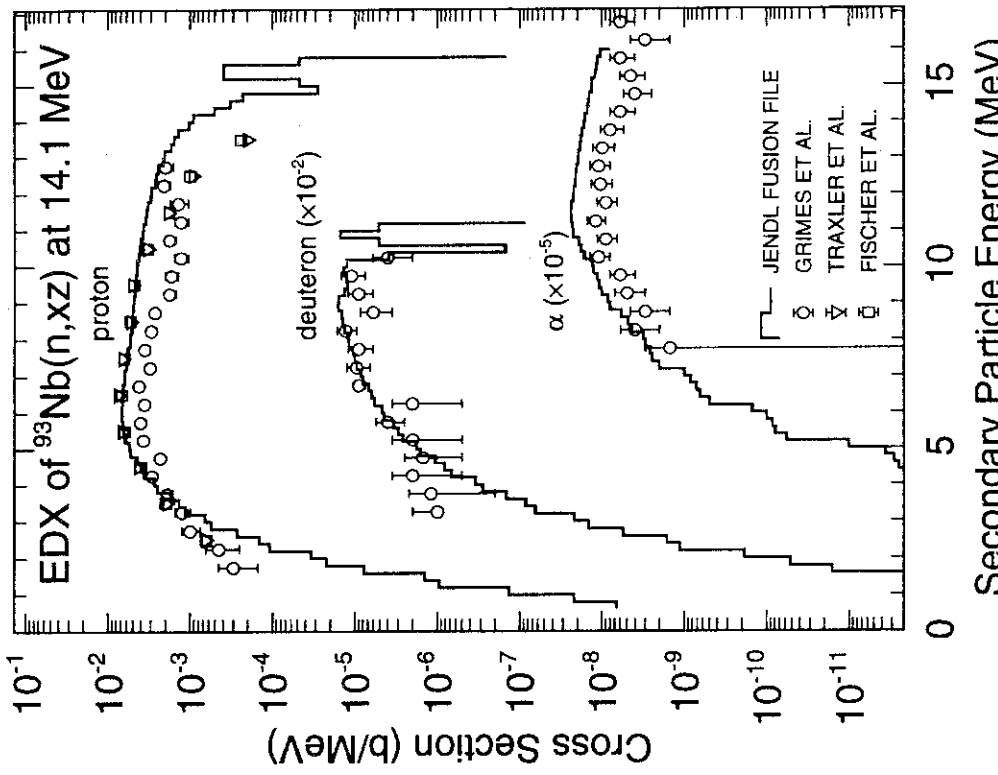

Fig. 7 DDX of ^{93}Nb(n,xz) at 14.1 MeV

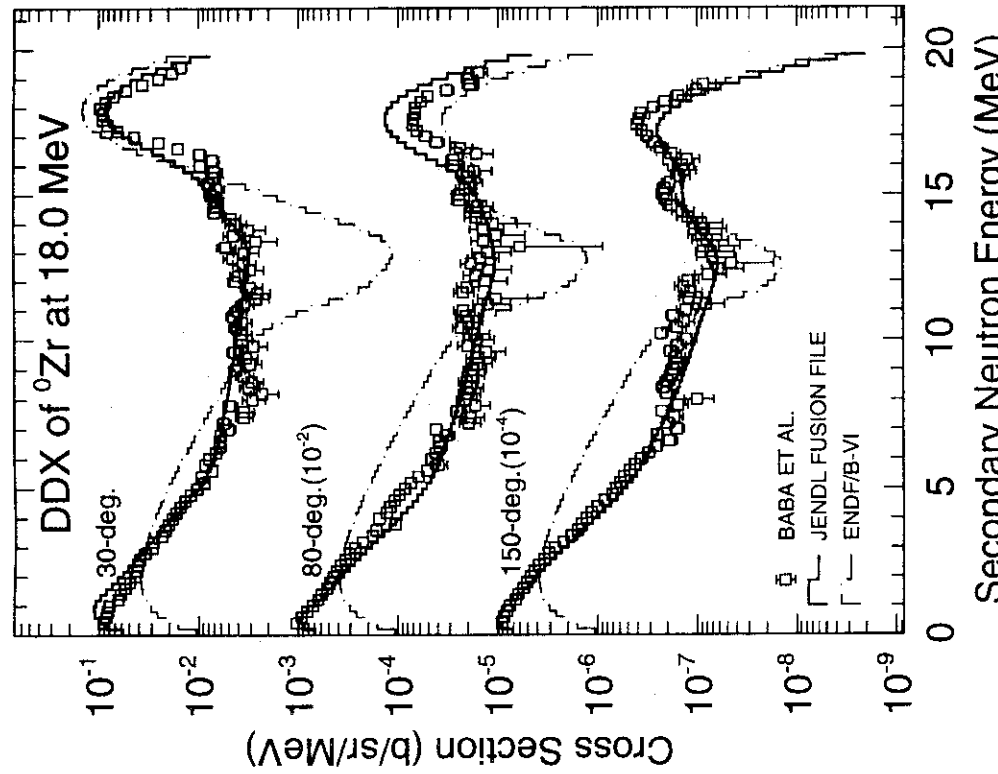

Fig. 6 DDX of ^{0}Zr(n,xn) at 18.0 MeV

2.3 The Present Status of Cross Section Libraries

Kazuaki KOSAKO
Sumitomo Atomic Energy Industries, Ltd.
Ryogoku, Sumida-ku, Tokyo 130

Various neutron cross section libraries using in the area of fusion reactor engineering in Japan were summarized characteristics in view of the present status. The libraries were explained distinctively a continuous energy type and a multigroup type, with priority given to recent libraries.

1. Introduction

In the area of fusion reactor engineering, various neutron cross section libraries are used to research on nuclear design and safty. In general, a cross section library is produced from cross section data that were processed an evaluated nuclear data file by a processing code. A library has a proper type depended on a transport code and the porper type is necessary in order to perform efficiently the transport calculation. Various libraries are classfied into two large groups of a continuous energy cross section library and a multigroup cross section library. The former spread rapidly according as the MCNP code[1] since the late 1980's. The latter is traditional type given actual result in the area of fission.

Since the Japanese Evaluated Nuclear Data Library Version 3 Revision-2 (JENDL-3.2)[2] was released in June 1994, several neutron cross section libraries based on JENDL-3.2 were produced for fusion field and has been provided for public use. Summarizing the present status of cross section libraries in Japan is very useful to user of library and is helpful in an appreciation for analyses of various benchmark experiments.

2. Continous Energy Cross Section Library

The primary feature of a continuous energy neutron cross section library is expression of cross sections by a large number of successive energy points (pointwise). An energy between two neighboring energy points is calculated by linear-linear interpolation. Angular distribution of secondary particle in the library is expressed by equal-probability cosine bins. The number of the bins is sufficient 32 to keep the precision of nuclear data file. Energy distribution of secondary particle in the library is the same expression as nuclear data file. The precision of calculated result with the library is equivalent to it of the evaluated nuclear data file. The library can be checked the content by comparing with original nuclear data file.

To use a continuous energy cross section library, it is necessary to simulate particle transport by each individual sampling of event. Therefore, the combination of the library and Monte Carlo method is optimum. Typical Monte Carlo codes using the library are MCNP and

MVP[3] in Japan. The format of a continuous cross section library for MCNP differs from one for MVP. The calculation results are recognized as standard results with high precision. The results might be fed back to the original nuclear data file. S(α,β) data could be used in order to calculate correctly neutron spectrum in thermal region of several materials.

Table 2.3.1 shows continuous energy neutron cross section libraries using in fusion field of Japan. The libraries for MCNP were processed by a nuclear data processing system NJOY[4]. The libraries for MVP were processed by a LICEM code[3]. The number of nuclides in Table 2.3.1 means ones processed at temperature of 300 K, but a part of nuclides in MVPLIB-J32[5] are 600 K and a part of ones in BMCCS[1] are 0 K. The recent library is FSXLIB-J3R2[6] and MVPLIB-J32 produced from JENDL-3.2, and the latest library is FSXLIB-JFF[7] produced from JENDL Fusion File[9] with ENDF-6 format[8]. In particular, FSXLIB-J3R2 contains all the 340 nuclides stored in JENDL-3.2 and thus covers many minor isotopes. FENDL/MC1[10] was produced from an nuclear data library, FENDL/E-1.0[10], collected from ENDF/B-VI[8], EFF-1 and JENDL-3.1[11] for ITER project and is available to only MCNP-4A[1]. RMCCS[1] based on ENDF/B-V[12] is the standard library in U.S.A. BMCCS is old library consisted of various nuclear data files. FSXLIB-J3[13] based on JENDL-3.1 was released as first library for MCNP made in Japan. MVPLIB-J3[3] and -J32 include nuclides processed at temperatures of 300, 600, 900, 1500 and 1800 K.

Calculations used FSXLIB-J3R2 and -JFF dominate in recent fusion neutronics field. Main specification of their libraries is shown in Table 2.3.2. The primary feature of FSXLIB-JFF is the correspondence of energy-angle relationship in energy distribution of secondary particle that is attributed to JENDL Fusion File. Therefore, FSXLIB-JFF is available to only MCNP-4A. Most of evaluations in JENDL Fusion File were incorporated into JENDL-3.2, but the energy-angle relationship was divided into energy distribution and angular distribution. Therefore, FSXLIB-JFF is better than FSXLIB-J3R2 and the element and isotopes of tungsten and lead were reevaluated in 1995. Utilization of FSXLIB-JFF optimized for fusion is expected in order to improve the calculational precision.

3. Multigroup Cross Section Library

The primary feature of a multigroup cross cross section library is expression by a finite number of groups for energy (groupwise). Cross sections, angular distribution and energy distribution are averaged by each group meant a specific energy range. A multigroup cross section library has been used for a long time and various multigroup transport codes using the library have been developed. But, the library has an intrinsic problem of approximation by the averaging. The library must be taken care about approximation as follows: 1) a finite number of groups and the energy group structure, 2) Legendre expandsion form or double differential cross section (DDX) form of angular distribution, 3) type of weight function and selfshielding

factor of resonance for averaging by group, and 4) without distinction of reaction type. In addition, the produced multigroup cross section library is impossible almost to check the content. DDX form is better than Legendre expandsion. In fusion field, weight function for averaging neutron cross sections is generally used a function combined Maxwell distribution in thermal region with 1/E in energy region above thermal, where E is energy. Weight function for photon is 1/E. Photon interaction cross section file is needed to produce a library coupled neutron and photon, and is generally used DLC-136/PHOTX[14] and DLC-146/HUGO-VI[15] at present.

Several nuclear data processing codes are available to produce a multigroup cross section library in Japan. Their codes are shown in Table 2.3.3. MACS-N[16], NJOY91[4] and RADHEAT-V4[17] have been used in general, but only NJOY91 corresponds to the latest ENDF-6 format at present.

Table 2.3.4 shows typical multigroup cross section libraries using in fusion field of Japan. JSSTDL-295/J32[18] and -295/J3[18] are generally used after the collapse to a small number of groups and the conversion to macroscopic cross sections of ANISN format[19]. The difference between FUSION-J3[20] and FUSION-40[20] is the numbers of groups. FENDL/MG1[10] was produced from FENDL/E-1.0 into MATXS format[4] with group structure of VITAMIN-J but the photon interaction cross section file is unknown. GICX40V4[21] is a old library and is be almost out of use at present. DDXLIB-J3[22] and BREMJ3[23] are neutron libraries of DDX form for a MORSE-DD[22] code and a series of BERMUDA codes[23]. The recent library is JSSTDL-295/J32, FENDL/MG1 and BREMJ3, and the successional libraries to FUSION-J3 and FUSION-40 also can be provided. The popular library is FUSION-J3, -40 and JSSTDL-295/J3 and thus Legendre expandsion is popular as expression of angular distribution. JSSTDL-295/J32, -295/J3 and FENDL/MG1 have the table of self-shielding factors depended to temperature and thus is taken account of self-shielding effect of resonance structure that is significant in deep penetration problem. Temperature of the others is only 300 K. In Japan, neutron 42-groups is standard in nuclear design of fusion reactor and neutron 125-groups are standard in benchmark calculation.

4. Response Library

A response library is a collection of data as reaction cross sections, gas production cross sections, displacement per atom (dpa), kerma factor, a multiplication factor, and dose equivalent conversion coefficients. These data can be used to calculate the reaction, muliplication or production rates from neutron and gamma-ray spectra obtained by a transport calculation. A response library is necessary to estimate parameters on fusion design by calculation.

A response libraries also are classfied into a continuous energy type and a multigroup type. In general, the former is used in post-processing of transport calculation result. The latter is used to estimate directly reaction rates at detector of a continous energy Monte Carlo

code and can be calculated with good precision than another in the case of giant resonance structure.

Table 2.3.5 shows typical response libraries using in fusion field of Japan. REACTXX[24] is a large response library of multigroup type contained many group sutructures of neutron and photon. FUSION-J3/KDG[25] is an neutron library of multigroup type corresponded to FUSION-J3 and -40. APPLE-3/LIB[26] is a library of multigroup type collected only important responses in fusion. MCNPDOS[1] and FSXDOS-J3 are neutron libraries of continous energy type as MCNP dosimetry file. The libraries for MCNP in Table 2.3.1 also can be used as MCNP dosimetry file. The libraries except libraries for MCNP were produced for fusion at JAERI.

References

1) Briesmeister J.F. (Ed.): "MCNP - A General Monte Carlo N-Particle Transport Code, MCNP-4A," LA-12625 (1993).
2) Nakagawa T., et al.: "Japanese Evaluated Nuclear Data Library Version 3 Revision-2: JENDL-3.2," J. Nucl. Sci. Technol., 32[12], 1259 (1995).
3) Mori T. and Nakagawa M.: "MVP/GMVP: General Purpose Monte Carlo Codes for Neutron and Photon Transport Calculations Based on Continuous Energy and Multigroup Methods," JAERI-Data/Code 94-007 (1994) (in Japanese).
4) MacFarlane R.E., Muir D.W. and Boicourt R.M.: "The NJOY Nuclear Data Processing System," LA-9303-M (ENDF-324) (1982).
5) Mori T.: To be published.
6) Kosako K., et al.: "FSXLIB-J3R2: A Continuous Energy Cross Section Library for MCNP Based on JENDL-3.2," JAERI-Code/Data 94-020 (1994).
7) Kosako K. and Oyama Y.: To be published.
8) BNL: "ENDF/B-VI: Evaluated Nuclear Data File, Version-VI" (1990); and Rose P.F. and Dunford C.L. (Ed.): "Data Formats and Procedures for the Evaluated Nuclear Data File, ENDF-6," BNL-NCS-44945 (ENDF-102) (1990).
9) Chiba S., et al.: "Evaluation of JENDL Fusion File," Proc. 1991 Symposium on Nuclear Data, JAERI-M 92-027, p.35 (1992).
10) IAEA: "FENDL/E-1.0: Fusion Evaluated Nuclear Data Library Version 1"
11) Shibata K., et al.: "JENDL-3: Japanese Evaluated Nuclear Data Library, Version-3," JAERI-1319 (1990).
12) BNL: "ENDF/B-V: Evaluated Nuclear Data File, Version-V" (1979); and Kinsey R. (Ed.): "Data Formats and Procedures for the Evaluated Nuclear Data File, ENDF," BNL-NCS-50496 (ENDF-102) (1979).
13) Kosako K., et al.: "FSXLIB-J3: A Continuous Energy Cross Section Library for MCNP Based on JENDL-3.2," JAERI-M 91-187 (1991) (in Japanese).

14) Trubey D.K., et al.: "Photn Cross Sections for ENDF/B-VI," Proc. of Advances in Nuclear Engineering Computation and Radiation Shielding, April 9-13, Santa Fe, USA (1989).
15) RSIC: DLC-146/HUGO-VI (1990).
16) Hasegawa A.: To be published.
17) Yamano N., et al.: "RADHEAT-V4: A Code System to Generate Multigroup Constants and Analyze Radiation Transport for Shielding Safety Evaluation," JAERI-1316 (1989).
18) Hasegawa A.: "Group Cross-section Processing Method and Common Nuclear Group Cross-section Library Based on JENDL-3 Nuclear Data File," Proc. 1990 Symposium on Nuclear Data, JAERI-M 91-032, p.133 (1991).
19) Engle W.W.: "A User's Manual for ANISN, A One-Dimensional Discrete Ordinate Transport Code with Anisotropic Scattering," K-1693 (1976).
20) Maki K., et al.: "Nuclear Group Constant Set FUSION-J3 for Fusion Reactor Nuclear Calculations Based on JENDL-3," JAERI-M 91-072 (1991) (in Japanese).
21) Seki Y. and Iida H.: "Coupled 42-Group Neutron and 21-Group Gamma Ray Cross Section Sets for Fusion Reactor Calculation," JAERI-M 8818 (1980).
22) Mori T., et al.: "One-, Two- and Three-Dimensional Transport Codes Using Multi-Group Double-Differential Form Cross Sections," JAERI 1314 (1988).
23) Nakashima H., et al.: "A New Library of Neutron Group Constants for BERMUDA Based on JENDL-3.2 Nuclear Data File," JAERI-Data/Code 95-006 (1995) (in Japanese).
24) Kosako K.: "INTERF: The Reaction Rates and Spectra Editing Code for Analysis of Fusion Neutronics Experiments," JAERI-M 90-199 (1990) (in Japanese).
25) Maki K., et al.: "Nuclear Heating Constant KERMA Library - Nuclear Heating Constant Library for Fusion Nuclear Group Constant Set FUSION-J3," JAERI-M 91-073 (1991) (in Japanese); Mori S., et al.: "Multi-Group Helium and Hydrogen Production Cross Section Libraries for Fusion Neutronics Design," JAERI-M 93-175 (1993).
26) Kawasaki H., et al.: "APPLE-3: Improvement of APPLE for Neutron and Gamma-ray Flux, Spectrum and Reation Rate Plotting Code, and of Its Code Manual," JAERI-M 91-058 (1991) (in Japanese).

Table 2.3.1 Continuous energy neutron cross section libraries using in fusion field of Japan

type	library name	nucliear data file	number of nuclides	temperatures [K]
MCNP	FSXLIB-JFF	JENDL Fusion File	82	300
	FSXLIB-J3R2	JENDL-3.2	340	300
	FSXLIB-J3	JENDL-3.1	116	300
	FENDL/MC1	ENDF/B-VI, etc.	56	300
	RMCCS	ENDF/B-V	91	300
	BMCCS	ENDF/B-IV, etc.	69	0, 300
MVP	MVPLIB-J32	JENDL-3.2	98	300, 600, 900, 1500, 1800
	MVPLIB-J3	JENDL-3.1	91	300, 600, 900, 1500, 1800

Table 2.3.2 Main specification of FSXLIB-J3R2 and FSXLIB-JFF

item	FSXLIB-J3R2	FSXLIB-JFF
original nuclear data file	JENDL-3.2	JENDL Fusion File
production year	1994	1995
the number of nuclides	340 (all the nuclides in JENDL-3.2)	82 (all the nuclides in JENDL Fusion File)
nuclear data processing code	NJOY83/6/FNS	NJOY91.108/FNS
version of available MCNP	MCNP-3 to -4A	MCNP-4A
temperature	300 [K]	300 [K]
type and number of nuclides of gamma-ray production data	expanded photon production format, and 66	expanded photon production format, and 35
energy distribution expression	MF=5	MF=5 and 6
neutron cross section identifiers in ZAID	36 (for meta-stable states) and 37 (for elements and ground states)	41
data size in text image	328 [MBytes]	120 [MBytes]

Table 2.3.3 The nuclear data processing codes to produce a multigroup cross section library in Japan

processing code	organization	angular distribution	ENDF format	comment
MACS-N	JAERI	DDX and P_L	4, 5	developed for JENDL
NJOY91	LANL	P_L	4, 5, 6	worldwide code
RADHEAT-V4	JAERI	DDX and P_L	4, 5	for shielding safty evaluation
AMPX-77	ORNL	P_L	4, 5	
PROF-DD	JAERI	DDX	4, 5	for only neutron

Table 2.3.4 Multigroup cross section libraries using in fusion field of Japan

name of library	nuclear data file		processing code		number of groups		nuclides	temperature [K]	angular distr.	self-shielding	weight function for neutron
	neutron	photon	neutron	photon	neutron	photon					
JSSTDL-295/J32	JENDL-3.2	PHOTX	MACS-N		295	104	65	300, 600, 900, 2100	P-5	$\sigma(\sigma_0,T)$	Maxwell + 1/E
JSSTDL-295/J3	JENDL-3.1	PHOTX	MACS-N		295	104	63	300, 600, 900, 2100	P-5	$\sigma(\sigma_0,T)$	Maxwell + 1/E
FUSION-J3	JENDL-3.1	HUGO	MACS-N	NJOY83	125	40	40	300	P-5		Maxwell + 1/E
FUSION-40	JENDL-3.1	HUGO	MACS-N	NJOY83	42	21	40	300	P-5		Maxwell + 1/E
FENDL/MG1	ENDF/B-VI, etc.	?	NJOY91		175	42	56	300, 600, 900, 1200	P-6	$\sigma(\sigma_0,T)$	Maxwell + 1/E + fusion
GICX40V4	ENDF/B-IV		NJOY	GAMLEG-JR	42	21	40	300	P-5		1/E
DDXLIB-J3	JENDL-3.1		PROF-DD		125		20	300	DDX		Maxwell + 1/E
BREMJ3	JENDL-3.2		MACS-N		125		30	300	DDX		Maxwell + 1/E

Table 2.3.5 Response libraries using in fusion field of Japan

name of library	type	kind of data	nuclear data file
REACTXX	multigroup of 32, 42, 125, 135 and 175 groups for neutron and 21, 40 and 42 groups for photon	reaction cross sections, dpa, kerma factor, dose equivalent, etc.	JENDL-3PR1, -3.1, -3.2, -Dosimetry File, ENDF/B-IV, -V, etc.
FUSION-J3/KDG	multigroup of 42 and 125 groups for neutron and 21 and 40 groups for photon	kerma factor, dpa and gas production cross sections	JENDL-3.1 and -Gas Production File
APPLE-3/LIB	multigroup of 42 groups for neutron and 21 groups for photon	reaction cross sections, kerma factor and dose equivalent	JENDL-3.1, ENDF/B-IV, etc.
MCNPDOS	pointwise for MCNP dosimetry file for neutron	reaction cross sections	ENDF/B-V and ACTL
FSXDOS-J3	pointwise for MCNP dosimetry file for neutron	reaction cross sections	JENDL-Dosimetry File

2.4 Present Status of Transport Calculation Codes for Fusion Neutronics

Takamasa MORI
Reactor System Laboratory
Japan Atomic Energy Research Institute
Tokai-mura, Naka-gun, Ibaraki-ken 319-11

In fusion neutronics, one needs to perform transport calculations to predict neutron and photon fluxes and a number of important nuclear responses. To treat the special features of fusion neutronics, the calculation methods developed for the fission reactors have been modified, and the prediction accuracy has been much improved. In this paper, transport codes used in this field are reviewed focusing on the continuous energy Monte Carlo codes widely used for recent integeral tests of nuclear data and nuclear design of fusion reactors.

1. Introduction

In fusion neutronics, transport calculations are required to predict neutron behavior and neutron-induced phenomena. Many transport calculation codes using various approximation methods have been developed for core and shielding analysis of fission reactors[1)2)]. However, specific features of fusion neutronics, such as highly anisotropic neutron and photon fields due to spatially and energetically localized neutron source, required improvement of the calculation methods to achieve sufficient accuracy. For the integral test of nuclear data, especially, high accuracy of calculation methods is important to reduce uncertainty caused by the method. In 1980s, many works were carried out to improve the multigroup method by using double-differential cross sections and several codes have been developed[3)4)5)6)]. These codes were successfully used in the integral test for JENDL-3 evaluation and the JAERI/US collaborative program on fusion neutronics[7)]. In late years, however, the continuous energy Monte Carlo method has been widely used as a main tool to obtain a reference solution or to analyze experiments as precisely as possible in this field. It is expected that the application area of this method becomes wider and wider keeping pace with an advent of computer environment such as vector and/or parallel super computers.

Transport calculation codes and approximation methods used in the fusion neutronics area

in Japan are summarized in Table 1. In the following, main capabilities of those codes are briefly presented focussing on the continuous energy Monte Carlo codes most widely used in recent analysis for integral test of nuclear data.

2. Deterministic codes

All the deterministic codes in Table 1 are based on the multigroup and discrete Sn method. These codes are classified into two groups depending on treatment of scattering anisotropy. One uses the Legendre expansion type cross sections (ANISN[8], DOT[9]). The other uses the double-differential form ones (NITRAN[3], *-DD series[4], BERMUDA series[5]). The former codes were developed for fission reactors, but are used in blanket and shielding design studies for fusion reactors because of inexpensive calculation cost and sufficiently prepared cross section libraries and auxiliary programs. The latter codes were developed for fusion neutronics before the previous specialist meeting on the nuclear data for fusion neutronics. The details are given in the reference of each code.

3. Monte Carlo codes

Since the first stage of fusion neutronics, the Monte Carlo codes have been used to precisely treat complicated geometry encountered in fusion neutronics calculations. The multigroup code MORSE-DD[4], which can use the multigroup double-differential form cross sections, has been developed in JAERI and successfully used in the JAERI/US collaborative program on fusion neutronics[7]. To achieve a higher speed Monte Carlo calculation by using a vector supercomputer, JAERI has developed a vectorized code GMVP[10] based on the multigroup model, which has similar functions to MORSE-DD.

According to recent progress of computer capability, more accurate continuous energy Monte Carlo codes have begun to be used as a powerfull tool for fusion neutronics calculations, especially for analyses of experiments. The recent versions of a widely used code MCNP and a domestically developed code MVP are presented below.

MCNP

The MCNP code is one of the most widely used continuous energy Monte Carlo codes in the world. The capabilities of the latest version MCNP 4A[11] released in 1993 are summarized in Fig.1. This code treats an arbitrary three-dimensional configuration in geometric cells bounded by first-,

second- and some special fourth-degree surfaces. Continuous energy cross section data are used, though multigroup data may also be used. Fixed-source adjoint calculation can be made with multigroup cross section data. For neutrons, all reactions given in evaluated data are taken into account. Both free gas and S(α,β) thermal treatments are available. Criticality sources are available as well as fixed volume and surface sources. A general source and tally structures are available. In the latest version, the tallies include extensive statistical analyses of convergence such as estimation of variance of variance to predict the reliability of calculation results from a statistics viewpoint. Rapid convergence can be achieved by a variety of variance reduction techniques. Parallel processing is available on a cluster of several workstation by using the PVM software package developed in ORNL.

At the present stage, the MCNP 4A code is only one code which is available for the file 6 data (energy-angle correlated distribution) of the ENDF/B-VI format.

MVP

Algorithmic studies of neutron and photon transport Monte Carlo simulation suitable for vector supercomputers have been made, and general purpose Monte Carlo codes MVP[10] has been developed in JAERI. This codes realized a higher computation speed by a factor of about 15 compared with the conventional Monte Carlo codes on the FACOM VP2600 vector supercomputer. In order to achieve more speedup, the code has been applied to the following three types of parallel computers or parallel processing environments[12].

(1) Vector-parallel: MONTE-4 at JAERI (equivalent to NEC SX-3) with 4 vector processors and a shared memory.

(2) Massive parallel: AP1000 developed by Fujitsu corporation with up to 512 RISC processors and 16 megabytes distributed memories.

(3) Workstation cluster: several workstations connected to a network by PVM.

On the vector-parallel supercomputers and the massive parallel computer, speedup almost proportional to the number of processors have been obtained by assigning particles uniformly to each processor. On the workstation cluster, on the other hand, effective parallel computations required the modification of particle assignment method taking into account the calculation power of each workstation.

In 1994, the MVP code has been released for public use in Japan, together with the multigroup version GMVP (version 94.1)[10]. Since then, these codes have been used at almost research institutes studying the nuclear engineering in Japan. Figure 2 summarizes the main

functions of the released version.

After the release at 1994, the following functions are added to the code.

(1) General Source Routine : equivalent to MCNP ?

(2) Tallies

- Time-dependent tallies
- Reaction rate tallies for MCNP dosimetry libraries
- Arbitrary energy bins and time bins

(3) Parallel computation on FACOM VPP-500/42 (vector-parallel Masine with distributed memories) : 16PEs at maximum

The capabilities of scattering analysis with the file 6 data of ENDF/B-VI format and point detector estimator are under development.

Reference

1) G.I. Bell and S. Glasstone, 'Nuclear Reactor Theory,' Van Nostrand Reinhold, 1970.
2) E.E Lewis and W.F. Miller, Jr., 'Computational Methods of Neutron Transport,' John Wiley & Sons, 1984.
3) A. Takahashi and D. Rusch, KfK 2832/I and II , Kernforschungszentrum Karlsruhe (1979)
4) T. Mori, et al., JAERI-1314, Japan Atomic Energy Research Institute (1988).
5) T. Suziki, et al., JAERI-1327, Japan Atomic Energy Research Institute (1992).
6) N. Yamano, et al., JAERI-1316, Japan Atomic Energy Research Institute (1989).
7) Fusion Technol., 28(1), 1995 and 28(2), 1995.
8) W.W. Engle, K-1693, Union Carbide Corporation, Computing Technology Center (1967).
9) W.A. Rhodes and F.R. Mynatt, ORNL-TM-4280, Oak Ridge National Laboratory (1973).
10) T. Mori and M. nakagawa, JAERI-Data/Code 94-007 (in Japanese), Japan Atomic Energy Research Institute (1994).
11) J. Briesmeister (Editor), LA-12625, Los Alamos National Laboratory (1993).
12) M. Sasaki, et al., Computer Assisted Mechanics and engineering Sciences, **1**, 177 (1994).

Table 1 Transport codes and their calculation methods used for fusion neutronics

<table>
<tr><th rowspan="2">Transport code (*)</th><th colspan="4">Calculation (approximation) method</th></tr>
<tr><th>Energy</th><th>Flight direction</th><th>Scattering anisotropy</th><th>Solution method</th></tr>
<tr><td>ANISN (1D)
DOT (2D)</td><td rowspan="5">multigroup</td><td rowspan="3">discrete S_N</td><td>Legendre expansion</td><td rowspan="2">finite difference</td></tr>
<tr><td>ANISN-DD, NITRAN (1D)
DOT-DD (2D)</td><td rowspan="2">DDX</td></tr>
<tr><td>BERMUDA (1D,2D,3D)</td><td>direct integration</td></tr>
<tr><td>MORSE (3D)</td><td rowspan="3">continuous</td><td>Legendre expansion</td><td rowspan="3">Monte Carlo</td></tr>
<tr><td>MORSE-DD, GMVP (3D)</td><td>DDX</td></tr>
<tr><td>MCNP, MVP (3D)</td><td>continuous energy</td><td>nuclear data + kinematics etc.</td></tr>
</table>

* 1D, 2D and 3D mean one-, two- and three-dimensional codes, respectively.

MCNP4A
Monte Carlo N-Particle Transport Code System
Dec., 1993, (LANL)

- Nature of Problem Solved:
  General-purpose, continuous-energy,
  generalized-geometry, time-dependent,
  coupled neutron-photon-electron Monte Carlo

- Geometry: 1-, 2-, 4-degree surfaces
  with repeated geometry

- Cross sections:
  Neutron: all reactions in evaluated data
  free gas and S(α, β) thermal treatments
  ENDF/B-VI, File 6
  Law=44:file 6 law=1 lang=2
  Kalbach-87 correlated E-A scattering
  Law=66:file 6 law=6
  N-body phase space distribution
  Law=67:file 6 law 7
  correlated E-A scattering
  Photon:

incoherent	with or without
cohrerent	electron binding effects
photoelectric	with fluorescent emission
pair creation	with annihilation radiation

- Very general source and tally structure
- Extensive statistical analysis
- Wide variety of variance reduction methods
- Available computers:
  UNIX WS, MS-DOS PCs, Cray, VAX, IBM mainframe
  etc.
- Multiprocessing on a workstation cluster (PVM)

Fig. 1 Main function of MCNP 4A

MVP/GMVP
General-purpose Monte Carlo Codes for
Neutron and Photon Transport Calculations
Based on Continuous and Multi-group Methods
(Version 94.1)
Aug., 1994, JAERI

Function of MVP

- Particles : Neutron、Photon (Bremsstrahlung X-ray included)
- Problem to be solved : fixed-source、eigenvalue(k_{eff})
- Cross sections : continuous energy
  Neutron : 10^{-5} eV～20 MeV
  Thermal scattering : Sαβ
  Unresolved resonances : cross section probability table
  File 6 of ENDF/B-VI Format is not available
  Photon : 1 keV～100 MeV(similar model to MCNP4A)
  Bremsstrahlung X-ray : thick target approximation
- Geometry model : Combinatorial geometry (CG) with repeated geometry capability by lattice
- Tally : keff, flux,
  reaction rates
  multi-group response function
  reactions used for transport calculations
  multi-group effective cross sections
- Estimator : Track length, Collision
  Analog (k_{eff})
- Variance Reduction Techniques :
  Russian roulette & splitting
  (cell importance, weight window)
- Speedup by vectorization : vs. scalar codes
  ～15 (on Facom VP-2600)
- Speedup by parallelization
  Vector-Parallel computer (NEC SX-3, 4 CPU)
  UNIX EWS Cluster (by using PVM)
  Massive parallel (Fujitsu AP-1000, 512 PEs)

Fig. 2 Main function of MVP 94.1

3. Integral Test of Neutron and Secondary Gamma-ray Data (I)

3.1 Integral Data Test of JENDL-3.2 and Fusion File Using FNS Benchmark Experiments

Yukio OYAMA, Fujio MAEKAWA and Masayuki WADA
Japan Atomic Energy Research Institute
Tokai-mura, Naka-gun, Ibaraki-ken 319-11
oyama@fnshp.tokai.jaeri.go.jp

JENDL-3.2 and JENDL Fusion File were tested by using benchmark experiments performed at FNS in JAERI. These experiments are the time-of-flight experiment measuring angular leakage flux and the insystem reaction rate measurements and the tested materials are Li, Be, C, N, O, Fe Cu, W, Pb for slab assemblies. The calculations were made by MCNP. The result shows that JENDL-Fusion File is the best agreements with the experiments in overall.

1. Introduction

JENDL-3.2[1]and JENDL Fusion File (JENDL-FF)[2] was developed for fusion application to solve the problems found in the previous JENDL 3.1 nuclear data file.[3] The JENDL Fusion File used ENDF-6 format[4] for energy-angular distribution for secondary emission neutrons and was submitted to IAEA/NDS for one of the FENDL-2[5] candidates. At the same time, Fusion Neutronics Integral Test Working Group was organized under Japan Nuclear Data Committee to perform benchmark testing for JENDL-3.2 and JENDL Fusion File. The working group selected the fusion integral experiments from the existing Japanese benchmark experiments.

The selected experiments include the FNS experiments on slab assemblies, i.e., the angular leakage neutron flux spectra measurement using the time of flight method and the insystem experiments on reaction rates and neutron and gamma-ray spectra.[6] The geometry of the experiments is slab. Materials included in the benchmark experiments are Li_2O, Be, C, N, O, Fe, Pb for the time-of-flight experiment and Li_2O, Be, C, Fe, Cu, W for the insystem experiments. Table 1 summarizes the materials and the experimental types used for those benchmark experiments. The international library FENDL/E-1[7] that is developing under the IAEA is also to be tested. Therefore, the benchmark calculations were performed for three nuclear data libraries, i.e., JENDL-3.2, JENDL-Fusion File and FENDL/E-1.

2. Calculation

The calculation was performed by using the MCNP-4A Monte Carlo code[8] with the

FSXLIB-J3R2[9] and the FSXLIB-JFF[10] libraries that were processed from the JENDL-3.2 and the JENDL Fusion File by NJOY83.6 and NJOY91.108[11], respectively. The FSXLIB-JFF includes 82 nuclides and 23 elements, and the FSXLIB-J3R2 for 340 nuclides. This version of the JENDL Fusion File was replaced for Pb and W data by re-evaluations due to the previous benchmark test. For FENDL/E-1, FENDL/MC-1[11] library was used which was provided the IAEA/NDS. In the MCNP calculations, the point estimator was adopted for the leakage experiment and the track length estimator was used for the insystem parameters. The reaction rate data were calculated by JENDL Dosimetry File. The calculated results were compared with the experimental values in terms of the calculated to experimental value ratio (C/E). This comparison was applied to the spectrum results by energy region-wise integration and the reaction rate results.

3. Results and Discussion

Li2O

Angular flux spectra from the slab calculated by JENDL-3.2 showed good agreements as well as the other nuclear data files. The C/Es of the tritium production rates, that is the most important reactions as $^{6}Li(n,\alpha)$ and $^{7}Li(n,n\alpha)$ inside the Li2O slab, also showed excellent agreements within experimental errors.

Be

Angular flux spectra from the slab calculated by JENDL-FF showed very good agreements with the measured spectra compared to the JENDL-3.2 because JENDL-FF was newly evaluated considering experimental data of α particle emission spectra. Specially in the energy region of 0.8 to 2 MeV, the spectrum was improved much as shown in Fig. 1(a). One can see in the figure 1(b) that this trend is similar to the reaction rate of $^{115}In(n,n')^{115m}In$ in the slab. In low energy, however, all the calculations overestimated $^{197}Au(n,\gamma)$ reaction.

C

For graphite, there is little difference between the experiment and both the results by JENDL-3.1 and JENDL-3.2, but large disagreement with the experiment in FENDL-1 as seen in Fig.2(a). The FENDL has softer spectrum for continuum inelastic neutrons. This also affect on high energy neutron transmission as shown in Fig.2(b) in which the C/E of $^{93}Nb(n,2n)$ reaction increases with depth.

N

Figure 3 shows that JENDL-3.2 is in good agreement between the other two libraries. However, all the calculations tend to underestimate the angular flux spectrum with increasing emission angle, but JENDLs are much better than FENDL-1.

O

Figure 4 shows that all the files show good agreements with the experiment, but still

somehow tends to underestimate the spectrum with increasing angle.

Fe

From the insystem response measurements, in overall the calculation by JENDL-FF showed good agreement as well as FENDL-1, but , for high energy flux, there exists a trend to underestimation with increasing the depth as shown in Fig. 5(a)-(c). In comparison between JENDL-FF and JENDL-3.2 for low energy region, one can find a little improvement in the C/E values for the energy range of 0.1 to 100 keV as shown in Fig.5(d)-(f). This is only one example which shows the effect to improve the calculation by ENDF-6 format representation.

Cu

For the insystem neutron spectrum in a copper slab, it can be seen that there is large underestimation of low energy neutron spectrum below 500 eV by 50% and overestimation in 5-50 keV range for all libraries .

W

In the insystem spectrum, JENDL-FF and FENDL-1 show good agreements with the experiment above 0.1 MeV, but below 0.1 MeV it seems that FENDL-1 is better than JENDLs though the experimental error is large. However, when the reaction rates of $^{93}Nb(n,2n)^{92m}Nb$ and $^{197}Au(n,\gamma)^{198}Au$ inside the tungsten slab were checked, JENDLs are better. For high threshold reaction, FENDL-1.0 shows trend of overestimation with increasing the depth while, for low energy sensitive reaction, FENDL-1.0 shows underestimation with depth. On the other hand JENDLs show better agreements for both reactions. Considering the experimental error, the low energy neutrons calculated by JENDLs may be correct.

Pb

The preliminary version of JENDL-FF that was basically the same as JENDL-3.2 showed large overestimation of the flux below 1 MeV. Since the present lead data of JENDL-FF was modified, the calculated angular flux spectra of JENDL-FF were in very good agreements with the experiment.

4. Concluding Remarks

JENDL-3.2 and JENDL Fusion File were validated by using the existing benchmark experiments. According to comparison to the JENDL-3.2, the JENDL Fusion File improved the low energy spectrum of the iron slab experiment by file-6 format representation. JENDL Fusion File also showed better results for Be, W and Pb than JENDL-3.2. For nitrogen and oxygen, agreements were slightly worse. In overall, the results of Li, Be, C, Cu and W are satisfactory, but for iron there may be problems in elastic cross section.

References

1) Nakagawa T.: "JENDL-3 Revision 2," JAERI-M 94-019, pp.68-78 (1994)

2) Chiba S., Yu B. and Fukahori T.: JAERI-M 94-027, pp. 35-44 (1992)
3) Shibata K. and JENDL-3 Compilation Group: JAERI 1319 (1990)
4) Rose P.F. and Dunford C.L.:" ENDF-6 Formats Manual," IAEA-NDS-76 (1992)
5) Ganesan S.: Summary Report of the IAEA Advisory Group Meeting, Tokai, Japan, 8-12 Nov., 1993, IAEA-NDS-297 (1994)
6) Sub Working Group of Fusion Reactor Physics Subcommittee: " Collection of Experimental Data for Fusion Neutronics Benchmark," JAERI-M 94-014 (1994)
7) Ganesan S. and MacLaughin P.K.: IAEA-NDS-128 (1995)
8) Briesmeister J. F., Ed.: LA-12625-M, Los Alamos National Laboratory (1993)
9) Kosako K., et al.: "FSXLIB-J3R2: A Continuous Energy Cross Section Library for MCNP Based on JENDL-3.2," JAERI-Data/Code 94-020 (1994)
10) Kosako K., et al.: "FSXLIB-JFF:A Continuous Energy Cross Section Library for MCNP Based on JENDL Fusion File," private communication (1995)
11) MacFarlane R.E. Muir D.W. and Boicourt R.M.: " The NJOY Nuclear Data Processing System," LA-9303-M (ENDF-324) (1982)

Table 1 Materials used in the benchmark experiments, and materials included in JENDL Fusion File.

Material	Angular Flux Experiment by Time-of-flight	Insystem Response Experiment	Inclusion to JENDL-Fusion File
Li_2O	Yes	Yes	No
Be	Yes	Yes	Yes
C	Yes	Yes	No
N	Yes	No	No
O	Yes	No	No
Fe	Yes	Yes	Yes
Cu	No	Yes	Yes
W	No	Yes	Yes
Pb	Yes	No	Yes

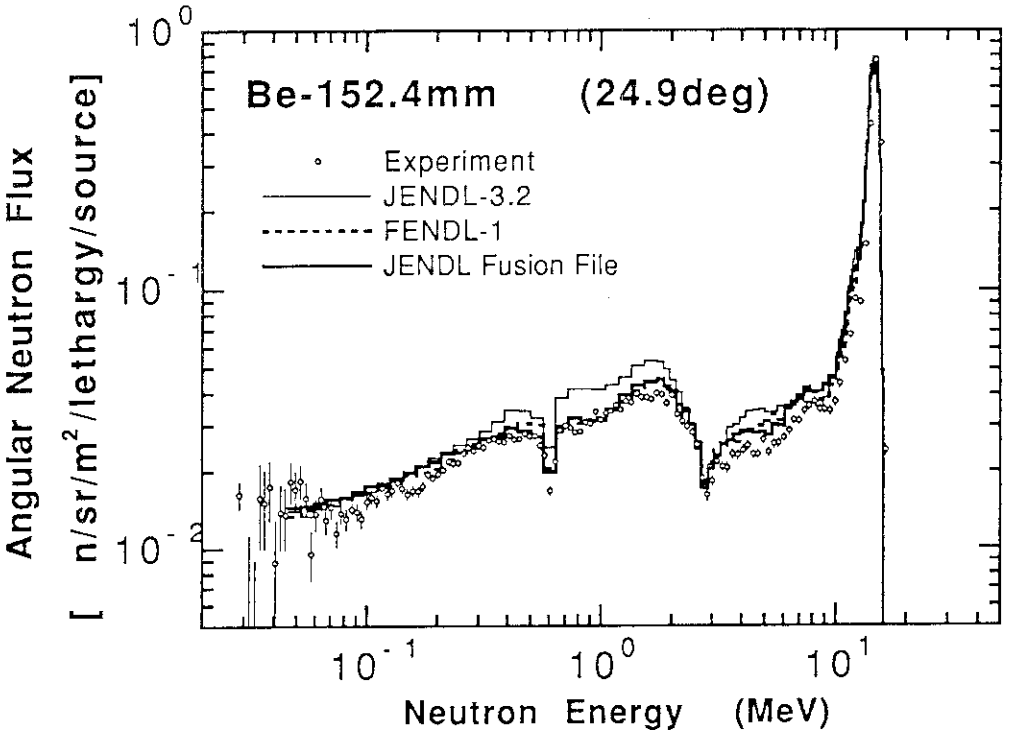

Fig.1(a) Angular neutron leakage flux from the beryllium slab of 152.4 mm in thickness.

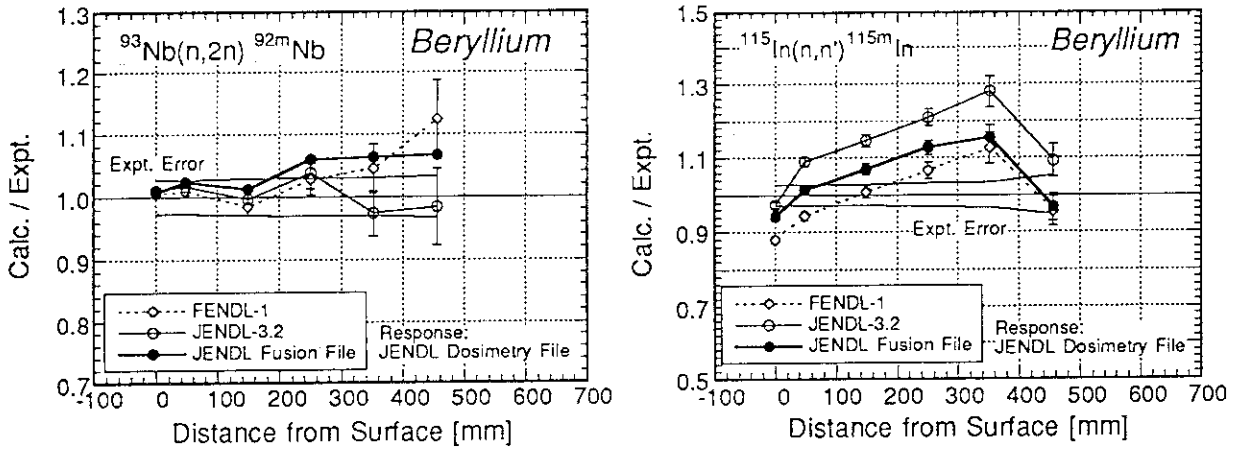

Fig.1(b) Comparison of the calculated to experiment ratio (C/E) of reaction rates of $^{93}Nb(n,2n)^{92m}Nb$ and $^{115}In(n,n')^{115m}In$ reactions inside the beryllium slab of 450 mm in thickness.

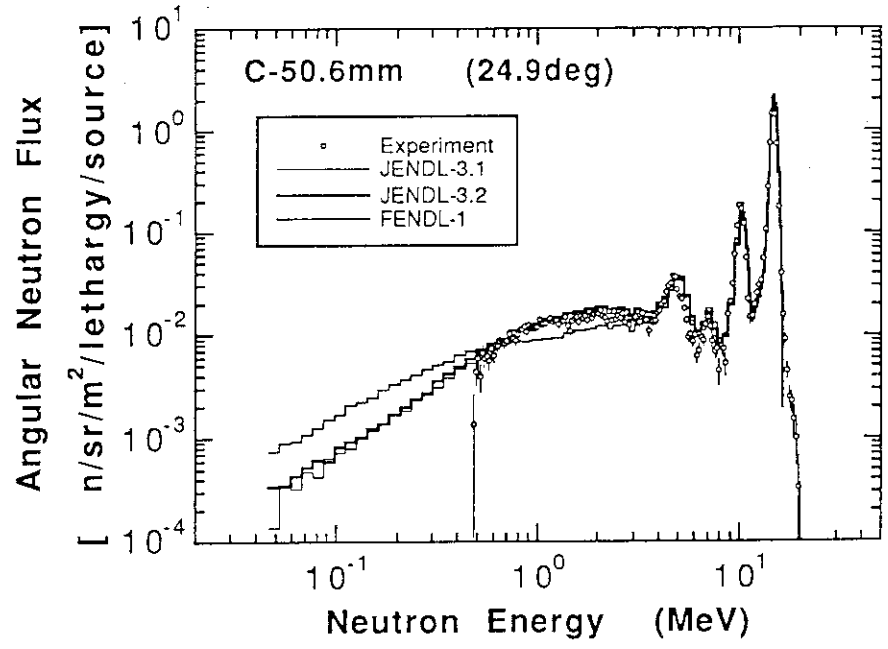

Fig.2(a) Angular neutron leakage flux from the graphite slab of 50.6 mm in thickness.

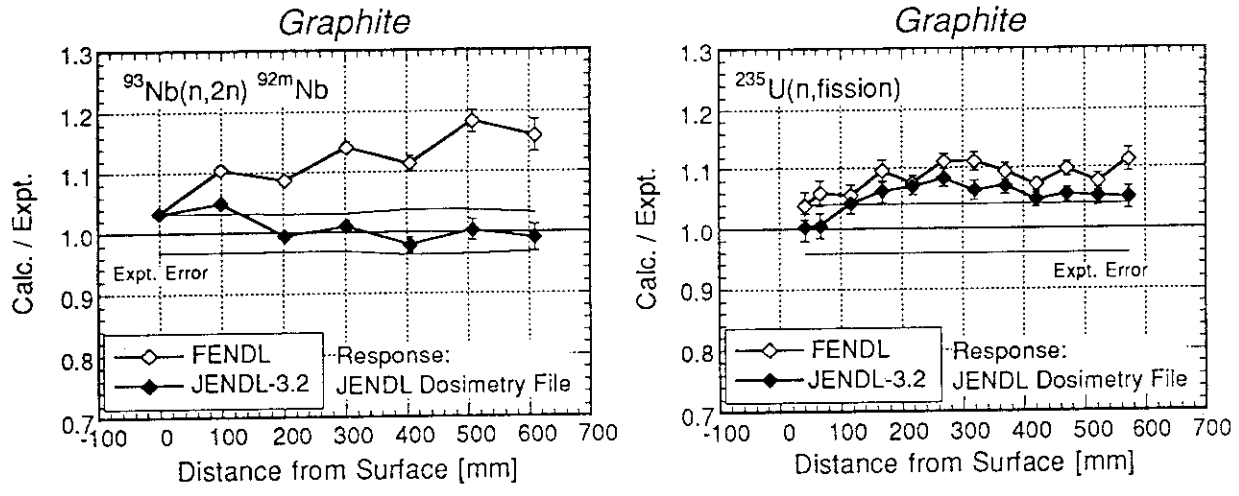

Fig.2(b) Comparison of the calculated to experiment ratio (C/E) of reaction rates of $^{93}Nb(n,2n)^{92m}Nb$ and $^{235}U(n,fission)$ reactions inside the beryllium slab of 600 mm in thickness.

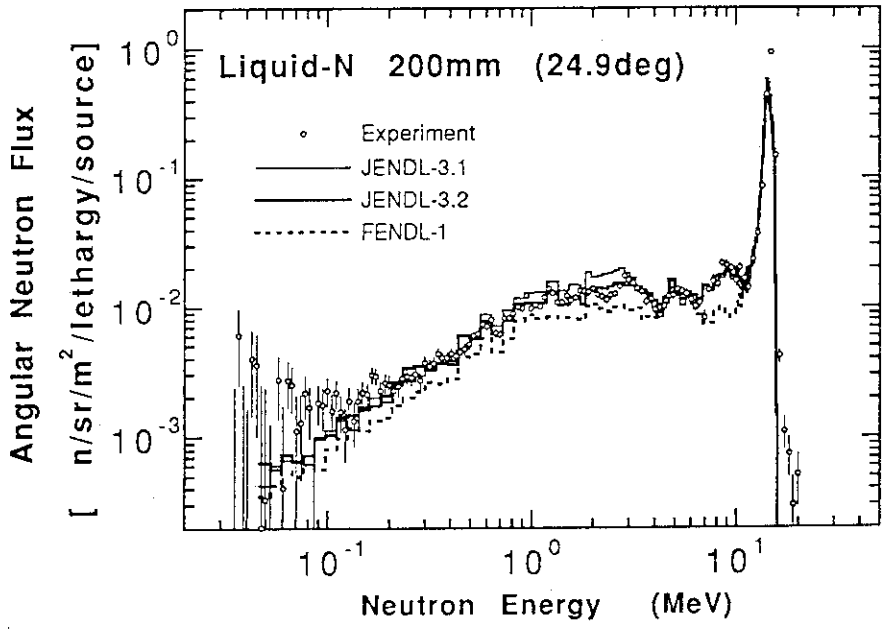

Fig.3 Angular neutron leakage flux from the liquid nitrogen slab of 200 mm in thickness.

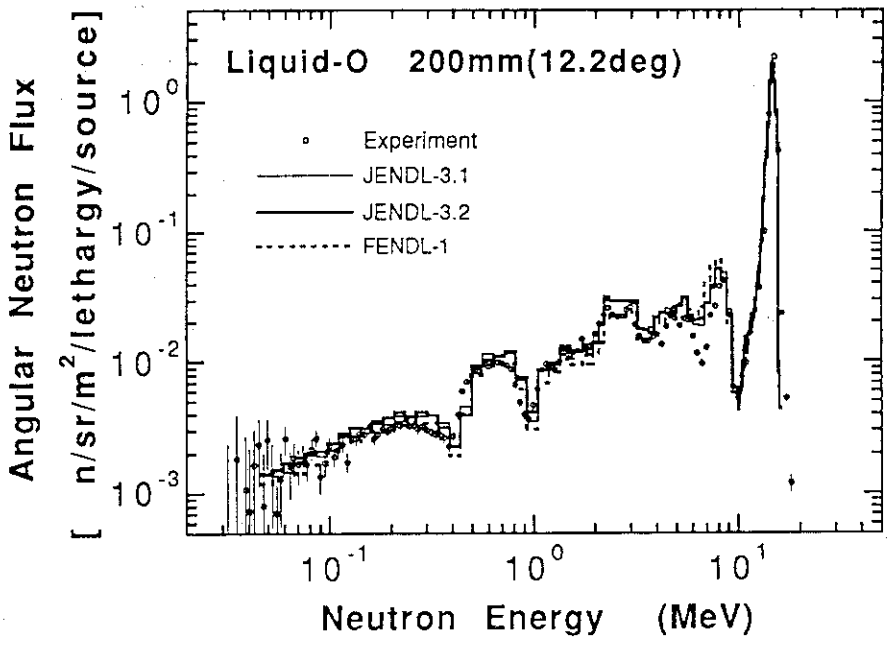

Fig.4 Angular neutron leakage flux from the liquid oxygen slab of 200 mm in thickness.

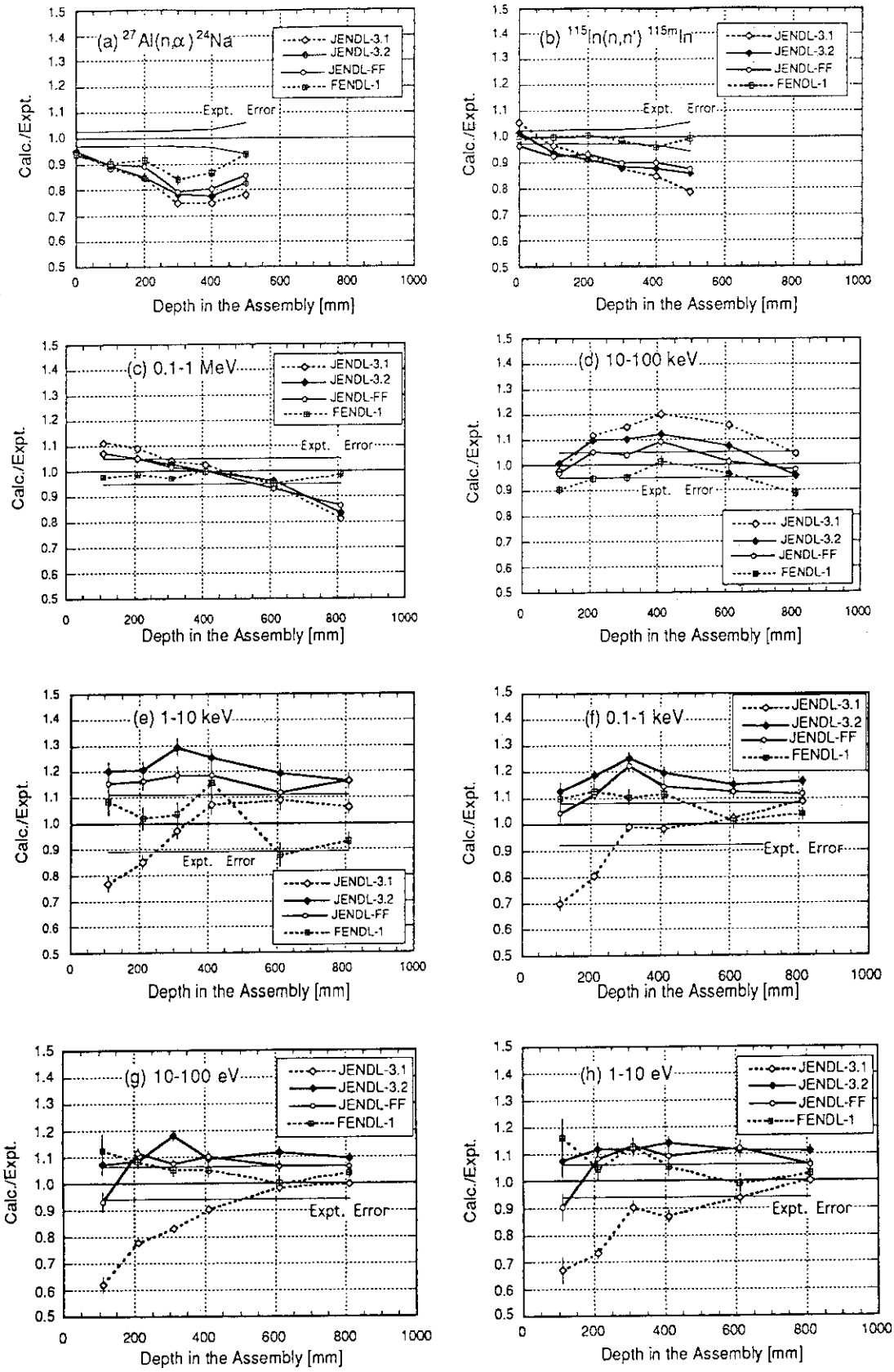

Fig.5 The C/E plots of integral flux in various energy ranges for the iron slab of 1 m in thickness

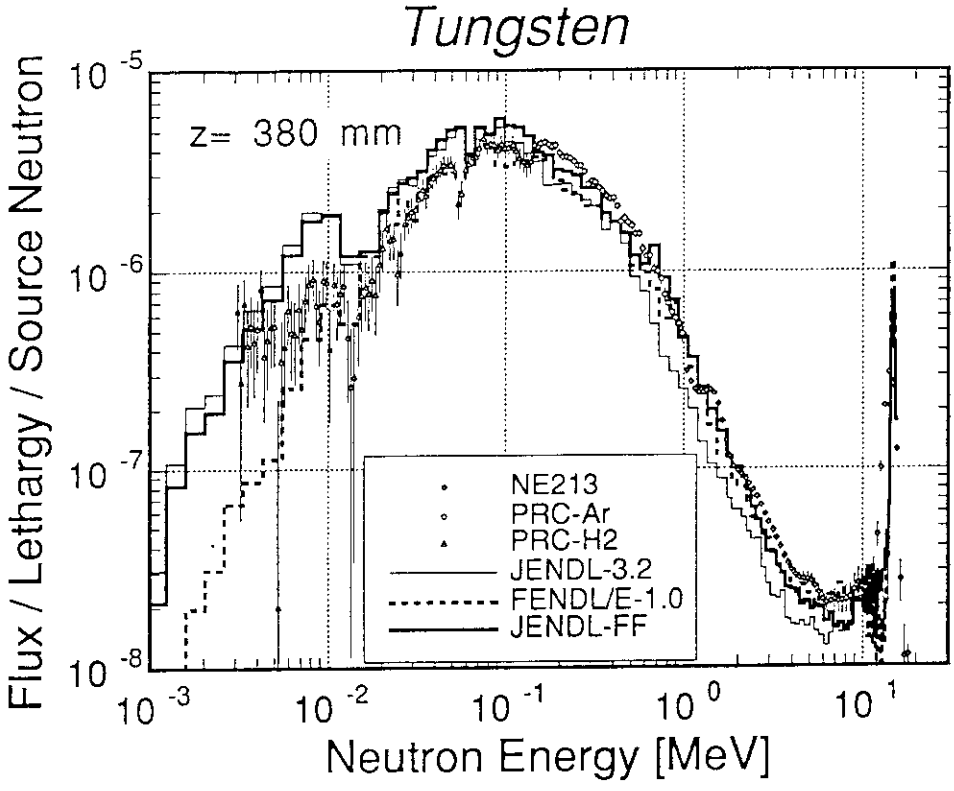

Fig.6(a) Insystem scalar neutron spectrum inside the tungsten slab of 500 mm in thickness

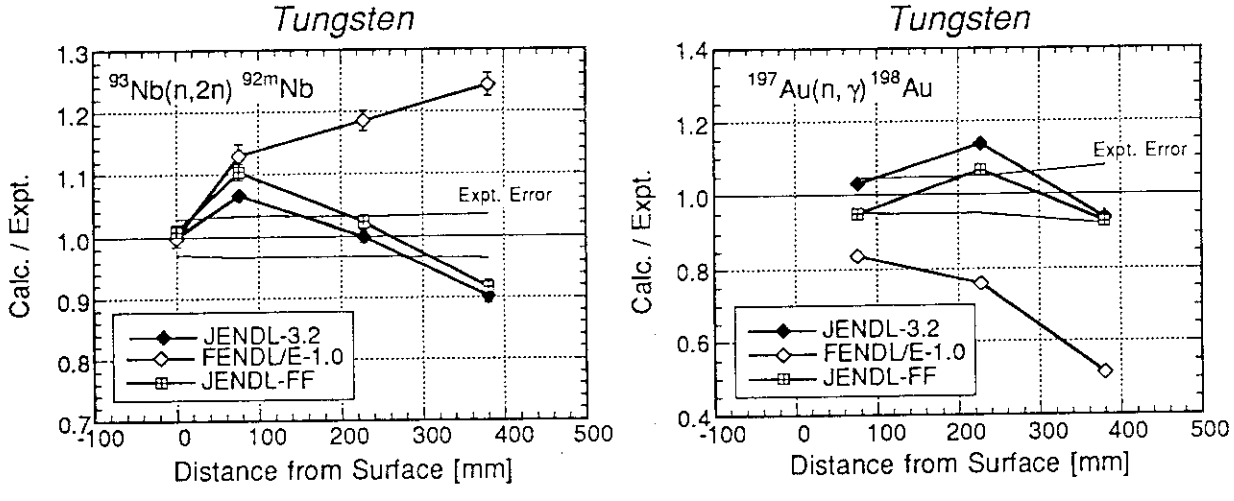

Fig.6(b) Comparison of the calculated to experiment ratio (C/E) of reaction rates of $^{93}Nb(n,2n)^{92m}Nb$ and $^{197}Au(n,\gamma)^{198}Au$ reactions inside the tungsten slab of 500 mm in thickness.

3.2 Benchmark Study on Neutron Cross Sections Based on Pulsed Sphere Experiment

Chihiro ICHIHARA[a], Shu A. HAYASHI[b], Itsuro KIMURA[c], Junji YAMAMOTO[d], Yo MAKITA[e], Akito TAKAHASHI[e], Kotaro UEKI[f] and Katsumi HAYASHI[g]

[a]*Research Reactor Institute, Kyoto University*
Kumatori−cho, Sennan−gun, Osaka 590−04, Japan

[b]*Institute for Atomic Energy, Rikkyo University*
Nagasaka, Yokosuka, Kanagawa 240−01, Japan

[c]*Department of Nuclear Engineering, Kyoto University*
Yoshida−honmachi, Sakyo−ku, Kyoto 606−01, Japan

[d]*Department of Engineering, Setsunan University*
Ikeda−nakamachi, Neyagawa, Japan

[e]*Department of Nuclear Engineering, Osaka University*
Yamada−oka, Suita, Osaka 565, Japan

[f]*Ship Research Institute, Ministry of Transport*
Shinkawa, Mitaka, Tokyo 181, Japan

[g]*Hitachi Engineering Co., Ltd.*
Saiwai−cho, Hitachi, Ibaraki, 317, Japan

Benchmark validation of neutron cross sections was performed by comparing theoretical calculated leakage spectra with measured ones by means of pulsed sphere experiment conducted at OKTAVIAN of Osaka university, FZK, German and IPPE Obninsk, Russia. It was found out that the nuclear data of Be in both JENDL Fusion File and ENDF/B−VI had similar trend in each experiment. However, there exists some discrepancy among the three different experiments, which suggests further study is needed to validate Be nuclear data.

Calculated spectra for Li, Cr, Mn, Cu, Zr, Nb and Mo using JENDL Fusion File predict the experiment fairly well. However, for LiF, $(CF_2)_n$, Si, Ti, Co and W, the calculated spectra are not in good agreement with the measurement. The prediction using FENDL−1.0 data gives ^N^N agreement in case of Li, Cr, Mn, Cu and Mo, whereas in other case, the prediction gives insufficient result.

The analysis of Fe and Pb experiment conducted at IPPE Obninsk showed that Fe data in JENDL Fusion File and JENDL−3.2 were much better than FENDL/E−1.0. Pb data in JENDL Fusion File appeared to have been much improved as compared with JENDL−3.2 evaluation.

1. Introduction

1) Nuclear data libraries

Nuclear data libraries are of essential importance for designing nuclear fusion reactors. For selecting an suitable evaluated nuclear data set for the future requirement including a fusion task, FENDL nuclear data project[1] is now being carried out under the auspices of nuclear data

section of IAEA. After the first release of FENDL/E-1.0[1], the selection of the next candidate file had already started. Recently, several nuclear data files have been published in the world. JENDL-3.2[2] has been released in 1995 as the second revision of JENDL-3[3]. JENDL Fusion File has been released as the special purpose file of JENDL-3.2 by adding DDX representation of secondary neutrons. As these files are positive candidate for the next FENDL libraries, it is important to make benchmarking these data files. In this paper, the calculations using cross section libraries processed from JENDL Fusion File, JENDL-3.2 and FENDL/E-1.0 are compared with the pulsed sphere experiment conducted at OKTAVIAN of Osaka university, Forschungs Zentrum Karlsruhe (FZK), Germany and IPPE Obninsk, Russia in order to validate neutron cross section data for several nuclide and elements including essential elements for fusion reactors such as Be, Fe, Pb, etc.

2. Experiment and Analysis

1) OKTAVIAN experiment and analysis

OKTAVIAN is an intense neutron source facility[4] of Osaka university. Series of the leakage neutron spectrum measurement from spherical samples have been performed at OKTAVIAN. The samples were Be, Li, LiF, $(CF_2)_n$, Al, Si, Ti, Cr, Mn, Co, Cu, As, Zr, Nb, Mo and W. All the samples except for Be were packed in spherical shells. For Be measurement, a set of beryllium spherical shells were used to make spheres with four different thickness by combining these shells. The thickness of Be sample covers from 4.55 to 11.65 cm. An NE218 liquid scintillation counter was used as a neutron detector and was located about 11 m from the center of a spherical sample. The detail of the experiment have been explained previously[5),6)]. The diameters, each weight of the sample and the thicknesses of the samples other than Be are listed in **Table-1**. The numerical data of the experimental result can be downloaded from IAEA Nuclear Data Section[7].

The theoretical calculation was performed using a continuous energy Monte Carlo code MCNP4A[8]. Neutron libraries used for the calculation were, 1) three JENDL based libraries – FSXLIB-J3[9] from JENDL-3.1, FSXLIB-J3R2[10] from JENDL-3.2 and FSXLIB-JFF[11] from JENDL Fusion File, 2) FENDL/MC1[12] from FENDL/E-1.0 which consists of ENDF/B-VI[13], JENDL-3.1 and BROND-2[14]. The source was assumed as an isotropic point source and surface crossing tally was adopted to get the results.

2) Analysis of KANT (KArlsruhe Neutron Transmission experiment) experiment

Leakage neutron spectra from a set of spherical beryllium shells of which thickness was 5, 10

and 17 cm have been measured at FZK Karlsruhe, Germany. The detailed description of this experiment is given in **Ref. 15**.

Theoretical calculation was performed by using MCNP4A with the above-mentioned libraries and an EFF-1 based library.

3) Analysis of Obninsk experiment

A Be spherical sample was used. The outer and inner radii were 11 and 6 cm, respectively. Spherical samples of Fe and Pb with a 12 cm outer radius and a 4.5 cm inner radius were used for the experiment. The analysis was also performed using MCNP4A. The calculations for the Be and Pb samples were performed with FSXLIB-J3R2 and FSXLIB-JFF. For the Fe sample FENDL/MC-1.0 was used in addition.

Table-1 Various parameters of the sphere samples

Sample	Diameter (cm)	Weight (kg)	Apparent density (g/cm^3)	Sample thickness	
				(cm)	MFP
Li	40	14.25	0.53	9.8	1.3
LiF	61	198.0	1.79	27.5	3.5
TEFLON	40	34.7	1.30	9.8	0.7
Al	40	32.8	1.22	9.8	0.5
Si	60	138.05	1.30	20.0	1.1
Si	40	34.85	1.30	9.8	0.55
Ti	40	41.20	1.54	9.8	0.5
Cr	40	99.7	3.72	9.8	0.7
Mn	61	480.0	4.37	27.5	3.4
Co	40	52.0	1.94	9.8	0.5
Cu	61	675.0	6.01	27.5	4.7
Zr	61	311.9	2.84	27.5	2.0
Nb	28	47.7	4.39	11.2	1.1
Mo	61	236.0	2.15	27.5	1.5
W	40	118.6	4.43	9.8	0.8

3. Results and discussion

1) Be experiment

The **Figs. 1 to 4** show measured and calculated leakage spectra from 4.55, 7.65, 10.45 and 11.65 cm thick Be spheres of the OKTAVIAN experiment. In case of the 4.55 cm thick sphere, JENDL-3.2 predicts the experiment rather well, whereas the other two data files underpredict the experiment below 2.5 MeV. In case of the 7.65 and 10.45 cm thick spheres, strong underprediction lies below about 9 MeV and above few MeV region. On the other hand, underprediction become lower for the 11.65 cm sphere.

In the **Figs. 5** to **7**, the measured and calculated leakage spectra from 5, 10 and 17 cm thick Be spheres of KANT experiment. The calculated spectra using Be data in JENDL Fusion File are fairly in good agreement with the measured ones. However, an underestimation of low-energy neutron leakage is observed with the thinner shells for the JENDL Fusion File as well as other libraries. Such discrepancy disappears with increasing beryllium thickness and may be due to a single-collision effect, i.e. emission of neutrons of such low energies directly from Be(n,2n) or Be(n,n') reactions.

The **Table-2** shows the C/E values for the experiment at IPPE Obninsk. The C/E trend of both calculation is quite different from the above two results.

To summarize the three different Be study, it should be emphasized that;

- The C/E trend in the 4.55 cm thick sphere case at OKTAVIAN is inconsistent with the 5 cm thick sphere case at IPPE Obninsk.
- Though there is a large underestimation of the OKTAVIAN experiment from 10.45 cm thick Be sphere, no such discrepancy can not be observed in the 10 cm sphere KANT experiment.

Table-2 Calculated to experimental ratio of integrated leakage current from 5 cm thick Be sphere

Energy (MeV)	JENDL-3.2	JENDL Fusion File
0.4-0.8	0.856	0.712
0.8-1.4	0.971	0.752
1.4-2.5	1.091	0.970
2.5-4.0	1.187	1.160
4.0-6.5	1.115	1.026
6.5-10.5	0.944	0.926
10.5-15.0	1.089	1.100

Table-3 Calculated to experimental ratio of integrated leakage current from 7.5 cm thick Fe sphere

Energy (MeV)	JENDL		FENDL/ MC-1.0
	3.2	Fusion File	
0.2-0.4	0.961	0.965	0.797
0.4-0.8	0.882	0.882	0.808
0.8-1.4	0.915	0.913	0.890
1.4-2.5	1.000	0.996	0.961
2.5-4.0	0.876	0.881	0.982
4.0-6.5	0.897	0.895	1.071
6.5-10.5	1.031	1.034	1.224
10.5-15.0	0.874	0.911	0.907

Since beryllium is a very important nuclide for fusion reactors, further study should be performed to get acceptable knowledge about Be cross sections.

2) Fe and Pb Experiment

In the **Table-3**, C/E values of integrated leakage current for the Fe sample are listed. JENDL-3.2 and JENDL Fusion File give much better prediction than the FENDL/E-1.0 one.

The C/E values of integrated leakage current from Pb sphere calculated using JENDL-3.2 and JENDL Fusion File are given in **Table-4**. The evaluation of Pb data in JENDL Fusion File is completely revised from JENDL-3.2. It can be seen that JENDL Fusion File gives improved prediction compared to the JENDL-3.2 one.

Table-4 Calculated to experimental ratio of integrated leakage current from 7.5 cm thick Pb sphere

Energy (MeV)	JENDL-3.2	JENDL Fusion File
0.4-0.8	1.17	1.03
0.8-1.4	0.824	0.816
1.4-2.5	0.797	0.804
2.5-4.0	0.864	0.926
4.0-6.5	0.869	0.850
6.5-10.5	0.845	0.902
10.5-15.0	1.082	1.19

3) Other OKTAVIAN experiment

In the **Figs. 8** to **22**, calculated and experimental spectra for the samples are shown. The C/E values of integrated current for the energy range between 0.1 and 1 MeV, 1 and 5 MeV, 5 and 10 MeV and higher than 10 MeV are also shown. The symbols in the figures express the C/E values of integrated spectrum within the corresponding energy range. As a whole, there is no much difference between the calculations with JENDL-3.2 and JENDL Fusion File. Both of the JENDL data files give almost calculation for Li, Cr, Mn, Cu, Zr, Nb and Mo having less than 10 % of discrepancy from the experiment. The calculations for Al leakage with JENDL files are fair except for the energy range below 500 keV.

FENDL/MC-1.0 prediction is satisfactory for the Li, Cr, Mn, Cu and Mo. However, for in case of Zr and Nb, for which JENDL files give good calculations, the calculations with FENDL/MC-1.0 are not satisfactory and calculation for Al gives larger discrepancy between 5 and 10 MeV.

Further study to find out specific problem in these cross section data will be continued.

References

1) Pashchenko A.B., *et al.*: FENDL/E-1.0, *IAEA-NDS-128 Rev 2.*, (1995).
2) NAKAJIMA T., *et al.: J. Nucl. Sci. Technol.*, **32**[12], 1259 (1995).
3) SHIBATA T., *et al.: JAERI* 1319, (1990).
4) SUMITA K., *et al.: Nucl. Sci. Eng.*, **106**, 249 (1990).
5) ICHIHARA C., *et al.*: The Measurement of Leakage Neutron Spectra from Various Sphere Piles with 14 MeV Neutrons, *Proc Int. Conf. Nuclear Data for Science and Technology, Mito, May 1988*, p.319, (1988), Saikon Pub.
6) ICHIHARA C., *et al.: JAERI-M* 94-014, (1994).
7) GANESAN S. (Compile), Improved Evaluations and Integral Data Testing for FENDL, *INDC(NDS)-312/GF*, (1994).
8) BRIESMEISTER J.F. (ed.): A General Monte Carlo N-Particle Transport Code, Version 4A, *LA-1265-M* (1993).
9) KOSAKO K., *et al.: JAERI-M* 91-187, (1991).
10) KOSAKO K., *et al.: JAERI-Data/Code* 94-020, (1994).
11) KOSAKO K., *et al.*: to be published.
12) MACFARLANE R.E. *et al.*: FENDL/MC-1.0, Library of continuous energy cross section in ACE format for neutron-photon transport calculations with the Monte Carlo

N-particle Transport Code system MCNP-4A, *IAEA-NDS-169*, (1995).

13) ROSE P.F. (ed.): 4th Edition of *BNL-NCS-17541*, (1991).

14) MANOKHIN V.N. *et al.: IAEA-NDS-90* Rev. 8, (1994).

15) MÖLLENDORF U. von *et al.: Fusion Eng. Design*, **28**, p.737, (1995)

16) GANESAN S.: Preparation of Fusion Benchmarks in Electronic Format for Nuclear Data Validation Studies, *Summary Report of the IAEA Consultants' Meeting at IAEA Headquarters Vienna, Austria, December 13-16, 1993, INDC(NDS)-298*, (1994).

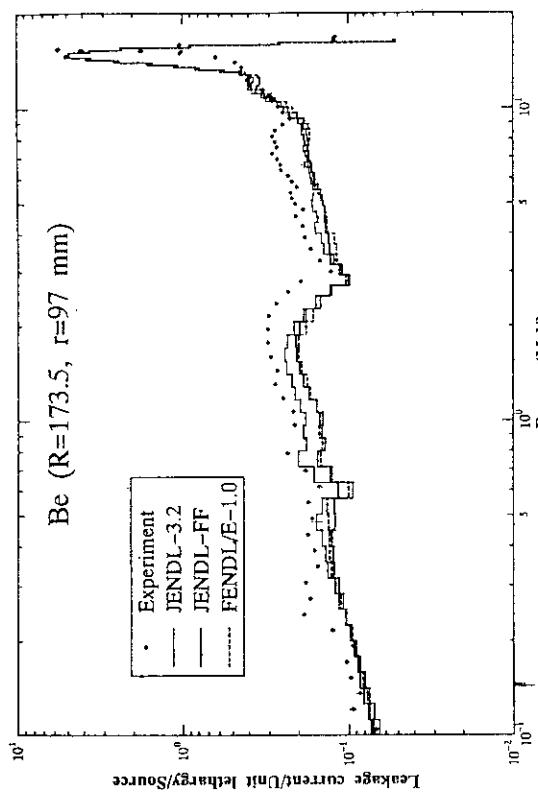

Fig. 1 Total leakage current from 4.55 cm thick Be sphere

Fig. 2 Total leakage current from 7.65 cm thick Be sphere

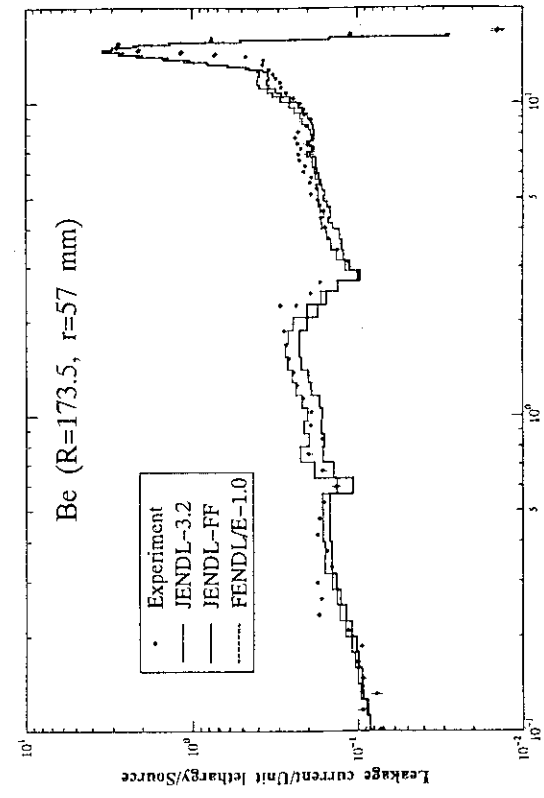

Fig. 3 Total leakage current from 10.45 cm thick Be sphere

Fig. 4 Total leakage current from 11.65 cm thick Be sphere

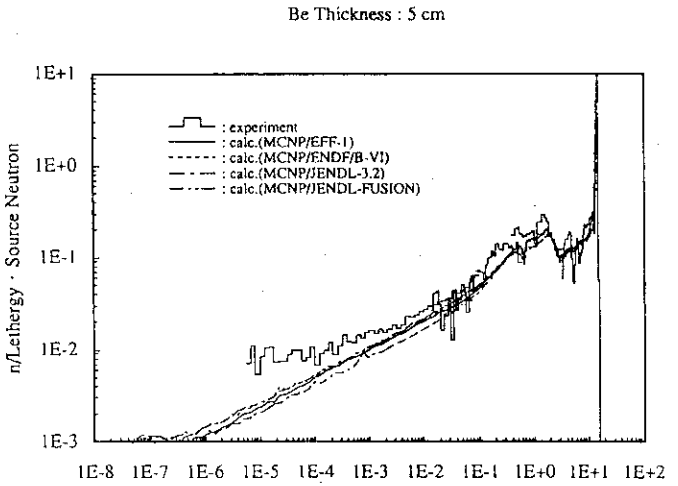

Fig. 5 Total leakage current from 5 cm thick Be sphere

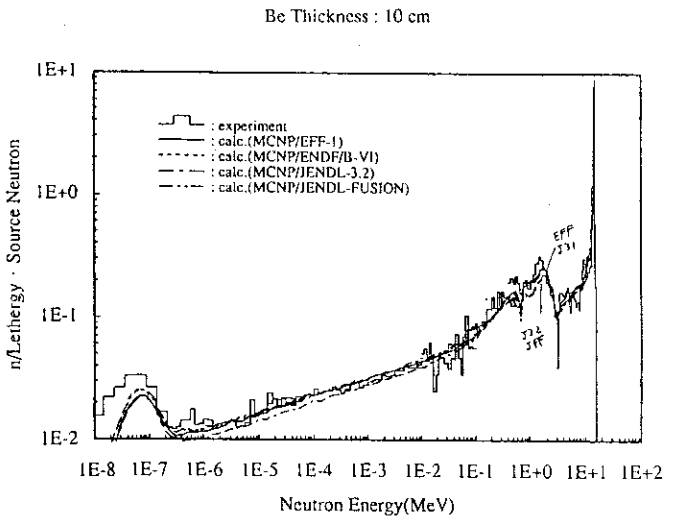

Fig. 6 Total leakage current from 10 cm thick Be sphere

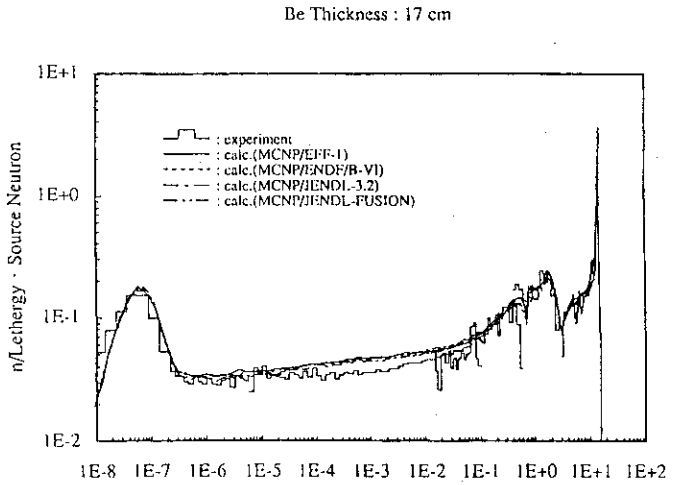

Fig. 7 Total leakage current from 15 cm thick Be sphere

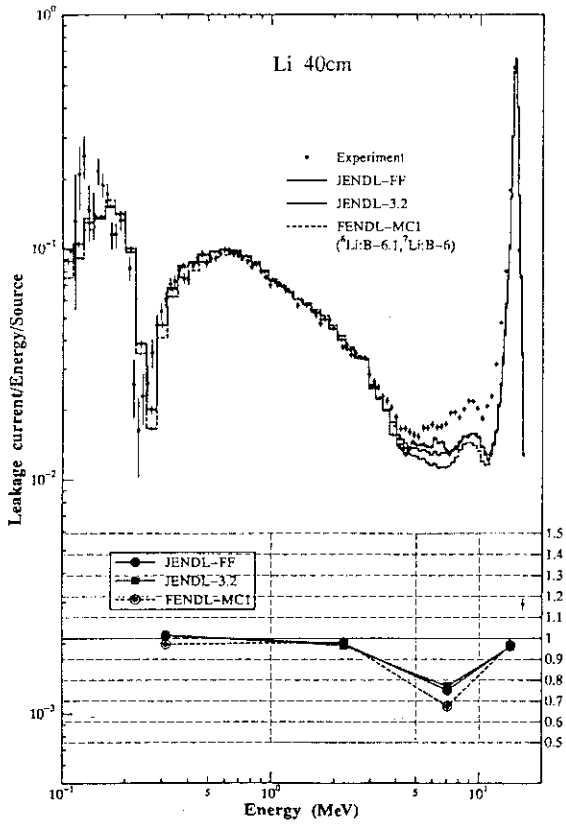

Fig. 8 Total leakage current from Li sphere

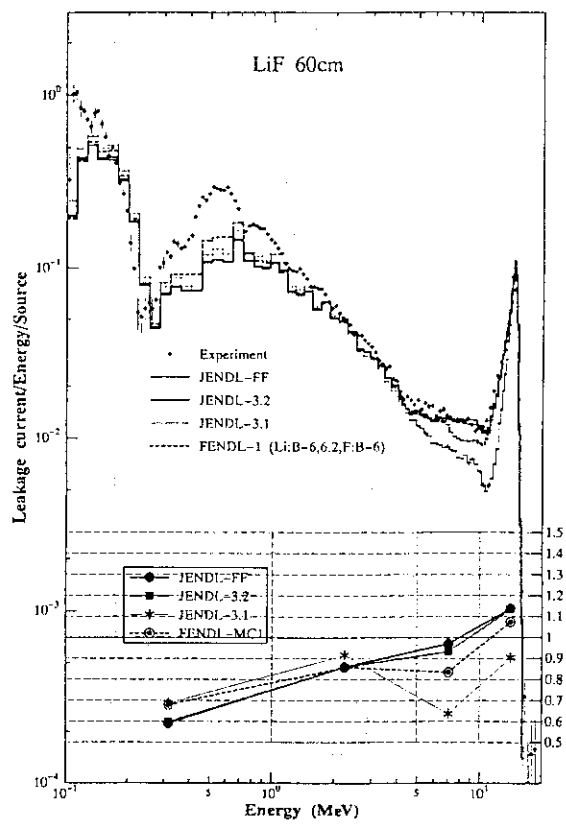

Fig. 9 Total leakage current from LiF sphere

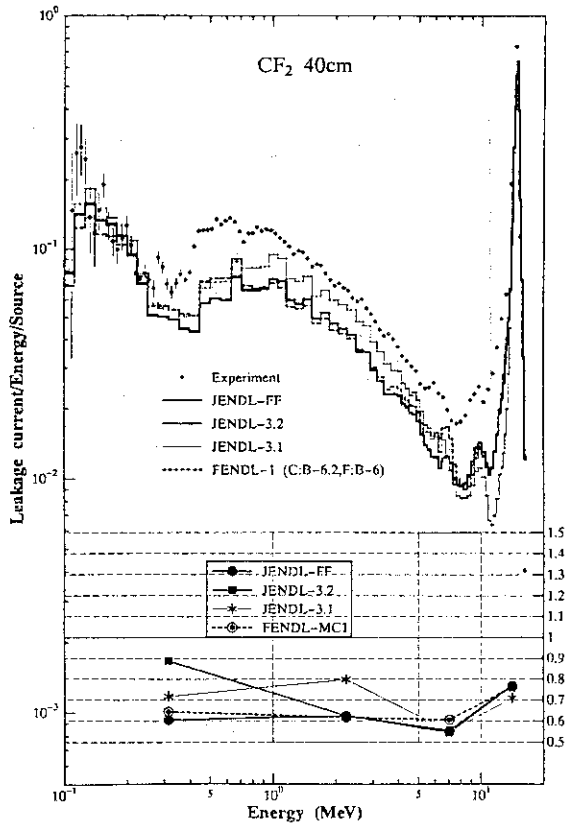

Fig. 10 Total leakage current from TEFLON sphere

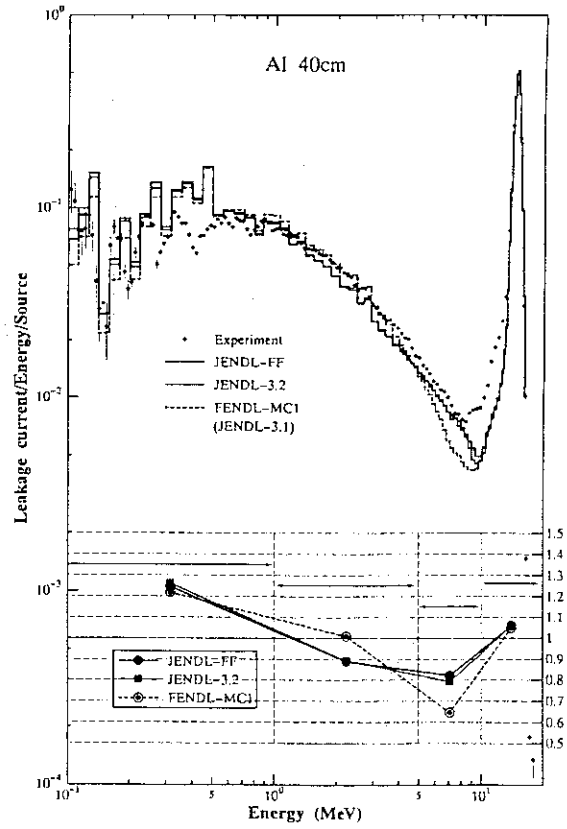

Fig. 11 Total leakage current from Al sphere

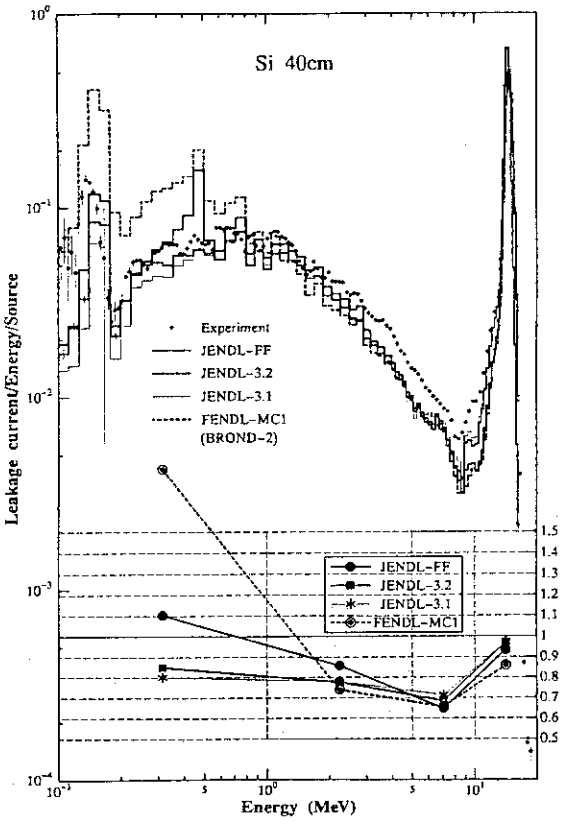

Fig. 12 Total leakage current from 40 cm Si sphere

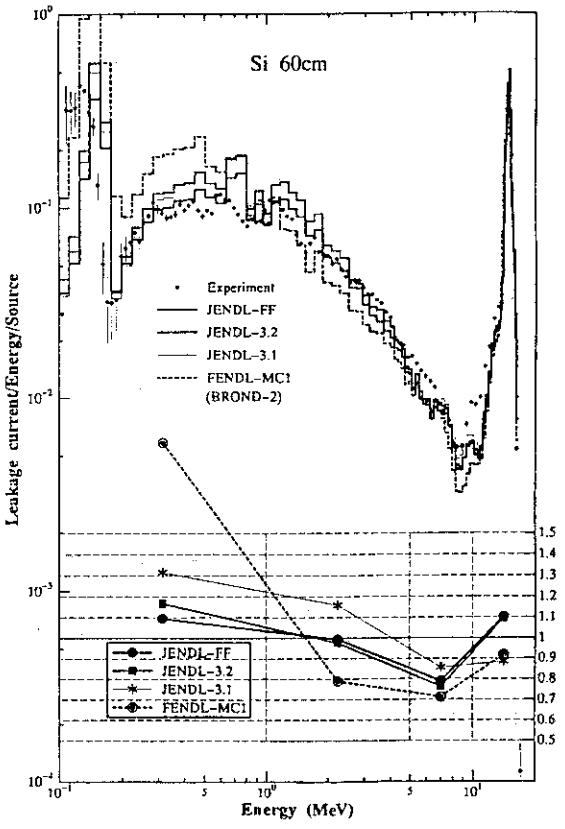

Fig. 13 Total leakage current from 60 cm Si sphere

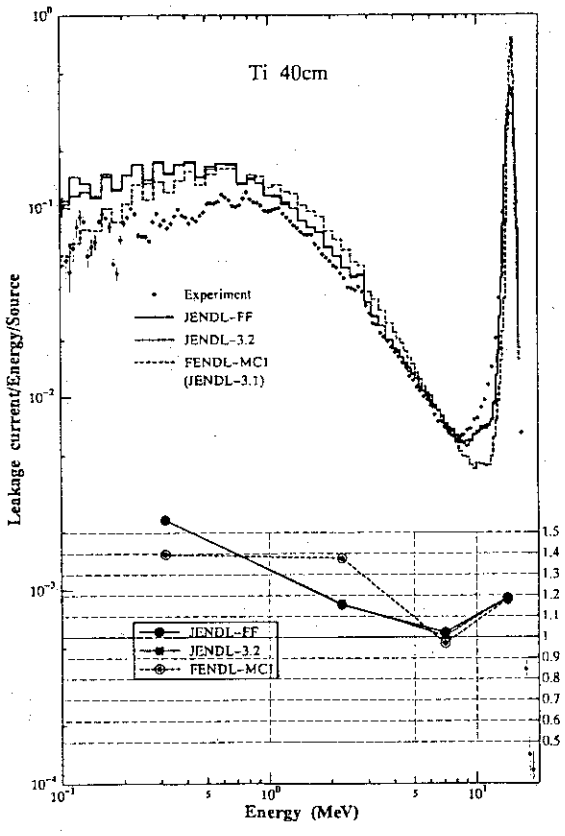

Fig. 14 Total leakage current from Ti sphere

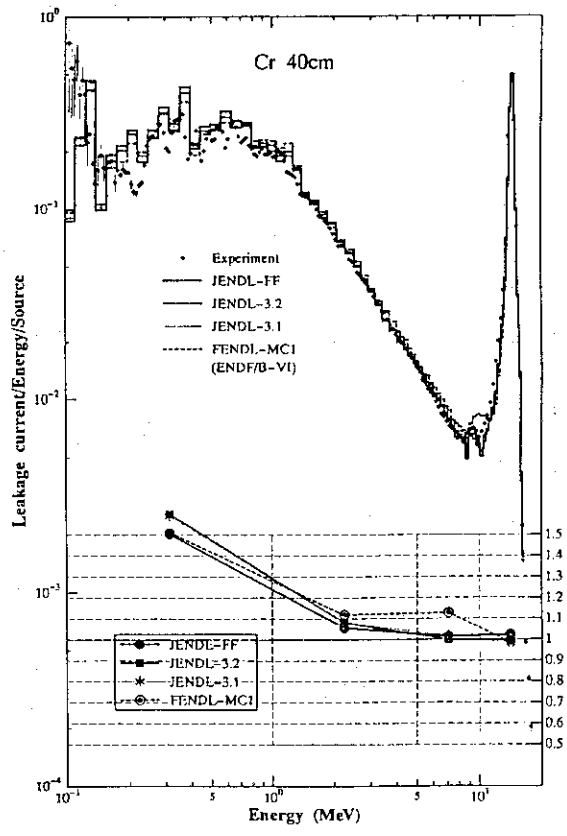

Fig. 15 Total leakage current from Cr sphere

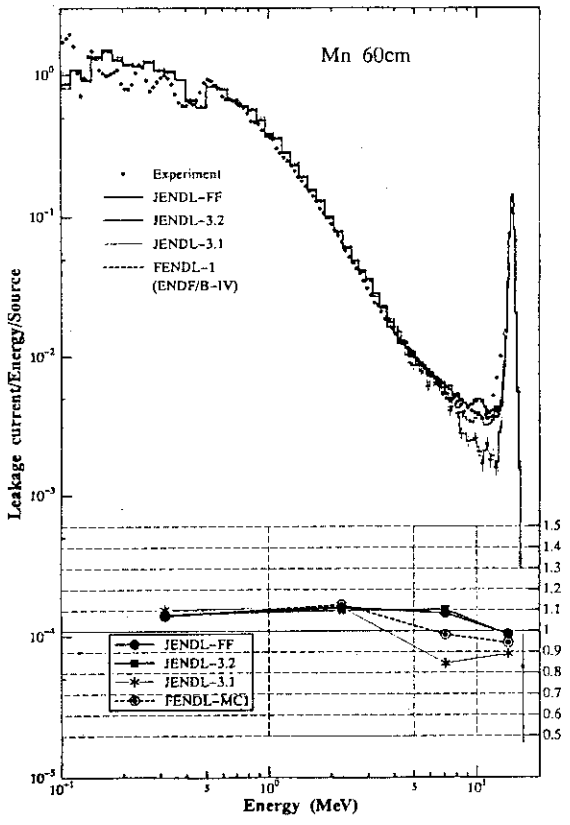

Fig. 16 Total leakage current from Mn sphere

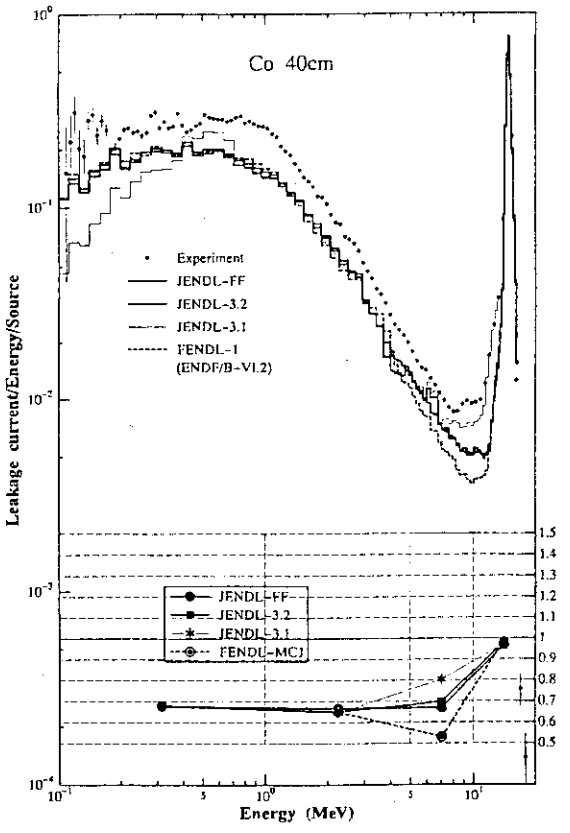

Fig. 17 Total leakage current from Co sphere

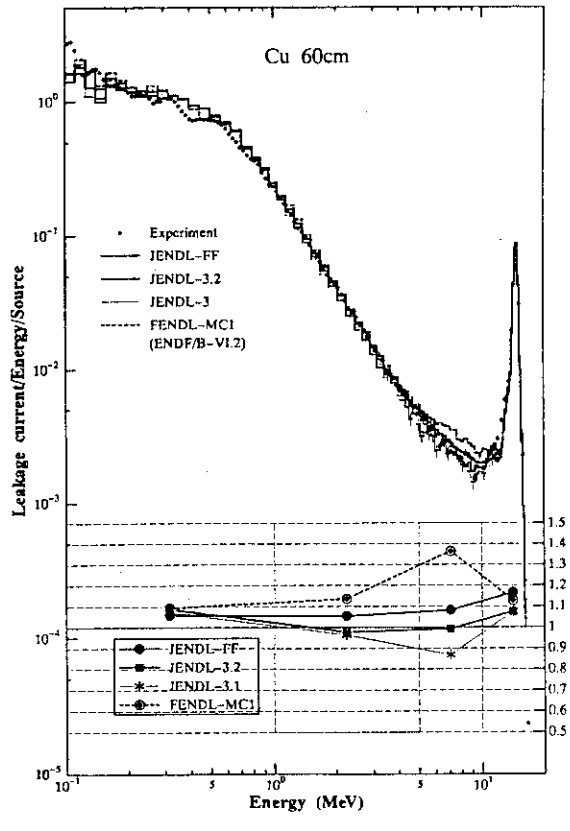

Fig. 18 Total leakage current from Cu sphere

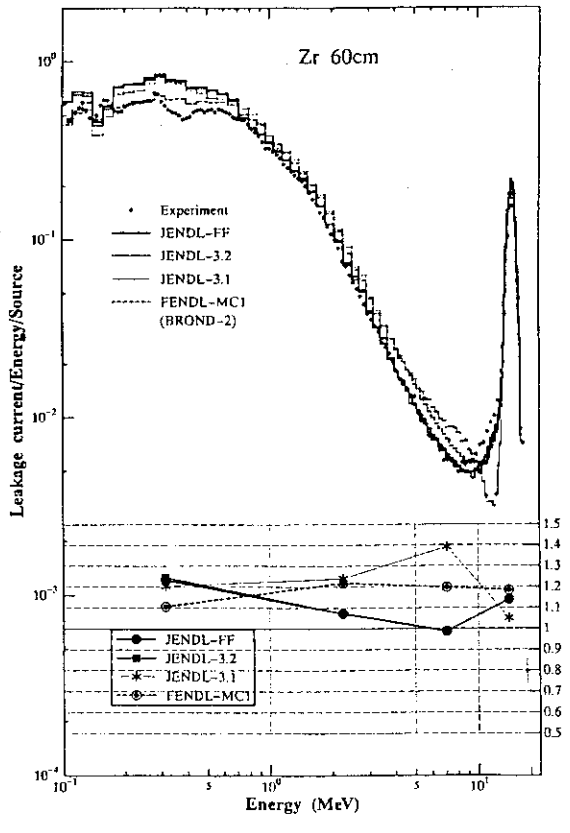

Fig. 19 Total leakage current from Zr sphere

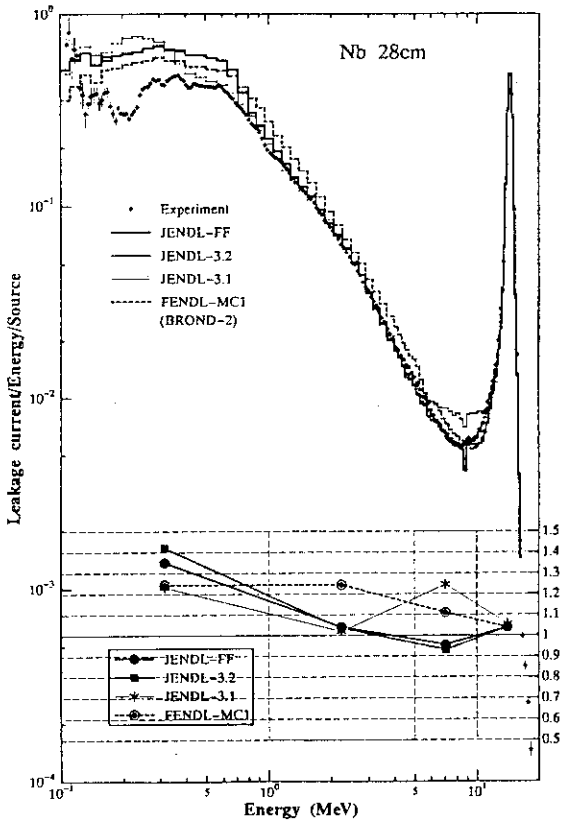

Fig. 20 Total leakage current from Nb sphere

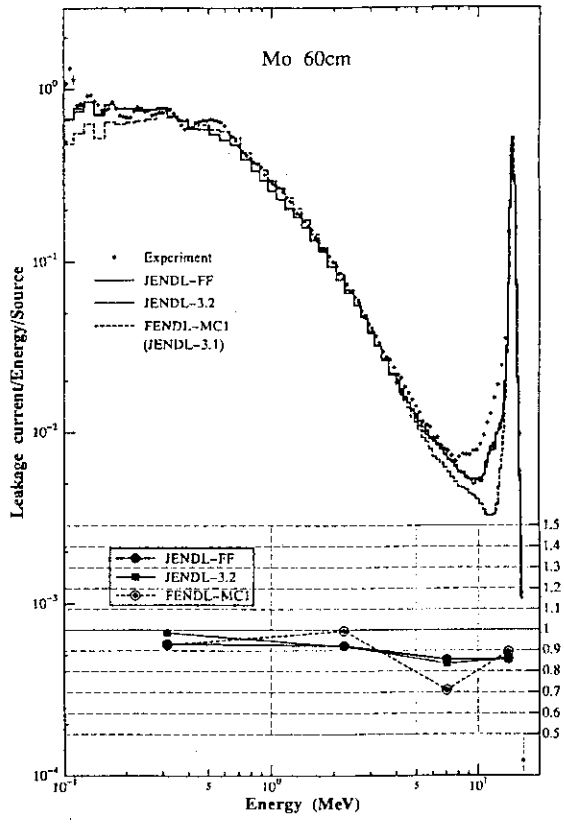

Fig. 21 Total leakage current from Mo sphere

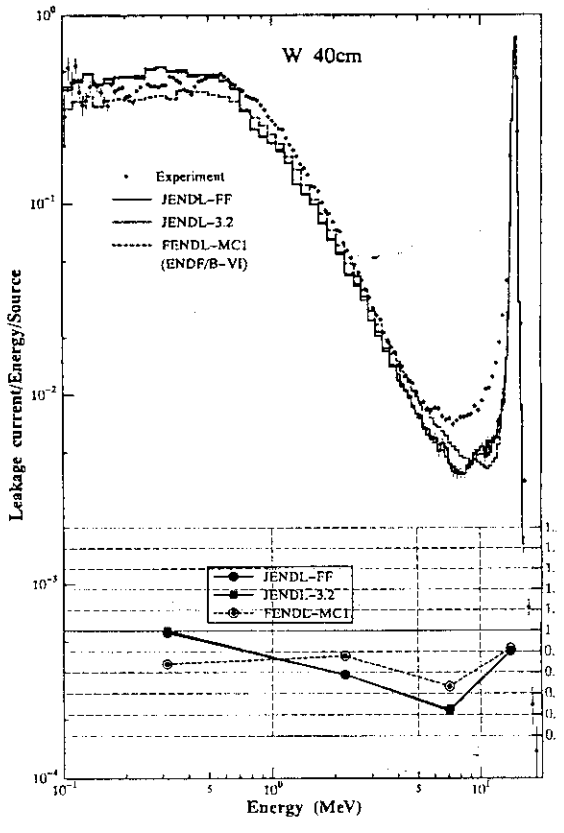

Fig. 22 Total leakage current from W sphere

3.3 Nuclear Data Test with Gamma-Ray Integral Experiments

Fujio MAEKAWA
Fusion Neutronics Laboratory
Japan Atomic Energy Research Institute
Tokai-mura, Naka-gun, Ibaraki-ken 319-11
e-mail: fujio@fnshp.tokai.jaeri.go.jp

Secondary gamma-ray data in JENDL-3.2, JENDL Fusion File and FENDL/E-1.0 were tested through benchmark calculations of two series of integral experiments with D-T neutrons performed at FNS/JAERI and OKTAVIAN/Osaka University. As a result, although discrepancies of gamma-ray spectra between experiments and calculations are found for several materials, the energy balance was found to be valid for the secondary gamma-ray data tested in JENDL Fusion File and FENDL/E-1.0. It was concluded that the secondary gamma-ray data in the two evaluated files could be utilized for designs of fusion reactors.

1. Introduction

One of the most crucial nuclear design parameters of International Thermonuclear Experimental Reactor (ITER) is nuclear heating of superconducting magnets (SCMs) [1]. As illustrated in Fig. 1, Neutrons do not cause significant nuclear heating in SCM because 14-MeV and high-energy neutrons are considerably attenuated in the SCMs region by thick shielding materials. On the other hand, a radiative neutron capture reaction with a low-energy neutron induces energetic gamma-rays of total energy around 8 MeV, and the gamma-rays mainly contribute the nuclear heating in SCM. The secondary gamma-ray data (SGD) are also needed for nuclear heating designs of plasma facing components, blankets, shields, vacuum vessels and so on. Therefore, accurate SGD are strongly required for fusion reactor designs in evaluated nuclear data libraries.

The SGD became available in JENDL-3 [2] released in 1989. Efforts have been devoted to the JENDL reevaluations to improve quality of the data and to extension of nuclides in which SGD were given, and the results were reflected in JENDL-3.2 [3] and JENDL Fusion File [4] released in 1994 and 1995, respectively. On the other hand, the Evaluated Nuclear Data Library for Fusion, Version 1, FENDL/E-1.0 [5], was compiled by International Atomic Energy Agency, and it is utilized as the official library for nuclear designs of ITER. Benchmark tests of SGD in these files have been partly carried out in some previous work [6, 7]. In this paper, latest results of the benchmark test for secondary gamma-ray data in JENDL-3.2, JENDL Fusion File and FENDL/E-1.0 (hereafter abbreviated as J-3.2, J-FF and FENDL, respectively) were described.

2. Secondary Gamma-Ray Integral Experiments for the Test

Two series of integral experiments [8-12] with D-T neutron sources in Japan, OKTAVIAN at Osaka university and FNS at JAERI, were employed for the present test.

OKTAVIAN Experiment: Leakage gamma-ray spectra from thirteen spherical piles were measured with an NaI(Tl) scintillation detector [8]. The sample piles were made of LiF, CF_2, Al, Si, Ti, Cr, Mn, Co, Cu, Nb, Mo, W and Pb, typically in 40 or 60 cm in diameter or thickness of 0.5-4.7 mean

free path for 14 MeV neutrons. Leakage neutron spectra above 0.1 MeV were also measured with the same piles [13]. Since the thicknesses of the spherical shells were not so large and the gamma-ray spectra were measured within a short time gate of about 70 ns to reject neutron events, most of the measured gamma-rays, roughly around 70 %, were generated with 14-MeV neutrons. Hence the experiments provided very useful benchmark data for verification of gamma-ray production data around 14-MeV.

FNS Experiments: Gamma-ray spectra and gamma-ray heating rates were measured by a liquid organic scintillation detector and thermoluminescence dosimeters, respectively, inside of four experimental assemblies made of Fe [9], Cu [10], W [11] and type 316 stainless steel (SS316) [12]. At the same detector positions, neutron spectra in a wide energy range from 14 MeV to 0.3 eV and many dosimetry reactions were also measured [9-12]. The most remarkable feature of the FNS experiment is that capture gamma-rays induced by lower-energy neutrons are measured as well as gamma-rays generated by threshold reactions with higher-energy neutrons. For the designs of fusion reactors, capture gamma-ray data are highly important to estimate nuclear heating in SCMs, as illustrated in Fig. 1. The FNS experiment is the unique experiment allowing a test of capture gamma-ray data, because low-energy neutrons spectrum down to 0.3 eV producing capture gamma-rays are also measured.

3. Policy of the Test

Most of the design parameters associated with gamma-rays, such as gamma-ray heating, dose and radiation damage of a material, have a close relation to total energies deposited to the material by gamma-rays. Therefore, for the test of SGD from a viewpoint of fusion engineering, total energies of gamma-rays should be primarily highlighted rather than the number of gamma-rays or the shape of gamma-ray spectrum. According to testing of the total energies, it can be verified whether the SGD are consistent with the law of the conservation of energy or not.

Gamma-ray heating rates of materials, which just correspond to the energies deposited to the materials by gamma-rays, were measured in the FNS experiment and could be utilized for test of the total energies. In the OKTAVIAN experiment, since no quantity was provided corresponding to the total energies, the measured gamma-ray spectra were integrated for both cases with and without multiplying gamma-ray energies as

$$I_E = \int \phi_\gamma(E) \cdot dE \quad \text{and}$$

$$I_N = \int \phi_\gamma(E) \cdot dE.$$

The total energy integral, I_E, along with the total number of gamma-rays, I_N, were discussed for the OKTAVIAN experiment.

In order to examine the details of the SGD, the gamma-ray spectra provided by both the FNS and OKTAVIAN experiments were also compared with the results of transport calculations.

The continuous energy Monte Carlo transport code MCNP-4A [14] was used for all the benchmark calculations with three cross section libraries, FSXLIB-J3R2 [15], FSXLIB-JFF [16] and FENDL/MC-1.0 [17] for J-3.2, J-FF and FENDL, respectively. The MCNP-4A was selected because of the following two reasons: (i) the continuous energy cross section could precisely treat the original cross section data in

evaluated nuclear data files with little approximation, and (ii) cross section libraries for MCNP were available for all the three evaluated files even though secondary neutron distribution was expressed in a DDX form in the latter two files.

4. Results of OKTAVIAN Experiment

Figures 2 and 3 shows leakage gamma-ray spectra from the silicon and the niobium spheres, respectively, in comparison with calculated ones with J-3.2, J-FF and FENDL. Discrete gamma-ray peaks seen in some of measured gamma-ray spectra are integrated to numerically compare with those obtained by the calculations as shown in Fig. 4. Calculated to experimental (C/E) value ratios for the total energy integral, I_E, and the total number of gamma-rays, I_N, are shown in Figs. 5 and 6, respectively, for all the thirteen materials.

As shown in Fig. 2, the spectra from silicon by J-3.2 and J-FF are almost the same, and they agree very well with the experiment. As for peak areas of the two discrete peaks at 1.8 and 2.8 MeV, agreements between the experiment and all the calculations are excellent. The spectrum by FENDL is, however, smaller than the measured one in the continuum spectrum region above 2 MeV. This underestimation is clearly exhibited in the small I_E value of 0.73 by FENDL.

The gamma-ray spectra of niobium by all the calculations shown in Fig. 3 are smaller than the measured one in the energy ranges below 2 MeV for J-3.2 and J-FF and between 1 and 4 MeV for FENDL. The spectra by all the calculations are about 20 % smaller than the measured one in view of both the I_E and I_N values.

For the rest of eleven materials, no remarkable discrepancy between the measured and all the calculated spectra is found although the calculated spectra do not always agree very well with the measured ones. In the comparisons of the peak areas presented in Fig. 4, all the calculated discrete peaks except 1.4 MeV line of chromium agree almost within 10 % with the experiments.

Since secondary gamma-ray data in J-3.2 are not significantly changed in the evaluation of J-FF for the tested thirteen materials, all the gamma-ray spectra by J-3.2 and J-FF are very similar. All the I_E and I_N values by J-FF except for lead, however, are 2 - 12 % smaller than those by J-3.2. The differences are due to the revision of gamma-ray production data for iron and nickel around 14 MeV in the evaluation of J-FF, as described later, because all the sample materials except lead used in the OKTAVIAN experiment are contained in iron or type 304 stainless steel container.

The most substantial finding in the OKTAVIAN results is that the total energy integrals, I_E, for all the materials and all the evaluated cross sections agree within about ± 20 % with the experiment. The following remarks can be derived as far as SGD for around 14-MeV are concern: (i) all the tested SGD are valid in view of energy balance although small differences of spectral shape are seen, and (ii) statistical-model calculation codes such as GNASH and TNG used for most of the evaluations can provide energetically consistent SGD.

5. Results of FNS Experiment

In the FNS experiment, most of gamma-rays near the front surfaces of the experimental assemblies are generated by threshold reactions with high-energy neutrons, while in deeper parts of the assemblies capture gamma-rays are dominant in the observed gamma-rays. This situation just corresponds to the real fusion reactors as represented in Fig. 1. If appropriate neutron data are not

given in evaluated nuclear data files, a neutron spectrum calculated with those cross section data does not agree with the true one. This leads to disagreement of calculated gamma-ray spectra and heating rates with the cross section data even though SGD are accurately evaluated. This consideration is needed especially for capture gamma-rays generated with low-energy neutrons rather than threshold gamma-rays mainly with 14-MeV neutrons because larger uncertainties are involved in a calculated low-energy neutron spectrum comparing with 14-MeV neutron transmission. Therefore, the results of neutron data test should be reviewed prior to the test of secondary gamma-ray data for the FNS experiment which includes capture gamma-rays.

Neutron data for iron in J-3.2, J-FF and FENDL are found to be highly accurate from the fact that the results of transport calculations and the experiment agree within 20 % for all the reaction rates and the integral neutron fluxes in each order of magnitude between 1 eV and 1 MeV [9, 18]. Similarly, the calculated results for SS316 with the three files agree within 30 % with the experiment for all the quantities [12]. Hence discussions of secondary gamma-ray data are allowed just by looking the results of gamma-rays. As for copper and tungsten, however, large discrepancies between the measured neutron spectra and calculated ones with the three evaluations are observed in lower-energy parts of neutron spectra [11,18]. In this case, a special way of the test is needed for the test as described later.

Figure 7 shows C/E ratios of gamma-ray heating rate in the iron assembly. Near the front surface of the assembly, very large C/E ratios up to 1.7 are found in J-3.2. Larger gamma-ray production cross section (GPX) around 14-MeV is suggested from the result. The GPX in J-3.2 was calculated with the GNASH code, and then it was adjusted to an experimental GPX data [19]. The integral experiment indicates that the experimental GPX data are not appropriate, and the adjustment procedure destroys the energy balance of the nuclear data in J-3.2. In evaluation of the GPX of iron for J-FF, the calculated value by GNASH was taken without the adjustment. As a result, very good agreement between the measured and the calculated gamma-ray heating rates are achieved as shown in Fig. 7. In the deeper part of the assembly, agreements of gamma-ray heating rates between the experiment and the three calculations are very good. The agreements suggest validity of GPX for (n,γ) reactions in all the three evaluations.

As shown in Fig. 8, excellent agreements are observed between the measured gamma-ray spectrum at a deep position in the iron assembly and the calculated ones with J-3.2 and J-FF. The calculated spectrum with FENDL, however, has a different shape comparing with the others: the 8 MeV gamma-ray peak, which is produced when a nucleus in the capture-state directly transits to its ground state, is too much enhanced so that the number of gamma-rays below 7 MeV is smaller. As for iron, the experimentally obtained spectral shapes of secondary gamma-rays by (n,γ) reactions [20] are stored in both JENDLs while the calculated ones in FENDL. This is the reason for the good agreement of JENDLs with the experiment.

The results similar to the iron are obtained for SS316 for both gamma-ray heating rate and spectrum. Figure 9 shows the C/E ratios of gamma-ray heating rates in the SS316 assembly. Improvement of the heating rates near the front surface of the assembly is mostly due to the change of GPX of iron around 14 MeV. In the deeper positions, the heating rates by J-3.1 are larger than the other three. This is due to the major modification of SGD in the evaluation of J-3.2, i.e., energy balance of (n,γ) reactions. The energy balance is not sufficiently conserved in J-3.1, however, it is modified in J-3.2 so as to be consistent with the low of conservation of energy.[5]

The energy balance of (n,γ) reactions can be easily checked for evaluated SGD as follows. Figure 10 is an example of the results for chromium data in J-3.1 and J-3.2. If the incident neutron energy is low, the total gamma-ray energies released by an (n,γ) reaction are close to the Q-value of the reaction around 8 MeV. As shown in Fig. 10, the total released energies are correctly assigned in J-3.2, however, the energies by J-3.1 are as large as more than 1.5 times the real one for incident neutron energies below 10 keV. This is the main reason for the larger gamma-ray heating rates of SS316 by J-3.1 in deeper positions. The same check of energy balance for (n,γ) reactions were carried out for Cr, Mn, Fe, Ni, Cu, Mo and W in J-3.2, J-FF and FENDL. As a result, almost valid energy balance was confirmed for all the data.

As mentioned earlier, since large discrepancies of low-energy neutron spectra between the experiments and calculations are found for copper and tungsten, direct comparisons of gamma-ray results including capture gamma-rays are not meaningful. Even in this case, however, a complete data test for SGD of (n,γ) reaction is possible by considering the two items, the energy balance and the shape of gamma-ray spectrum. For copper and tungsten, since the validity of energy balance is confirmed as mentioned in the above, the shapes of gamma-ray spectra are compared as shown in Figs. 11 and 12, respectively. As for copper, the spectra by all the three calculations have a very similar shape, but they do not agree well with the measured one. In the three evaluations, as similar to the iron data in FENDL, the 8 MeV gamma-rays produced by direct transition of nucleus in the capture-state to the ground state is too strong, accordingly the number of lower-energy gamma-rays below 7 MeV are too small. As for tungsten, the spectra by all the three calculations are also similar. The figure implies that the shape of secondary gamma-rays by (n,γ) reactions in all the evaluations are somewhat softer than the measured one.

6. Concluding Remarks

According to the present benchmark test of the secondary gamma-ray data, the following remarks are derived.

(i) As for shapes of secondary gamma-rays mostly produced by 14-MeV, the results are summarized as follows.

JENDL-3.2, -FF	Good agreement for	C, F, Al, Si, Co, Cu, Mo, W and Pb
	Small discrepancies for	Ti, Cr, Mn and Pb
FENDL/E-1.0	Good agreement for	C, F, Al, Cr, Cu, Mo and W
	Small discrepancies for	Si, Ti, Mn, Co, Nb and Pb

(ii) The larger gamma-ray production cross section of iron around 14-MeV in J-3.2 is improved in J-FF. As a result, a good energy balance within 20 % is achieved for all the materials tested in this work for both J-FF and FENDL as far as 14-MeV neutrons are concerned.

(iii) As for secondary gamma-ray data for capture gamma-rays, a good energy balance is confirmed for Cr, Mn, Fe, Ni, Cu, Mo and W for both J-FF and FENDL, although the shapes of secondary gamma-rays of Fe for FENDL and Cu and W for both J-FF and FENDL differ a little from the measured ones.

Consequently, the energy balance, which is the most important quantity for engineering design of fusion reactors, is found to be valid for all the secondary gamma-ray data tested in J-FF and FENDL. Hence both two comprehensive evaluated files can be utilized for designs of fusion reactors with firm

confidence.

References

1) Gohar Y., Parker R. and Rebut P.-H.: Fusion Eng. Des, 27, 52 (1995).
2) Shibata K. and JENDL-3 Compilation Group: JAERI 1319 (1990).
3) Nakagawa T., et al.: J. Nucl. Sci. Technol., 32, pp. 1259-1271 (1995).
4) Chiba S., Yu B. and Fukahori T.: JAERI-M 92-027, pp. 35-44 (1992).
5) Ganesan S. and McLaughin P. K.: IAEA-NDS-128 (1995).
6) Maekawa F. and Oyama Y.: "Benchmark Test of 14-MeV Neutron Induced Gamma-Ray Production Data in JENDL-3.2 and FENDL/E-1.0 through Analysis of the OKTAVIAN Experiments," submitted to Nucl. Sci. Eng. (1995).
7) Maekawa F. and Oyama Y.: INDC(NDS)-334, pp. 139-145 (1995).
8) Yamamoto J., et al.: JAERI-M 94-014, pp. 32-62 (1994).
9) Oishi K., et al.: Proc. 7th Int. Conf. on Radiation Shielding, Bournemouth, UK, September 12-16, 1988, pp. 331 (1988); Konno C., et al.: Fusion Eng. Des., 18, 297 (1991); Maekawa F. and Oyama Y.: "Measurement of Neutron Energy Spectrum below 10 keV in an Iron Shield Bombarded by D-T Neutrons and Benchmark Test of Recent Evaluated Nuclear Data from 14 MeV Down to 1 eV," submitted to Nucl. Sci. Eng. (1995); Maekawa F., et al: to be submitted to Nucl. Sci. Eng. (1996).
10) Maekawa F., et al.: Fusion Eng. Des., 28, 753 (1995); Konno C., et al.: ibid., 28, 745 (1995); Maekawa F., et al.: JAERI-M 94-038 (1994).
11) Maekawa F., et al.: JAERI-Review 95-014, pp. 133-135 (1995).
12) Konno C., et al.: JAERI-Research 94-043 (1994); Maekawa F., et al.: JAERI-Research 94-044 (1994).
13) Ichihara C., et al.: JAERI-M 94-014 pp. 63-125 (1994).
14) Briesmeister J. F., Ed., LA-12625-M, Los Alamos National Laboratory (1993).
15) Kosako K., et al.: JAERI-Data/Code 94-020 (1994).
16) Kosako K., private communication (1995).
17) Ganesan S. and Wienke H.: IAEA-NDS-169 (1995).
18) Oyama Y.: "Nuclear Data Test with FNS Slab Experiments," in this proceedings (1996).
19) Chapman G. T., Morgan G. L. and Perey F. G.: ORNL/TM-5416 (1976).
20) Igashira M., et al.: Proc. Int. Conf. on Nucl. Data for Science and Technology, Mito, May 30 - June 3, 1988, pp. 67-70 (1988).

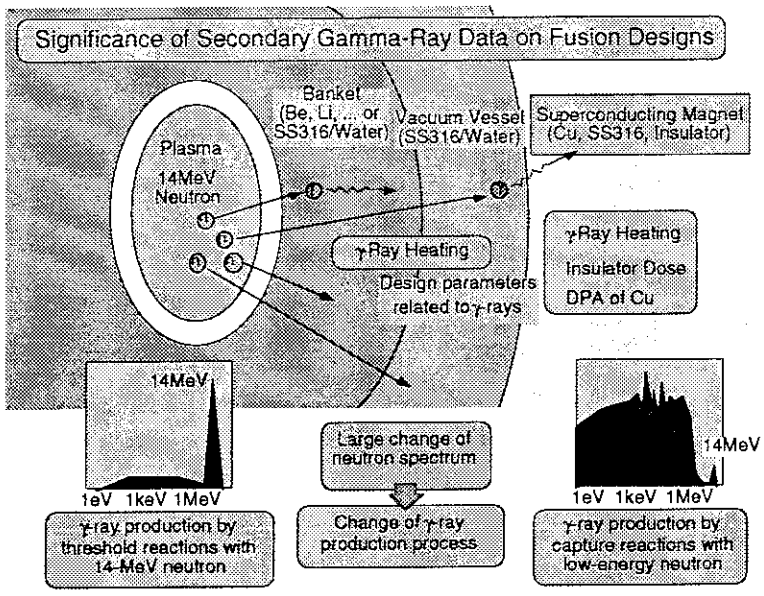

Fig. 1 Significance of secondary gamma-ray data on fusion designs.

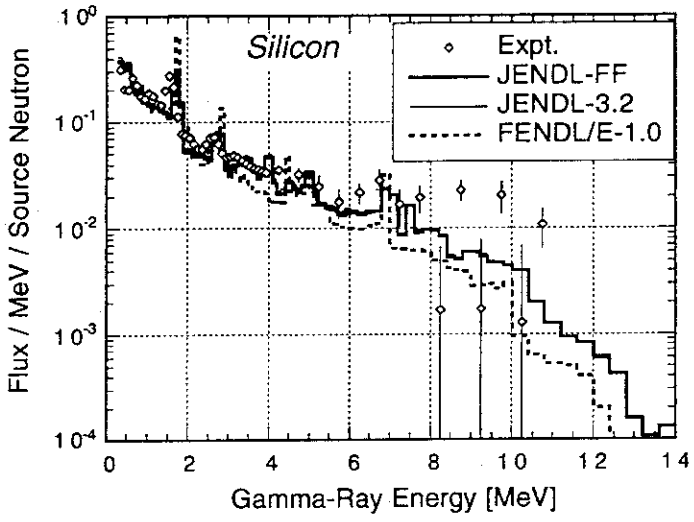

Fig. 2 Comparison of leakage gamma-ray spectra from the silicon pile of 60 cm in diameter measured and calculated with JENDL Fusion File, JENDL-3.2 and FENDL/E-1.0.

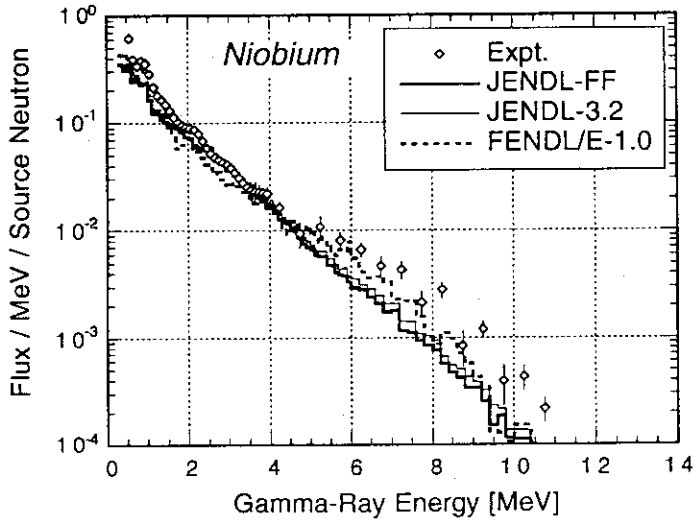

Fig. 3 Comparison of leakage gamma-ray spectra from the niobium pile of 28 cm in diameter measured and calculated with JENDL Fusion File, JENDL-3.2 and FENDL/E-1.0.

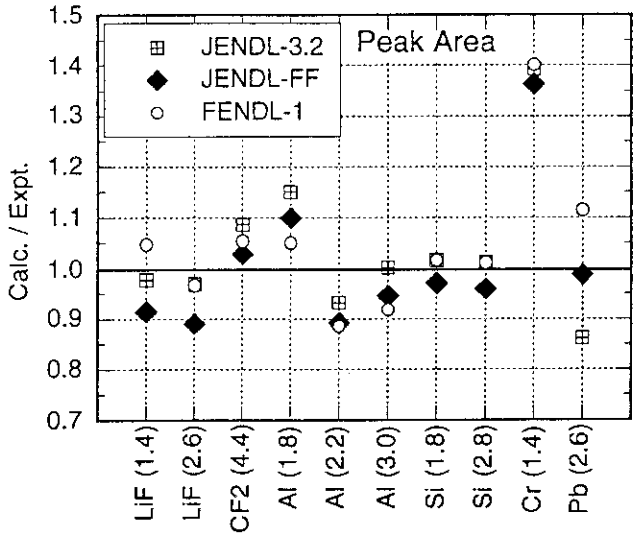

Fig. 4 Caluculated to experimental ratios for the discrete gamma-ray peaks observed in the OKTAVIAN experiment. Numbers in parensis indicate gamma-ray energies.

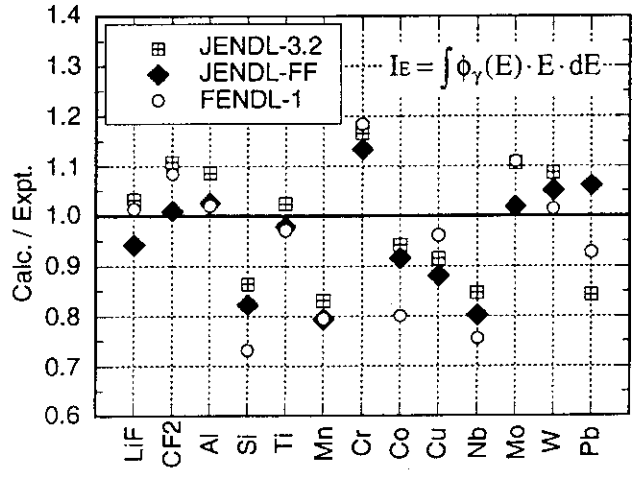

Fig. 5 Caluculated to experimental ratios for the total energy integrals, I_E, for the spectra observed in the OKTAVIAN experiment.

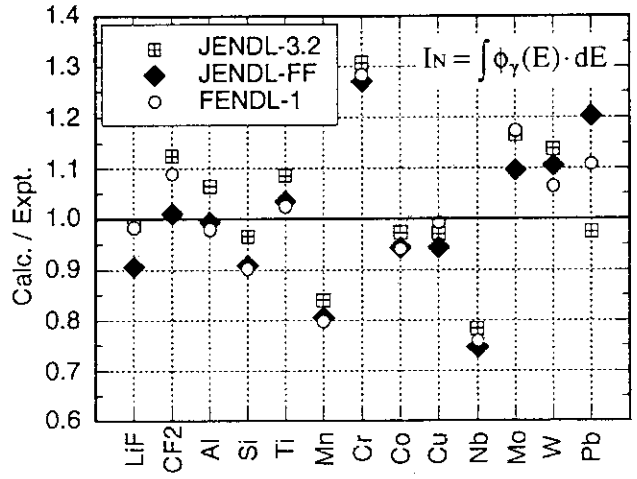

Fig. 6 Caluculated to experimental ratios for the total number of gamma-rays, I_N, for the spectra observed in the OKTAVIAN experiment.

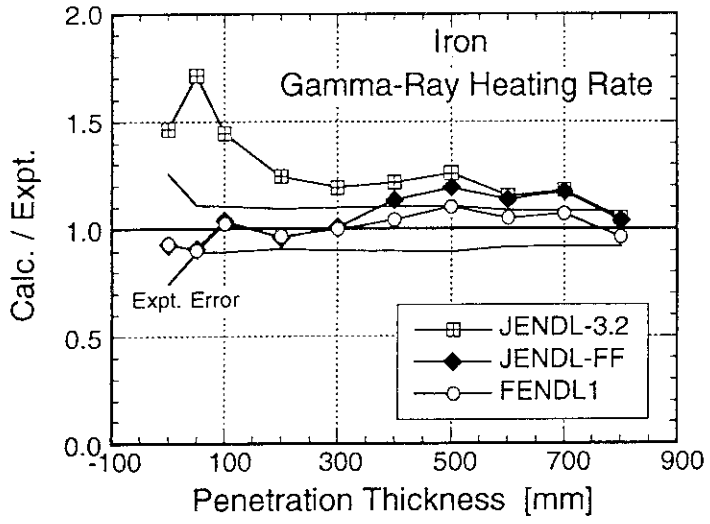

Fig. 7 Caluculated to experimental ratios for gamma-ray heating rates of iron obtained by the FNS experiment as a function of penetration thickness.

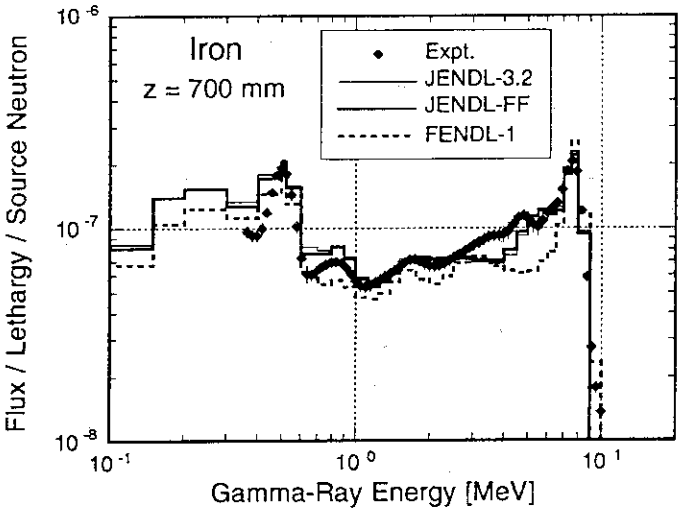

Fig. 8 Comparison of gamma-ray spectra at the 700 mm depth position in the FNS iron assembly measured and calculated with JENDL Fusion File, JENDL-3.2 and FENDL/E-1.0.

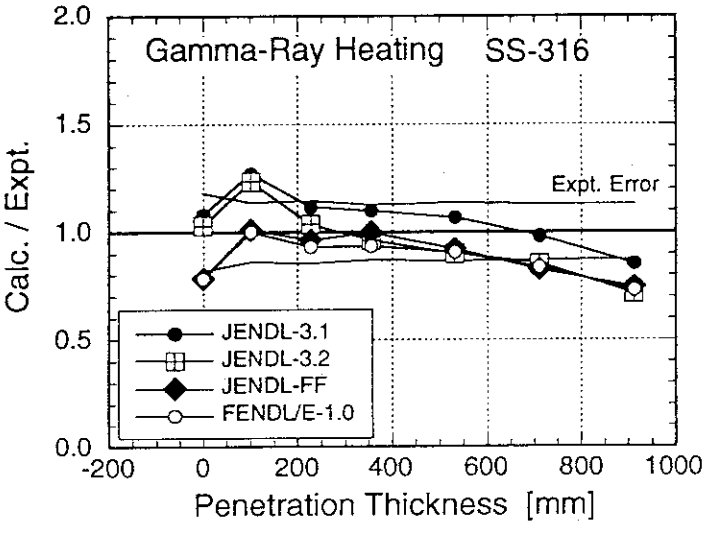

Fig. 9 Caluculated to experimental ratios for gamma-ray heating rates of SS316 obtained by the FNS experiment as a function of penetration thickness.

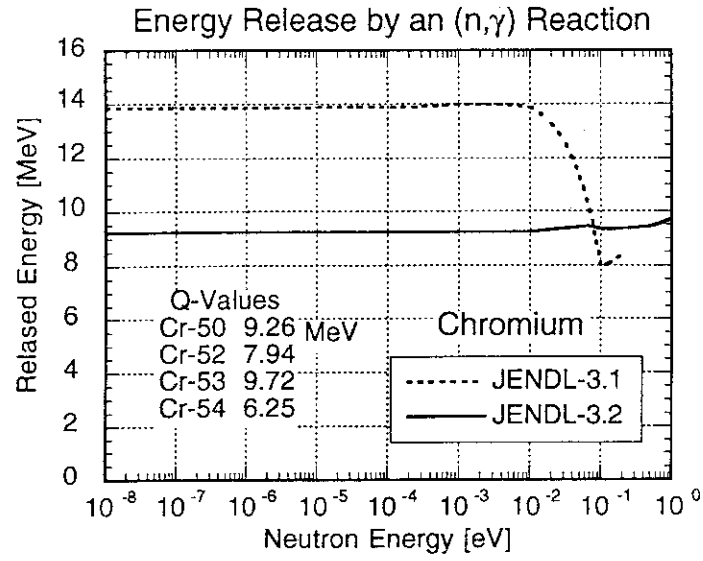

Fig. 10 Released energy by an Cr(n,γ) reaction as a function of incident neutron energy derived from JENDL-3.1 and -3.2.

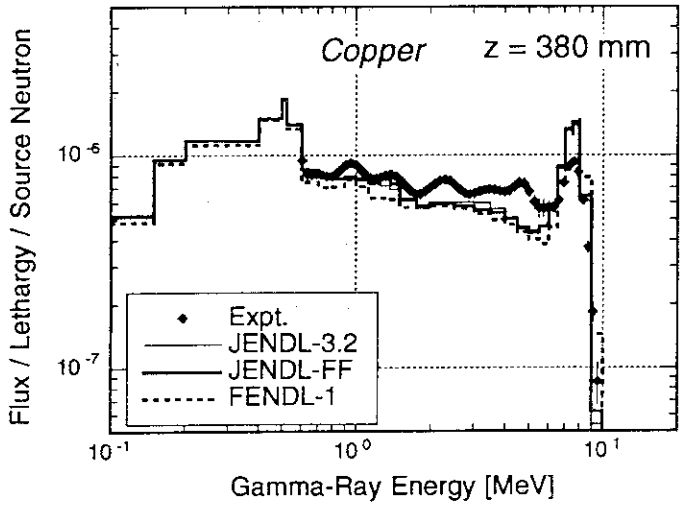

Fig. 11 Comparison of gamma-ray spectra at the 380 mm depth position in the FNS cooper assembly measured and calculated with JENDL Fusion File, JENDL-3.2 and FENDL/E-1.0.

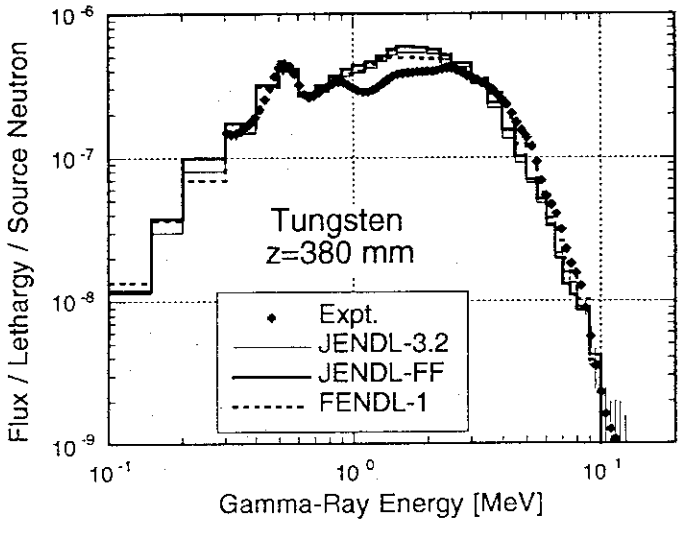

Fig. 12 Comparison of gamma-ray spectra at the 380 mm depth position in the FNS tungsten assembly measured and calculated with JENDL Fusion File, JENDL-3.2 and FENDL/E-1.0.

4. Integral Test of Neutron and Secondary Gamma-ray Data (II)

4.1 ITER Bulk Shielding Experiments at FNS

Chikara KONNO, Fujio MAEKAWA, Yukio OYAMA, Masayuki WADA,
Yujiro IKEDA, Yoshitomo UNO and Hiroshi MAEKAWA

Department of Reactor Engineering
Japan Atomic Energy Research Institute
Tokai-mura, Naka-gun, Ibaraki-ken, 319-11

Bulk shielding experiments on SS316 and SS316/water for D-T neutrons were performed under one of the ITER/EDA R&D tasks at FNS. The various experimental data for neutron and gamma-ray, particularly neutron spectra below 1 MeV and gamma-ray heating rate, were measured to the depth of 914 mm. The MCNP and DOT3.5 codes were used with nuclear data libraries based on JENDL-3.1, -3.2, -Fusion File and FENDL/E-1.0 for the analyses of these experiments. The MCNP calculations with JENDL-Fusion File and FENDL/E-1.0 agreed with the measurements of the SS316 and SS316/water experiments within 30 %. It was pointed out that the group constants of JENDL-3.2 had some problems in the thermal group and that the self-shielding correction was inadequate in the group constants of the FENDL/E-1.0.

1. Introduction

One of the most promising candidates of shielding materials in International Thermonuclear Experimental Reactor (ITER) is the configuration of type 316 stainless steel (SS316) and water. Bulk shielding experiments[1-4] on SS316 and SS316/water were performed under the '94 ITER/EDA R&D task (T-16) at FNS to examine the shielding performance of SS316 and SS316/water. This paper explains these experiments briefly and discusses the analyses based on the libraries of JENDL-3.1[5], -3.2[6], -Fusion File[7] and FENDL/E-1.0[8].

2. Experiments

The experimental assembly of SS316 was consist of a test region and source reflector as shown in Fig. 1. The test region was a cylindrical SS316 of 1200 mm in diameter and 1118 mm in thickness, which was located at 300 mm from the D-T neutron source. The source reflector, which was SS316 of 200 mm in thickness surrounding the D-T neutron source, adjusted neutron energy spectrum incident to the test region. In the SS316/water experiment, the test region was modified as shown in Fig. 2 to a layered structure of SS316

and water (volume ratio is 4 : 1) and the water tanks or polyethylene blocks of about 150 mm in effective thickness were added to the rear region of the test region to decrease the influence of room-returned background neutrons.

Neutron spectra above 2 MeV, from a few keV to 1 MeV and below 1 keV were measured at the positions from 0 to 914 mm in depth using a 14 mm-diam. NE213 spectrometer, small proton recoil gas proportional counters and a BF3 gas proportional counter (slowing down time method), respectively. A 40 mm-diam. C6D6 spectrometer and thermoluminescence dosimeter were used to measure gamma-ray spectra and heating rates, respectively. As neutron spectrum indices, fission and activation reaction rates were also measured by micro fission chambers of ^{235}U and ^{238}U, and foils of aluminum, niobium, indium and gold.

3. Analyses

The analyses of the experiments were performed by two calculation codes; continuous energy Monte Calro code MCNP-4A[9] and two-dimensional S_N transport code DOT 3.5[10]. The FNSUNCL[11] code which is a modified code of the GRTUNCL was used to calculate the first collision sources for the DOT calculations. The nuclear data libraries for MCNP were FSXLIB-J3[12], -J3R2[13], -JFF[14] and FENDL/MC-1.0[15] processed from JENDL-3.1, -3.2, -Fusion File and FENDL/E-1.0, respectively. Those for DOT were JSSTDL-3.1[16] (neutron : 125 groups, gamma : 40 groups), JSSTDL-3.2[17] (preliminary version, neutron : 125 groups, gamma : 40 groups) and FENDL/MG-1.0[18] (neutron : 175 groups, gamma : 42 groups) processed from JENDL-3.1, -3.2 and FENDL/E-1.0, respectively. The self-shielding correction and P_5S_{16} approximation were adopted in the DOT calculations.

4. Results and Discussion

SS316 Experiment

Figure 3 shows the ratios of the calculation values to the experimental ones (C/E) for neutron flux above 10 MeV, which were obtained from neutron spectra. All the calculations agree with the measurement within 30 %. The C/Es for neutron flux from 100 keV to 1 MeV are shown in Fig. 4. The MCNP calculations with FSXLIB-J3, -J3R2 and -JFF tend to underestimate as the depth (underestimation of 30 - 40 % at the depth of 914 mm). This tendency is more prominent in the DOT calculations. This underestimation is improved in the MCNP calculation with FENDL/MC-1.0, which agrees with the measurement within 15 %. The C/E of the DOT calculation with FENDL/MG-1.0 is, however, worse than those with JENDL libraries. Figure 5 shows the neutron spectra at the depth of 914 mm calculated by MCNP and DOT with JENDL-3.2 and FENDL/E-1.0. Though the DOT calculation with JENDL-3.2 agrees with the MCNP one, the DOT calculation with FENDL/E-1.0 is much smaller than the MCNP one in the whole energy regions below 1 MeV. It is considered that

the self-shielding correction is inadequate in FENDL/MG-1.0. The C/E of ^{235}U fission rate is shown in Fig. 6. All the calculations agreed with the measurements within 30 %, but the discrepancy between the DOT calculation with FENDL/E-1.0 and the MCNP one also appears in this figure. Figure 7 shows the C/E of gamma-ray heating rate of SS316. The C/E of JENDL-3.2 is smaller than that of JENDL-3.1 and JENDL-Fusion File improves the overestimation in the front region. The C/E of MCNP calculation with FSXLIB-JFF is very similar to that of FENDL/MC-1.0, which decreases as the depth inside the assembly.

SS316/Water Experiment

The C/Es for neutron fluxes above 10 MeV and from 100 keV to 1 MeV are shown in Figs. 8 and 9, respectively. All the calculations agree with the measurements within 20 %. The tendency of underestimation for neutron flux from 100 keV to 1 MeV is not eminent. The discrepancy between the DOT and MCNP calculations with FENDL/E-1.0 is much smaller, since the influence of the self-shielding is small in the SS316/water configuration. Figure 10 shows the C/E of ^{235}U fission rate. All the MCNP calculations agree with the measurement within 30 %. The DOT calculations with JSSTDL-3.1 and FENDL/MG-1.0 also agree with the measurement within 20 % except for the front region where the distribution of thermal neutrons was very different from the Maxwell distribution since neutrons were not well thermalized, but the C/E of the DOT calculation with JSSTDL-3.2 is much larger. Figure 11 shows the fission rate profile of ^{235}U calculated by DOT with JSSTDL-3.1 and -3.2 at the depth of 127 mm. The fission rate of the thermal group, which is more than 50 % of the total fission rate, in the DOT calculation with JSSTDL-3.2 is quite different from that with JSSTDL-3.1. Probably JSSTDL-3.2 has some problems in the thermal group. The C/E of gamma-ray heating rate of SS316 is shown in Fig. 12. The variations of C/E from JENDL-3.1 to -3.2 and from JENDL-3.2 to -Fusion File are the same as those in the SS316 experiment. The MCNP and DOT calculations with JENDL-Fusion File and FENDL/E-1.0 agree with the measurement within 30 %, though they tend to decrease as the depth.

5. Concluding Remarks

Bulk shielding experiments on SS316 and SS316/water for D-T neutrons performed at FNS were analyzed by the MCNP-4A and DOT3.5 codes with the nuclear data libraries of JENDL-3.1, -3.2, -Fusion File and FENDL/E-1.0. The MCNP calculations with JENDL-Fusion File and FENDL/E-1.0 agreed with the measurements of the SS316 and SS316/water experiments within 30 %, though they tended to decrease as the depth. It was, however, pointed out that the self-shielding correction was inadequate in the group constants of the FENDL/E-1.0 and that the group constants (preliminary version) of JENDL-3.2 had some problems in the thermal group.

References

1) Konno C., et al.: "Bulk Shielding Experiments on Large SS316 Assemblies Bombarded by D-T Neutrons, Volume I : Experiment," JAERI-Research 94-043 (1994).
2) Maekawa F., et al.: "Bulk Shielding Experiments on Large SS316 Assemblies Bombarded by D-T Neutrons, Volume II : Analysis," JAERI-Research 94-044 (1994).
3) Konno C., et al.: "Bulk Shielding Experiment on a Large SS316/Water Assembly Bombarded by D-T Neutrons, Volume I : Experiment," JAERI-Research 95-017 (1995).
4) Maekawa F., et al.: "Bulk Shielding Experiment on a Large SS316/Water Assembly Bombarded by D-T Neutrons, Volume II : Analysis," JAERI-Research 95-018 (1995).
5) Shibata K., et al.: "Japanese Evaluated Nuclear Data Library, Version-3 --JENDL-3 --," JAERI 1319 (1990).
6) Kikuchi Y.: "JENDL-3 Revision-2 -JENDL-3.2 -," Proc. Int'l Conf. on Nuclear Data for Science and Technology, Gatlingburg, Tennessee, May 9 - 13, pp. 685-691 (1994).
7) Chiba S., et al.: "Evaluation of JENDL Fusion File," JAERI-M 92-027, pp. 35-44 (1992).
8) Ganesan S. and McLaughlin P.K., "FENDL/E, Evaluated Nuclear Data Library of Neutron Interaction Cross Sections, Photon Production Cross Sections and Photon-Atom Interaction Cross Sections for Fusion Applications," IAEA(NDS)-128, Rev. 1 (1995).
9) Briesmeister J.F. (edited): "MCNP - A General Monte Carlo Code for Neutron and Photon Transport, Version 4A," LA-12625 (1993).
10) Rhodes W.A. and Mynatt F.R., The DOT-III two dimensional discrete ordinates transport codes, ORNL-TM-4280 (1973).
11) Oyama Y., et al.: "Phase-III experiments of the JAERI/USDOE collaborative program on fusion neutronics - Line source and annular blanket experiments - Volume I : Experiment," JAERI-M 94-015 (1994).
12) Kosako K., et al.: "FSXLIB-J3 MCNP Continuous Cross Section Library based on JENDL-3," Proc. New Horizons in Radiation Protection and Shielding, Pasco, Washington, pp. 357-363 (1992).
13) Kosako K., et al.: "FSXLIB-J3R2: A Continuous Energy Cross Section Library for MCNP based on JENDL-3.2," JAERI-Data/Code 94-020 (1994).
14) Kosako K.: private communication (1995).
15) MacFarlane R.E.: private communication (1995).
16) Hasegawa A.:, "Development of a Common Nuclear Group Constants Library System: JSSTDL-295n-104γ Based on JENDL-3 Nuclear Data File," Proc. Int'l Conf. on Nuclear Data, Jülich, Germany, pp. 232-234 (1991).
17) Nakagawa T.: private communication (1995).
18) MacFarlane R.E.: private communication (1995).

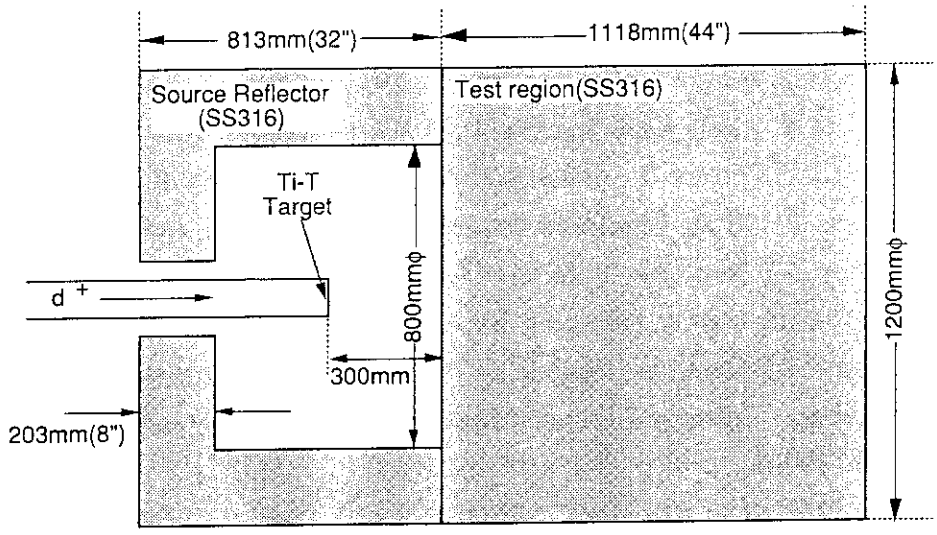

Fig. 1 Experimental assembly of the SS316 experiment.

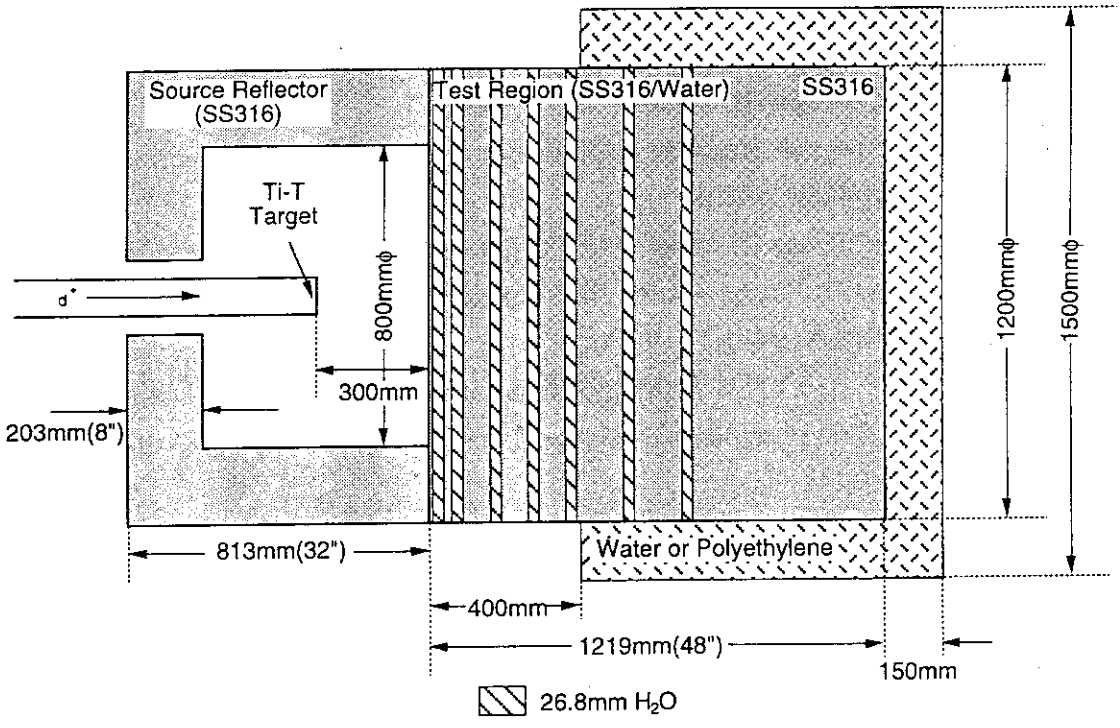

Fig. 2 Experimental assembly of the SS316/water experiment.

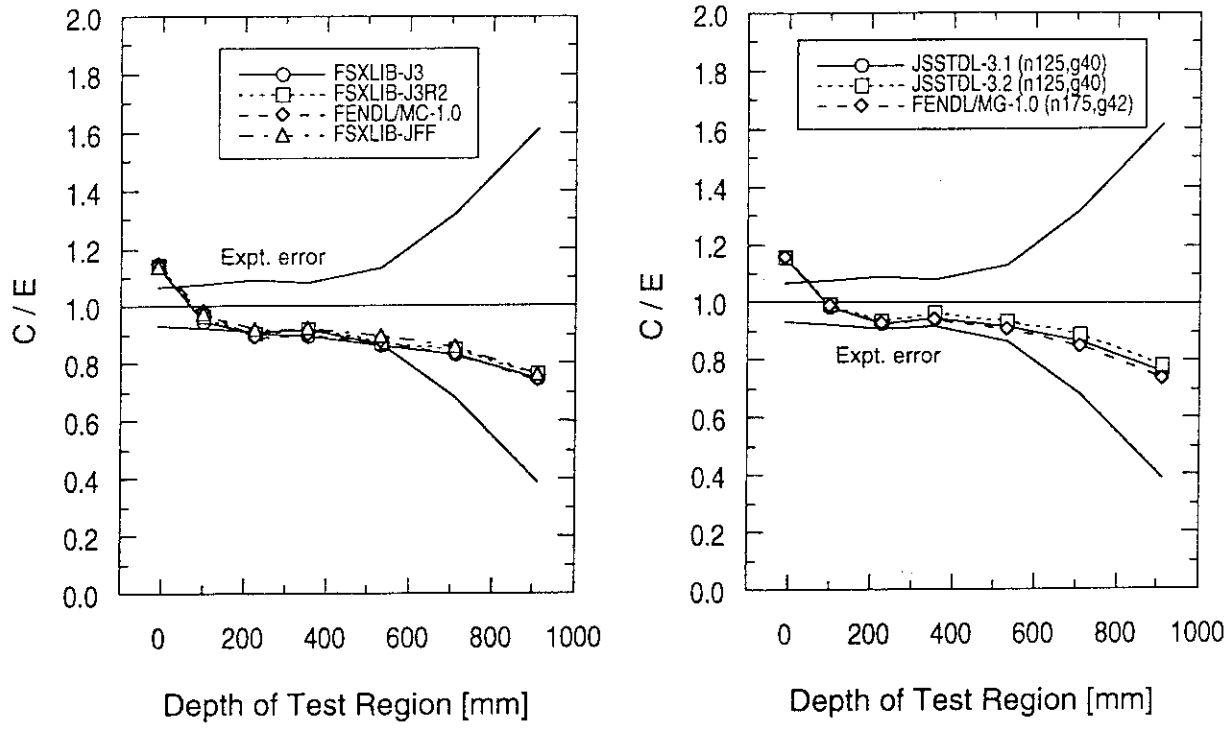

(a) MCNP　　(b) DOT

Fig. 3　C/E values of neutron flux above 10 MeV in the SS316 experiment.

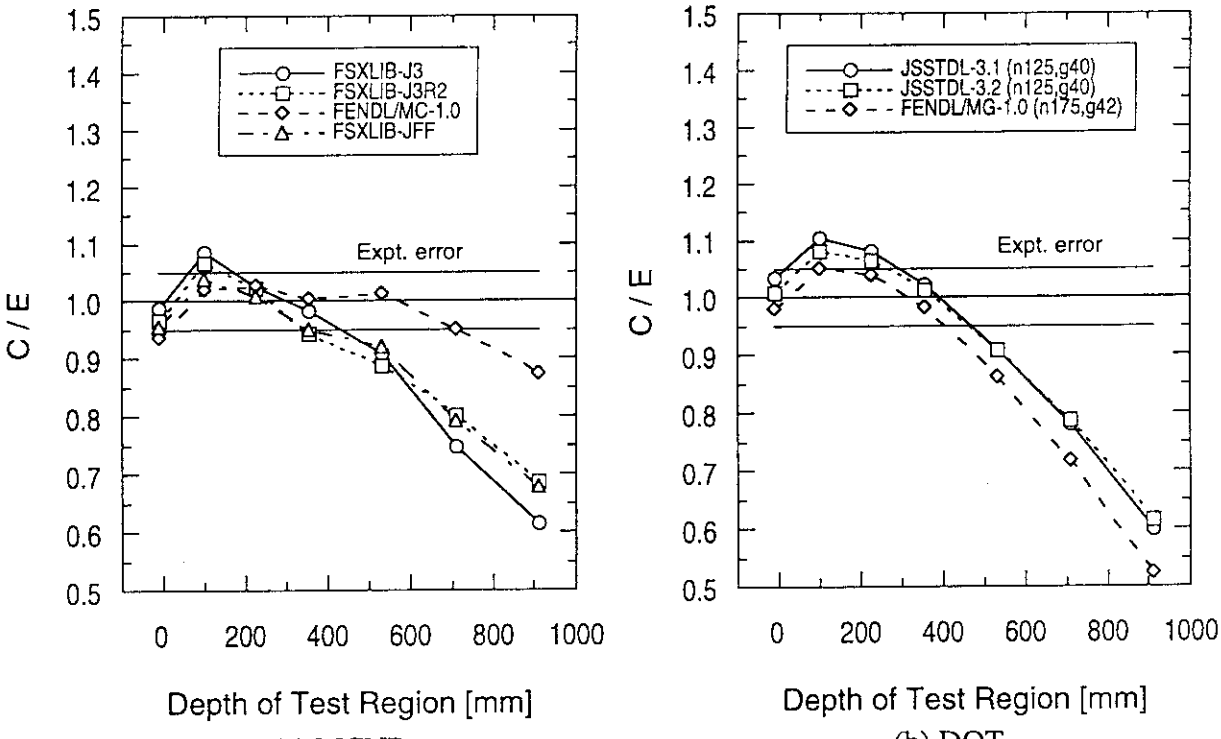

(a) MCNP　　(b) DOT

Fig. 4　C/E values of neutron flux from 100 keV to 1 MeV in the SS316 experiment.

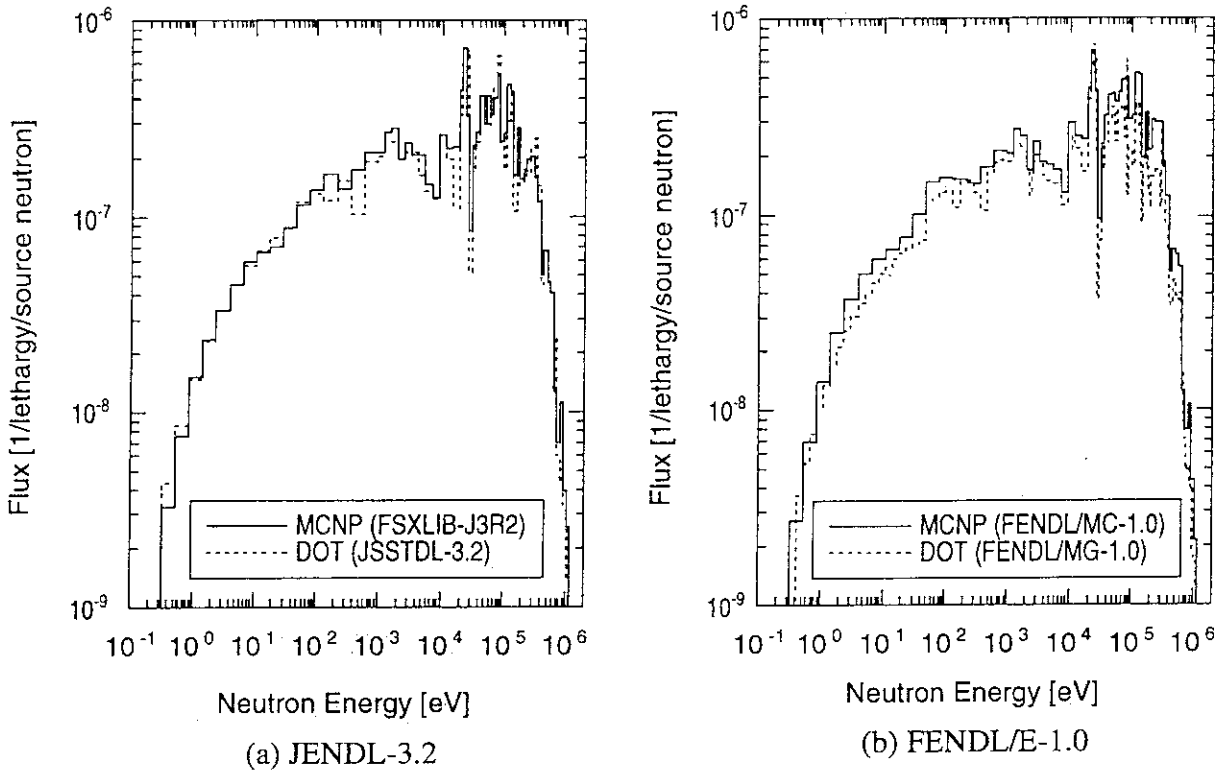

Fig. 5 Neutron spectra at the depth of 914 mm in the SS316 experiment calculated by MCNP and DOT with JENDL-3.2 and FENDL/E-1.0.

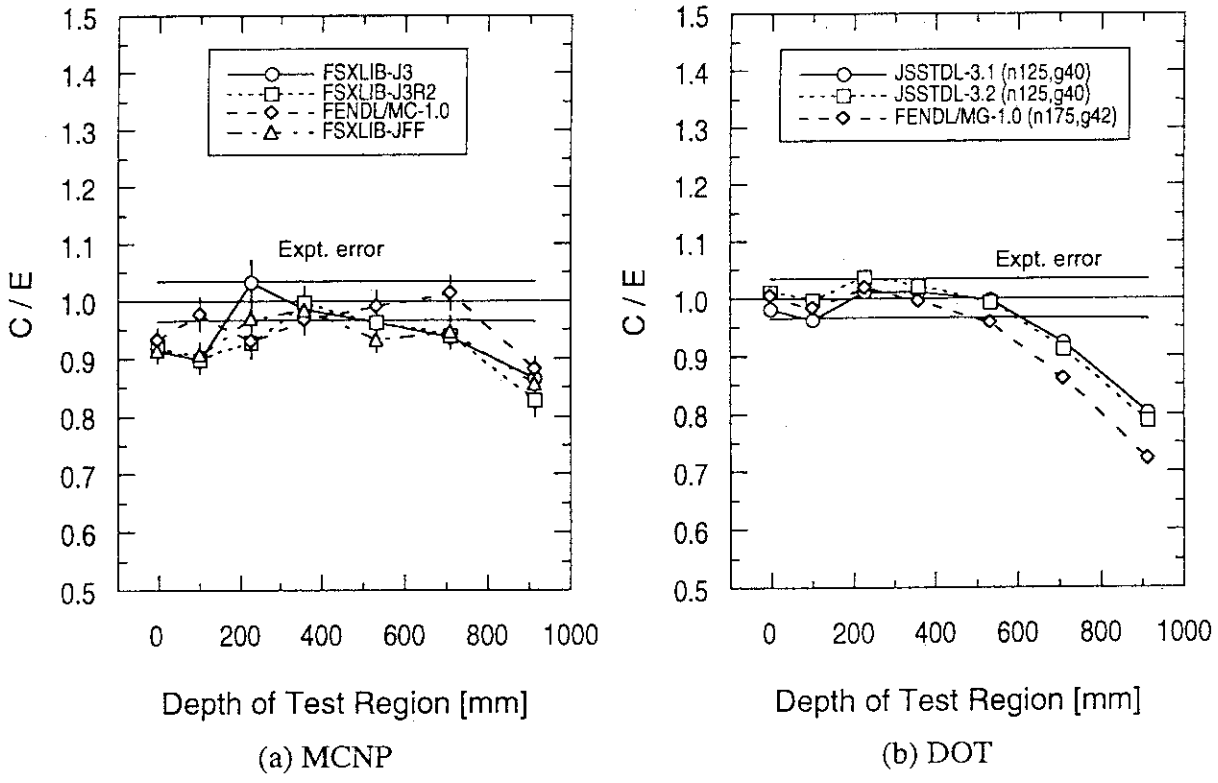

Fig. 6 C/E values of fission rate of ^{235}U in the SS316 experiment.

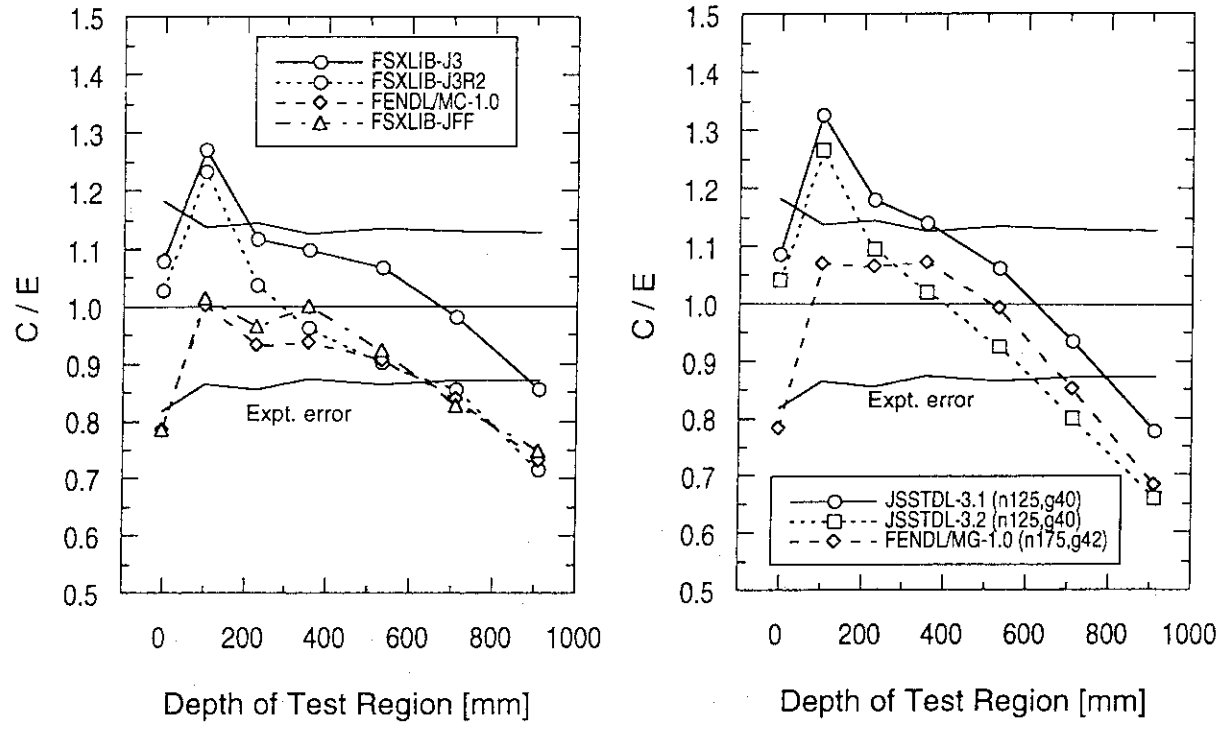

(a) MCNP　　(b) DOT

Fig. 7　C/E values of gamma-ray heating rate of SS316 in the SS316 experiment.

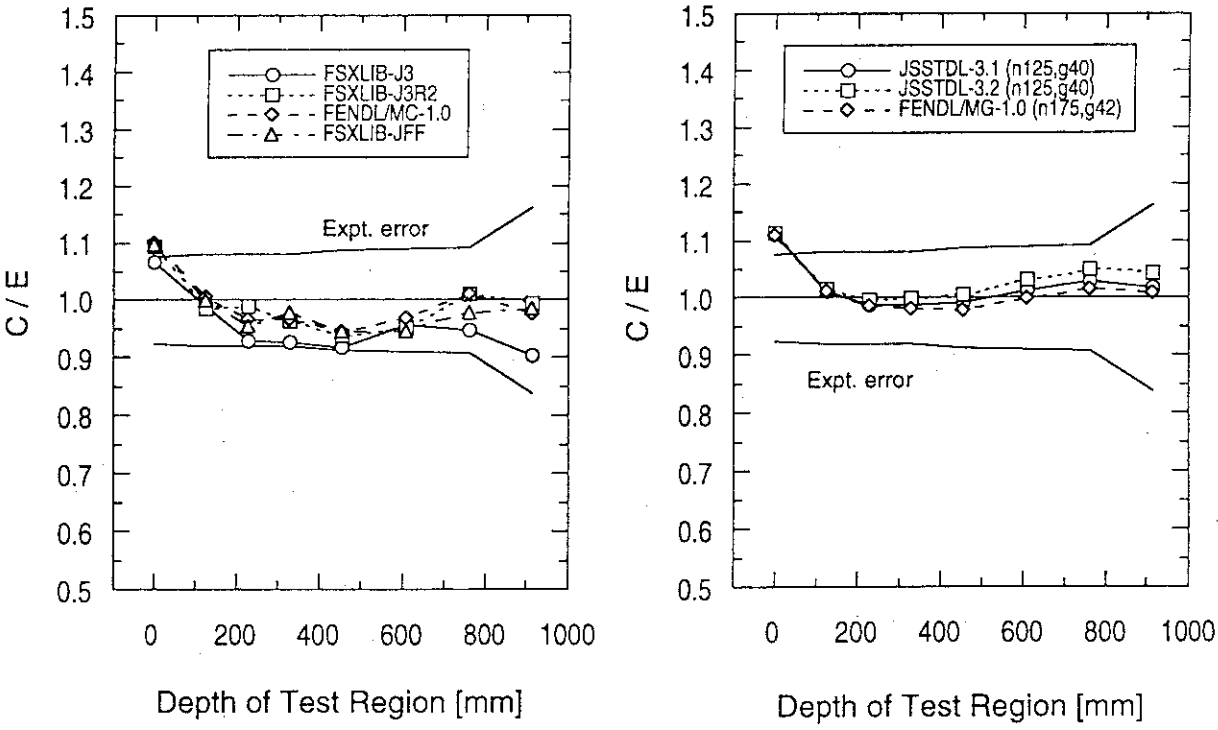

(a) MCNP　　(b) DOT

Fig. 8　C/E values of neutron flux above 10 MeV in the SS316/water experiment.

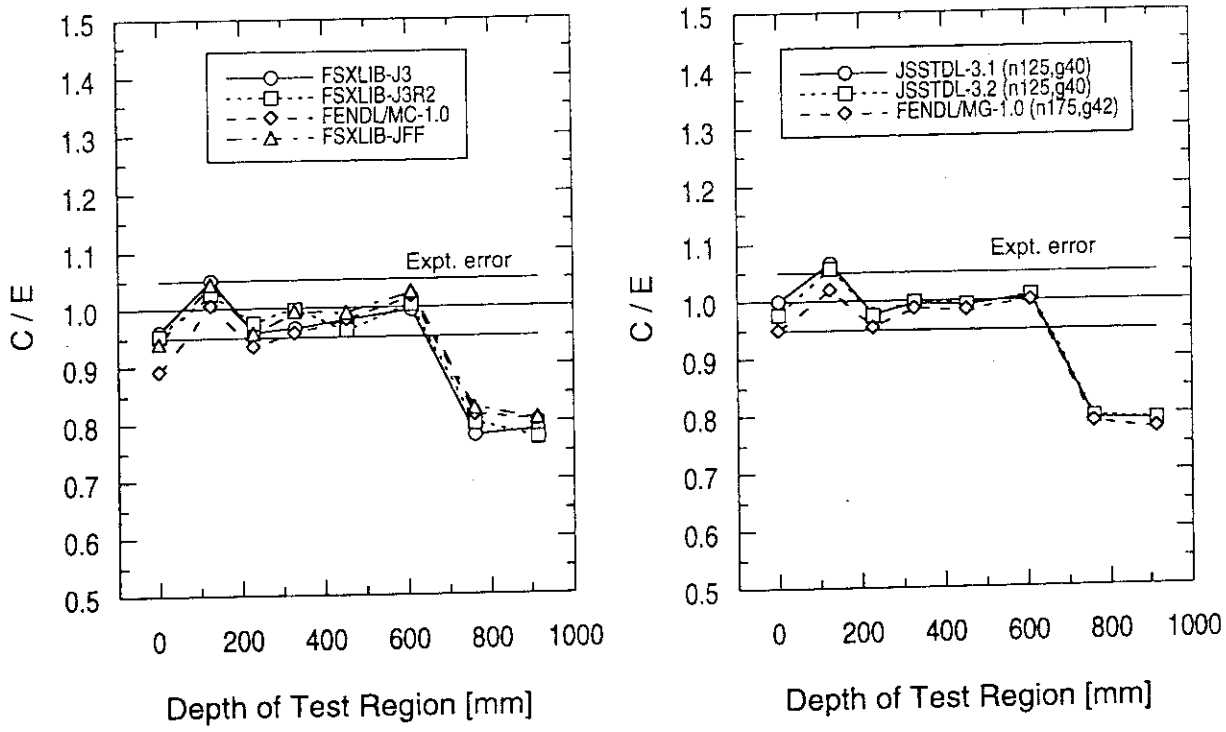

(a) MCNP　　(b) DOT

Fig. 9 C/E values of neutron flux from 100 keV to 1 MeV in the SS316/water experiment.

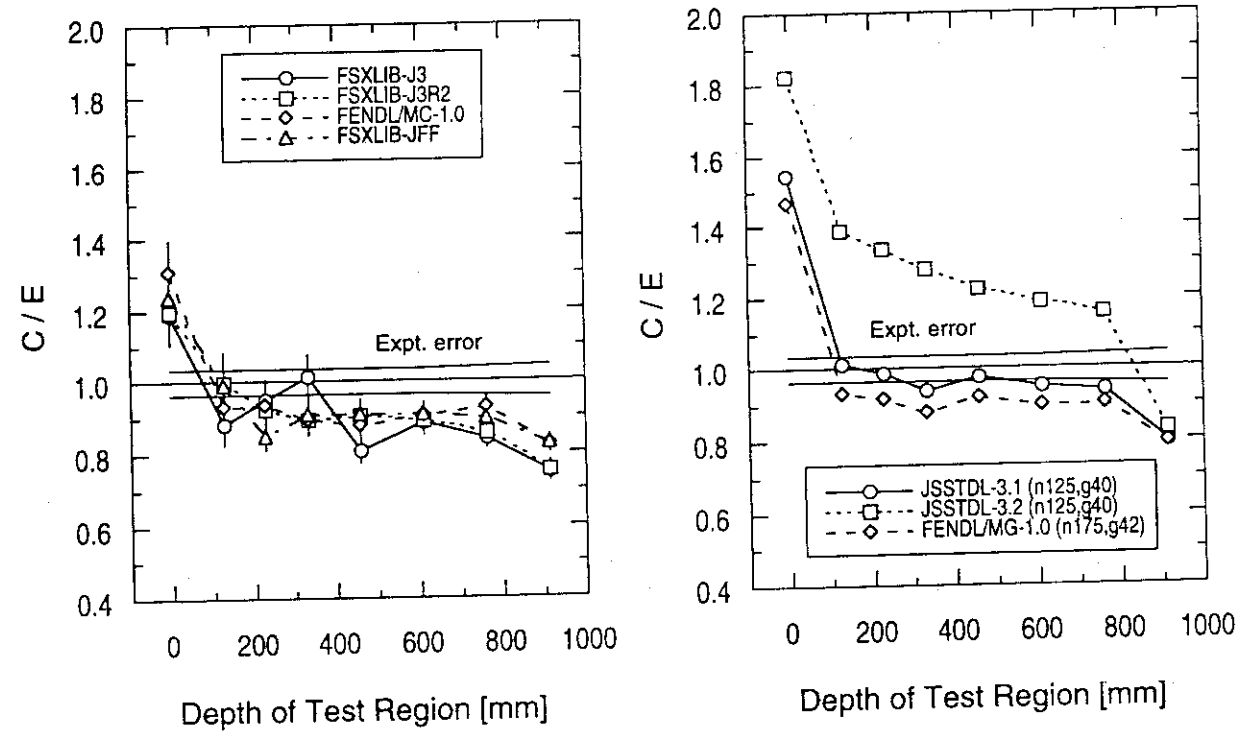

(a) MCNP　　(b) DOT

Fig. 10 C/E values of fission rate of ^{235}U in the SS316/water experiment.

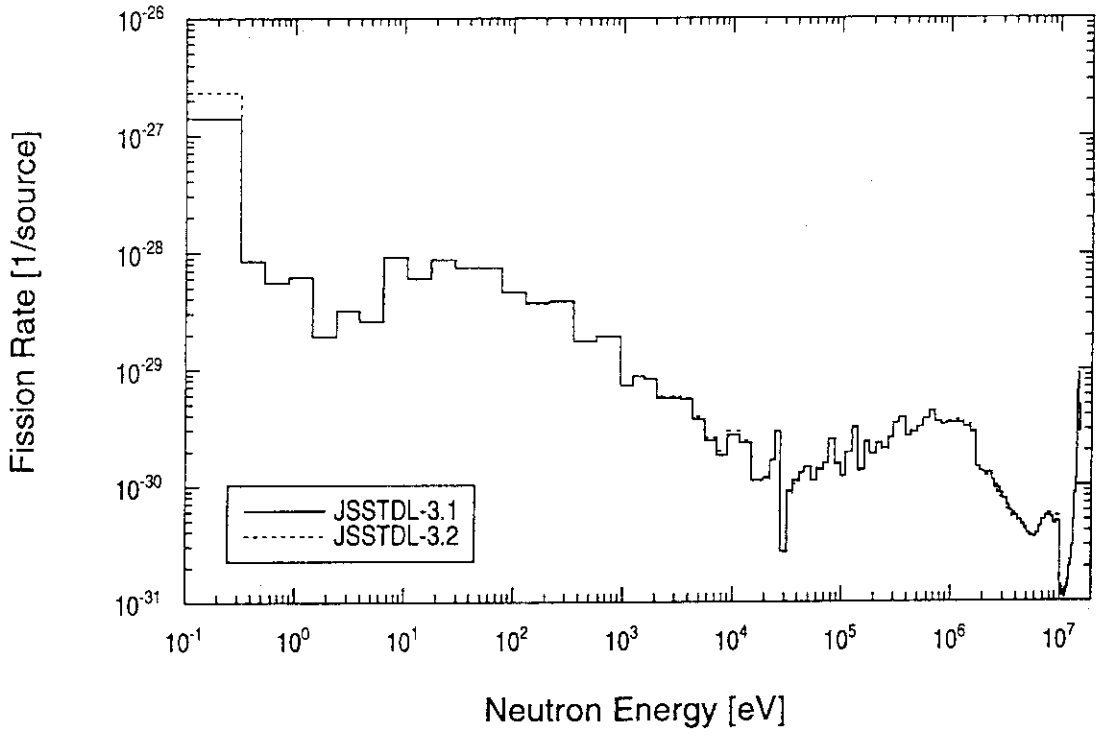

Fig. 11 Fission rate profile of ^{235}U at the depth of 127 mm in the SS316/water experiment calculated by DOT with JSSTDL-3.1 and -3.2.

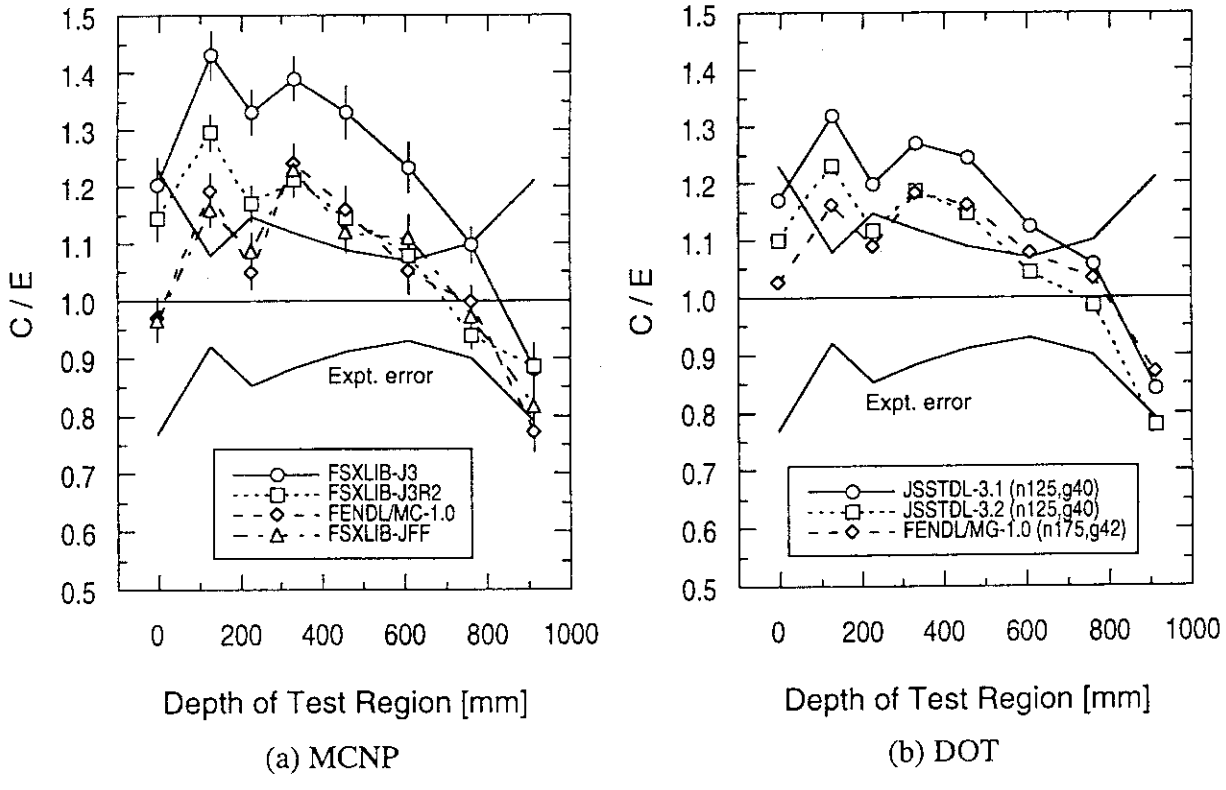

Fig. 12 C/E values of gamma-ray heating rate of SS316 in the SS316/water experiment.

4.2 Test of JSSTDL3.2 Multigroup Cross Section Library by Analysis of FNS Benchmark Experiment

Katsumi Hayashi
Hitachi Engineering Company
Saiwai-cho, 3-2-1, Hitachi, Ibaraki, 317

Yukio Oyama, Fujio Maekawa, Hiroshi Maekawa
Japan Atomic Energy research Institute
Tokai-mura, Naka-gun, Ibaraki-ken, 319-11

Koubun Yamada
Business Automation
Toranomon, Minato-ku, Tokyo, 105

JSSTDL3.2 multigroup cross section library which was created from JENDL 3.2 was tested by analyzing FNS benchmark experiments. FEND/MG-1 multigroup cross section library was also tested. Both libraries are found to be applicable for Carbon, Lithium Oxide and Beryllium analysis except for thermal region and over 10MeV region by FENDL/MG-1. The discrepancy comes from the energy group structure of FENDL 171 group.

1. Introduction

In the shielding design of fusion experimental reactor, discrete ordinate Sn code is still the most effective and powerful design tool because of its nice features to get the flux information on whole system within reasonable computer time. One of the important point we must confirm is whether the multigroup cross section set used is appropriate or not.

To test two multigroup cross section sets, we did benchmark analyses using FNS fusion shielding benchmark experiments. One is JSSTDL3.2 multigroup library which is made from JENDL3.2. The other is FENDL/MG-1.0 based on FENDL/E.

2. Analysis

Multigroup cross section libraries are tested using three FNS integral experiments, i. e.

(1) Graphite cylinder geometry
(2) Lithium Oxide cylinder geometry
(3) Beryllium cylinder geometry

The aim of this work is to validate the multigroup cross sections by simply comparing with the MCNP results.

FENDL/MG-1 (175 groups, P5) and JSSTDL3.2 (175 groups collapsed from 295 groups, P5) are used with GRTUNCL - DOT3.5 (S16) analysis. Reaction cross section used in both analysis is JENDL dosimetry file.

C/E values versus depth from the surface are shown in attached figures.

Figures with odd figure number show the C/E results using FENDL/MG-1(+DOT3.5) and FENDL MC-1(+MCNP).

Figures with even figure number show the C/E results using JSSTDL3.2(+DOT3.5) and FSXLIB-J3R2 (+MCNP).

3. Results

(1) Graphite cylinder geometry

Both multigroup cross section give almost similar results as those obtained by pointwise

cross sections. From these results, both multigroup cross sections are applicable for carbon analysis. However, there are some discrepancies in multigroup and continuous energy analysis in the reaction ^{58}Ni(n, 2n) and ^{90}Zr(n, 2n) in both libraries. This problem may come from the coarse group structure at higher energy region in FENDL 175 group structure. Also, both multigroup libraries give higher reaction rate of ^{235}U(n, fission).that may come from the two group treatment of thermal energy.

(2) Lithium Oxide cylinder geometry

Both multigroup cross section give almost similar results as those obtained by pointwise cross sections. From these results, both multigroup cross sections are also applicable for Lithium Oxide analysis. However, there are some discrepancies in multigroup and continuous energy analysis in the reaction ^{58}Ni(n, 2n) in JENDL. Also, there are some discrepancies in multigroup and continuous energy analysis in the reaction ^{27}Al(n, α) in FENDL.

(3) Beryllium cylinder geometry

Both multigroup cross section give a little bit different results from those obtained by pointwise cross sections. However, we can result that both multigroup cross sections are almost applicable for Beryllium analysis. There are some discrepancies in multigroup and continuous energy analysis in the reaction ^{58}Ni(n, 2n) and ^{90}Zr(n, 2n) in JENDL. Also, there are some discrepancies in multigroup and continuous energy analysis in the thermal reaction as ^{197}Au(n, γ), ^{235}U(n, fission) and ^{6}Li(n, α) in both libraries.

4. Conclusion

From these results, both multigroup cross sections are applicable for carbon, Lithium Oxide and Beryllium analysis.

There are some discrepancies in multigroup and continuous energy analysis in high energy threshold reactions that may come from the coarse group structure at higher energy region in FENDL. Also, the weighting function of these multigroup libraries are different. FENDL uses fusion spectrum weighting and JSSTDL uses 1/E spectrum weighting. This may be the reason why the C/E results for high energy threshold reaction are different.

The discrepancy at thermal energy region observed in FENDL may be caused by two group treatment of thermal energy. Upscatter calculations is necessary in that occasion in DOT3.5 calculation. But normally in design analysis, upscatter calculation is unusual. Consequently, it is better to use one thermal group structure for future FENDL multigroup library.

Acknowledgment

The authors thank to members of fusion neutronics working group for discussion and giving useful suggestions.

References

1. Shibata K., Nakagawa T., Asami T., et al.: "Japanese Evaluated Nuclear Data Library, Version-3-JENDL-3-," JAERI1319 (1990)
2. "Collection of Experimental Data for Fusion Neutronics Benchmark", JAERI-M 94-014 (1994)

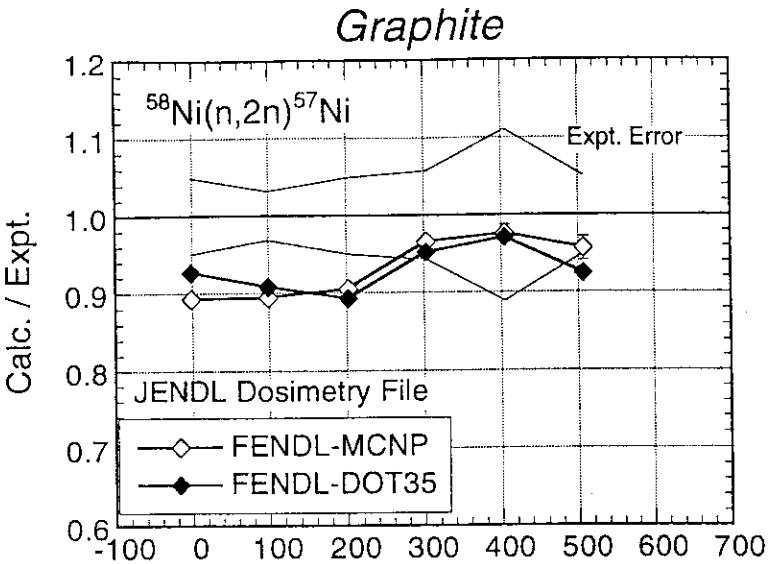

Fig. 1

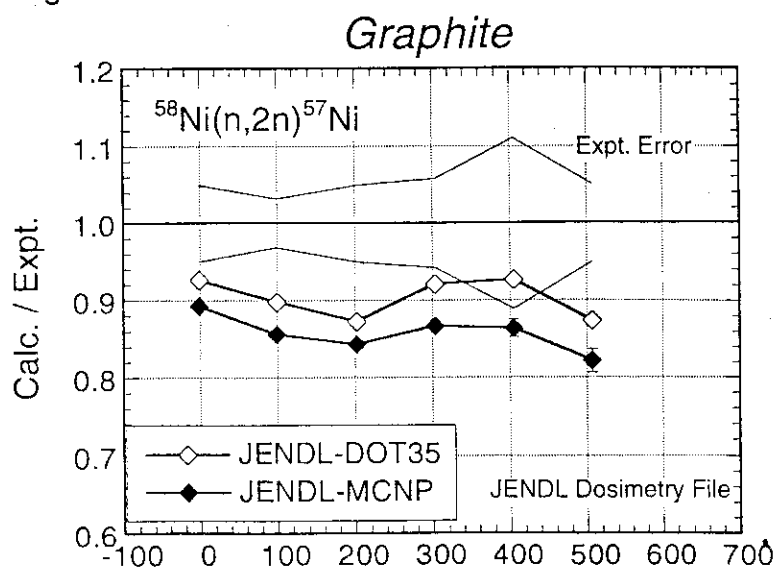

Fig. 2

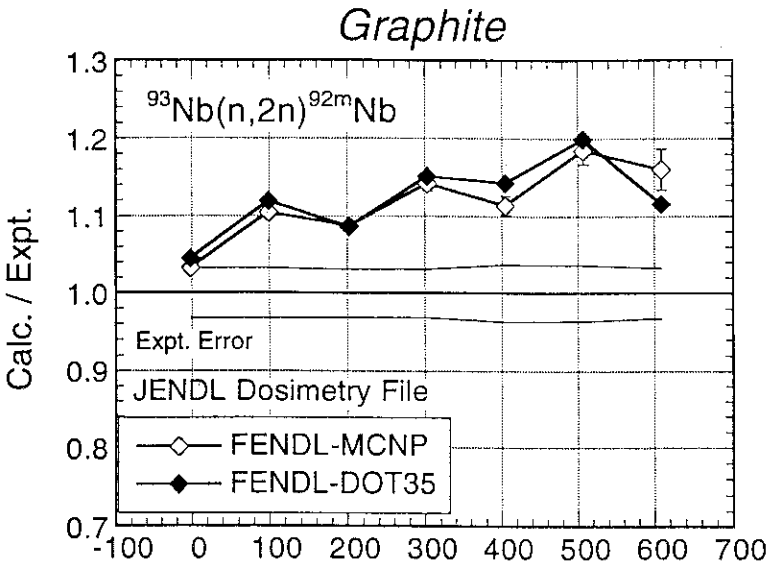

Fig. 3

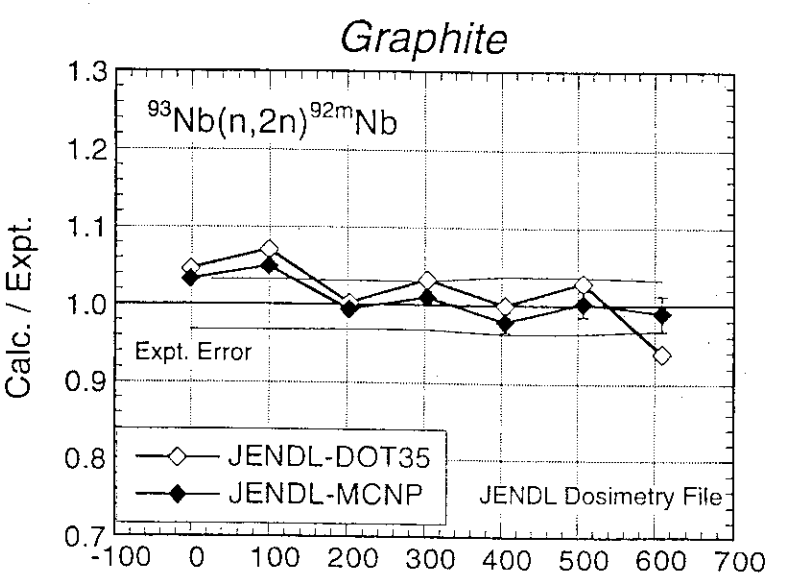

Fig. 4

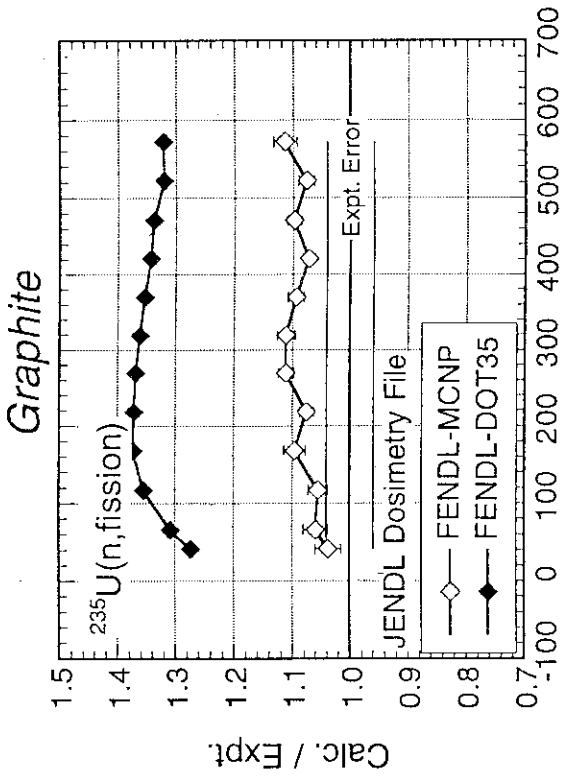

Fig. 7

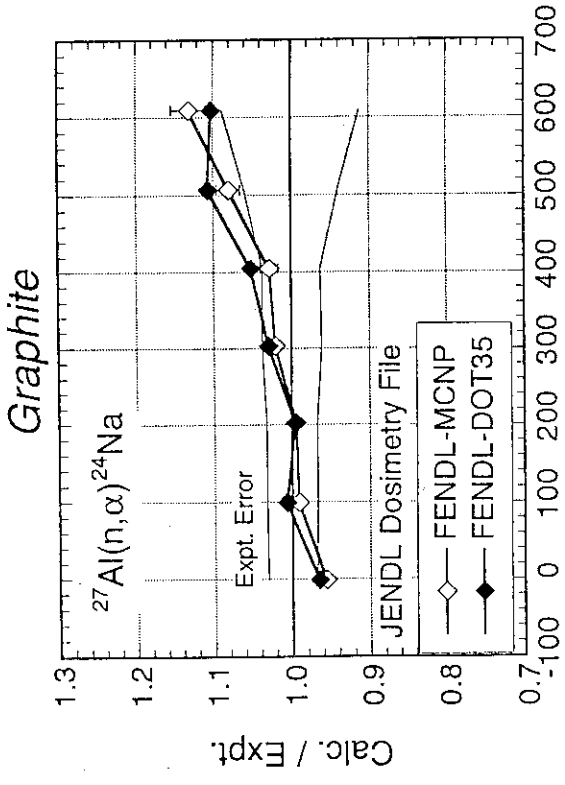

Fig. 5

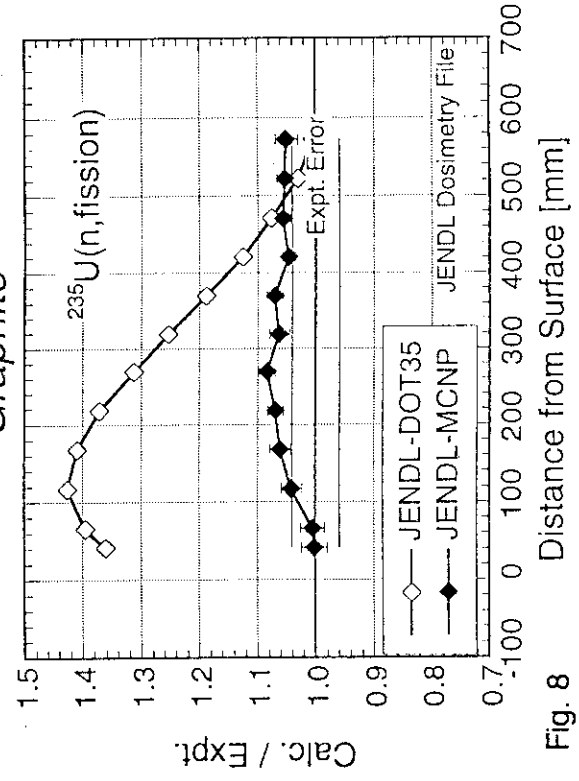

Fig. 8

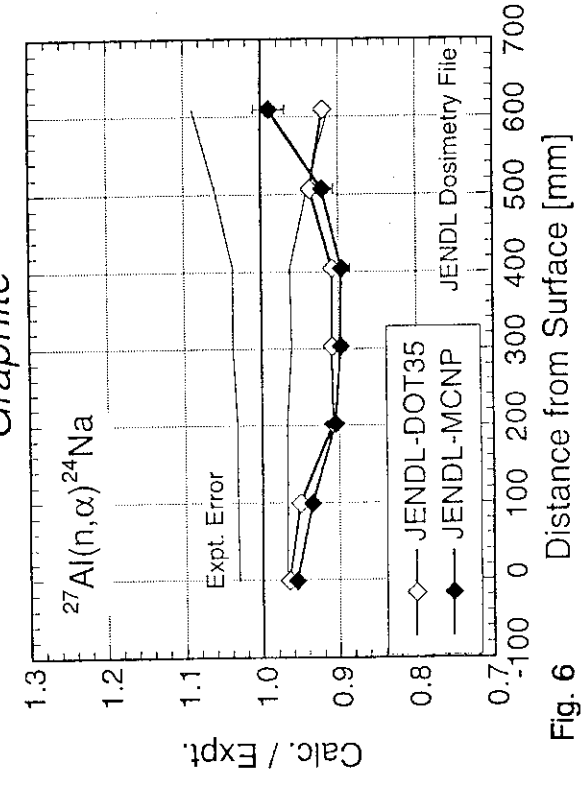

Fig. 6

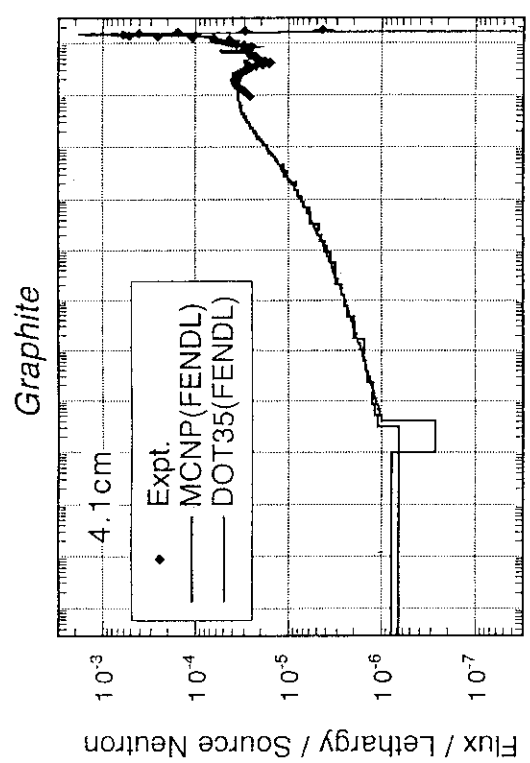

Fig. 9

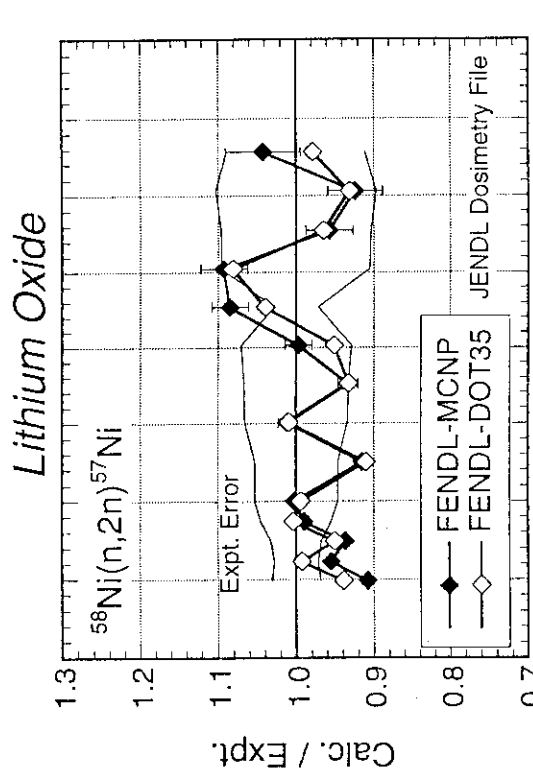

Fig. 11

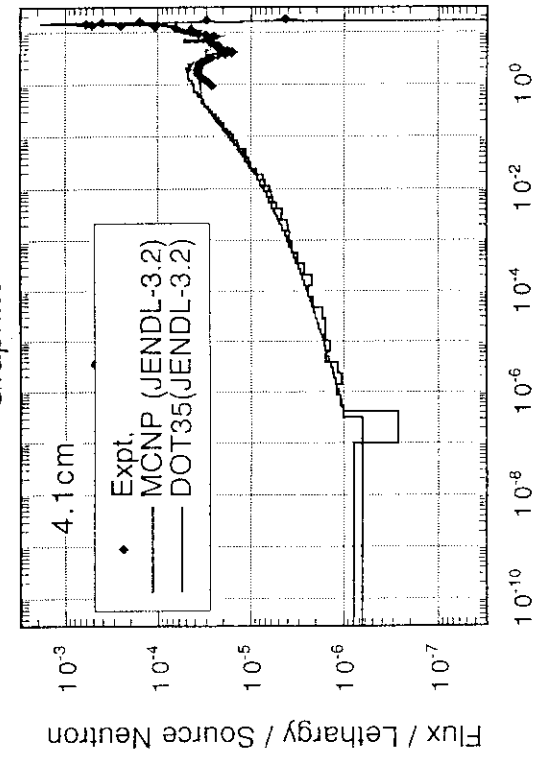

Fig. 10

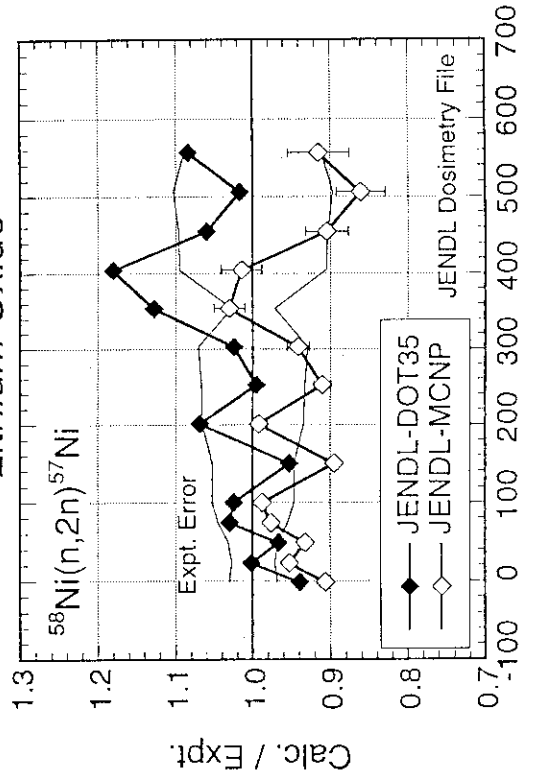

Fig. 12

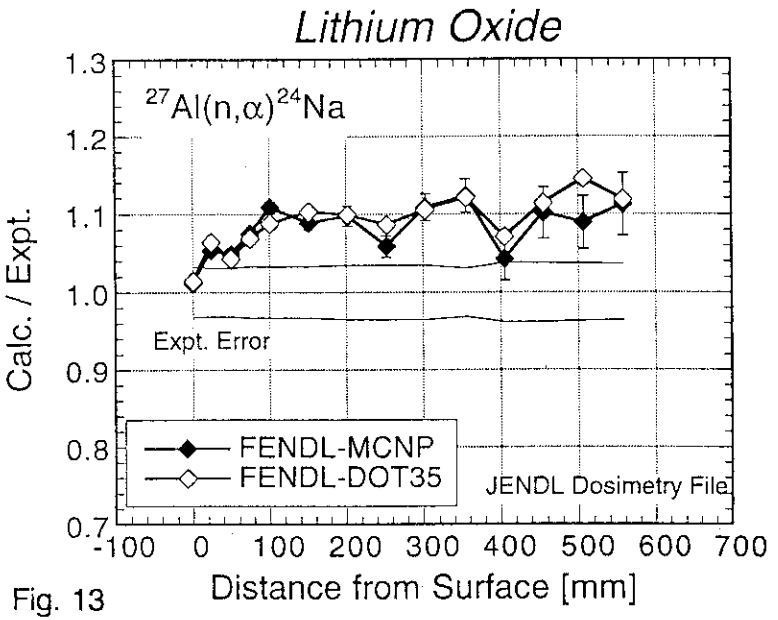

Fig. 13

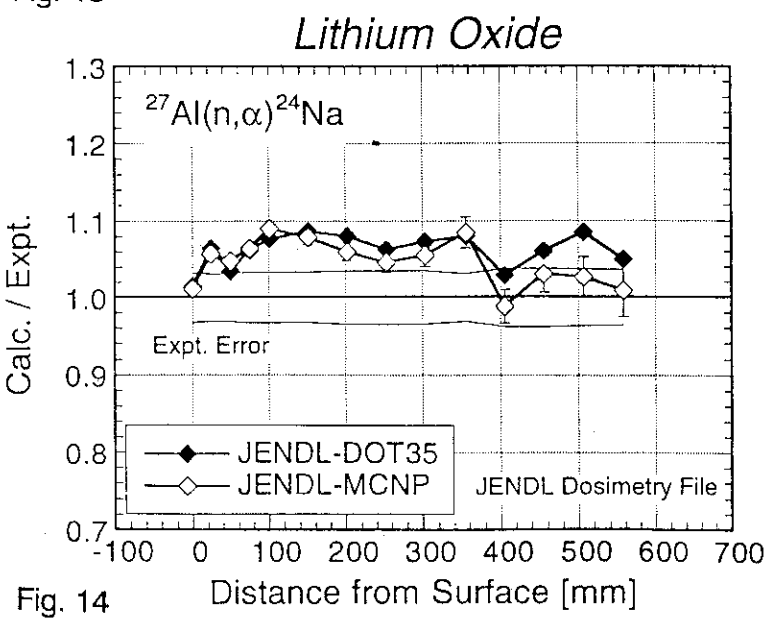

Fig. 14

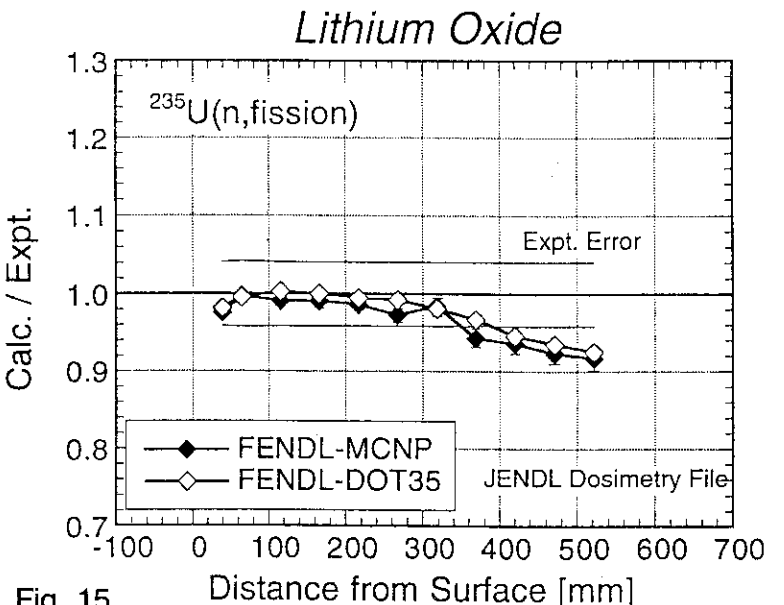

Fig. 15

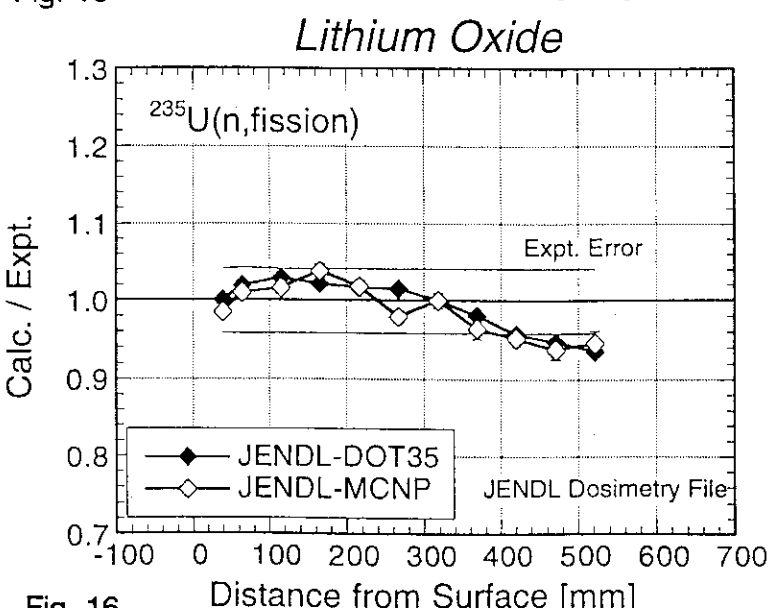

Fig. 16

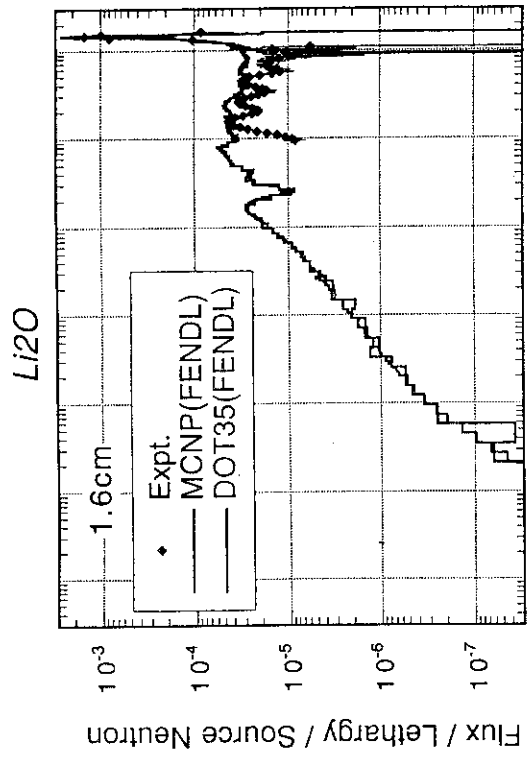

Fig. 17

Fig. 18

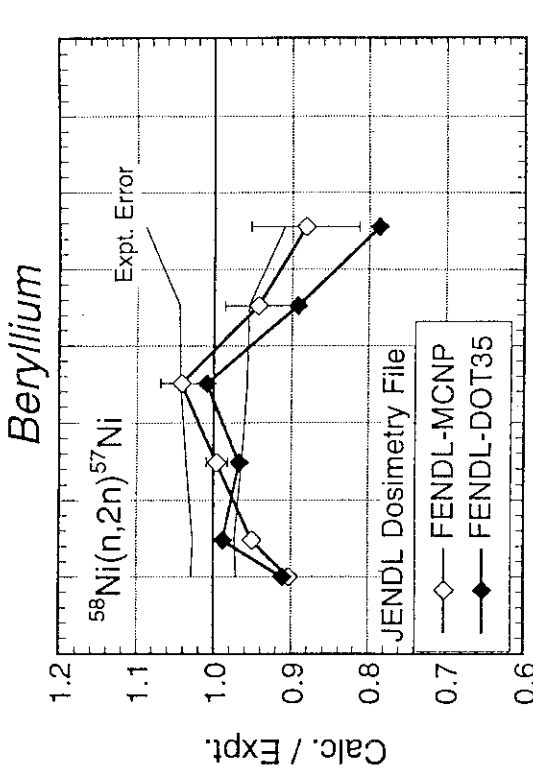

Fig. 19

Fig. 20

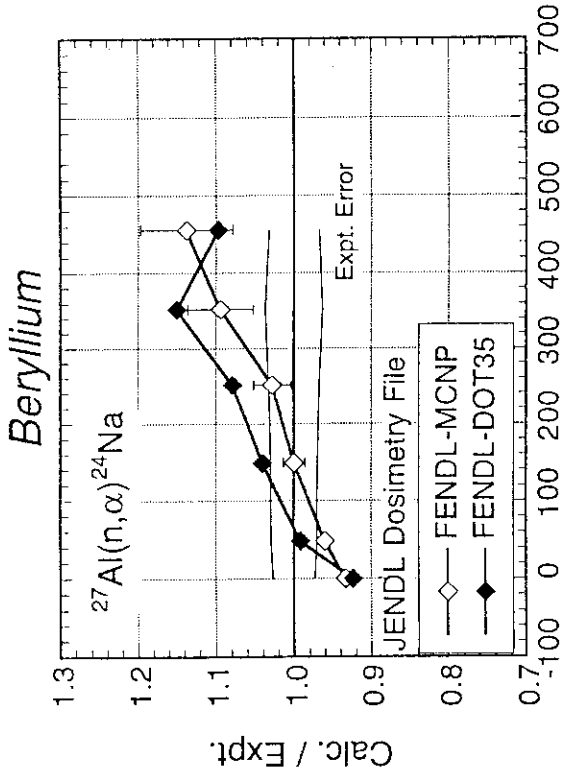

Fig. 23

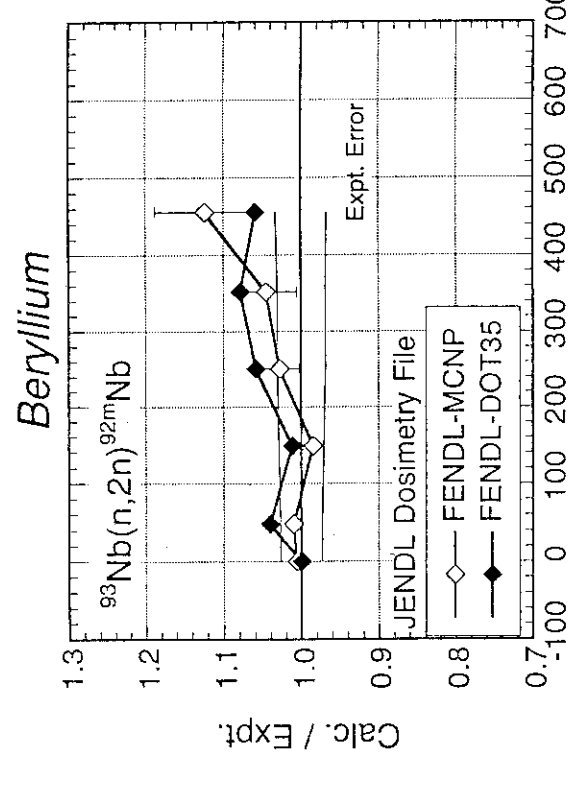

Fig. 21

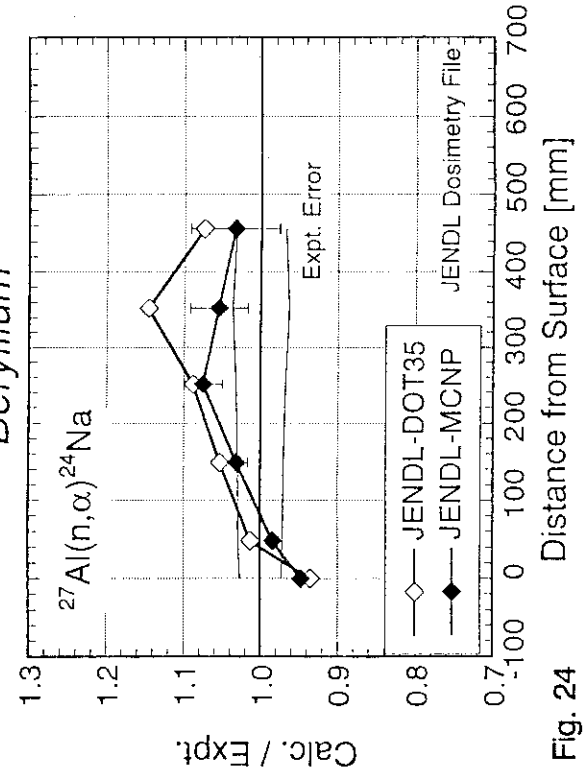

Fig. 24

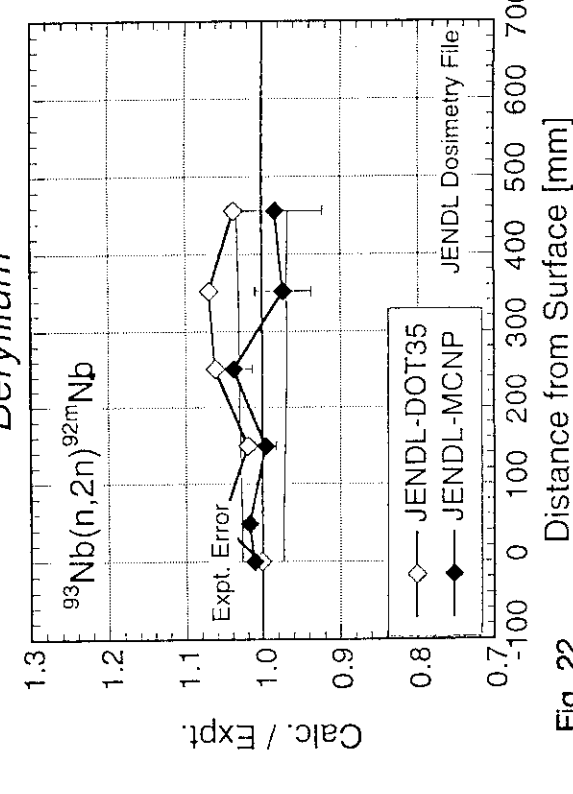

Fig. 22

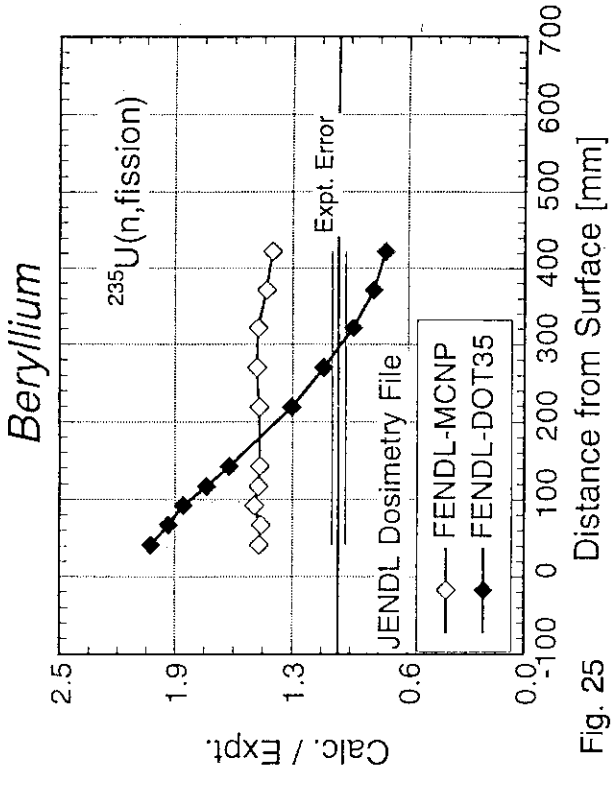

Fig. 25

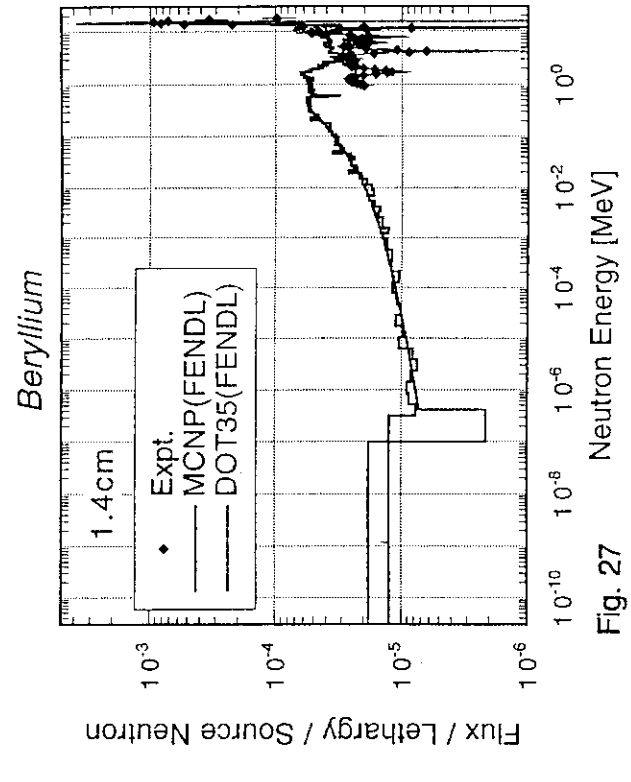

Fig. 27

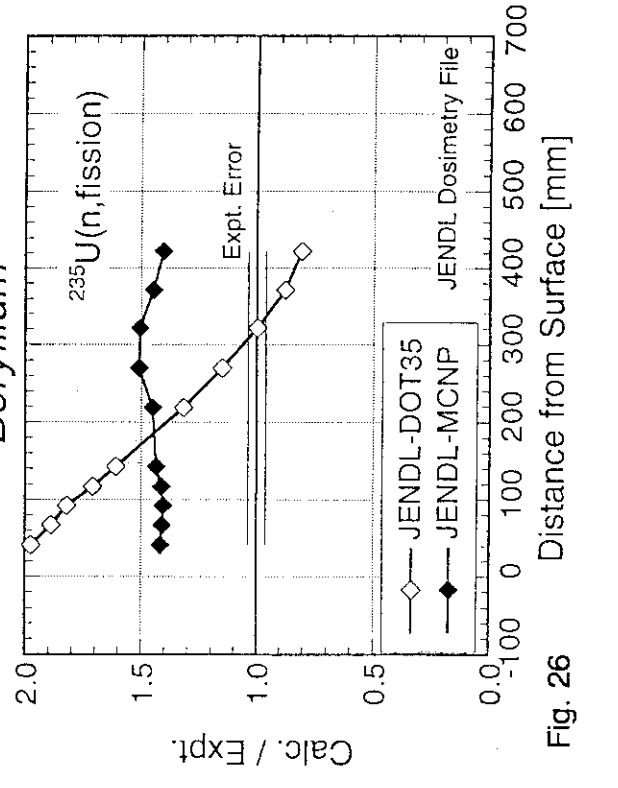

Fig. 26

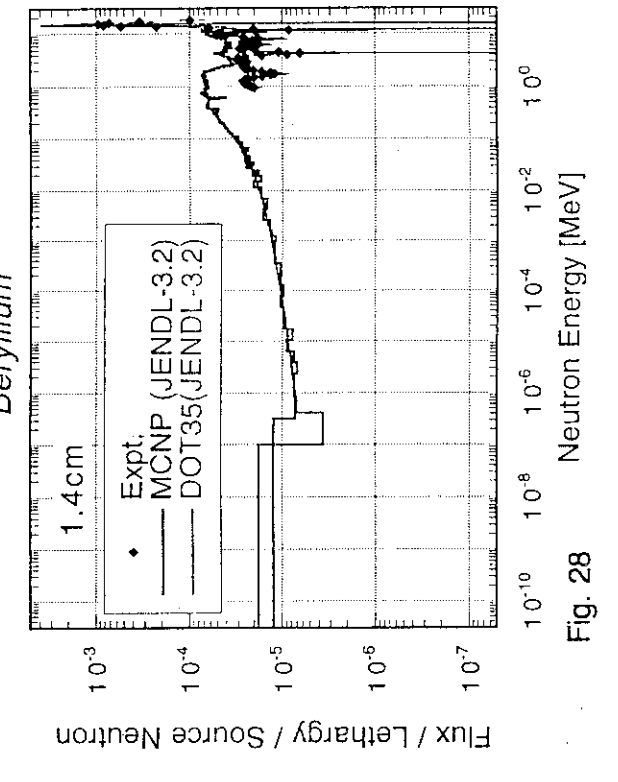

Fig. 28

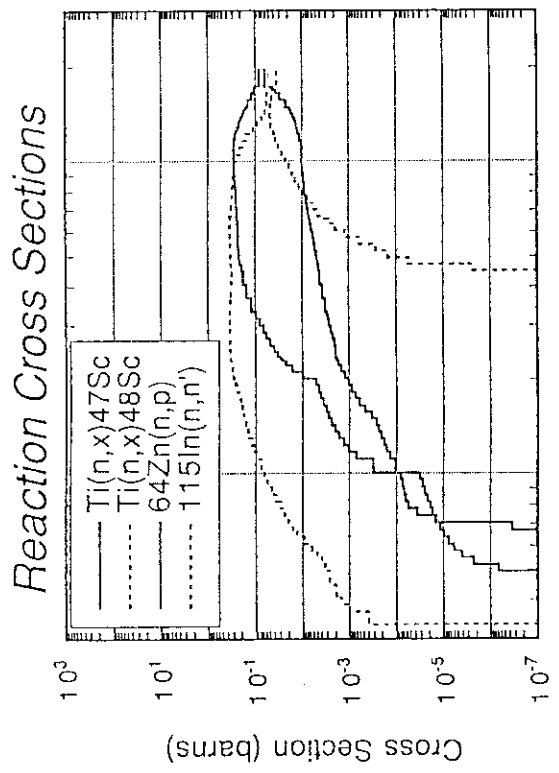

Fig. 31

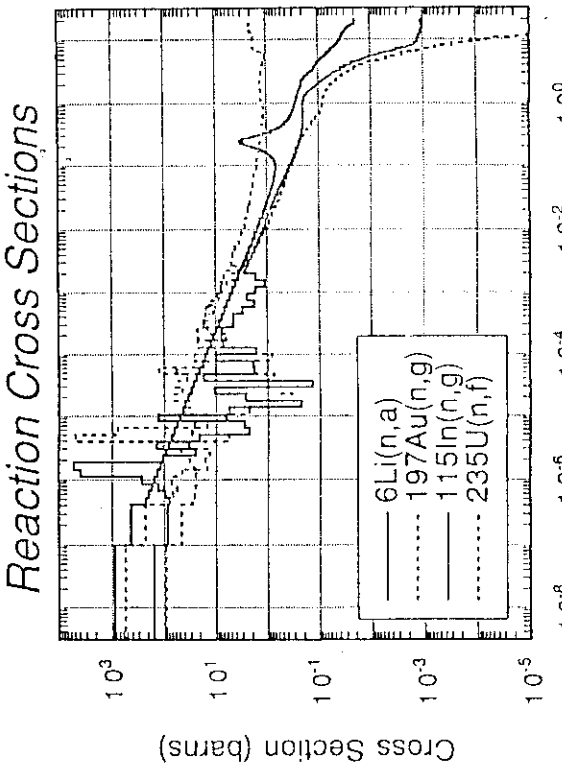

Fig. 32

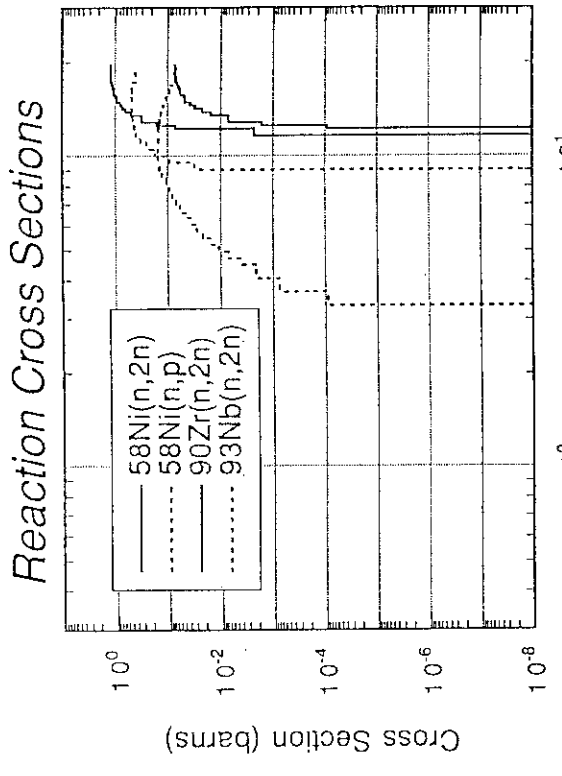

Fig. 29

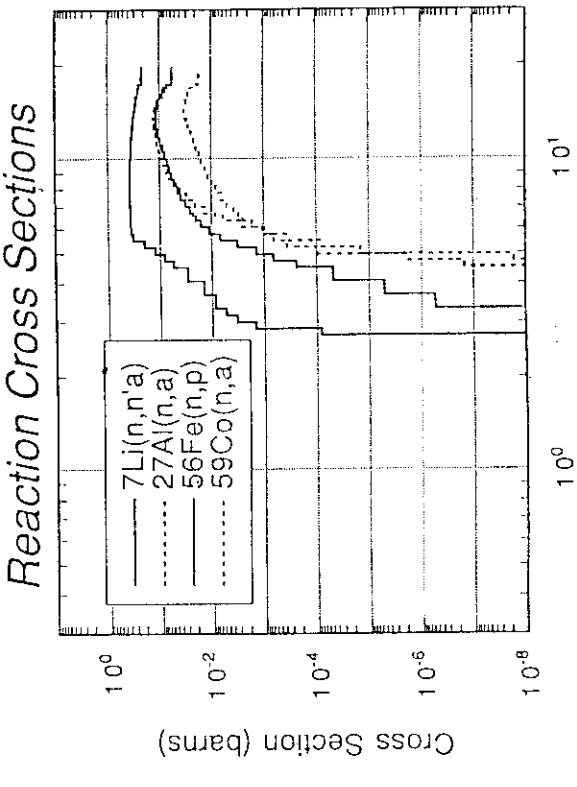

Fig. 30

5. Activation Cross Section File

5.1 Evaluation of the JENDL Activation File

Yutaka NAKAJIMA

Japan Atomic Energy Research Institute,
Tokai-mura, Ibaraki-ken 319-11, Japan
e-mail : nakajima@cracker.tokai.jaeri.go.jp

and

Japanese Nuclear Data Committee activation-cross-section data working group[1]

The preliminary JENDL activation file was accomplished in February 1995 and has been used in the Japanese Nuclear Data Committee and as one of the data sources for the Fusion Evaluated Nuclear Data Library in IAEA. In the preliminary file 1,158 reaction cross sections have been compiled for 225 nuclides up to 20 MeV. Evaluation was made so as to reproduce reliable experimental data. While a number of data are included in the file from JENDL-3.2, reevaluation has been made based on the SINCROSS-II system[1)]. The overall consistency with experimental data has been improved. The detail of the evaluation of cross sections for the JENDL activation file has been described in the proceedings of the 1995 Symposium on Nuclear Data[2)].

References

1) Yamamuro N.: JAERI-M 90-006(1990).

2) Nakajima Y, , et al.: To be published in JAERI-Conf.

[1]Members of the activation-cross-section-data working group

T. Asami*, M. Hachiya, Y. Ikeda, S. Iwasaki, K. Kobayashi, Y. Nakajima, Y. Seki, N. Yamamuro*, M. Yano, T. Yoshida, T. Watanabe*, (S. Iijima*).

*Evaluators

5.2 Integral Tests of Current Activation Libraries And Comparisons

Yujiro Ikeda

Japan Atomic Energy Research Institute
Tokai, Ibaraki 319-11 Japan

The results for the integral tests of JENDL activation file along with other currently available libraies are given. The tests are based on the benchmak experiments in D-T neutron fields carried out at FNS.

1. Introduction

Neutron activation reactions are one of most serious issues in the fusion reactor development, in terms of induced radioactivity production, dose rate and decay heat after shutdown and long-lived waste disosal scenario. In particlar, the data are strongly needed from reactor safety and environment assessment. In order to meet the data request, large efforts have been placed on the establishment of comprehensive activation cross section data files not only in Japan as JENDL activation file, nut also world wide regional libraires ,e.g., EAF (Europian Activation File), US activation file, FENDL activation library, and so forth. In any data file, however, it is required to validate the quality of data and the adequacy for the application. The extensive validation study has been conducted for this purpose at FNS with emphasis of integral experiments on the radioactivity in the potential candidate of materials for fusion reactor apprication. The experimental procedure and the first results for the data testing were given in Ref-1,2), where the the first version of JENDL activation files[3] showed the most reliable evaluation among tested libraries of FENDL-1[4], REAC*3[5] library ,EFA-3.1[6] and Russian file of ADL3T[7].

This paper summarizes the status of the data tests and recommendations for improving the data. give a guid line of adoption of a data liburary for the fusion application. In viewing the ITER/EDA progress, it should be noted that this type of integral data test is of valuable for the ITER design. Also some notes on the procedure for FENDL/Activation Library verison-2 are given, which is to be the official data base for the licensing matter.

2. Activation Libraries and inventory codes

At the present moments, following activation liburaries are available for data test; JENDL -A3.2 (1,400 reactions), FENDL/A-1.1 (9,000 reaction), EAF-3.2 (11,000 reactions), ADL3T (35,000 reactions) and REAC-175 (10,000 reactions). In the present study, the code module of ACT4 in the THIDA code system[8] was mainly used. Some of calculation was done by REAC*3[5] code. The data libraries were made in 125 neutron groups structure and 175 neutron groups of VITAMIN-J format.

3. Material Wise Benchmark Experiments and Data Testing:JAERI/USDOE

The data have been distributed in the world through the IAEA-NDC. The data are the products in the JAERI/USDOE collaboration on fusion neutronincs. All detailed data necessary for the calculation in terms of materials, neutron sectrum, activities of interest are given in the reprot.[1,2] Given below is the summary of the results for the test in material wise and produced radioactivity wise.

Mg:

^{24}Na: All calculations agree within 3 % (REAC175 is 10 % high to the present ACT4 calculation) No change from J3.1 to J3.2. FENDL-175/ACT4 and FENDL/REAC gives the same result. FENDL and EAF3.1 are almost identical.

^{27}Mg: JENDL doesn't have the corresponding reaction. Other library give almost same results.

^{24}Ne: FENDL and EAF3.1 are identical/ ADL3T gives 7 orders of magnitudes lower value.

Al:

^{24}Na: FENDL/EAF3.1/JENDL agree within 3 %. ADL3T is higher by about 8 % than those others.

^{27}Mg: FENDL/EAF3.1/JENDL agree within 4 %. ADL3T is lower by about 8 % on the contrary to the ^{24}Na case.

^{26}Al: JENDL is slightly larger than others by 30 %.

Si:

^{28}Al: FENDL and EAF3.1 are almost identical. ADL3T and JENDL give close results which are more than a factor of three lower than those of FENDL/EAF3.1. Further verification of the cross sections are needed by experiment. (No experimental data is available)

^{27}Mg: ADL3T and JENDL reasonably agree with the experiment, but FENDL/EAF3.1 give a factor of 7 larger values than the experiment.

^{29}Al: All calculations except ADL3T agree within 2 % with the experiment. ADL3T is lower by 6 % than others. FENDL/REAC gives 6 % lower that FENDL/ACT4. Therefor, there is a possible difference in the decay library data.

^{28}Mg: No experimental data. FENDL/EAF3.1 give unreasonable large values, which was pointed out in the previous discussion for the REAC175. The data should be revised. ADL3T and JENDL seems reasonable, but further experimental verifications are needed.

^{31}Si: JENDL doesn't have corresponding reaction cross section, (n,γ). It will be added soon. There are scattered results among FENDL/EAF3.1/ADL3T. Considerably large reduction of the value from 175g to 125g in the EAF3.1 indicate group structure dependency for the capture reaction cross section. Cross sections should be compared directly. New experimental data are needed for the next test.

Ti:

^{45}Ti: All calculations give almost same values, overestimating more than 40 %. About 10 % difference between calculations with 125 and 175 group structures. It is due to steep exciting function near 14 MeV neutron peak. Experimental value should be checked because of large uncertainty in the 511γ-ray counting efficiency. The cross section with high threshold energy near 14 MeV should be re-examined.

^{46}Sc: All calculation agree within 20 %. JENDL gives the closest agreement with experiment. ADL3T gives largest value.

^{47}Sc: All calculation overestimate experiment. ADL3T gives the best agreement with experiment by 11 %. FENDL/EAF3.1 largely overestimate by 50 %.The cross section needs to be examined.

^{48}Sc: Generally all calculations agree within 15 % with the experiment. JENDL gives the best agreement within 6 %.

^{49}Sc: No experimental data due to the lowγ-ray branching. Large discrepancies more than 40 % are found among the calculations. New experimental data are needed.

^{51}Ti: There is no data in JENDL due to short life discrimination. It will be added.

V: FENDL/REAC gives always 5 % higher value than FENDL/ACT4 due to higher number density in REAC*3 element library.

^{47}Sc: There is a large difference in the calculations. FENDL and EAF3.1 are identical. ADL3T and JENDL3.2, respectively, gives 3 and 2 orders of magnitude lower value than FENDL/ EAF3.1. FENDL/EAF3.1 seem not realistic.

^{51}Ti: All calculation give almost same results. However, those are lower by 50 % than experiment. Both cross sections and experiment should be re-examined.

^{48}Sc: ADL3T is 10 % higher than others. JENDL gives closest agreement with experiment with C/E of 1.04

^{52}V: FENDL/ADL3T/EAF3.1 calculations give almost same results, which overestimate experiment by 15 %. The self-shielding of the (n,γ) reaction should be considered. JENDL gives one order of magnitude lower value than others. JENDL should be check. New experimental data are needed.

Cr:

^{49}Cr: Large overestimations are observed. JENDL is closest with C/E of 1.27. However, there is unreasonable anomaly in the cross section curve at 14 MeV. The revision of evaluation is under way. ADL3T follows JENDL. FENDL/EAF3.1 overestimate by a factor of two.

^{49}V: Very few cross section measurements are available. There are large differences among the calculations. JENDL took lower cross section by discarding the highest experimental cross section data.

^{51}Cr: Calculations agree within 10 %. JENDL gives the best agreement with the experiment (C/E = 1.05)

^{48}V: JENDL gives two orders of magnitude lower values than others.

^{51}Ti: Calculations are in the same range.

Mn:

^{54}Mn: All calculations reasonably agree with the experiments.

^{55}Cr: No experimental data due to short-lived and extremely small γ-ray branching. The calculation scattered within 60 %. JENDL gives the lowest value.

^{52}V: All calculations overestimate the experiment. JENDL gives the closest value with C/E = 1.27.

^{56}Mn: All calculations overestimate the experiment. There is a large difference in the calculations. The processing of group cross sections for (n,γ) reactions should be check.

Fe:

^{53}Fe: All are in a same range.

^{55}Fe: JENDL is 10 % higher than others.

^{54}Mn: All calculations seem O.K. Agreements with the experiments are excellent.

^{51}Cr: All calculations agree within 5 % with the experiments.

^{56}Mn: All calculations are in good agreements within 10 % with the experiment. JENDL gives the best results. with C/E from 0.95 to 1.01.

^{59}Fe: JENDL is higher by 15 % than others.

Co:

^{58}Co: Except JENDL, all calculation show C/E range from 1.12 to 1.25. From the preliminary

analysis, JENDL overestimated the experiment largely.

^{58m}Co: On the contrary to the ground state production, JENDL underestimated the experiment.

^{59}Fe: FENDL/EAF3.1 agree within 10 % with the experiment. However, ADL3T/JENDL underestimated it by more than 30 %.

^{56}Mn: The experimental value of case A11 seems suspicious. All calculations agree within 10 % with the experiments.

Ni:

^{57}Ni: JENDL/ADL3T agree with the experiments within 5 %. Others overestimated the experiment by 10 %.

^{57}Co: All calculations except ADL3T are identical within 4 %. The agreement with the experiment is generally good within 10 %. ADL3T is 30 % larger than others.

^{59}Ni: All calculations are in a same range.

^{58}Co: Except ADL3T, all calculations agree with the experiment within 15 %. ADL3T give lower value by 30 % than others.

^{58m}Co: JENDL is a factor of two smaller than others. There should be a systematic change in the calculation of $^{58m+g}$Co production.

^{60}Co: JENDL is lower by 20 % than others. From the recent status of the cross sections measurement for ^{60}Ni(n,p)$^{60m+g}$Co reaction, JENDL should be raised by 20 %.

^{60m}Co: All calculations give almost the same results.

^{61}Co: Large discrepancies more than 30 % exist between FENDL/EAF3.1 and JENDL. ADL3T is in between.

^{63}Ni: All calculations are in a same range.

^{62}Co: All calculation give almost identical values.

^{62m}Co: All calculation except FENDL/REAC calculation give more than one order of magnitude lower value than the experiment. The decay chain of the ACT4 code is suspicious. Decay chain should be check. However, according to the current decay scheme, almost all 1174 γ-ray should be associated with the ^{62m}Co decay. Thus, isomer ratio for this production should be re-examied.

^{59}Fe: All calculation give almost same results.

^{65}Ni: Except ADL3T, all calculation are in a same range. ADL3T is 70 % higher than others.

Cu:

^{62}Cu: All calculations agree with the measurement. However, the ^{62}Cu decay rate was obtained from 511 annihilation gamma-ray intensity assuming that all γ-rays are associated with ^{62}Cu. This was not true. Actually there was same 511 γ-rays due to the ^{64}Cu decay. If the ratios of ^{62}Cu and ^{64}Cu decay rates could be reasonable, all calculations should overestimate by about 15% the experiment. According to the new measurement at FNS, the cross section of ^{63}Cu(n,2n)-^{62}Cu should be lowered by more than 10 % from the currently evaluated value. The new evaluation is highly recommended.

^{64}Cu: The efficiency of 511 keV annihilation γ-rays are different from geometry by geometry. Thus, large uncertainty should be taken into account. Generally, the agreements between calculations and experiments are good.

^{63}Ni: All calculation give close results each other.

^{60}Co: ADL3T is larger by 50 % than JENDL. FENDL/EAF3.1 are in between.

^{60m}Co: JENDL is lower by 50 % than others.

^{65}Ni: All results are in a same rage.

^{62}Co: There are a large difference between FENDL/EAF3.1 and ADL3T/JENDL. JENDL/ADL3T give a factor of two larger than FENDL/ADL3T.

^{62m}Co: The situation is the same as ^{62}Co. It should be noted that FEND:/REAC gives 5 times larger value than FENDL/ACT4. Thus, there should be some inconsistency in the decay chain library in ACT4. It should be investigated.

^{61}Co: All calculations give results in a same range.

^{66}Cu: All calculations are very close each other.

Zr:

^{89}Zr: All calculations except ADL3T give slightly overestimated results by 10 %. ADL3T is a factor of 2.5 larger the others.

^{89m}Zr: ADL3T is twice as much larger as JENDL. FENDL is in between.

^{90m}Y: JENDL agrees reasonably with the experiment. FENDL/EAF3.1 underestimated experiments by a factor of two. ADL3T, on the other hand, a factor of 4 overestimated the experiment.

^{87m}Sr: FENDL/EAF3.1 underestimate the experiment by 70 %. ADL3T overestimates it by 30 %. JENDL gives the closest value to the experiment with C/E of 0.92 - 1.15.

^{91m}Y: ADL3T is larger by a factor of 2 than the experiment. FENDL/EAF3.1 and JENDL underestimate and overestimate the experiments by 20 %, respectively.

^{92}Y: FENDL/ADL3T/EAF3.1 agree within 5 %. JENDL give an about 15 % overestimation.

^{94}Y: All calculations overestimate the experiment by more than 30 %. JENDL gives closest results to the experiment. FENDL/ADL3T/EAF3.1 are a factor of 2.5 higher than the experiment.

^{97}Zr: FENDL is closest to the experiment, but still there is a 30 % overestimation. ADL3T/EAF-3.1/JENDL are more than a factor of 2 larger than the experiment.

Nb:

^{92m}Nb: Although this production is well known, there are scattered calculated values. FENDL is a factor of two smaller than the experiment. ADL3T is a factor of four higher than the experiment. EAF3.1 seems reasonable but still more than 10 lower than the experiments. JENDL gives on the contrary 10 % higher than the experiments. According to the new experiment at FNS, the new evaluation should be taken place.

^{90}Y: FENDL and JENDL are very close. ADL3T and EAF3.1 give twice as much as FENDL/ JENDL. New experimental data is desirable.

^{90m}Y: FENDL and JENDL are in good agreements with the experiments. EAF3.1 give a factor of two higher value.

^{92}Y: ADL3T and EAF3.1 are a factor of two higher the FENDL.

Mo:

^{91}Mo: ADL3T gives a reasonable agreement with the experiment. Other calculations largely overestimate the experiment by more than 30 %.

^{89}Zr: JENDL underestimate the experiment by 30 %. FENDL/EAF3.1 largely underestimate it by 60 %. ADL3T gives a result in between.

^{93m}Mo: FENDL/JENDL are more than a factor of 2 larger than the experiment. ADL3T/EAF3.1 overestimate the experiment by more than 50 %.

^{92m}Nb: All calculation give almost the same results, which are lower by 30 % than the experiment.

^{95}Nb: JENDL and ADL3T give reasonable agreements with the experiments. FENDL/EAF3.1 overestimate the experiment by more than 50 %.

^{95m}Nb: FENDL/EAF3.1 overestimate the experiment by 50 %. JENDL underestimates it by 45 %. ADL3T give the closest results with C/E of 0.83.

^{95}Zr: All calculation agree within 20 % with the experiment

^{96}Nb: FENDL/EAF3.1 an ADL3T/JENDL give lower and higher values than the experiment. However, they are within 20 %.

^{97}Nb:All calculation underestimate the experiment by more than 50 %.

^{98m}Nb: The experimental value distributed should be revised to be one order high. JENDL/ADL3T give C/E around 1.2. However, FENDL/EAF3.1 are smaller by more than a factor of two than the experiment.

^{99}Mo: All calculation give identical results. They underestimate the experiment by 20 %.

Ta:

^{182}Ta: Large overestimation are found in all calculation. The self-shielding in the Ta sample should be treated correctly.

^{182m}Ta:There is large discrepancies among the ^{182m}Ta production more than 3 orders of magnitudes. The results reflect to the ^{182}Ta decay rate.

Others: FENDL and EAF3.1 are identical. There are considerably large differences among the calculations.

W:

^{181}W: FENDL/EAF3.1/JENDL give almost same results. ADL3T is about twice as much as others. All calculates largely underestimate the experiment. As the activity was very low, new experimental measurements are desired.

^{184}Ta: JENDL is 20 % lower than the experiment. The others agree within 10 %. ADL3T gives the best agreement.

^{187}W: FENDL/ADL3T/EAF3.1 overestimate the experiment by 25 %. Whereas, JENDL underestimates it by 15 %.

^{186}Ta: JENDL is in a good agreement with the experiment. Others underestimate it by more than 80 %.

^{183}Hf: All calculations except JENDL give reasonable agreements with the experiment. JENDL is almost a factor of 2 lower the experiment.

4. Summary of results

Throughout the present test of the libraries, it can be said that JENDL gives reasonable agreement with the experiment. However, for some of the productions, FENDL gives the best results. In general, there is no drastic change in JENDL3.2 from JENDL3.1. FENDL and EAF3.1 are almost identical except some cases. ADL3T gives results closer to JENDL rather than to FENDL/EAF3.1. For about 70 % of productions tested, the C/Es are in a range from 0.7 to 1.5. The decay chain should be examined for the productions with large differences between ACT4 and REAC*3. The present study is still on the way to be finalized due to time constraint. The comparison of cross section curves will be included to provide more graphical understanding the source of the discrepancies.

5. Recommendations

(1) As a next action for the integral test, new experimental data with short half-lives less than 10 min. and with long half-lives longer than 1 years should be needed. In particular, the data for W, Mo, Cu, Ni are elements with high priority.

(2) For the verification of the (n,γ) reaction products, also, it is highly desired to do new experiments on various elements in several different neutron spectra.

(3) The multigroup cross section process should be examined in terms of the weighting function, group structure.

(4) Tests with other inventory codes are recommended to check the associated decay chain and gamma-ray source libraries.

The experimental data under ITER R&D task will be available after the reporting to ITER JCT by the end of this year. (A new experimental measurements under pulse mode operations has been done at FNS in last July.)

REFERENCES

1. Y. Ikeda, A. Kumar, C. Konno, K. Kosako, Y. Oyama, T. Nakamura, H. Maekawa, M.Z. Youssef and M.A. Abdou, "Joint Report of JAERI/USDOE Collaborative Program on Fusion Neutronics --Induced Radioactivity Measurements in Fusion Neutron Environment --," JAERI-M 93-018 (1993), UCLA-ENG-91-32, UCLA-FTN-53
2. Y. Ikeda, C. Konno, T. Nakamura, A. Kumar, M.A. Abdou, "Experiment on Induced Activities and Decay-Heat in Simulated D-T Neutron Fields: JAERI/USDOE Collaborative Program on Fusion Neutronics," Fusion Technol. 19 , (1991) 1961-1966.
3. Y. Nakajima, "JENDL Activation Cross Section File, " JAERI-M 91-032 (1991) pp43-57.
4. A.B. Pashchenko, "Status of FENDL activation file and plans for the future developments," Proc. Int. Workshop on Nuclear Data for Fusion Reactor Technology, Del Mar, California, USA, 3 - 6, May 1993.
5. F. M. Mann, "REAC*3 Nuclear Data Libraries," Proc. Intl. Conf. on Nucl. Data for Sci. and Technol., Jülich, Germany, 12-17 May 1991, pp936-938.
6. J. Kopecky, H. Gruppelaar, and R. A. Forrest, "European Activation File for Fusion," Proc. Int. Conf. on Nuclear Data for Science and Technol., Jeilich, Germany, May 1991, p 828.
7. Catalog of ADL3 Library (1993).
8. Y. Seki, H. Iida, H. Kawasaki and K. Yamada, "THIDA-2: An Advanced Code System for Calculation of Transmutation, Activation, Decay Heat and Dose Rate, " RSIC computer code collection, CCC-410 (April 1987).

6. PKA and KERMA Data

6.1 Process of PKA/KERMA File for FENDL from JENDL Fusion File

T. Fukahori, S. Chiba
Nuclear Data Center, JAERI,
Tokai-mura, Naka-gun, Ibaraki-ken, 319-11 Japan
fukahori@cracker.tokai.jaeri.go.jp, chiba@cracker.tokai.jaeri.go.jp
and
M. Kawai
Nuclear Engineering Laboratory, Toshiba Co.,
4-1 Ukishima-cho, Kawasaki-ku,Kawasaki, 210 Japan
kaw@rcg.nel.rdc.toshiba.co.jp

The project of JENDL PKA/KERMA File is introduced as a file for radiation damage calculations in the incident neutron energy range below 50 MeV. The code ESPERANT using an effective single particle emission approximation (ESPEA) was developed for nucleus except light mass elements as a processing method from an evaluated nuclear data file. The code SCINFUL/DDX is used for light mass nuclides. As a trial task of ESPERANT usage, PKA file for the FENDL project in the energy range below 20 MeV was processed from the JENDL Fusion File. The processed PKA file was compared with results of Monte-Carlo calculation by MCEXCITON and calculated results from ENDF/B-IV. The results of three methods gave similar trends. It was concluded that the processing method with ESPEA was applicable to produce PKA File.

1. Introduction

In the Japanese Nuclear Data Committee, the PKA/KERMA file containing primary knock-on atom (PKA) spectra, KERMA factors and displacement per atom (DPA) cross sections in the energy range between 10^{-5} eV and 50 MeV is prepared from the evaluated nuclear data, for radiation damage calculations used to such as the International Fusion Material Irradiation Facility (IFMIF)[1] which is an FMIT-type accelerator facility using Li(d,n) neutron source for irradiation tests of fusion reactor materials. The processing code system, ESPERANT, was developed to calculate quantities of PKA, KERMA and DPA from evaluated nuclear data for medium and heavy elements by using an effective single particle emission approximation (ESPEA). For light elements, the PKA spectra are evaluated by the

SCINFUL/DDX[2] and EXIFON[3] codes, simultaneously with other neutron cross sections. Finally, the PKA/KERMA file will contain the data for 78 isotope of 29 elements in the energy region up to 50 MeV.

As a trial task of ESPERANT, a file of PKA spectra for 69 nuclides from ^{19}F to ^{209}Bi in the energy region up to 20 MeV has been generated for fusion application from the JENDL Fusion File[4], in order to supply the PKA data to the FENDL-2 project[5]. The considered reactions to process were elastic (MT=2) and discrete inelastic (MT=51-90) scattering, continuum neutron emission reaction (MT=201) and charged particle emission reactions (MT=203-207). Damage energy spectra were also processed. The PKA spectra file was compared with the results of Monte Carlo calculation using MCEXCITON[6] and of Doran's processing[7] ENDF/B-IV[8], as data check and benchmark test. It was concluded that processed result of present work had an good accuracy for PKA spectra.

In this report, the processing method, ESPEA, is explained and the results of comparison are discussed. The project of JENDL PKA/KERMA File is also described.

2. PKA/KERMA FILE

The PKA/KERMA File is producing mainly to estimate the radiation damage in solid materials, for instance, applications like the IFMIF project which needs PKA spectra by neutron- induced reactions below 50 MeV. **Table 1** shows physical quantities included in PKA/KERMA File as well as MF number defined in ENDF-6 format. Generally, PKA File will be processed by the ESPERANT code from neutron data in the JENDL High Energy File up to 50 MeV by using effective single particle emission approximation (ESPEA) which is explained in the section 3. For light mass nuclides, nuclear data and PKA spectra are evaluated simultaneously by the SINFUL/DDX code. The PKA/KERMA File contains the data for 29 elements, 78 isotopes which are summarized in **Table 2** and is planed to release in 1998. For ^{1}H and ^{12}C, evaluations have been finished and compilation is in progress. For the other nuclides, evaluations is now going on.

3. Effective Single Particle Emission Approximation (ESPEA)

It is often impossible to calculate PKA spectra exactly for reactions emitting two or more particles from evaluated nuclear data file which usually has no separated spectrum of each reaction step and channel. For these cases, the effective single particle emission approximation (ESPEA) has been developed to calculate spectra. In ESPEA, it is assumed that the particles are emitted from sequential reactions, which can not emit the particles simultaneously, and only the first emitted particle contributes to determination of energy and angular distributions of PKA.

Processing method of ESPERANT code is explained in this section as well as ESPEA. Basic notations are indicated in **Fig. 1** where superscripts of C and L mean center-of mass system (CMS) and laboratory system (LAB), subscripts of p, t, 1 and 2 show incident particle, target nucleus, outgoing particle and residual nucleus, and symbols of E, V, m and θ are energy, velocity, mass and emitted angle ($\mu = \cos\theta$). Double-differential cross section (DDX) of emitted particle in CMS, $DDX_1{}^C(E_p{}^L, E_1{}^C, \mu_1{}^C)$, is assumed to be given in evaluated nuclear data files. PKA spectrum in CMS, $DDX_2{}^C(E_p{}^L, E_2{}^C, \mu_2{}^C)$, is directly calculated by using energy and momentum conservation lows. That for particle emission reaction is written

$$DDX_2^C(E_p^L, E_2^C, \mu_2^C) = \frac{m_2}{m_1} DDX_1^c(E_p^L, E_1^C, \mu_1^C) ,$$
$$E_2^C = \frac{m_1}{m_2} E_1^C , \quad \mu_2^C = -\mu_1^C$$

and that for γ-ray emission reaction is

$$DDX_2^C(E_p^L, E_2^C, \mu_2^C) = \frac{m_2 c^2}{E_\gamma} DDX_\gamma(E_p^L, E_\gamma, \mu_\gamma) ,$$
$$E_2^C = \frac{E_\gamma^2}{2m_2 c^2} , \quad \mu_2^C = -\mu_\gamma$$

where c is light speed. Since particle production cross sections (MT=201, 203-207 in ENDF-6 format, similar as following) are compiled by summing up individual production cross sections, which are given as a product of reaction cross section and particle multiplicities, exceeds the total reaction cross section, some re-normalization is necessary to treat as single particle emission. A normalization factor, R, for ESPEA is given as following.

$$R = \frac{\sigma_R}{\sum_x \int_{\varepsilon_x^{(min)}} d\varepsilon_x \int d\mu_x \sigma_x(E_p^L, \varepsilon_x, \mu_x)}$$

where σ_R and σ_x indicate cross sections of total reaction and each particle emission channel, and $\varepsilon_x{}^{(min)}$ is lower limit of energy for spectrum considered, which means the first emitted particles are distributed in higher energy region in the emitted spectra. A schematic diagram is shown in **Fig. 2**. It is assumed that no PKA is created by light particles emitted below this energy. The lower energy limit, $\varepsilon_x{}^{(min)}$, is determined to be satisfied the following equation of average energy for light particle emitted from the reaction x.

$$\int_{\varepsilon_x^{(min)}} \varepsilon_x f_x(\varepsilon_x)\, d\varepsilon_x = \left(\frac{m_t}{m_p+m_t}E_p^L+Q_x\right) \Big/ \left[1+\left(\frac{m_{1x}}{m_{2x}}\right)^2\right]$$

$$\int_0^\infty f_x(\varepsilon_x)\, d\varepsilon_x = 1$$

where Q_x is Q-value of reaction x, and f_x the normalized DDX_1^C of reaction x.

DDX of PKA in LAB, $DDX_2(E_P,E_2,\mu_2)$, is obtained after conversion from CMS to LAB (hereafter the superscript 'L' is abbreviated), then the damage energy spectra, σ_D, can be given by

$$\sigma_D(E_p,E_2,\mu_2) = E_D(E_2) \cdot DDX_2(E_p,E_2,\mu_2)$$

and E_D is given by Lindhard-Robinson model[9] as following.

$$E_D(E_2) = \frac{E_2}{1+k\,g(\varepsilon)}\ , \quad E_2\ [MeV]\ ,$$
$$k = 0.13372\, Z^{2/3} / A^{1/2}\ ,$$
$$g(\varepsilon) = 3.48008\, \varepsilon^{1/6} + 0.40244\, \varepsilon^{3/4} + \varepsilon\ ,$$
$$\varepsilon = E_2 / 86.931\, Z^{7/3}$$

DPA Cross Section, σ_{DPA}, can be obtained by using the above damage energy spectra,

$$\sigma_{DPA}(E_p) = \int \nu(E_2)\ \sigma_D(E_p,E_2,\mu_2)\ dE_2\, d\mu_2\ ,$$
$$\nu(E_2) = \frac{\kappa}{2\,\varepsilon_d} E_D(E_2)\ , \quad \kappa = 0.8$$

where ε_d is the threshold energy for knock-on atom displaced from lattice point, and its amount strongly depends on materials. The kerma factor for x-Reaction, $KERMA_x(E_p)$, is also calculated by using double differential PKA spectrum as following.

$$KERMA_x(E_p) = \int (E_{1x}+E_{2x})\ DDX_2(E_p,E_{2x},\mu_{2x})\ dE_{2x}\, d\mu_{2x}$$

For neutron and photon emission reactions, the term of E_{1x} is eliminated.

4. PKA File for FENDL

The PKA File for FENDL-2 Project has been processed to supply the PKA data as a trial task of ESPERANT, generating from the JENDL Fusion File below 20 MeV. Nuclides

included in JENDL Fusion File (69 isotopes) is processed and they are summarized in **Table 3**. Considered reactions are elastic (MT=2) and discrete inelastic scattering (MT=51-90), continuum neutron emission reaction (MT=201), and charged particle emission reactions (MT=203-207). Damage energy spectra has been also processed.

In **Table 4**, the energy meshes in PKA File for FENDL-2 Project is given. The processing accuracy was 5.0 %, including CMS-LAB conversion accuracy, averaging accuracy, PKA energy calculation accuracy, and so on.

The results of PKA spectra processed by ESPERANT from JENDL Fusion File were compared with those calculated with MCEXCITON and given by Doran. Since the PKA spectrum strongly depends on emitted light particle spectrum, the particle spectra in PKA file and calculated by MCEXCITON were also compared. For example, the particle and PKA spectra for ^{27}Al and ^{56}Fe at incident neutron energies of 10 and 20 MeV are shown in **Figs. 3-10**. The light particle spectra for neutron, proton and α-particle in **Figs. 3, 5, 7 and 9**, indicate that both ESPERANT and MCEXCITON results are generally consistent with each other, although the nuclear model parameters used for the JENDL Fusion File evaluation are not entirely the same as those of the MCEXCITON calculation. The PKA spectra processed by ESPERANT are in good agreement with those calculated by MCEXCITON with considering the large secondary particle energy meshes (**Figs. 4,6,8 and 10**). In **Fig. 4**, the PKA spectra given by Doran at incident energies of 9 and 11 MeV is also indicated. Doran processed the PKA spectra from ENDF/B-IV with assuming evaluation spectra for charged particles, since ENDF/B-IV does not have charged particle spectrum. However, his processing gives similar result to present result. From above discussion, it is concluded that the approximation used in ESPERANT can well process PKA spectrum data from the evaluated nuclear data file.

5. SUMMARY

The project of JENDL PKA/KERMA File is introduced. The present status of the JENDL PKA/KERMA File was also reviewed, especially for FENDL usage (En < 20 MeV). The processing method, ESPEA, was explained and the results of comparison are discussed. It was confirmed by comparing with the results of Monte-Carlo code, MCEXCITON, calculation and of Doran's processing by using ENDF/B-IV, as data check and benchmark test that ESPEA was well worked for processing PKA spectra from the evaluated file.

Acknowledgements

The authors wish to thank the members of PKA Spectrum WG in Japanese Nuclear Data Committee for their fruitful discussion about the ESPEA and the ESPERANT code development. The authors would also like to give acknowledgements to Mr. Kazuaki Kosako for his

helping to improvement of the ESPERANT code.

References

1) Noda K.; "International Fusion Material Irradiation Facility (IFMIF) Program," *Proc. 1994 Symposium on Nuclear Data, Tokai, Ibaraki, Nov. 17-18, 1994, JAERI-Conf 95-008*, p.112 (1995).

2) Kashimoto H., Watanabe Y., Koyama Y., Shinohara H. and Chiba S.; "Study of the ^{12}C Breakup Process and Carbon Kerma Factor," *Proc. 1992 Symposium on Nuclear Data, Tokai, Ibaraki, Nov. 26-27, 1992, JAERI-M 93-046*, p.287 (1993).

3) Kalka H.; "Statistical Multistep Reaction Model for Nuclear Data", *Proc. Int. Conf. on Nuclear Data for Science and Technology, Julich, May 13-17, 1991*, p.897 (Springer-Verlag, Berlin, Heidelberg, 1992).

4) Baosheng Y., Chiba S. and Fukahori T.; *J. Nucl. Sci. Technol.*, **29**, 677 (1992).

5) e.g. for FENDL-1: Ganesan S. and McLaughlin P.K.; "FENDL/E: Evaluated Nuclear Data Library of Neutron Nuclear Interaction Cross-Sections and Photon Production Cross-Sections and Photon-Atom Interaction Cross-Sections for Fusion Applications," *IAEA-NDS-128 Rev.1* (1995).

6) Kishida N. and Kadotani H.; "On the Validity of the Intranuclear-Cascade and Evaporation Model for High Energy Proton Induced Reactions," *Proc. Int. Conf. on Nuclear Data for Science and Technology, Mito, May 30 - June 3, 1988*, p.1209 (Saikon Publishing, Tokyo, 1988).

7) Doran D.G. and Graves N.J.; "Displacement Cross Sections and PKA Spectra: Table and Applications," HEDL-TME 7670 (1976).

8) (Ed.) Garber D.; "ENDF/B Summary Documentation," *BNL-17541*, 2nd Edition (1975).

9) Lindhard J., et al.; *Kgl. Danke Vidensk Selsk. mat-fis. Medd.*, **33**, Np.10 (1963) and Robinson N.T.; *Proc. BNES Conf. on Nuclear Fission Reactors, Culham 1969*, p.346 (BNES, London, 1969).

Table 1 Physical Quantities Included in the PKA/KERMA File (En=10^{-5} eV - 50 MeV)

MF	quantities
3	Cross sections and KERMA factor
4	Angular distributions for discrete levels
6	Double-differential light particles and PKA cross sections
63	DPA cross sections
66	Damage energy spectra

Table 2 Elements Included in the PKA/KERMA File (En=10^{-5} eV - 50 MeV)

29 elements, 78 isotopes
H, Li, Be, B, C, N, O, Na, Mg, Al, Si, Cl, K, Ca, Ti, V, Cr, Mn, Fe, Co, Ni, Cu, Ge, Zr, Nb, Mo, W, Pb, Bi

underline: Evaluation was finished.

Table 3 Nuclides Included in PKA File for FENDL-2 Project (En=10^{-5} eV - 20 MeV)

69 isotopes included in JENDL Fusion File is processed.
^{19}F, ^{27}Al, ^{28,29,30}Si, ^{40,42,43,44,46,48}Ca, ^{46,47,48,49,50}Ti, ^{51}V, ^{50,52,53,54}Cr, ^{55}Mn, ^{54,56,57,58}Fe, ^{59}Co, ^{58,60,61,62,64}Ni, ^{63,65}Cu, ^{75}As, ^{90,91,92,94,96}Zr, ^{93}Nb, ^{92,94,95,96,97,98,100}Mo, ^{121,123}Sb, ^{112,114,115,116,117,118,119,120,122,124}Sn, ^{182,183,184,186}W, ^{204,206,207,208}Pb, ^{209}Bi

Table 4 The Energy Meshes in PKA File for FENDL-2 Project

- Incident Energy Mesh [eV]: 37
  1.00E-5,2.53E-2,5.00E-1,1.00E+0,2.00E+0,5.00E+0,1.00E+1,2.00E+1,5.00E+1,
  1.00E+2,2.00E+2,5.00E+2,1.00E+3,2.00E+3,5.00E+3,1.00E+4,2.00E+4,5.00E+4,
  1.00E+5,2.00E+5,5.00E+5,1.00E+6,2.00E+6,3.00E+6,4.00E+6,5.00E+6,6.00E+6,
  7.00E+6,8.00E+6,9.00E+6,1.00E+7,1.20E+7,1.40E+7,1.50E+7,1.60E+7,1.80E+7,
  2.00E+7
- Outgoing Energy Mesh [eV]: 53
  1.00E-5,2.53E-2,5.00E-1,1.00E+0,2.00E+0,5.00E+0,1.00E+1,2.00E+1,3.00E+1,
  4.00E+1,5.00E+1,6.00E+1,7.00E+1,8.00E+1,9.00E+1,1.00E+2,2.00E+2,3.00E+2,
  4.00E+2,5.00E+2,6.00E+2,7.00E+2,8.00E+2,9.00E+2,1.00E+3,2.00E+3,5.00E+3,
  1.00E+4,2.00E+4,5.00E+4,1.00E+5,2.00E+5,5.00E+5,1.00E+6,2.00E+6,3.00E+6,
  4.00E+6,5.00E+6,6.00E+6,7.00E+6,8.00E+6,9.00E+6,1.00E+7,1.10E+7,1.20E+7,
  1.30E+7,1.40E+7,1.50E+7,1.60E+7,1.70E+7,1.80E+7,1.90E+7,2.00E+7

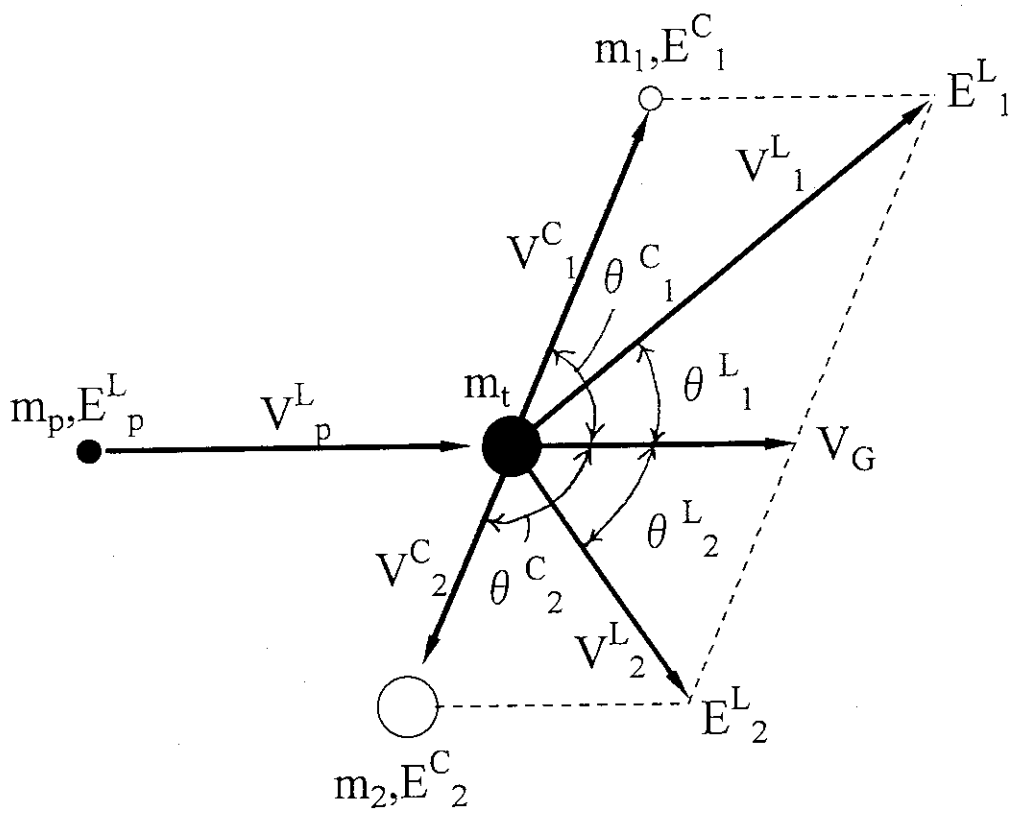

Fig. 1 Kinematics for PKA Calculation

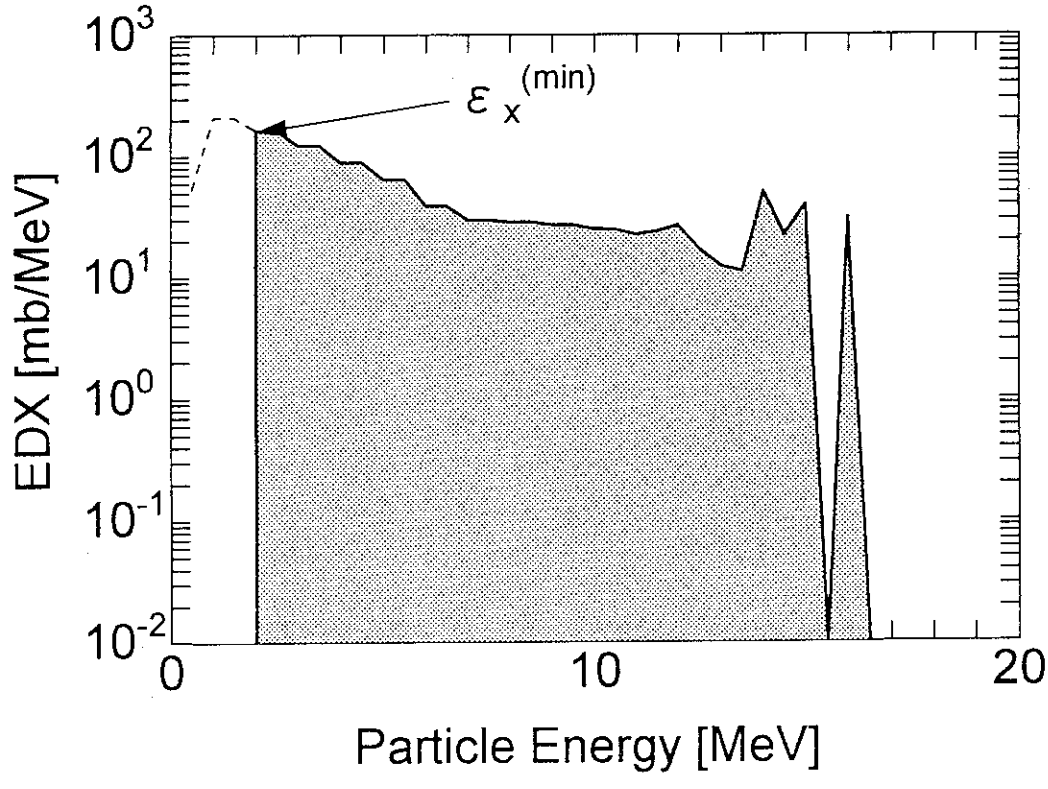

Fig. 2 Schematic Diagram for Determination of $\varepsilon_x^{(min)}$

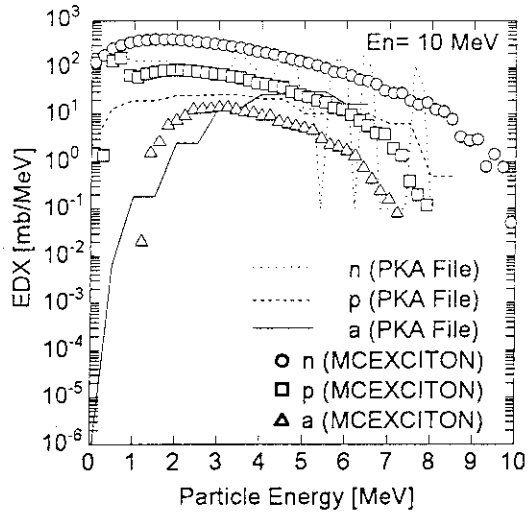

Fig. 3 Particle Spectra of PKA File and MCEXCITON for ^{27}Al at En=10 MeV

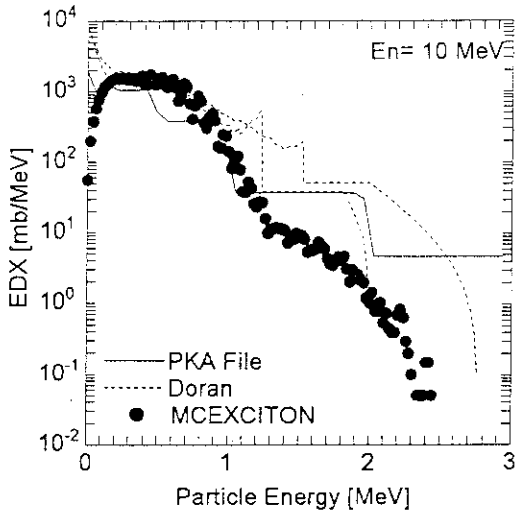

Fig. 4 PKA Spectrum for PKA File and MCEXCITON Compared with Doran's Calculation for ^{27}Al at En=10 MeV

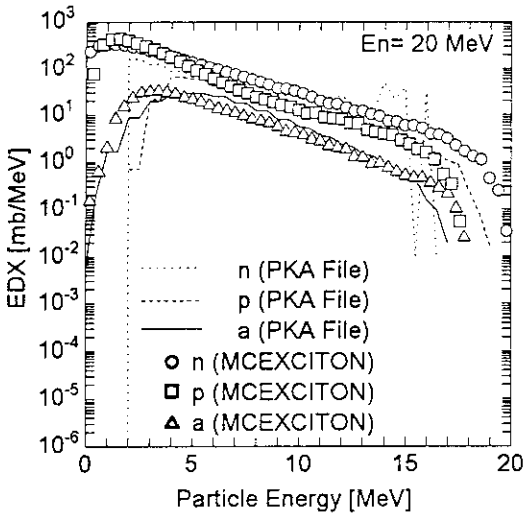

Fig. 5 Particle Spectra for PKA File and MCEXCITON for ^{27}Al at En=20 MeV

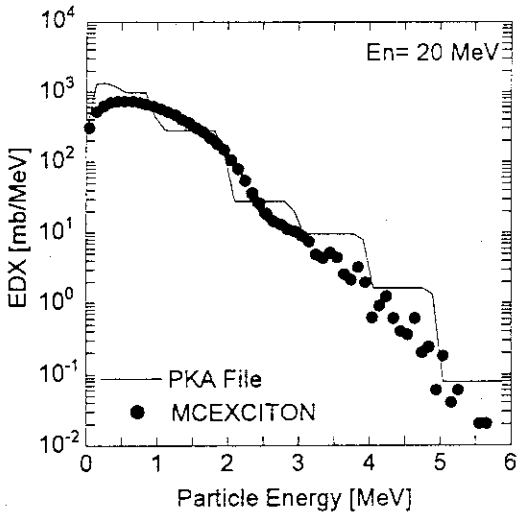

Fig. 6 PKA Spectrum for PKA File and MCEXCITON for ^{27}Al at En=20 MeV

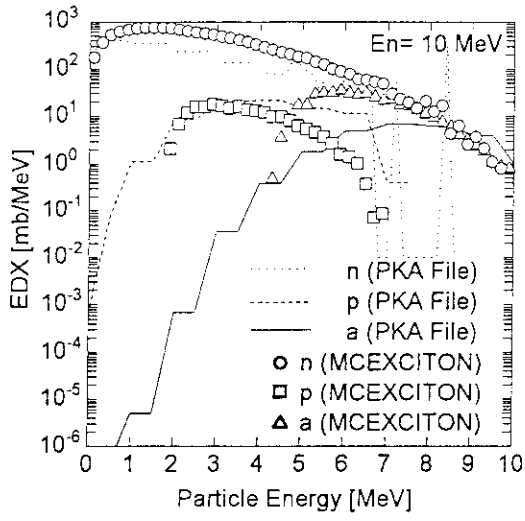

Fig. 7 Particle Spectra for PKA File and MCEXCITON for ^{56}Fe at En=10 MeV

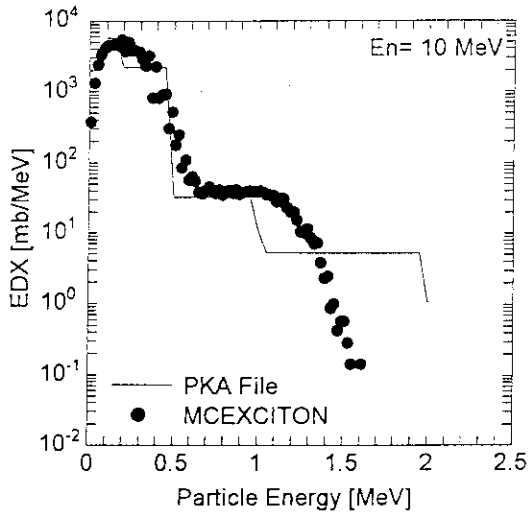

Fig. 8 PKA Spectrum for PKA File and MCEXCITON for ^{56}Fe at En=10 MeV

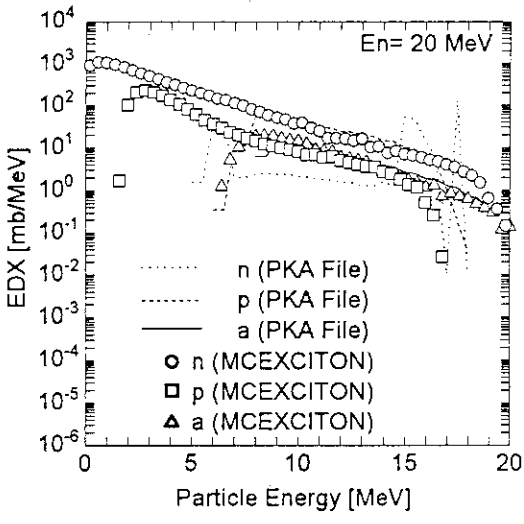

Fig. 9 Particle Spectra for PKA File and MCEXCITON for ^{56}Fe at En=20 MeV

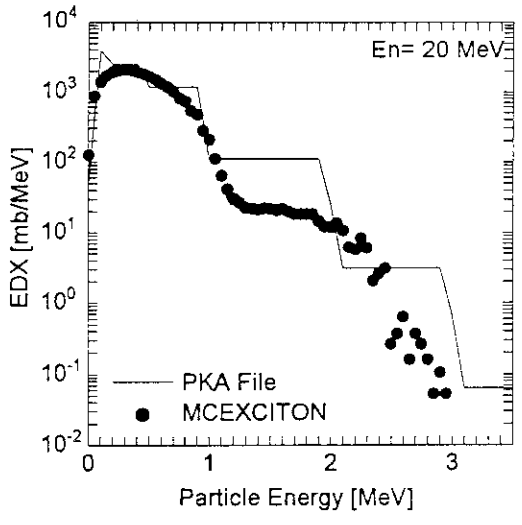

Fig. 10 PKA Spectrum for PKA File and MCEXCITON for ^{56}Fe at En=20 MeV

6.2 Direct Nuclear Heating Measurements and KERMA Data Test

Yujiro Ikeda and Anil Kumar*

Department of Reactor Engineering, Japan Atomic Energy Research Institute,
Tokai-mura, Naka-gun, Ibaraki-ken 319-11 Japan

* School of Engineering and Applied Science, University of California at Los Angeles (UCLA),
Los Angeles, CA 90024, USA

An experimental technique based on the microcalorimeter has been developed in order to meet the strong need for validating the nuclear data relevant to nuclear heat deposition in fusion reactor structural components. The experimental measurements of the nuclear heating conducted on stainless steel 316, beryllium, graphite, copper, zirconium, and tungsten, demonstrated the applicability and reliability of the technique in terms of detection sensitivity and accuracy for the relevant neutronic data validation. The experiment covered measurements of gamma-heating with TLD and reaction rate distribution measurements with foils activation technique. The calculations have been performed using MCNP and DOT3.5 with JENDL-3.2 and FENDL-1 data libraries. The comparison of calculation (C) to experiment (E) shows considerable deviation between the two, in particular for beryllium and zirconium. The sources of potential discrepancies in C and E are discussed.

1. Introduction

The importance of nuclear heating in the structural materials has been recognized from a view point of critical system design in ITER. Requirements for reduction of design margin are stringently addressed in the design criteria. The uncertainty of the data base relevant to nuclear heating is considered as one of most crucial problems in the designs, not only for inboard shielding against the superconducting magnet heating, but for the plasma facing component configurations also. Many data libraries have been compiled and implemented in the neutron transport code systems[1-6]. Adequacy of the these data libraries of kerma factors has, however, not been thoroughly tested due to lack of suitable experimental data.

The present work was carried out under the TER/EDA R&D Task T-16 focusing on further technical development for the detection of very small signals in structural materials, and on demonstration of the feasibility of the technique for precise measurements of nuclear heat depositions in a configuration based on the comprehensive ITER First Wall/Blanket /Shield design for validating the relevant nuclear data. The calorimetric measurements of total nuclear heating measurements were complemented by preliminary measurements of gamma-heating component through TLD's, on one hand, and dosimetry activation rates at various locations inside a stainless steel assembly that housed the probes, on the other. In addition, comprehensive analysis of the measured heating rates was carried out to see the adequacy of the available kerma factor libraries, and the particle transport libraries to predict the measured rates. In this report, the results for experimental analyses based on JENDL-3.2[7] and a part of FENDL-1[8] are mainly given.

2. Experiments

2.1. Neutron Source

The D-T neutrons were generated by bombarding a tritiated rotating target (~ 900 Ci) with a 20

mA deuteron beam accelerated to 350 kV at FNS[9]. The absolute neutron yield was monitored by a ^{232}Th fission chamber which was calibrated by the associated α-particle counting method[10]. The D-T neutron target was located at the center of target room with dimensions of 5 m x 5 m x 4.5 m, surrounded by 2.5 m thick ordinary concrete walls. The neutron irradiation history was recorded with MCS (Multi-Channel Scaling) with 10 seconds duel time bin.

2.2 Experimental Assembly

The schematic cross sectional views of the experimental assembly are given in **Fig. 1**. The central zone of the assembly consisted of SS-316 blocks with a central channel hole of 50 mm in diameter. The cross section of the central zone of SS-316 measured 150 mm x 150 mm. The outer region of the SS-316 zone, about 100 mm thick SS-304 region were stacked, followed by a 100 mm polyethylene layer. The assembly was contained in a SS304 container to insulate ambient change of room temperature. This configuration minimizes the thermal conduction and convection from the surrounding area. The outer dimension of the container was 600 mm x 600 mm x 600 mm. All probe materials to be tested were placed into the center channel. The assembly was set in front of the D-T neutron target as the distance between the target outer surface and the front surface of the assembly was 15 mm. The axis of the central channel was aligned to the d^+ beam direction in order to keep good symmetric configuration. The height of the d^+ beam line was 1.8 m from the ground flower.

2.3. Microcalorimeter System

We have considered the microcalorimetor as the principal technique to measure the total nuclear heating rate of the materials in the neutron and gamma-ray mixed radiation field as expected in the fusion reactor environment. The microcalorimetric technique comprises three components; (i) the material (probe) to be tested, (ii) thermal sensors for detecting the temperature rise and (iii) a data acquisition system. Probes made of stainless steel 316, beryllium, graphite, copper, zirconium and tungsten were tested to demonstrate the feasibility of the presently developed technique for nuclear heating in D-T neutron environments. The material properties and dimensions of the probes are listed in **Table 1**.

The probe materials were placed inside a cylindrical central channel fashioned inside rectangular blocks of stainless steel 316. Six separate probes of stainless steel 316 were aligned one after another in this channel in the first set of measurements. The dimension of the material configuration in the experimental assembly are given in **Fig. 2**. In next set of measurements, the very first stainless steel probe of the reference assembly was replaced by a probe of other material. One by one, probes of beryllium, graphite, copper, zirconium, and tungsten were inserted in the reference SS-316 assembly and nuclear heating measurements were repeated. The distance of the lead probe from neutron source target surface was estimated to be ~27 mm. The material probes tested were placed on the axis of the assembly. As the thermal sensor, thermistors (TM) with 10 kΩ at 25 °C were used and placed at the front, middle side surface and rear surface of the probe. The probe was supported by a thin carbon papers in order to reduce thermal conduction. The sensors were contacted directly on the probe materials with use of a small piece of organic tape. The sensors were connected by thin wires with voltmeters. The coefficient of the sensors for the temperature change were 2.27×10^{-3} °K/Ωfor a TM at 25 °C. The temperature rise of 10^{-5} °K/sec corresponded to a voltage change of 4.4×10^{-8} volt/sec with 10μA current applied on 10 kΩ, resulting in the last two or three digits change of the nano-voltmeters-voltmeters used (Keithley 182) during 10s of nuclear heating.

2.4 Thermo-Luminescent Dosimeter (TLD)

As conventional applied in many dosimetry study, TLD has been employed as the gamma-ray heating detector. The gamma-ray data separated from neutron events are expected be complementary to the data with microcalorimetor. Five kinds of TLDs, that is, BeO (Zeff = 7.12), 7LiF (Zeff = 8.24), MSO (Mg_2SiO_4, Zeff = 11.1), SSO (Sr_2SiO_4, Zeff = 32.5) and BSO (Ba_2SiO_4, Zeff = 49.9),

were used to measure g-ray heating rates of beryllium (Z = 4), carbon (Z = 6), SS316 (Zeff = 26.4), copper (Z = 29), zirconium (Z = 40) and tungsten (Z = 74). Gamma-ray heating rates of SS316, copper and zirconium could be derived from interpolation of measured heating rates by TLDs because the Z-numbers of the materials, 26.4, 29 and 40, were inside the range of the TLD's Z-number between 7.12 and 49.9. But extrapolation or other assumptions were needed for beryllium, carbon and tungsten since no TLDs which Z-numbers were smaller than 7.12 or larger than 49.9 were available. All the TLDs in powder form were sealed in glass capsules of 2 mm in outer diameter and 12 mm in length. The TLD capsules were washed by ultrasonic cleaner with ethyl alcohol. Three kinds of TLDs, BeO, ^{7}LiF and MSO, were selected for the beryllium and carbon measurement, while the other three kinds of TLDs, MSO, SSO and BSO, were used for the SS-316, copper, zirconium and tungsten measurements. Four capsules out of each kind of TLD were packed in an aluminium foil. The aluminium foil prevent the TLDs from being exposed by light which increases the background signals.

2.5 Foil Activation Technique

The foil activation technique was applied for the measurement of reaction rates at the detector positions of the microcalorimeter and the TLD. The data proved a fundamental mean for validation of the neutron flux calculation to be used experimental analysis of nuclear heating. The representative set of reactions were selected for this purpose. The dosimetry reactions applied were ^{93}Nb(n,2n)^{92m}Nb, ^{197}Au(n,2n)^{196}Au, ^{27}Al(n,α)^{24}Na, ^{115}In(n,n')^{115m}In and ^{197}Au(n,γ)^{198}Au. The cross-sections are from JENDL dosimetry file[11]. The first three reactions allow to look at harder part of the neutron energy spectrum- from ~7 MeV up to ~15.48 MeV. The fourth reaction covers from ~0.5 MeV to ~15.48 MeV. The last reaction cover energy range below ~ 1 MeV, but preferably neutrons in keV to eV range. The decay data for the reactions are given in **Table 2**.

3. Measurement

3.1. Measurement of Nuclear Heating with Micro-Calorimeter

The calorimeter was placed at very close position to the D-T neutron target, and irradiated with 3 to 5 minute duration neutron pulses separated by 3 to 5 minute. A constant current of 10 μA was applied to the thermal sensors through out the irradiation to detect the signal during the irradiation. The temporal derivative is demonstratively shown in **Figs. 3** for very first probes of stainless steel 316 in the reference assembly. There is a TM each at front and rear of this probe.

The raw resistance change data for a sensor is treated to obtain net resistance change rate and then they are converted to the corresponding heat deposition rate by using specific heat (Cp) of each material, neutron yeild (Yn) and temperature coefficient of the sensor (CRT). The specific heat of each probe material used in the reported experiments is given in **Table 1**. The overall response time of the sensor in a duration of 10 seconds was estimated by a calculation with a heat transport code ADINAT[12]. The ADINA code treated all possible heat transfer phenomena in terms of heat conduction, convection and radiation. The response time was needed to correct the heating rate at the very beginning and end of the neutron pulses. The heat source distribution was given by the result of neutron and gamma-ray fluxes calculated by DOT3.5[13] with FUSION-J3[14]. Simulating the probe configuration, time dependent temperature change was calculated with DOT3.5/ADINAT coupled code for the position of the front surface of the first SS-316 probe. We derived the volume averaged experimental data from the derivatives of the several points at very end of the irradiation. It could be assumed the temperature rise becomes in equilibrium after 5 min even though the thermal conduction of SS-316 is relatively low in comparison with other metallic materials.

The self-heating driven by the joule heat in the resistance of the thermistor sensor gives a constant heating load which contributes a constant change of the temperature. If the weight of the 10 k

Ω thermistor sensor is assumed to be 10^{-3} g, the heat generation with 10μA was equivalent to 10^{-3} W/g, resulting in a much higher rate than that produced in the nuclear heating process ranging from 10^{-4} to 10^{-5} W/g. The other factor to be considered is the contribution to the temperature change from heat conduction even though it is small and slow in our experimental assemblies. Even with regulated air conditioning, a change of 10^{-2} °K is unavoidable. This change makes a steep gradient in the temperature between the probe and the surrounding environment in comparison to the temperature change induced by the nuclear heating. The overall fluctuation of the drift line was, as a result, governed by the constant self-heating and the slow component due to the ambient temperature change in the room along with electrical noise. As the signal of nuclear heating is superimposed on that slow component, the stability of the drift-line determines the error for the nuclear heating derivation. The nominal error due to the fluctuation of the drift-line ranged from 3 to 5 % with respect to the net nuclear heating signal in a well stabilized condition. If the stability of the system was not sufficient, the error was in a range from 10 to 15 % with respect to the net nuclear heating signal.

The nuclear heating in the first probe, in particular, depends critically on its distance from the source, owing to its close proximity to the source. For example, transport calculations show that (i) a change of 1 mm in the distance of 24 mm makes a maximum change of 5 % in the heating rate of the first probe, and (ii) an increase of distance from 24 mm to 28 mm brought down volume-averaged nuclear heating typically by ~11%. It is thus evident that the uncertainty in the determination of distance needs also to be taken into account as the experimental error. Other factors of error sources are the source neutron yield, coefficients of the thermal sensors and specific heat data. The experimental errors and uncertainties are summarized in **Table 3**.

3.2 Gamma-Ray Heating Rate by TLD

The TLD packages were placed at seven positions for the SS316 configuration; on the front surface of the first probe, in the six gaps between each two probes and on the rear surface of the last probe. The gap between the container box and the first probe and the six gaps between each two probes were kept by spacers to set TLD packages in the gaps. As for the rest of configurations except SS316, TLD packages were placed on the front and the rear surfaces of the first probe made of the materials of interest. Neutron irradiation was carried out for 1 minutes with deuteron beam of 1 mA for all the six configurations. A longer irradiation for 15 minutes with 1 mA of deuteron beam was also made for the SS316 configuration because some TLD packages were set far from the D-T neutron source where gamma-ray heating rates were small. For the SS316 configuration, positions of TLD packages for the shorter irradiation were 2.0, 52.6, 103.4, 154.0 and 204.7 mm, and those for the longer irradiation were 154.0, 204.7, 255.5 and 306.0 mm. One TLD package without an irradiation was kept together in the box.

One week later from the irradiation, thermoluminescences (TLs) were read out by a TLD reader. The measured TLs were in the unit of equivalent exposure dose of ^{60}Co in air, and they ranged between 1 x 10^{-4} and 2 x 10^{-2} [C/kg]. The range of exposure dose was adequate for the TLDs because high signal to noise ratio larger than 150 was attained and the linearity of the TLDs were assured as it was better than 3 % in the range.

The TLs after the subtraction of the neutron contribution were converted to gamma-ray heating rates in the unit of [Gy/source neutron] by considering the differences of mass energy absorption coefficients of air and the TLD materials. Gamma-ray heating rates of SS316 and copper were derived from the measured absorbed doses of MSO and SSO by linear-linear interpolations since the effective atomic numbers of the two materials were between those of MSO and SSO. Gamma-ray heating rates of zirconium were obtained from the measured absorbed doses of SSO and BSO in the same way. The measured gamma-ray heating rates of BeO and ^{7}LiF for the beryllium and carbon configurations, and SSO and BSO for the tungsten configuration were, instead of the extrapolating

method, averaged taking their experimental errors as the weighting coefficients to obtain gamma-ray heating rates for the configurations. Error sources of the measured gamma-ray heating rates were as follows; (1) deviation among a group of four TLDs ranged 5 - 17 %, (2) neutron yield was 2 % , (3) calibration of the TLD reader was 5 %. In the subtraction of neutron response, the following uncertainties were added to the errors according to the law of error propagation; (i) Neutron response function was 30 %, and (ii) neutron energy spectra was 10 %.

3.3. Reaction Rates Measurement

A set of four dosimetry foils of niobium, gold, aluminum, and indium each was located in between the SS-316 probes in the central channel of the reference assembly and was irradiated for 2 hours in a separate run. One set was placed right in front of the first probe of the stainless steel 316. The total neutron yield was 1.45 x 10^{16} at the target. After irradiation, the sample foils were taken from the assembly and the g-ray spectra from the activated foils were measured with a Ge detector. The net gamma-ray peak count of interest was derived by gamma-ray spectrum analysis.

Each reaction rate is normalized to one source neutron for one atom of the activating isotope. The experimental errors comprise g-ray count statistics, detector efficiency (2.0 %), errors in foil weight, times of irradiation, cooling and counting, decay half-lives, gamma-ray branching ratios, and the error of source neutron yield (1.5 %).

4. Experimental Analysis

Three dimensional code MCNP[15] and two dimensional code DOT3.5 were used for modeling the rotating target geometry and the probe-vacuum chamber system. Whenever present, a cylindrical jacket surrounding the core of the probe was also modeled. The background contribution was found negligible due to close proximity of the probe to the neutron source and hence it was subsequently ignored in all the computations. The JENDL-3.2 based library has 125 neutron groups and it was obtained from basic JENDL-3.2 data files using NJOY processing code[16,17]. In the DOT3.5 calculation, a P_5S_{16} approximation was used for the R-Z model and the first collision source was calculated by the GRTUNCL code. The library, FSXLIB-J3.2[18], was used for neutron interactions and photon production in MCNP calculation in the whole system. Also FENDL-1 library was applied for the MCNP calculation.

Heating numbers from FUSION-J3.2 and DLC-99[19] for neutron and gamma-ray, respectively, were used for a computing the nuclear heating rates. Nuclear heat deposition rate, expressed in J/g, is derived and compared with experimental data which were converted from the temperature to the same energy deposition unit in J/g. The D-T neutron target and other important structural components nearby were included in the modeling.

The measured heating rates were compared with the calculated ones. Of course, the comparison should stand as an indication of the feasibility of these calorimetric experiments themselves. For this purpose, the volume averaged heating rate in the first probe of each of the six experimental assemblies was compared. Before we present the comparison between the calculation (C) and the experiment (E), it is very helpful to understand also the potential sources of discrepancies that can creep into the calculations in the same spirit as was done earlier for the experimental sources of error.

5. Results and Discussion

Figure 4 shows C/E for all the 5 foil activation reaction rates as obtained with DOT3.5 with FUSION-J3.2 library for the reference assembly. It is evident that the C/E's except for the $^{197}Au(n,\gamma)^{198}Au$ reaction, mostly lie in a C/E band extending from 0.9 to 1.1. Only the reaction rate for the $^{197}Au(n,\gamma)^{198}Au$ reaction shows larger deviation from unity and C/E. For other threshold reactions,

calculations for reaction rates agreed within 10 % with measurements throughout the assembly. It thus appears that the transport of neutrons within stainless steel 316 can be characterized quite satisfactorily, at least up to a depth of 30 cm, with DOT3.5 used with FUSION-J3.2.

5.1. Total Nuclear Heating Rate Profiles

The volume averaged nuclear heating rate in each SS316 probe were calculated by DOT3.5 and MCNP with FUSION-J3.2 and FSXLIB-J3.2, respectively, JENDL-3.2 base nuclear data libraries along with FENDL-1 based libraries. **Figure 5** shows the measured distribution of the volume averaged heating rates in the probes along the central channel along with values calculated by both DOT3.5 and MCNP. As observed in **Fig. 5**, there are excellent agreements among the data in the distributions. It is demonstrated more clearly in **Fig. 6** for the C/Es.

Both calculations gave almost same C/Es throughout the assembly. However, MCNP gave slightly lower the DOT3.5. This may be due to the difference in modeling. All measurements are in good agreements within 10 % with calculations up to 270 mm depth in the assembly. At least the data in 200 mm depth, the C/Es demonstrate that the nuclear heating calculations for the SS-316 are validated. **Figure 7** shows plots of the C/Es for the indication of the calculation adequacy. The appreciable overestimations about 40 % are observed for the tungsten and zirconium cases. On the other hand, the JENDL and FENDL calculations for Be underestimated by 20 % and overestimated by 10 %, respectively. The explanation is given below for each material.

Tungsten: The 30 % overestimation in the calculation with JENDL-3.2 was already pointed out in the pervious study[20,21]. As the present calculation used the same library, the reproducibility was confirmed by the present experiments on the tungsten materials.

Zirconium: It was indicated that the new KERMA for zirconium is giving 10 % larger integrated value for the product of neutron spectrum and KERMA over the whole energy range than the old version. Thus, the agreement between measurement and calculation will be better.

Beryllium: The calculation with DOT3.5 and MCNP with JENDL-3.2 gave an underestimation with C/E of 0.80. Since the experimental was about 5 %, there should be an underestimation in the neutron KERMA data of JENDL-3.2. Because, the gamma-ray contribution to the total amounted to less than 10 %, it can be said that mostly the neutron response dominated the nuclear heating. On the other hand, the FENDL calculation agreed within 10 % with the measurement. This discrepancy is explained by **Fig. 8**, which shows the KERMA factors created from JENDL and FENDL files. Apparently, JENDL gives unreasonably small KERMA in the energy range higher than 6 MeV. In JENDL, a part of contribution of α-particle due to (n,2n) is missing. The FENDL seems adequate.

Copper: The C/E of 1.06 seems very satisfactory by taking into account the experimental error of 6 %. As the gamma-ray contribution to the total heating was appreciably large, the present experimental configuration was disadvantage because the copper probe is surrounded by SS-316. In the next stage, it is desirable to configure the assembly with copper in order to test the nuclear heating of copper.

Graphite: The C/E of 1.12 obtained in the present experiments is consistent with the previous result.[20,21] As the neutron contribution dominates the total heating rate for graphite as for beryllium, this slight overestimate could be attributed to the neutron KERMA of JENDL-3.2. There is no significant difference between JENDL3.1 and JENDL-3.2. In any case, it is concluded that the neutron KERMA data is acceptable.

5.2 Comparison of TLD Measurement with Calculation

The measured gamma-ray heating rates are compared with the DOT3.5 calculation. Ratios of the calculated to the experimental gamma-ray heating rates (C/E ratios) are shown in **Fig. 9.** Gamma-ray heating rates are given as values at positions between two adjacent probes.

The calculated heating rates are about 50 % larger to the measured ones up to the 204.7 mm position. This overestimation is qualitatively consistent with the results of the bulk shielding

experiments on large SS316 assemblies conducted at FNS.[22] At 255.5 and 306.0 mm position, the C/Es rapidly decrease as the depth increases. This fact might be due to the insufficient calculation model around the rear part of the SS316 configuration as described in the previous section for the unreasonable underestimation in the reaction rates for the $^{197}Au(n,\gamma)^{198}Au$ reaction. Because the beryllium probe are surrounded by the massive SS316 blocks, most part of the measured gamma-ray heating rates are arisen from gamma-rays produced in the SS316 blocks. Although the experimental error is very large, the calculation agrees with the experiment within the error range at the 2.0 mm position. The reason of the small C/E ratios at the 34.5 mm position of about 0.5 is attributed to the inadequate modeling of the beryllium configuration in the calculation. The size of the beryllium probe, 30.1 mm f x 30.0 mm, is smaller than the others, 48.0 mm ϕ x 48.0 or 50.0 mm. But the smaller size is not taken into the calculation correctly. As for carbon configuration, the calculated heating rates agree with the experiment within the experimental error ranges which are rather large as 79 % and 33 % at the 2.0 and 52.6 mm position, respectively. The C/E ratios for the copper and the zirconium configurations, which range between 1.3 and 2.0, are larger than unity even at the second position of 52.6 and 54.5 mm for the copper and the zirconium configurations, respectively, where the experimental errors are small as about 10 %. One of the possible reasons of the large C/E ratios is that, as mentioned earlier, excessive gamma-rays are produced in the surrounding SS316 blocks according to the cross section data used. The C/E ratios of the tungsten configuration of about 3 are considerably larger than the unity. The overestimation can not be attributed just only to the excess gamma-ray emission of SS316 because the C/E ratios of the SS316 configuration of about 1.5 are much smaller than the case of tungsten. Hence it is pointed out that gamma-ray production cross sections of tungsten in JENDL-3.2 is overpredicted.

5.3. Discussion

The 14 MeV neutron flux component decreases rapidly with the depth. The flux components in the lower energy below 1 MeV shows slower decease than that of 14 MeV. The gamma-ray spectrum distributed broadly in the energy below 10 MeV and decrease as a function of depth in the assembly. The gamma-ray flux decreasing rate is in between rates for 14 MeV neutron flux and for low energy flux.

It is apparent that most of neutron heating is produced by 14 MeV at the first probe. However, as already described, neutron contribution is only 40 % of the total even at the first probe. The results in the previous experiment demonstrated that there was a good agreement between calculation and measurement of the heating rate for SS-316 in a better field where neutron contribution is almost 70 % of the total. The good agreement between calculation and measurement shown in the present experiment confirmed the validity of the gamma-ray heating calculation if the validity of the neutron response holds. In contrast to the indirect results for the gamma-ray heating, the results with TLD gave rather large overestimations (C/E ~ 1.5) throughout the SS-316 assembly. In view of possible overestimation of gamma-ray production cross sections for SS-316 in JENDL3.2, as it was pointed out in other experimental analysis, the agreement of calculation with data obtained in the microcalorimeter doesn't indicate the overall validity for the gamma-ray heating data, in particular for the secondary gamma-ray production cross section in JENDL-3.2. In any case, the systematic discrepancy between experimental results with the microcalorimeter and TLD should be investigated carefully in the next stage.

6. CONCLUSION

In general, we observed reasonable agreements between the calculation and the experiment for threshold type reaction rates. The comparison of volume-averaged heating rates from the calculation

and the experiment for all the six materials. The calculations were in good agreements with experimental value for volume averaged heating rate in SS-316 probes throughout the assembly. We observed, however, large differences between the calculation and the experiment, particularly for probe materials of tungsten and zirconium.

In summary, the experimental approach with a microcalorimeter has demonstrated that this technique offers a promising way to arrive at production of experimental data for validating the adequacy of design calculations and associated nuclear data libraries. Though FENDL-1 calculations for SS-316 were more than 12 % larger than JENDL3.2 for neutron Kerma at high energy region, the differnce from JENDL calculation was small due to domination of γ-ray heating. However, FENDL tends to overestimate the heating rate at deep position of SS316 assembly.The results of comparison of calculation and the experiment show that while JENDL-3.2 based nuclear data libraries could be considered to predict relatively satisfactory nuclear heating rates in probes of graphite, copper, and SS-316, they carry rather large uncertainty for beryllium, tungsten and zirconium. In particular, although FENDL-1 shows resonable agreement with experiment, JENDL-3.2 underestimates experiments by 20 %. The treatment of a particle energy deposition seems inadequate. Thus, KERMA data based on JENDL-FF should be processed and to be applied for the test.

It is recommended strongly to build up on the present effort and improve the attainable experimental accuracy further.

REFERENCES

1. M. A. Abdou, C. W. Maynard and R. Q. Wright, "MACK: A Computer Program to Calculate Neutron Energy Release Parameters(Fluence-to-Kerma Factor) and Multigroup Reaction Cross Sections from Nuclear Data in ENDF Format," ORNL- TM-3994 (Jul. 1973).
2. M. A. Abdou and C. W. Maynard, "Calculation Method for Nuclear Heating -Part I: Theoretical and Computational Algorithms," Nucl. Sci. Eng.. 56 (1975) 360.
3. M. A. Abdou and C. W. Maynard, "Calculation Methods for Nuclear Heating- Part II: Applications to Fusion Reactor Blanket and Shields," Nucl. Sci. Eng.. 56 (1975) 381.
4. Y. Farawila, Y. Gohar and C. W. Maynard;"KAOS/LIB-V: A Library of Nuclear Response Functions Generated by KAOS-V Code from ENDF/B-V and Other Data Files," ANL/FPP/TM-241 (1989).
5. K. Maki, H. Kawasaki, K. Kosako and Y. Seki, "Nuclear Heating Constant KERMA Library," JAERI-M 91-073 (1991). (in Japanese)
6. M. Kawai, et al., "Review of the Research and Application of KERMA Factor and DPA Cross Section," JAERI-M 91-043 (1991). (in Japanese)
7. K. Shibata, e al., "Japanese Evaluated Nuclear Data Library, Version-3," JAERI-1319 (1990).
8. S. GANESAN and P. K. McLAUGHIN, "FENDL/E Evaluated Nuclear Data Library of Neutron Nuclear Interaction Cross-Sections and Photon Production Cross-Sections and Photon-Atom Interaction Cross Sections for Fusion Applications Version 1.0 of May 1994," IAEA-NDS-128, International Atomic Energy Agency (1995)., S. GANESAN and H. WIENKE, "FENDL/MC-1.0 Library of Continuous Energy Cross Sections in ACE Format for Neutron-Photon Transport Calculations with the Monte Carlo N-Particle Transport Code System MCNP 4A," IAEA-NDS-169, International Atomic Energy Agency (1995).
9. T. Nakamura, H. Maekawa, J. Kusano, Y. Oyama, Y. Ikeda, C. Kutsukake, S. Tanaka and Shu. Tanaka: Present Status of the Fusion Neutron Source(FNS), Proc. 4th Symp. on Accelerator Sci. Technol., RIKEN, Saitama, 24 - 26 November (1982) 155-156.
10. H. Maekawa, Y. Ikeda, Y. Oyama, S. Yamaguchi and T. Nakamura: Neutron Yield Monitors for the Fusion Neutronics Source (FNS), JAERI-M 83-219 (1983).

11. Y. Nakajima, "Present Status of JENDL Activation File," proceedings of FENDL-AGM, September 13 - 17, 1994, at Garching, Germany.
12. ADINAT, "Finite Element Program for Automatic Dynamic Incremental Nonlinear Analysis of Temperature," ADINA Engineering, Inc., 1984.
13. W. A. Rhoades and F. R. Mynatt, "The DOT III Two-Dimensional Discrete Ordinates Transport Code," ORNL/TM-4280 (1979).
14. K. Maki, K. Kosako, Y. Seki and H. Kawasaki, "Nuclear Group Constant Set FUSION-J3 for Fusion Reactor Nuclear Calculations Based on JENDL-3.1," JAERI-M 91-072 (1991).
15. J. F. Breismeister, editor, "MCNP- A General Monte Carlo Code for Neutron and Photon Transport: Version 3A," report no. LA-7396-M, Rev. 2 (Sep. 1988), along with MCNP3B newsletter dated July 18, 1988, Los Alamos National Laboratory.
16. R. E. MacFarlane, D. W. Muir, and R. M. Boicourt, "The NJOY Nuclear Data Processing System, Volume II: The NJOY, RECONR, BROADR, HEATR, and THERMR Modules," Los Alamos National Laboratory report LA-9303-M, Vol. II (ENDF-324) (May 1982); In latter half of 1993, ENDF/B-VI based MATXS libraries were also made available for use by U.S.
17. R. MacFarlane, "Energy Balance of ENDF/B-V," Trans. Am. Nucl. Soc., 33, 681 (1979).
18. K. KOSAKO, F. MAEKAWA, Y. OYAMA, Y. UNO and H. MAEKAWA, "FSXLIB-J3R2: A Continuous Energy Cross Section Library for MCNP Based on JENDL-3.2," JAERI-Data/Code 94-020, Japan Atomic Energy Research Institute (1994).
19. R. W. Roussin, J. R. Knight, J. H. Hubbell, and R. J. Howerton, "Description of DLC 99/HUGO Package of Photon Interaction Data in ENDF/B-V Format," ORNL/RSIC-46 (ENDF-335) (1983).
20. Y. Ikeda, A. Kumar, et al., "Measurement and Analysis for Nuclear Heat Depositions in Structural Materials Induced by D-T Neutrons," Fusion Technol. 21 (1992) 2190.
21. A. Kumar, Y. Ikeda, et al., "Measurement and Analysis of Nuclear Heat Deposition rate in Plasma Facing Components by D-T Neutron Irradiation," to be published in Fusion Technology as the special issue.
22. C. Konno , et al., "Bulk Shielding Experiment on Large SS316 Assemblies Bombarded by D-T Neutrons Volume I: Experiment," JAERI-Research 94-043 (1994).

Table 1 Material properties and dimensions of probes

Material	Specific Heat (at 300 K)	Dimension (mm)
SS-316	0.445 J/g/K	48ϕ x 48
graphite	0.712 J/g/K	48ϕ x 48
tungsten	0.134 J/g/K	48ϕ x 50
beryllium	1.75 J/g/K	30ϕ x 30
copper	0.383J/g/K	48ϕ x 48
zirconium	0.272J/g/K	48ϕ x 50

Table 2 Reactions Investigated and Associated Decay Data

Reaction	Half-life	Abundance	γ-Energy	γ-ray branching	Atomic mass
$^{27}Al(n,\alpha)^{24}Na$	15.02 h	1.0	1368.6	1.0	26.98154
$^{93}Nb(n,2n)^{92m}Nb$	10.15 d	1.0	934.53	0.990	92.9064
$^{115}In(n,n')^{115m}In$	4.486 h	0.957	336.26	0.458	114.82
$^{197}Au(n,2n)^{196}Au$	6.183 d	1.0	355.58	0.87	196.9665
$^{197}Au(n,\gamma)^{198}Au$	2.694 d	1.0	411.80	0.955	196.9665

* Data are taken from Table of Radioactive Isotopes (1986):
E. Brown, R. B. Firestone, V. S. Shirley, Editor, John Wiley & Sons Publ. Inc.

Table 3 Experimental errors and uncertainties range for heat deposition

Items
1. Neutron flux determination
Probe positioning 4 %
Absolute neutron yield 2 %
2. Net temperature rise derivation
Fluctuation of drift-line < 5 %
Determination of background <5 %
3. Conversion coefficient of sensors 1 %
4. Volume averaging procedure 2 %[a)]
5. Heat loss/gain through conduction, convection and radiation 2 %[b)]
6. Specific heat data 2 % [c)]
Overall <10 %

a) The error was tentatively assigned from the difference of data at the front and the rear.
b) The error was tentatively given.
c) There is no explicit error for the specific heat data in the literature. The uncertainty is considered from the difference in the values taken from the different sources.

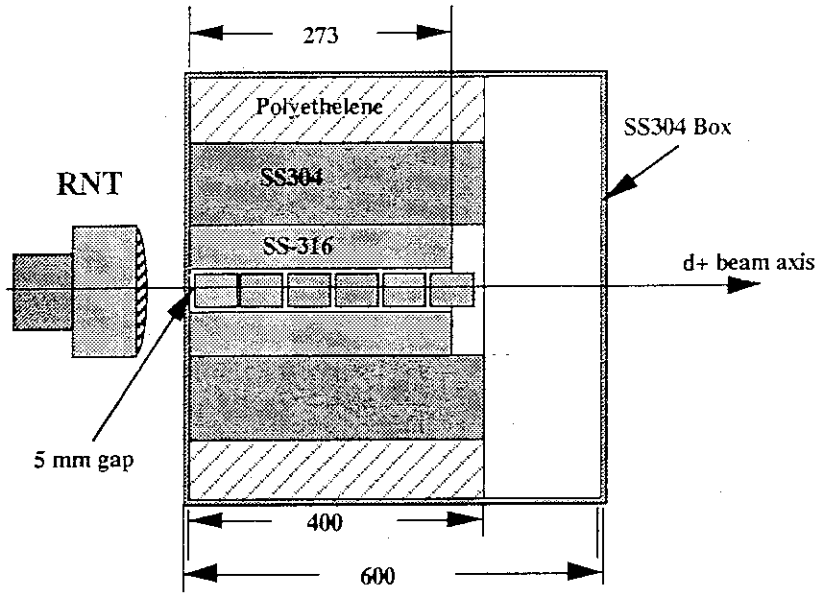

Fig. 1 Schematic Cross Secitonal View of the Experimental aasembly

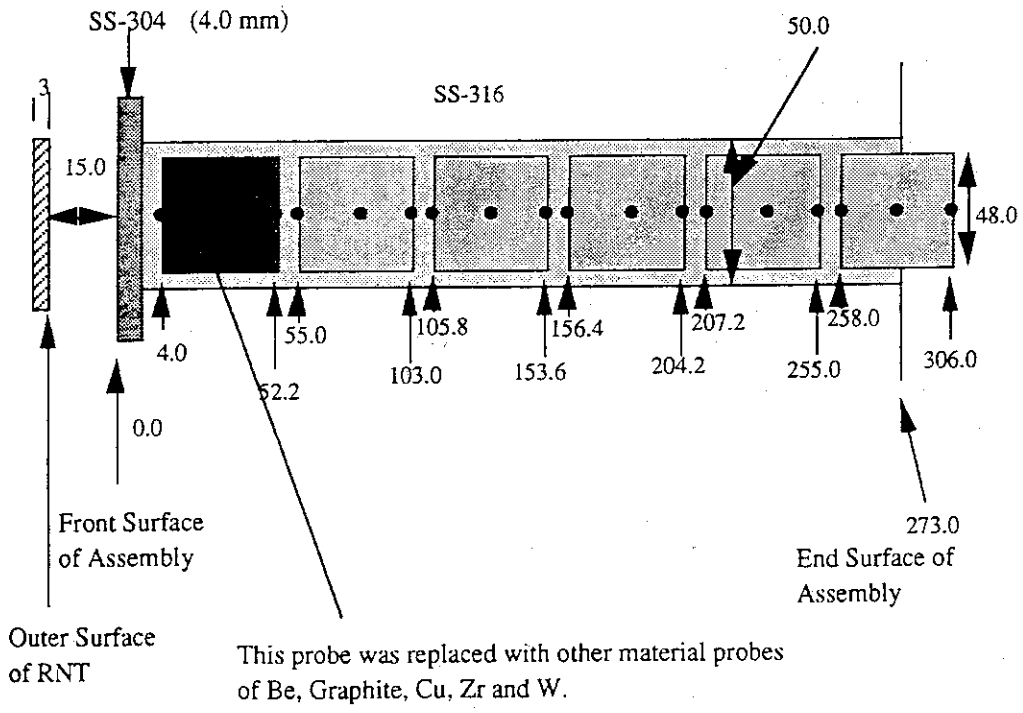

Fig.2 Probe Arrangement in SS-316 Assembly

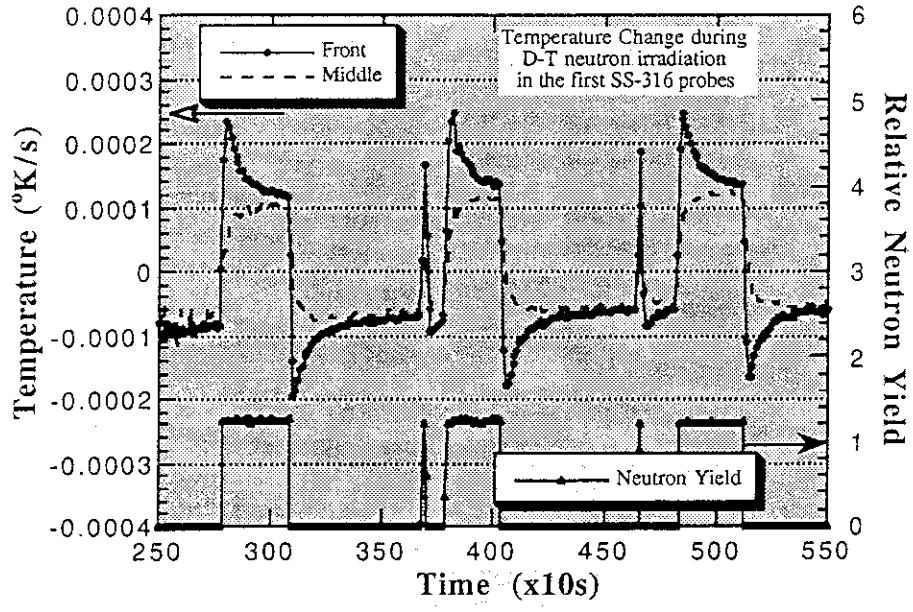

Figure 3. Temporal derivative of temperature of a stainless steel 316 probe subjected to spaced D-T neutron pulses (Actually resistance change per cycle is shown. It is proportional to the temporal derivative of the temperature).

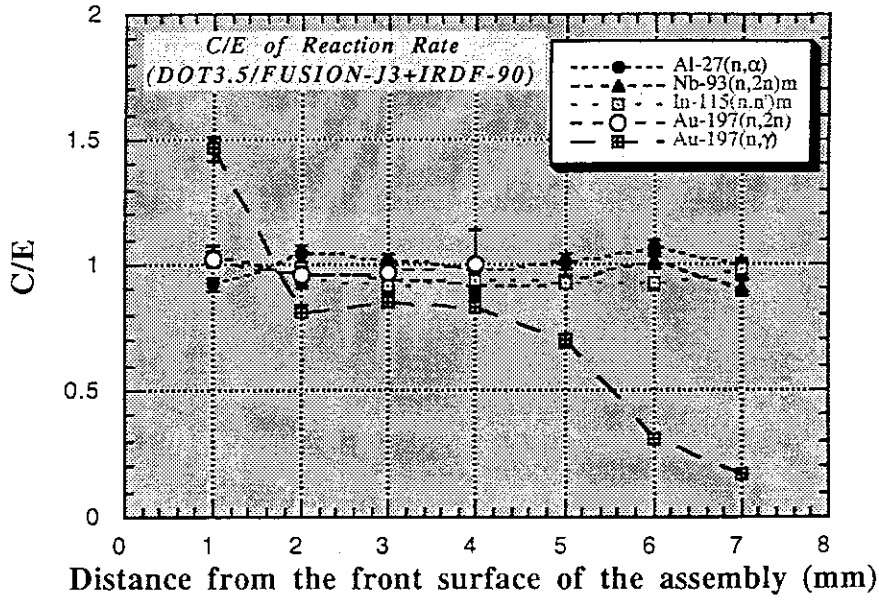

Figure 4 Ratio of calculation to experiment (C/E) for the dosimetry reactions of $^{93}Nb(n,2n)^{92m}Nb$, $^{197}Au(n,2n)^{196}Au$, $^{27}Al(n,a)^{24}Na$, $^{115}In(n,n')^{115m}In$, and $^{197}Au(n,g)^{198}Au$, at different depths inside the reference experimental assembly. The calculations done with DOT3.5/JENDL-3.1 and IRDF-90 dosimetry file.

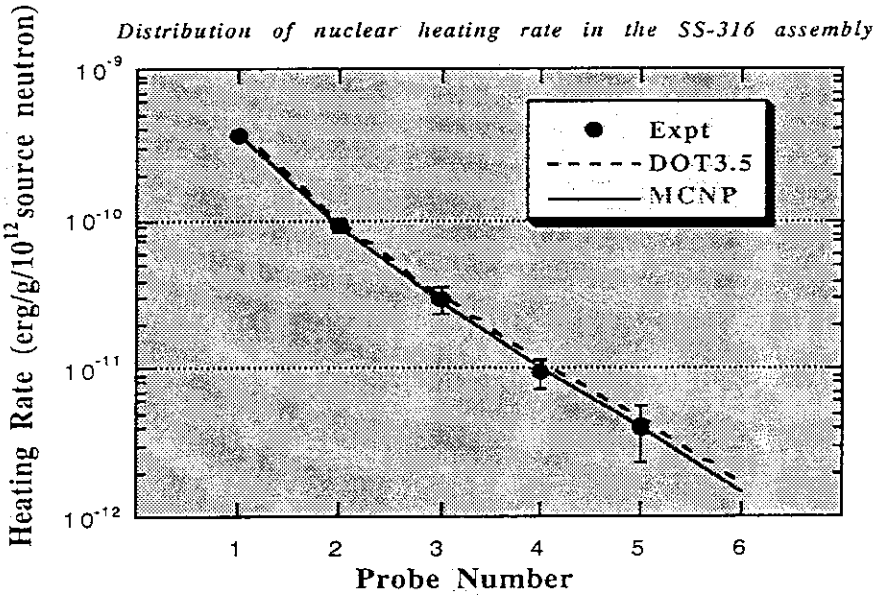

Figure 5 Comparison of calculation and measurement for distribution of volume averaged nuclear heating rates over each probe of SS-316 inside the reference assembly. The calculations have been done using MCNP with FSXLIB-J3 and DOT3.5 with FUSION-J3.

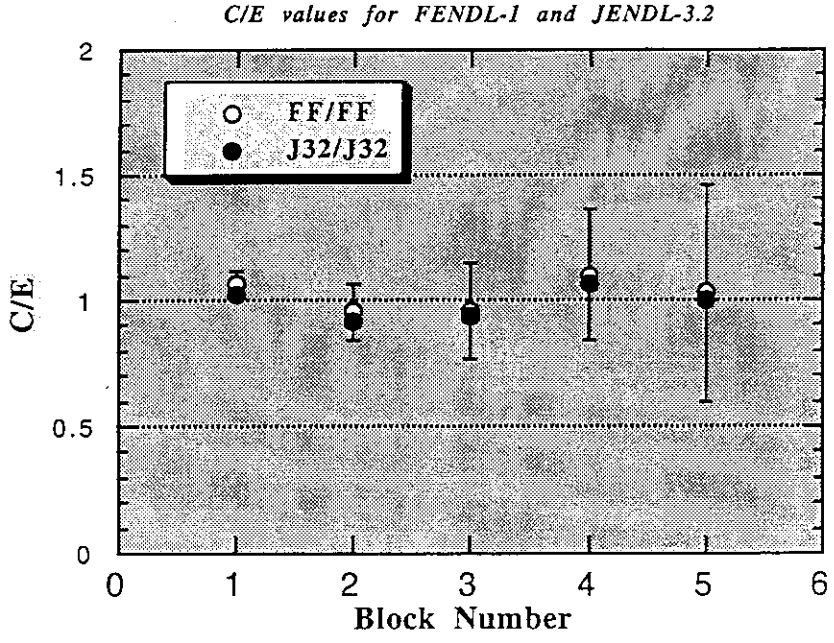

Figure 6 Comparison of calculated and experimental nuclear heating rates inside the reference experimental assembly, using various codes and nuclear data libraries. The heating rates have been "averaged" over respective probe volumes.

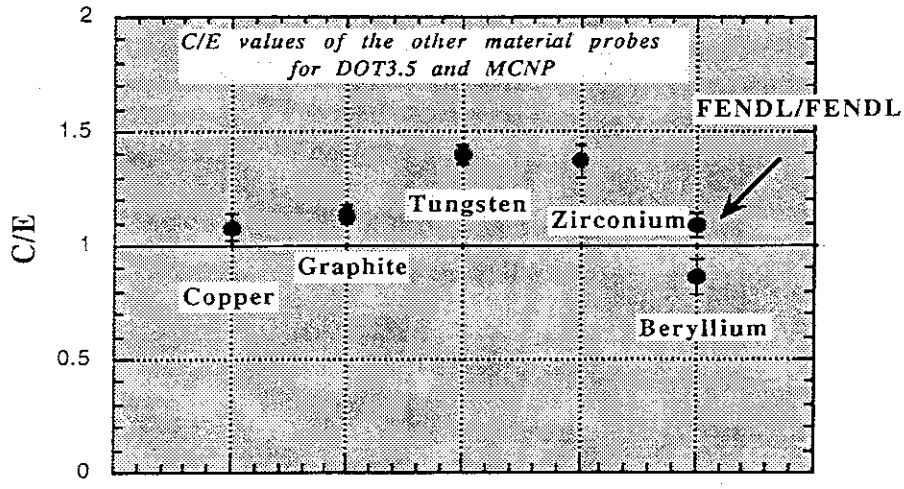

Figure 7 Comparison of calculated and experimental nuclear heating rates inside leading probes (probe #1) of all six experimental assemblies, using various codes and nuclear data libraries. The heating rates have been averaged over respective probe volumes.

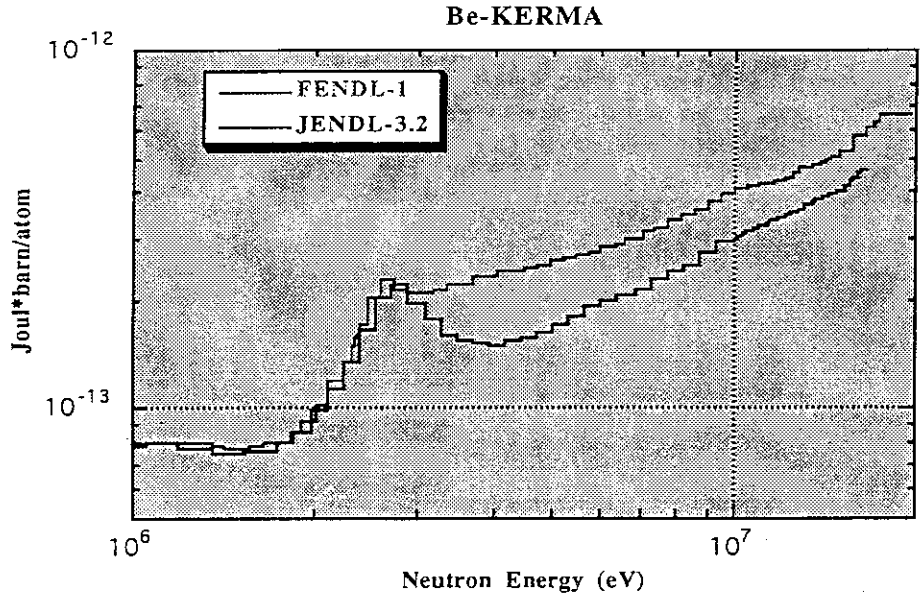

Figure. 8. Comparison of KERMA data between JENDL3.2 and FENDL-1

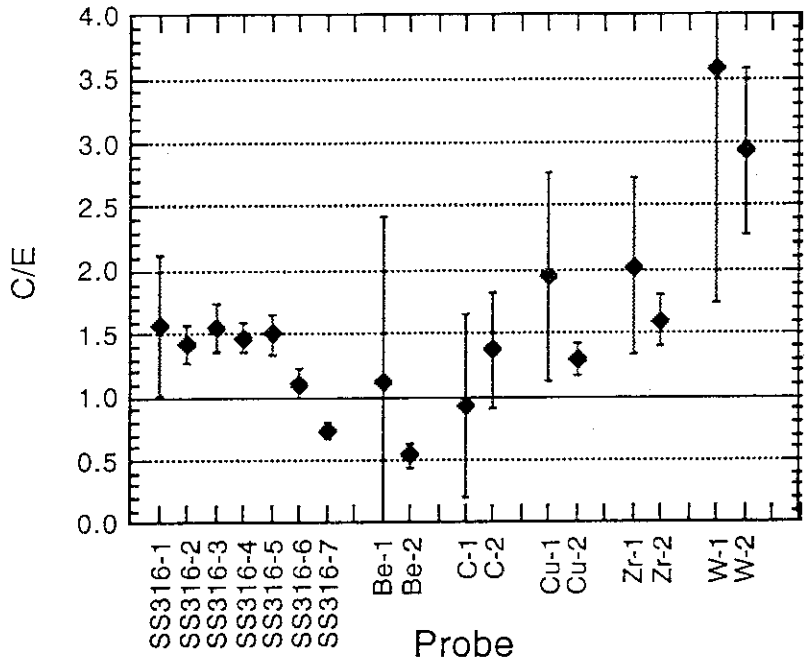

Figure 9 C/Es of the gamma-ray heating rates for the six configurations in the TLD measurements.

7. Discussion and Summary

7.1 Summary of Integral Data Test

7.1(a) Summary of Integral Data Test for Neutron Nuclear Data

Yukio OYAMA
Japan Atomic Energy Research Institute
Tokai-mura, Naka-gun, Ibaraki-ken 319-11
oyama@fnshp.tokai.jaeri.go.jp

Results of Integral data test were reported thorough this meeting for JENDL-3.2, JENDL Fusion File and FENDL/E-1 by using benchmark experiments performed at FNS/JAERI and OKTAVIAN/Osaka university. Qualities of these nuclear data file are evaluated and classified corresponding to degrees of agreement with the experiments.

The types of experiments were distinguished between the sphere and the slab geometries, because these experiments were performed at different facility each other. The features of the two experiments may also be different, i.e., the slab geometry is more sensitive to forward scattering. The point is given each nuclear data file corresponding to the level of agreement with the experiment. For example, For the case with agreement within 10%, 3 points are given to the nuclear data file, and for the case agreement within 10-20% and more than 20%, 2 and 1 points are given respectively. Therefore the maximum point is 3 points. These evaluations are presented in Table 1 along with the comments in which the problems found through the test are described.

In the results, there are inconsistency or ambiguity were found for some materials such as beryllium, nickel, cobalt. For beryllium, the results of the slab and the sphere experiments were inconsistent each other. For the slab, JENDL-FF showed good agreement but for the sphere JENDL-3.2 was in much better agreement. However, in general, JENDL-FF showed more than 2 points, i.e., less than 20% deviation and only a few exceptions are fluorine and cobalt.

Table 1 Evaluation Results by Integral Data Test (Neutron)

Nuclear Data File	JENDL-3.2		JENDL-FF		FENDL-1		Comments
Experiment Type	Sphere	Slab	Sphere	Slab	Sphere	Slab	
Breeder Constituents							
Beryllium	2	2	1	3	1	3	Inconsistency between sphere and slab , and between sphere experiments
Lead	--	1	--	3	--	3	Revised evaluation
Lithium	3	3	3	3	3	3	TPR within experimental error
Aluminum	2	--	2	--	2	--	C/E=+ 20% < 1MeV
Silicon	2	--	2	--	1	--	C/E=+10% < 1MeV
Zirconium	2	--	2	--	2	--	C/E=+10 > 10MeV, +15% < 1MeV
Structural/Shielding							
Iron	--	2	--	2	--	3	elastic XS is small ? MeV response
Chromium	3	--	3	--	2	--	C/E=+50% < 1MeV ? Experiment ?
Manganese	3	--	3	--	3	--	
Nickel	?	--	?	--	?	--	Normalization of Experiment ?
Copper	3	2	3	2	3	2	C/E < -40% for En <1keV in slab
Tungusten	1	2	(1)	3	2	1	C/E=-20-30% for 1-10MeV in sphere, but good for slab
Others							
Graphite	--	3	--	3	--	1	Softer continuum emission spectrum (FENDL)
Oxygen	--	3?	--	--	--	2?	Angular Distr. > 10 MeV
Nitrogen	--	2	--	--	--	1	8 MeV peak in expt., and inconsistent with DDX experiment.
Fluorine	1	--	1	--	1	--	large underestimation for CF2, LiF data
Cobalt	1?	--	1?	--	1?	--	Experiment ?
Niobium	2	--	2	--	1	--	Overestimation < 1 MeV
Titanium	2	--	2	--	1	--	Overestimation < 5 MeV
Molybdenum	2	--	2	--	2	--	C/E=-15% > 10 MeV
Arseric	--	--	2	--	--	--	

Criteria : (3)Good= < 10% (2)Satisfactory= 10-20% (1)Unsatisfactory= 20% < (?)Unclear= inconsistency, need further study

7.1 (b) Gamma-Ray Data

Fujio MAEKAWA
Fusion Neutronics Laboratory
Japan Atomic Energy Research Institute
Tokai-mura, Naka-gun, Ibaraki-ken 319-11
e-mail: fujio@fnshp.tokai.jaeri.go.jp

According to the results of the benchmark test, evaluations of secondary gamma-ray data in JENDL-3.2, JENDL Fusion File and FENDL/E-1.0 were summarized.

1. Policy of the Evaluation

According to the results of the benchmark test [1], evaluations of secondary gamma-ray data in JENDL-3.2, JENDL Fusion File and FENDL/E-1.0 were summarized. Two indices were selected for the summary; (1) energy balance and (2) shape of gamma-ray spectrum with the help of number of gamma-rays. The first index, energy balance, is the most important quantity of nuclear data required for fusion designs as described elsewhere [1]. In order to evaluate the energy balance, the calculated to experimental (C/E) ratios of gamma-ray heating rates measured in the FNS experiment and those of the total energy integrals, I_E, defined for the OKTAVIAN experiment were used. For the second index, C/E ratios of the total number of gamma-rays, I_N, for the OKTAVIAN experiment were used. In addition, agreement of shape of gamma-ray spectra between the measurement and the calculations for both the FNS and OKTAVIAN experiment were referred in the second index although it was subjective. Goodness of the data was classified into three grades, 3, 2 and 1 with the criteria of < 10 %, 10-20 % and >20 %, respectively, by taking account of the agreement of C/E ratios.

2. Results of the Evaluation

The evaluation results are shown in Table 1. The classification into the three grades is rather rigid because the experimental errors sometimes exceed 10 % and the modeling of the experiment in the Monte Carlo calculation, especially for the OKTAVIAN experiment, is not very accurate. Hence the data in the grades 3 and 2 which correspond to agreement within 20 % are judged as valid, while accuracy of the data in the grade 1 is regarded as unsatisfactory. The following remarks were derived.

(i) Secondary gamma-ray data in JENDL-3.2 were improved in JENDL Fusion File. As a result, energy balance of all the materials in JENDL Fusion File is in the grade 3 and 2.

(ii) Energy balance of Si and Nb in FENDL/E-1.0 is in the grade 1.

(iii) As for number of gamma-rays and shape of spectrum, data of Cr and Nb in both JENDL

Fusion File and FENDL/E-1.0 are in the grade 1.

3. Concluding Remarks

According to the evaluations, energy balance of all the secondary gamma-ray data in JENDL Fusion File and FENDL/E-1.0 except for Si and Nb in FENDL/E-1.0 was found to be valid. These data can be utilized for designs of fusion reactors with firm confidence.

Qualities of secondary gamma-ray data in JENDL Fusion File was validated by the benchmark calculations, and as a whole, found to be superior to those in FENDL/E-1.0. Hence cross section data in JENDL Fusion File are recommended as candidate substitutions for the next FENDL/E-2.0.

Reference

1) Maekawa F.: "Nuclear Data Test with Gamma-Ray Integral Experiments," in this proceedings (1996).

Table 1 Evaluation results for secondary gamma-ray data.

Material	Experiment	JENDL-3.2	JENDL-FF	FENDL-1	Comments
	FNS / OKT	IN+spec / IE	IN+spec / IE	IN+spec / IE	
Breeder Constituents					
Beryllium	-	-	-	-	
Lead	OKT	3 2	2 3	2 3	Revised JENDL-FF
Lithium	-	-	-	-	
Aluminum	OKT	3 3	3 3	3 3	
Silicon	OKT	3 2	3 2	2 1	
Zirconium	-	-	-	-	
Structural/Shielding					
Iron	FNS	1 1	3 2	2 3	Revised JENDL-FF FENDL (n,g)_spec not good
Chromium	OKT	1 2	1 2	1 2	Experiment ?
Manganese	OKT	2 2	2 2	2 2	Shibata's Evaluation for JENDL&B-VI
Nickel	-	-	-	-	
Copper	FNS / OKT	2 3	2 2	2 2	J-FF, FEN (n,g)_spec not good
Tungusten	FNS / OKT	2 3	3 3	3 3	Revised JENDL-FF
SS316 (Fe,Cr,Ni)	FNS	3 1	3 2	2 2	FEN (n,g)_spec not good
Others					
Graphite	OKT	3 3	3 3	3 3	4.44MeV only
Oxygen	-	-	-	-	
Nitrogen	-	-	-	-	
Fluorine	OKT	3 3	3 3	3 3	
Cobalt	OKT	3 3	3 3	2 2	
Niobium	OKT	1 2	1 2	1 1	
Titanium	OKT	2 3	2 3	2 3	
Molybdenum	OKT	2 2	2 3	2 2	
Arseric	-	-	-	-	

Judgement: (3) Good = < 10% (2) Satisfactory = 10-20% (1)Unsatisfactory = > 20%

7.1 (c) Activation File

Yujiro Ikeda

Japan Atomic Energy Research Institute.
Tokai-mura, Naka-gun, Ibaraki-ken 319-11, Japan

1. FENDL-A2 Selection Procedure and Status

FENDL-A2 selection procedure was agreed at FENDL-AGM in 1994, Garching. The Selection panel members were nominated from regional participating parties and assigned to execute the procedure. The candidate files were submitted by February 15, 1995 to IAEA and De. F. Mann who compiled all files into appropriate format to be compared with the experiments. The files are JENDL Activation File (Japan), EAF-4.0 (EU), ADL3 (Russia), FENDL-A1(IAEA) and US-Act (US). A selection kit, plots of all library data for specific reactions, were prepared by IAEA/NDS and distributed to the selection panel members. Accordingly, the first meeting of the selection panel was held at St. Petersburg in conjunction with the last IAEA-RCM on Activation cross sections for Long-Lived Radio-nuclide Generation with each representative member of the participating organization. The meeting was successfully conducted, starting with recommending the most appropriate libraries by comparing the library data with the available experimental data. The first effort ended with the selections for the first and second priority reaction sets according to the list of the high priority reactions of concern for the fusion applications. As scheduled, in December 1995 at Del Mar, U.S.A., the FENDL-AGM was held to finalized the FENDL-A2 selection procedure. As the result of the FENDL-AGM, the most adequate candidate libraries for about 400 high priority reactions were determined. Among the reactions, all (n,γ) reactions were agreed to be replaced with EAF-4 by taking accounts of previous contributions on the comprehensive evaluation for these particular (n,γ) reactions. Also, it was agreed that EAF-4 will serve as the base-line library which data are to be used for the reactions other than those high priority 400 reactions.

2. Recommendation

As far as the FENDL-A2 is concerned, the JENDL Activation File committed reasonably. It is not possible JENDL Activation File to cover all reactions requested as the FENDL-A from the completeness requirement for the fusion application. Thus, it is noted that if JENDL will commit to an international activity, the number of reactions to be contained should be enlarged by considering reactions with unstable radionuclides as the target, resulting in the multi-step higher order reaction process. It is matter of discussion from further data requirements for the application.

The second issue is an extension of the neutron energy. The FENDL library limit the energy to 20 MeV according to the fusion application requirement. Higher energy region, however, should be stressed in the next step for the activation cross section data because of increase of large demands on the data from accelerator based high intense neutron source projects. The IFMIF need data up to 50 MeV. A Spallation neutrons source with GeV order protons requires data al least to several hundreds MeV. It is of course need data developments by theoretical model calculation as well as new experimental measurements. It is, thus , strongly recommended that a new coordination on the development for the high energy neutron activation cross section should be realized as soon as possible. It is worth IAEA to take initiative in addition.

7.1 (d) Overall Quality of Neutron and Secondary Gamma-ray Data

Yukio OYAMA and Fujio MAEKAWA
Japan Atomic Energy Research Institute
Tokai-mura, Naka-gun, Ibaraki-ken 319-11
oyama@fnshp.tokai.jaeri.go.jp

From both evaluations of neutron and gamma-ray data described in the previous summaries, overall evaluation of all the nuclear data files was attempted. Each evaluation for neutron and gamma-ray data described in 7.1(a) and (b) are summarized in Table 1. In this table, sum present overall quality where neutron data point is multiplied by two because the gamma-ray accounts for both the number of photon and the energy integral, i.e., the maximum point are 6 points. Then the maximum of the total point is 12 points.

Figures 1 and 2 show the histograms for the above points for each material and for each nuclear data file. From the figures, one can easily see that JENDL-FF have higher point for both the neutron and the total points. The worst material for JENDL-FF is Ti, while for FENDL-1, Nb and Si. Consequently, these two graphs give summary of the present data test.

Table 1 Evaluation Results by Integral Data Test

Material	JENDL-3.2			JENDL-FF			FENDL-1			Best Selection
	neutron	gamma-ray ϕ_γ $\phi_\gamma E$	Sum	neutron	gamma-ray ϕ_γ $\phi_\gamma E$	Sum	neutron	gamma-ray ϕ_γ $\phi_\gamma E$	Sum	
Breeder Constituents										
Beryllium	2 ?	------	(4)	2 ?	------	(4)	2 ?	------	(4)	all
Lead	1	3 2 (5)	7	3	2 3 (5)	11	3	2 3 (5)	11	J-FF,FEN
Lithium	3	------	(6)	3	------	(6)	3	------	(6)	all
Aluminum	2	3 3 (6)	10	2	3 3 (6)	10	2	3 3 (6)	10	all
Silicon	2	3 2 (5)	9	2	3 2 (5)	9	1	2 1 (3)	5	J-FF,J-3.2
Zirconium	2	------	(4)	2	------	(4)	2	------	(4)	all
Structural/Shielding										
Iron	2	1 1 (2)	6	2	3 2 (5)	9	3	2 3 (5)	11	FEN
Chromium	3	1 2 (3)	9	3	1 2 (3)	9	2	1 2 (3)	7	J-FF,J-3.2
Manganese	3	2 2 (4)	10	3	2 2 (4)	10	3	2 2 (3)	9	J-FF,J-3.2
Nickel	?	------	?	?	------	?	?	------	?	?
Copper	3?	2 3 (6)	12?	3?	2 2 (4)	10?	3?	2 3 (5)	11?	J-3.2
Tungusten	2	2 3 (5)	9	2	3 3 (6)	10	2	3 3 (6)	10	J-FF,FEN
Others										
Graphite	3	3 3 (6)	12	3	3 3 (6)	12	1	3 3 (6)	8	J-FF,J-3.2
Oxygen	3?	------	(6)	------	------	------	2?	------	(4)?	J-3.2
Nitrogen	2	------	(4)	------	------	------	1	------	(2)	J-3.2
Fluorine	1	3 3 (6)	8	1	3 3 (6)	8	1	3 3 (6)	8	all
Cobalt	1?	3 3 (6)	8	1?	3 3 (6)	8	1?	2 2 (4)	6	J-FF,J-3.2
Niobium	2	1 2 (3)	7	2	1 2 (3)	7	1	1 1 (2)	4	J-FF,J-3.2
Titanium	2	2 3 (5)	9	2	2 3 (5)	9	1	2 3 (5)	7	J-FF,J-3.2
Molybdenum	2	2 2 (4)	8	2	2 3 (5)	9	2	2 2 (4)	8	J-FF
Arseric	------	------	------	2	------	(4)	------	------	------	J-FF

Criteria: (3)Good= < 10% (2)Satisfactory= 10-20% (1)Unsatisfactory= 20% < (?)Unclear= inconsistency, need further study

Sum = Neutron x 2+ Gamma(ϕ_γ+$\phi_\gamma E$)

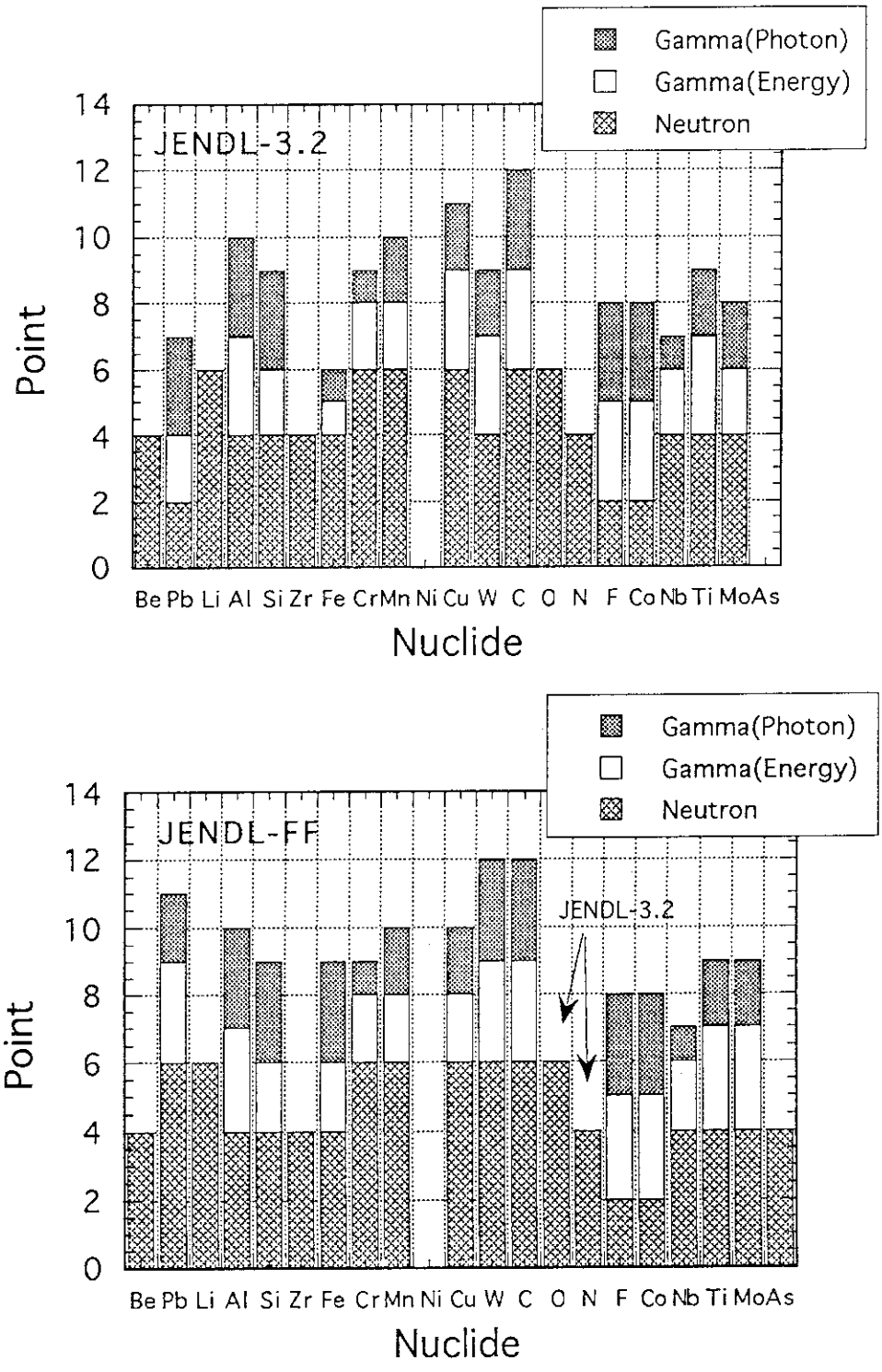

Fig.1 Comparison of overall quality of JENDL-3.2 and JENDL Fusion File from the integral data tests.

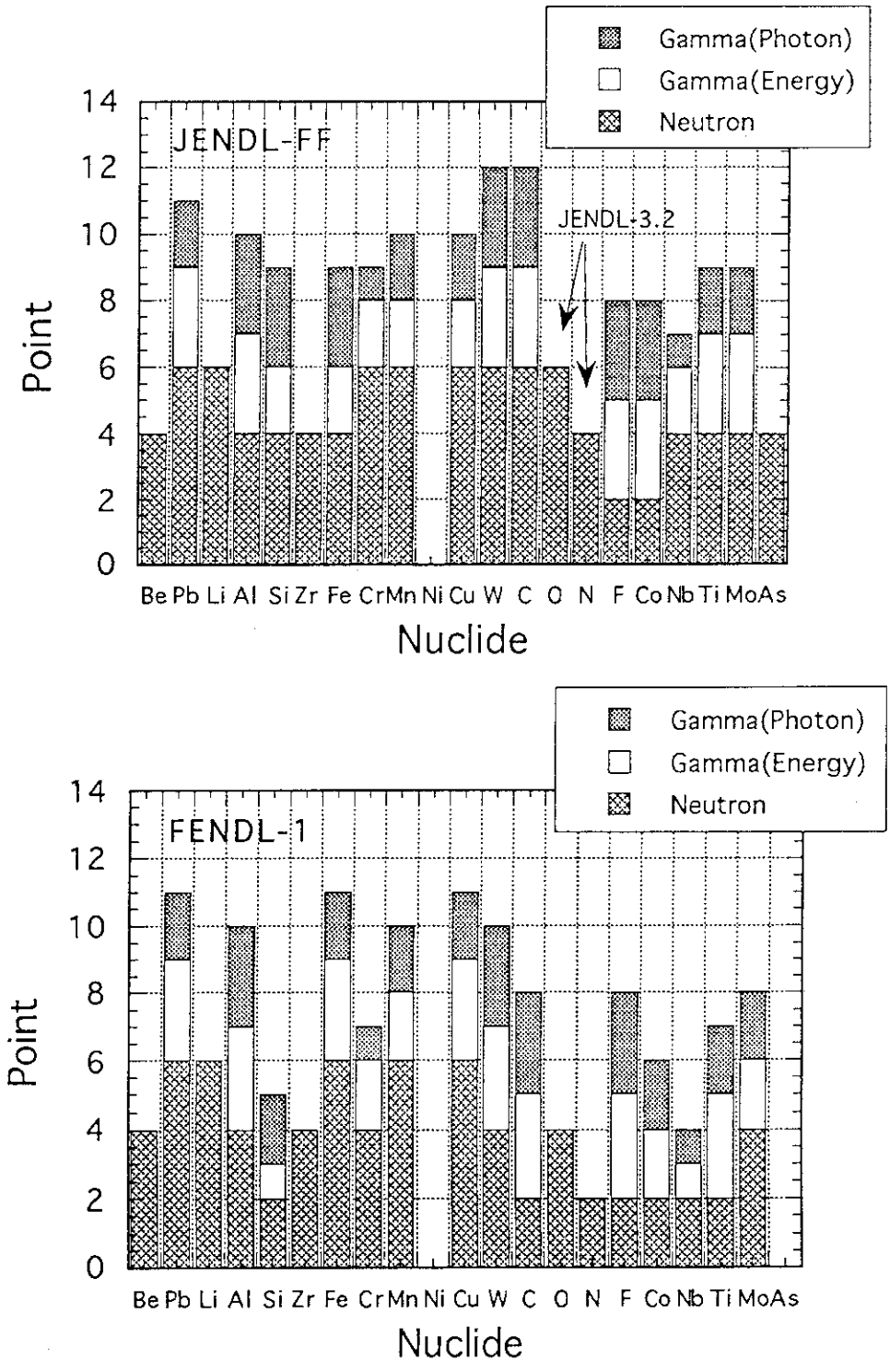

Fig.2 Comparison of overall quality of JENDL Fusion File and FENDL/E-1 from the integral data tests.

7.2 Future Subjects

7.2 (a) Comment 1 from Neutronics

Akito TAKAHASHI
Department of Nuclear Engineering
Osaka University
Suita, Osaka 565

Comments are given on major subjectives of future fusion neutronics works. Desired experimental efforts are mentioned for nuclear data, radiation shielding, neutronics design and reactor instrumentation and diagnostics of DT fusion reactors.

1. Introduction

Answers to a questionare on desired fusion neutronics activities in future, collected from neutronics researchers in Japan, will be summarized in the following with a bit modification by the commenter.

What is fusion neutronics may be defined as "research field on physics and instrumentation of nuclear－reaction－related subjectives of fusion devices and reactors". Major subjectives are categorized as fusion－nuclear data, radiation shielding, nuclear designing, and diagnostics and reactor instrumentation. Topics which requires especially experimental efforts are discussed in the following.

2. Establishment of Methodology for Nuclear Design of DT Reactors

Establishmernt of neutronics methodology for reliable nuclear designing of DT reactors has been a first priority target of Japanese neutronics activities in the last 15 years. Improvements of accuracies on predictabilities of tritium breeding ratios (TBR) and local tritium production rates (TPR) and nuclear heating distributions by radiation transport calculations have been done by accumulating and evaluating more accurate fusion－nuclear data, improving nuclear－data processing codes to access to transport codes, and improving radiation transport codes.

Reaction cross sections like ^{7}Li(n,n't) and double differential neutron emission cross sections, especially ones measured at Japanese laboratories have made great contributions to the improvements of evaluated nuclear data, such as JENDL3.2, ENDF/B－VI and FENDL1 for fusion applications. Integral benchmark experiments of pure material piles, simple model blankets and mock－up type model blankets done by the joint－University team using OKTAVIAN and the

JAERI－USDOE team using FNS have made also a great contribution to improve the methodologies. Most data of these integral benchmark experiments are compiled nowas electronic data base of IAEA and researchers for benchmark tasks can access to it via INTERNET. Integral benchmark of FENDL1 are under way in this guide line (see Proceedings of Del Mar '95 Meeting on FENDL).

Target accuracy of TBR has been set up to be within 2 %. Best accuracies obtained upto now by integral experiments on TBR are estimated to be within 4－5 %, and we need therefore further experimental efforts to improve the accuracies and hence to improve the predictability of TBR values by design calculations of DT reactors. Current trend of breeding blanlket designs is to employ "thermal blankets" based on ^{6}Li(n,t) reactions with neutron multiplications by ^{9}Be(n,2n) reactions. Therefore the improvement of Be nuclear data has been one of major efforts by the neutronics community. Conclusions of integral benchmark studies on Be nuclear data, especially (n,2n) cross ections and secondary neutron angle－energy distribution data, are not satisfactory: There are found systematic differences beteen 4 major experiments by FNS, OKTAVIAN, Obninsk and KfK. There are disagreements between these experiments and transport calculations with evaluated nuclear data (JENDL3.2, ENDF/B－VI, EFF2 and FENDL1). In order to resolve the disagreements on Be data, reexperiments with Be－spheres possibly by inertational collaboration should be encouraged.

Vanadium (or V－alloy) is a candidate of low－activation first wall material. However, we have no experimental data of integral benchmark ever done and therefore an intergal experiment like pulsed sphere leakage spectrum measurement should be strongly encouraged. Benchmark studies using available leakage neutron spectra data from spheres for many elements have shown that one of available evaluated nuclear data, for example JENDL3.2, at least can best fit to measured data for many elements and nuclides, but for some elements like F, Ti and Co we have no satisfactory evaluated nuclear data. For Ni, we have no reliable integral data available. Further benchmark studies for V, Ni, F, Ti and Co using some new experimental data should be therefore encouragaed.

Due to lack of experimental data for nuclear heating distributions (though a trial experiment is started at JAERI－FNS), new idea of experiments and construction of new intense DT neutron sources to realize nuclear heating experiments are strongly desired.

Scope of blanket neutronics can be also extended to fusion－fission hybrid systems and beam driven fusion neutron sources.

To resolve causes of disagreements between experiments and calculations, applications of sensitivity analyses are really needed.

3. Shielding and Safety

Shielding of neutrons and gamma－rays, to protect components , instrumentation－sensors and to keep working and living conditions around reactor and plant facility, is regarded as urgent tasks in constructing DT－burning plasma devices like ITER, from safety issue.

Neutron deep penetrations and streamings through geometrically complicated systems like ITER and LHD have been studied in last more than 20 years to develope and establish methodologies for 3D exact particle transport calculations (Monte Carlo codes and deterministic Sn codes), estimations by simplified equations, and special purpose nuclear data libraries (dosimetry, activation and decay－heat, KERMA, PKA data etc.) . Several serieses of integral benchmark experiments have been done at FNS and OKTAVIAN using from rather pure systems for deep penetration problems and streamings through slits and bent ducts to more complicated mock－up type assemblies simulating ITER/EDA designs. These experimental data have been efficiently used for benchmarking available shielding codes and estimating margin factors (safety factors) for key criteria of components and biological shieldings, and will be further utilized to improve codes for shielding calculations. Neutron and gamma－ray sky－shine data taken by existing 14 MeV neutron source facilities like OKTAVIAN are very valuable to evaluate environmental dose distributions from DT plasma facilities and plants.

Integral shielding data are however newly required for mock－up assemblies of ITER/EDA and helical systems to benchmark shielding capabilities, activation rates and nuclear heating rates (especially in SCM). A series of experiment is under way at FNS.

Conserning the safety issue of materials, special purpose nuclear data are under evaluation at JAERI for PKA, DPA and KERMA for future customers in damage and life－time analyses. Differential cross section measurements, e.g., double differential charged particle emission cross sections for nuclides of reactor－candidate materials are fundamental data for these evaluations, but no many data are available. Experimental efforts on charged particle emission DDX measurenments should be therefore encouraged, together with gamma－ray emission data.

Special shielding problems will be raised up in the planned construction of d－Li type intense neutron source (i.e., IFMIF) to cover source neutron energy range exteded up to 50 MeV, so that measuremenets of reaction cross sections and DDX data for neutron and charged particle emissions in 20－50 MeV region should be encouraged.

4. Intense Neutron Sources

Concept design study of IFMIF which is based on the d－Li reaction is under way as IEA international collaboration. Realization of IFMIF construction will surely impact the fusion neutronics community to be activated again.

Constructions of more intense DT sources than FNS and OKTAVIAN should be seriously recommended to provide lacked nuclear data for charged particle emissions and nuclear heating, promote further accurate integral benchmark experiments for shielding mock－up and blanket development purposes and surve as standard DT neutron sources for general fusion science purposes (many calibration purposes for diagnistic sensors, detectors, damage references, spectropy techniques, etc.). FNS21 and OKTAVIAN2 as 10 times more intense source than FNS and OKTAVIAN are current paper plans, and realization of one or both will be indispensable for the neutronics activity and equally for the main－stream fusion development program.

5. Characterization of Fusion Radiation Field

To clear the safety issue of fusion reactor plants, characterizations of fusion－induced radiation field (neutrons, gamma－rays, X－rays, radio activity distributions) will be importnat. Diagnostics and control of burning plasma, setting－up of radiation－resistant detectors and sensors, radiation damage monitoring instruments, and environmental radiation monitorings should be done under the support of reliable technology. Calculational methodologies of radiation field characterizations should be also established. To evaluate items of continuous monitoring of environmental radiation fields, benchmark data by experiments measuring field strengths (doses) and spectra inside, outside of reactor, in－room, ouside plant building and far environment should be encouraged.

7.2 (b) Comment 2: DEMO Reactor and Safety Related Nuclear Data

Yasushi Seki
Naka Fusion Research Center
Japan Atomic Energy Research Institute
Naka-machi, Naka-gun, Ibaraki-ken 311-01

Material used in Fusion DEMO Reactor is reviewed. The nuclear data needed in safety analyses of fusion reactor are identified. An interesting topic of radioactive nuclides produced from multi-step neutron reaction and charged particle nuclear reactions is introduced.

1. Materials used in DEMO reactor designs

In the review paper[1] on fusion DEMO reactors, I have reviewed recent DEMO reactor designs and the following materials are found to be used in the design.

Table 1 Materials used in DEMO fusion reactor studies

Function	Material
Plasma facing surface	Beryllium, Copper, Molybdenum, Tungsten, TiC
Structural materials	Austenitic steel, Ferritic steel, Martensitic steel, Vanadium alloy
Coolant	Water, Liquid lithium, Molten salt (FLIBE), Helium gas
Tritium Breeder	Lithium oxide, Liquid lithium, Molten salt (FLIBE), Lithium Lead
Neutron Multiplier	Beryllium

2. Nuclear Data needed for Safety Analyses

In the last meeting on Nuclear Data for Fusion Reactors, I gave a review[2] on the nuclear data needs for safety analyses. In this review, I summarize the type of nuclear data needed for safety analyses. In the safety analyses of a fusion reactor, the following needs to be analyzed. Radiation dose to the plant personnel and the general public in normal operation and in accident conditions. Nuclear heating during operation and transient states needs to be accurately for the evaluation of thermal-hydraulic conditions. Radiation damage of materials need to be evaluated to assure the reliability of reactor components and replacement frequency. Induced radioactivity evaluation is necessary for the release of radioactive material, decay heat and decay gamma-ray dose for personnel dose during maintenance and radioactive waste management evaluation. The nuclear data needs for various safety analyses are summarized in Table 2.

Table 2 Nuclear Data Needed for Safety Analyses

Safety Analyses	Type of Nuclear Data needed	Application
Radiation shielding analysis	Transport cross sections of neutron and gamma-rays Gamma-ray production cross sections Flux to dose conversion factors	Bulk shielding evaluation Streaming calculation Skyshine evaluation
Nuclear heating analyses	Kerma factors	Steady state and transient heat analyses
Radiation damage analyses	Flux to DPA conversion factor, Gas Production cross section, Transmutation cross section	DPA evaluation Helium and hydrogen gas production Alloy fraction change evaluation
Activation analyses	Activation reaction cross section Nuclide decay data (decay scheme, half-life) Decay gamma-ray energy spectra	Dose rate evaluation for routine and accidental release and radwaste disposal Decay heat evaluation for maintenance operation, loss of cooling events and radwaste Personnel dose during maintenance and radwaste disposal

3. Nuclear data for heavy irradiation activation analyses

In a recent study of radwaste study[3] of fusion power reactors with heavy irradiation fluences over 10 MWa/m^2, the importance of multi-step nuclear reactions became apparent. As an example, the generated transmutants from ^{186}W through multi-step reactions are shown as a function of irradiation time in Fig. 1. The importance of the sequential (x,n) reactions, namely the nuclear reactions caused by charged particles for the dose rate evaluation for heavy irradiation of 12.5 MWa/m^2, has been demonstrated by S. Cierjacks.[4] It has been shown that the dose rate from the activation of fluorine differs more than 10 orders of magnitude higher when (x,n) reactions are considered compared with the case without consideration of (x,n) reactions.

References

(1)SEKI, Y.: Review of Fusion DEMO Reactor Studies, this proceeding

(2)SEKI, Y.: Data Needs from Fusion Reactor Safety Analysis, JAERI-M 91-062 (1991)

(3)SEKI, Y., AOKI, I., YAMANO, N. and TABARA, T.:to be submitted to ANS Topical Meeting on Fusion Energy at Reno, 1996

(4)CIERJACKS, S., OBLOZINSKY, P. and RZEHORZ, B.: Nuclear Data Libraries for the Treatment of Sequential (x,n) Reactions in Fusion Materials Activation Calculations, KfK-4867 (1991)

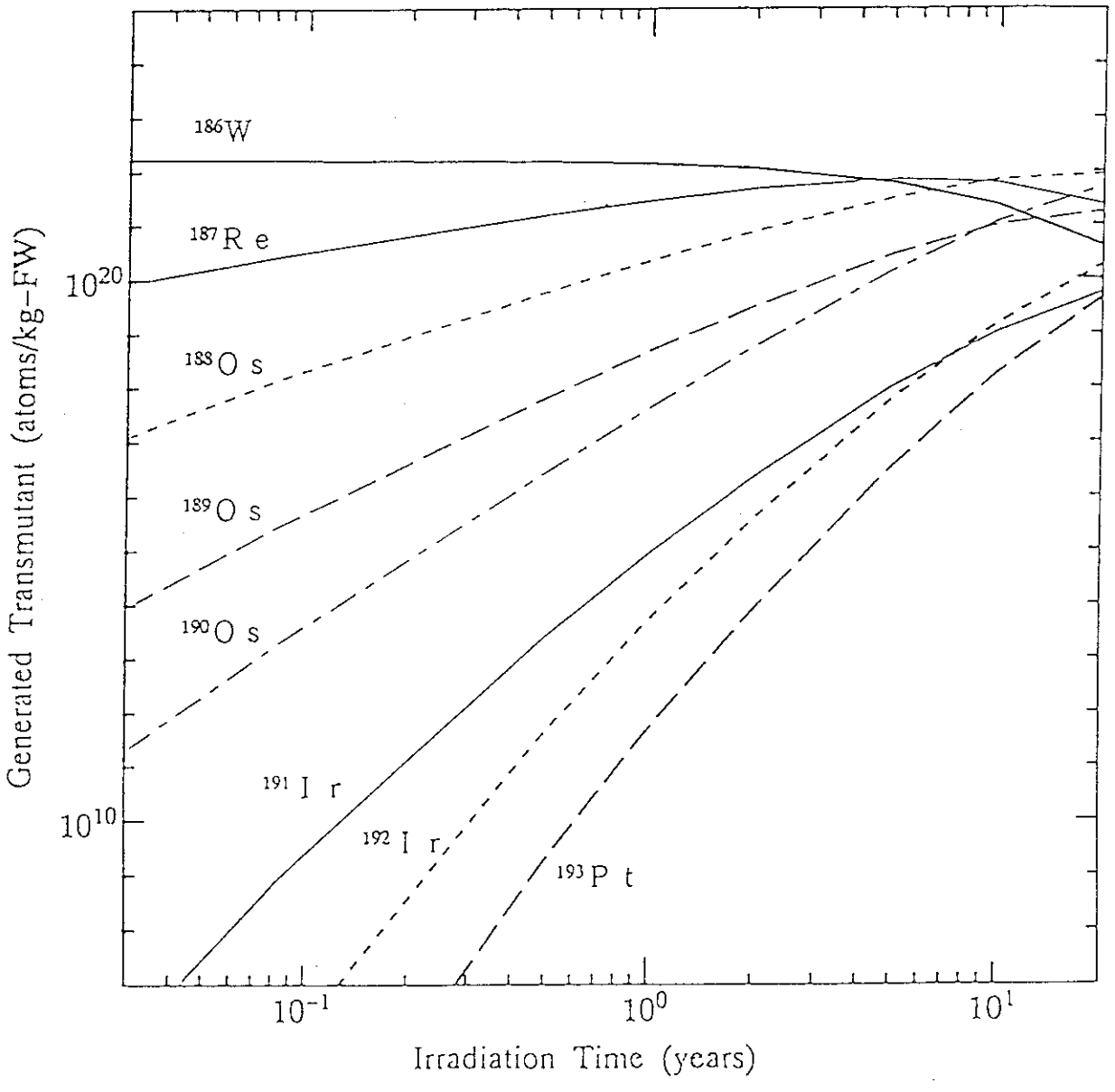

Fig. 1 Nuclide Densities of Generated Transmutants and ^{186}W in the First Wall of SSTR with Irradiation Time at Neutron Flux of 1 MW/m^2

7.2 (c) Comment 3 from Nuclear Design in International Thermonuclear Experimental Reactor (ITER)

Koichi Maki
Hitachi Research Laboratory, Hitachi Ltd.
7-1-1 Omika-cho, Hitachi-shi, Ibatraki-ken 319-12

1. Consequence of nuclear design to fusion reactor design

(1) In fusion reactors, shielding design for protecting facility itself against radiation must be held a important position in reactor design differently from fission reactors and accelerators, in which biological shielding is main shielding design. Especially shielding design for superconductive magnets (SCM) against radiation is held a main part of position together with structural design in fusion reactor design.

(2) Biological shielding can be considered separately from reactor core design since the former has small effect on the latter.

(3) Considering (1) and (2), we emphasize that we cannot put fusion reactor development forward without nuclear shielding design.

(4) It is indispensable to appeal consequence of nuclear design to the persons promoting fusion reactor development and those around them in order that they recognize the matter.

2. Requirements to nuclear data

(1) Activation cross sections in unstable nuclides, for example induced from W, Fe and Ni, etc., are necessary to evaluate radiation waste and safety analysis, etc., concerning induced activities.

(2) Accuracies in response function cross sections, Kerma factor, dpa, helium production rate, and hydrogen production rate, etc., are necessary to be heightened. In order to perform them accuracies in energy spectra of charge particles created in neutron reaction, and those of secondary neutron and gamma-ray are required to be heightened.

(3) Sensitivity analysis of nuclear data to integral data is necessary in order to understand clearly the efficiency of nuclear data to nuclear design characteristics.

7.2 (d) Comments on Nuclear Data Base Study from a Viewpoint of the JT-60SU Conceptual Design

Naoyuki MIYA
Japan Atomic Energy Research Institute
Naka Fusion Research Establishment
Naka-machi, Naka-gun, Ibaraki-ken, Japan

Neutron shielding structures of vacuum vessel with low activation materials are proposed for the JT-60 super-upgrade (JT-60SU) design. Titanium alloy and tungsten are used for the candidate vessel materials. These give the results consistent with the design requirements of the nuclear shielding. Production of accurate activation data and evaluation based on measurements and calculations for the candidate materials under the high D-D neutron fluxes are required in future nuclear data base study.

1. Introduction

Demonstration of feasibility of steady state operation is the important step to the goals of DEMO and a commercial reactor. We proposed the JT-60SU (Super Upgrade) [1-3] with a plasma current of 10MA, as the next to the JT-60U experimental programs. Mission of the research program using the device is the integrated study of steady state, high-power physics and technology. A present candidate design is to use superconducting magnet systems and long pulse operation exceeding 2000s mainly by 60MW-500keV negative-ion beam injector with non inductive current drive.

Activation of the device and nuclear heating in the superconducting magnet will be critical design problems due to long pulse discharges and high neutron fluxes. It is required to study the vacuum vessel structure which enables both the human access on the occasion of a major machine failure and the reduction of nuclear heating in the coil by shielding neutron irradiation. From the viewpoint of this, use of titanium (Ti) alloy, tungsten (W) materials and boron doped water are proposed for the shielding design of the vacuum vessel. In this paper some comments on nuclear data base study are described from a viewpoint of this conceptual design study of JT-60SU.

2. JT-60SU Device

An elevation view is shown in Fig.1. The plan view of the JT-60 torus hall is shown in Fig.2. The JT-60SU tokamak system is located inside an evacuated cryostat and biological shield. The device uses superconducting (SC) toroidal field (TF) coil and poloidal field (PF) coil magnet systems.

The JT-60SU assumes that approximately $4x10^{22}$ D-D fusion neutrons are produced per one year operation and a maximum neutron production rate is $1x10^{18}$/s. D-D neutron flux reaches ~$1x10^{12}$ n/s cm^2 on the vacuum vessel surface. Allowable limits of the biological shielding for in-vessel working section is ~10mrem/h(0.1mSv/h) at 1 year after shutdown. For the nuclear heating rate in the superconducting material (SCM) of the inboard TF SC-coil, an allowable limit of ~0.2 mW/cc is applied in an operation phase.

3. Low activation materials and Shielding Structure

Figure 3 shows two proposed structures for JT-60SU. In the structure A(left), Ti alloy is used for the vacuum vessel as a candidate for the low activation material[4]. Nuclear group constant set FUSION-40 is adopted for the calculation. The dose rate is ~15 mrem/h at 1 year after the shutdown. The vacuum vessel is a double-walled vessel filled with Boron (1% of ^{10}B) doped water. This water tank-type vacuum vessel with 30-80cm thick in total provides a one-turn resistivity of ~50μΩ and a nuclear heating rate of ~0.2mW/cc in the SCM. However, some technical problems of Ti alloy vessel such as hydrogen embrittlement, thermal /mechanical analysis for the water tank-type structure and manufacturing R&D including welding are considered to be necessary in future design studies, since the titanium would be the first application to large tokamak devices. Structure B (right) shows alternative plan for vessel materials. In this structure SS-316 (with low Co:<0.05 wt%), which is referred on the basis of much experience gained in the development as nuclear components, is used for the vessel material with pure water. High-Mn steel is also possible, cobalt concentration of which is extremely low. For the case of using only SS-316, total dose rate is estimated to be ~300 mrem/h. Thus Tungsten blocks of 1-2 cm thick, which decrease to ~5 mrem/h, is adopted as inner shielding wall in the case B.

4. Comments

Two types of the structure A and B are proposed for the vacuum vessel with low radioactivity. These give the results consistent with the design requirements of the nuclear shielding of JT-60SU.

In order to improve the accuracy of the activation calculation in a fusion reactor, there have been an number of activities to improve the quality and quantity of activation cross sections so far. This work is, however, focused on the accurate evaluation for the activation products generated by 14 MeV neutrons of D-T fusion reaction. In JT-60SU, high D-D neutron flux is estimated to be ~$1x10^{12}$ n/s cm^2 on the vacuum vessel surface. It is required to produce accurate activation data and have evaluation based on measurements and calculations for candidate materials such as Ti, W under the intensive D-D neutron field.

Impurity concentration is another problem to be considered. Radio nuclide ^{60}Co with

long half-life, for example, is dominant in the dose rate at 1 year after the shutdown even it is a very small quantity. Evaluation of impurity concentration for low activation materials based on measurements and calculations is also essential in the future work.

References

[1] M. Nagami, N. Miya, S. Nakajima et al., Preliminary Design Study of a Steady State Tokamak Device,33rd APS DPP,9T-58, 1991,Tampa.

[2] H. Ninomiya, et al., Conceptual Design of JT-60 Super Upgrade,15th IAEA conf., Seville, Spain, 1994, IAEA-CN-60/F-1-I-1.

[3] M. Kikuchi, et al., Conceptual Design of JT-60SU,16th Symposium on Fusion Engineering, Illinois, 1995

[4] N. Miya., et al., Fusion Engineering and Design, 23(1993)351.

machine parameters	
major radius	4.8 m
minor radius	1.3 - 1.5 m
ellipticity	1.8
triangularity	0.3 - 0.8
plasma current	10 MA
toroidal field	6.25 T
number of toroidal coils	18
heating power	60 MW
pulse length	
(full current drive)	≤ 3600 s
(inductive)	≤ 200 s

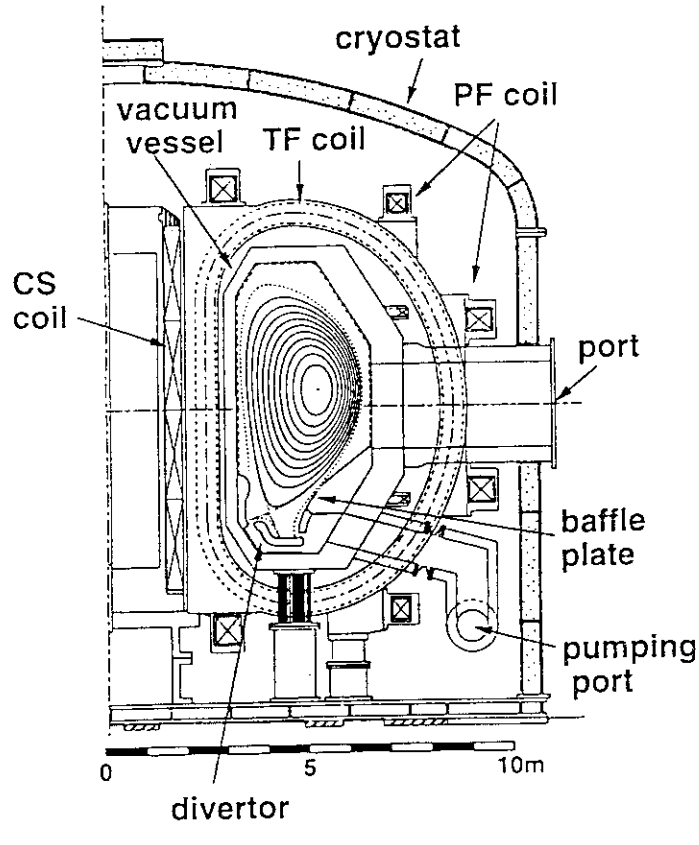

Fig. 1 Elevation view of JT-60SU.

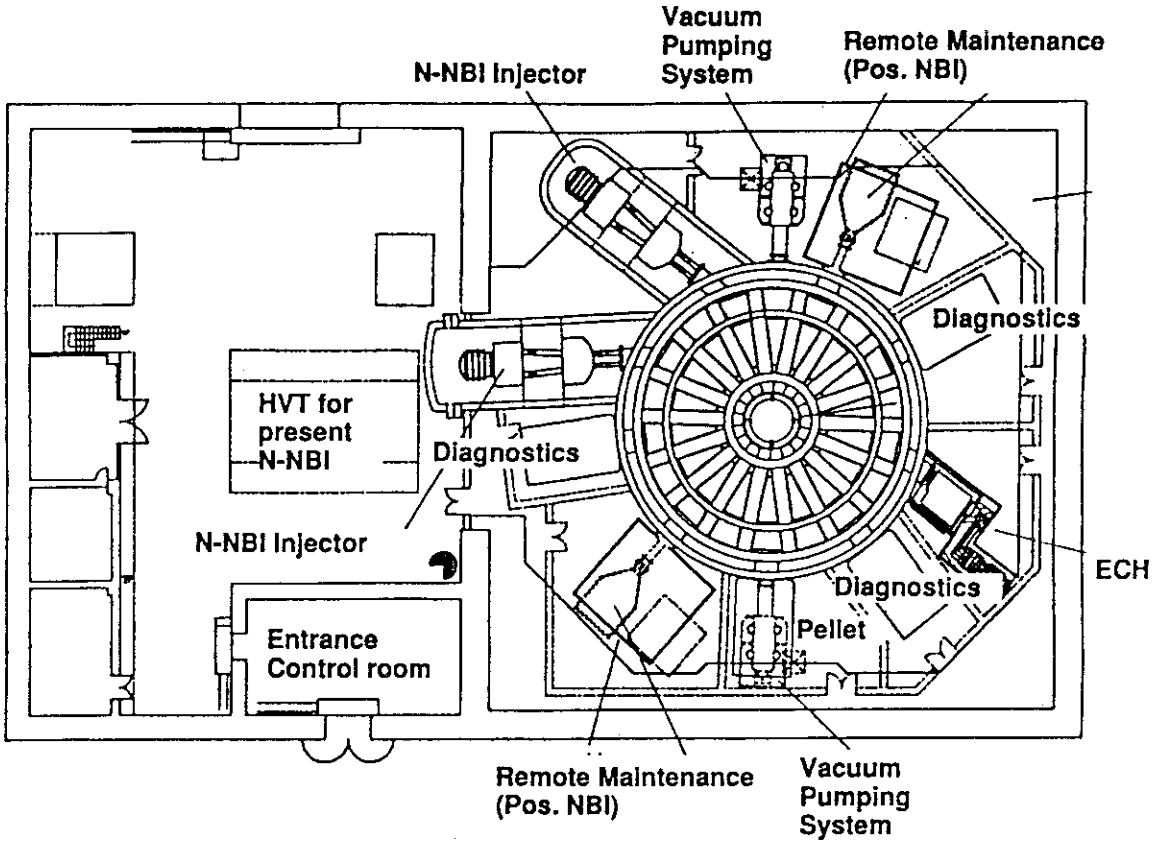

Fig. 2 Plan view of JT-60 torus hall.

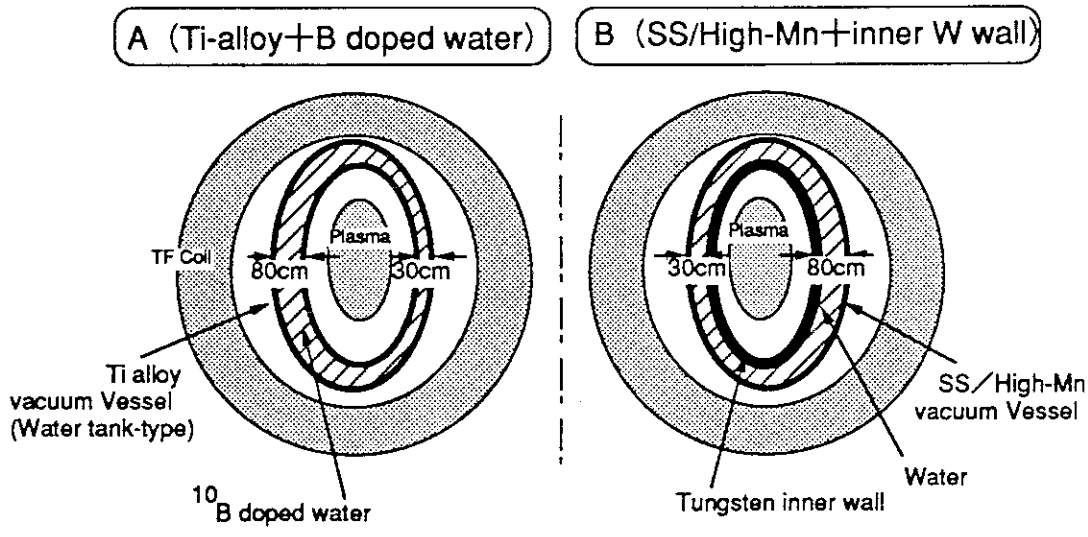

Fig.3 Shielding structures for JT-60SU

Appendix I Program of the Meeting

November 29

10:30-10:50

Opening Address — Y. Murao (JAERI)

Scope of the Meeting — Y. Oyama (JAERI)

10:50-12:05

1. Fusion Reactor Design — Chairman H. Maekawa (JAERI)
   - 1.1 Review of ITER Nuclear Design — K. Maki (Hitachi)
   - 1.2 Topics of ITER Nuclear Design — S. Sato (JAERI)
   - 1.3 R&D Task of ITER/EDA — Y. Ikeda (JAERI)

12:05-13:10 Lunch

13:10-13:45

- 1.4 Review of Fusion DEMO Reactor Study — Y. Seki (JAERI)

13:45-15:35

2. Nuclear Data Evaluation and Library — Chairman Y. Kanda (Kyushu Univ.)
   - 2.1 Evaluation of Light-Nuclei and Gamma-ray Production Data — K. Shibata (JAERI)
   - 2.2 Evaluation of Medium-Heavy Nuclei Data — S. Chiba (JAERI)
   - 2.3 Present Status of Cross Section Libraries — K. Kosako (SAEI)
   - 2.4 Present Status of Transport Calculation Codes for Fusion Neutronics — T. Mori (JAERI)

15:35-15:55 Coffee Break

15:55-17:40

3. Integral Test of Neutron and Secondary Gamma-ray Data
   - Clean Benchmark Experiment - — Chairman M. Baba (Tohoku Univ.)
   - 3.1 Nuclear Data Test by Using FNS Slab Experiments — Y. Oyama (JAERI)
   - 3.2 Benchmark Test by Using OKTAVIAN Sphere Experiments — C. Ichihara (Kyoto Univ.)
   - 3.3 Nuclear Data Test of Secondary Gamma-rays by Integral Experiments — F. Maekawa (JAERI)

November 30

9:30-10:30

4. Integral Test of Neutron and Secondary Gamma-ray Data

Appendix I (continued)

- Engineering Applicability - Chairman Y. Kikuchi (JAERI)

4.1 ITER Bulk Shielding Experiments at FNS C. Konno (JAERI)

4.2 Applicability of Multigroup Cross Section Library
K. Hayashi (Hitachi Eng.)

10:30-10:50 Coffee Break

10:50-11:50

5. Activation Cross Section File Chairman T. Asami (Data Eng.)

5.1 Evaluation for JENDL Activation Cross Section File
Y. Nakajima (JAERI)

5.2 Integral Test on Activation File Y. Ikeda (JAERI)

11:50-13:00 Lunch

13:00-13:50

6. PKA and KERMA Data

6.1 Production of JENDL PKA/KERMA File Based on JENDL Fusion File
T. Fukahori (JAERI)

6.2 Data Test by Nuclear Heating Measurement
Y. Ikeda (JAERI)

13:50-14:10 Coffee Break

14:10-15:50

7. Discussion and Summary Chairman A. Takahashi (Osaka Univ.)

7.1 Summary of Integral Data Test

a) Neutron Data Y. Oyama (JAERI)

b) Gamma-ray Data F. Maekawa (JAERI)

c) Activation Cross Section Y. Ikeda (JAERI)

7.2 Future Subjects

a) Comment 1 from Neutronics A. Takahashi(Osaka Univ.)

b) Comment 2 from DEMO Reactor and Safety Y. Seki (JAERI)

c) Comment 3 from ITER and JT60-SU N. Miya (JAERI) and
K. Maki (Hitachi)

15:50-16:00

Concluding Remarks Y. Kikuchi (JAERI)

Appendix II List of Participants

Takeo	ARUGA	Japan Atomic Energy Research Institute
Tetsuo	ASAMI	Data Engineering, Inc.
Mamoru	BABA	Tohoku University
Satoshi	CHIBA	Japan Atomic Energy Research Institute
Tokio	FUKAHORI	Japan Atomic Energy Research Institute
Masanori	HACHIYA	Data Engineering, Inc.
Katsumi	HAYASHI	Hitachi Engineering Co., Ltd.
Chihiro	ICHIHARA	Kyoto University
Yujiro	IKEDA	Japan Atomic Energy Research Institute
Osamu	IWAMOTO	Japan Atomic Energy Research Institute
Yukinori	KANDA	Kyushu University
Yoshimi	KASUGAI	Japan Atomic Energy Research Institute
Shigeto	KIKUCHI	Toshiba
Yasuyuki	KIKUCHI	Japan Atomic Energy Research Institute
Chikara	KONNO	Japan Atomic Energy Research Institute
Kazuaki	KOSAKO	Sumitomo Atomic Energy Industries, Ltd.
Vitaly	KOVALCHUK	Japan Atomic Energy Research Institute
Fujio	MAEKAWA	Japan Atomic Energy Research Institute
Hiroshi	MAEKAWA	Japan Atomic Energy Research Institute
Koichi	MAKI	Hitachi, Ltd.
Hiroyuki	MATSUNOBU	Sumitomo Atomic Energy Industries, Ltd.
Naoyuki	MIYA	Japan Atomic Energy Research Institute
Takamasa	MORI	Japan Atomic Energy Research Institute
Yoshio	MURAO	Japan Atomic Energy Research Institute
Tetsuo	NAKADA	Kawasaki Heavy Industries, Ltd.
Yutaka	NAKAJIMA	Japan Atomic Energy Research Institute
Masayuki	NAKAGAWA	Japan Atomic Energy Research Institute
Tsuneo	NAKAGAWA	Japan Atomic Energy Research Institute
Tsutomu	NARITA	Japan Atomic Energy Research Institute
Yukio	OYAMA	Japan Atomic Energy Research Institute
Satoshi	SATO	Japan Atomic Energy Research Institute
Yasushi	SEKI	Japan Atomic Energy Research Institute
Keiichi	SHIBATA	Japan Atomic Energy Research Institute
Peter	SIEGLER	Japan Atomic Energy Research Institute

Appendix II (continued)

Akito	TAKAHASHI	Osaka University
Keiichiro	TSUCHIHASHI	Japan Atomic Energy Research Institute
Yoshitomo	UNO	Japan Atomic Energy Research Institute
Masayuki	WADA	Japan Atomic Energy Research Institute
Naoki	YAMANO	Sumitomo Atomic Energy Industries, Ltd.
Michinori	YAMAUCHI	Toshiba